AUG 1 1931

VOLUME 38 SECOND SERIES NUMBER 3

THE PHYSICAL REVIEW

A JOURNAL OF EXPERIMENTAL AND THEORETICAL PHYSICS

CONDUCTED BY

THE AMERICAN PHYSICAL SOCIETY

BOARD OF EDITORS

Managing Editor, JOHN T. TATE, University of Minnesota, Minneapolis
Assistant Editor, J. W. BUCHTA, University of Minnesota, Minneapolis
E. U. CONDON, C. J. DAVISSON, F. K. RICHTMYER, K. F. HERZFELD, A. W. HULL,
F. W. LOOMIS, A. J. DEMPSTER, DAVID M. DENNISON, J. C. SLATER

AUGUST 1, 1931

Effect of Electric Fields on the Emission of Photoelectrons from Oxide Cathodes — W. S. HUXFORD 379
Some Photoelectric Properties of Mercury Films — DUANE ROLLER, W. H. JORDAN AND C. S. WOODWARD 395
The Effect of Adsorbed K^+ Ions on the Photoelectric Threshold of Iron — A. KEITH BREWER 401
Photoelectric Properties of Zinc Single Crystals — J. H. DILLON 408
The Fall of Potential in the Initial Stages of Electrical Discharges — J. C. STREET AND J. W. BRAMS 416
The Cathode Fall of an Arc — R. C. MASON 427
An Experimental Test of the Ionization Chamber Method of Measuring the Relative Intensities of X-ray Spectrum Lines — SAMUEL K. ALLISON AND VICTOR J. ANDREW 441
Ionization of Helium, Neon, and Argon — R. L. WOMER 454
The Infrared Spectrum of SN I — H. M. RANDALL AND NORMAN WRIGHT 457
On the Hyperfine Structure of Heavy Elements — G. BREIT 463
The Effect of Hyperfine Structure on the Polarization of Cadmium Resonance Radiation — ALLEN C. G. MITCHELL 473
Absorption Line Width in Sodium Vapor — S. A. KORFF 477
Selective Thermal Radiation of Colored and Pure Fused Quartz — R. W. WOOD 487
A Canonical Transformation and the Vibrations of a Loaded String — R. B. LINDSAY 491
The Motion of a Dirac Electron in a Magnetic Field — L. D. HUFF 501
Pictorial Representations of the Dirac Electron Cloud for Hydrogen-Like Atoms — H. E. WHITE 513
The Temperature Variation of the Electric Moment of Ethylene Choride — C. T. ZAHN 521
Magnetization and the Magneto-Caloric Effect — FRANCIS BITTER 528
Mobilities of Na^+ Ions in N_2 and H_2 as a Function of Time — LEONARD B. LOEB 549
Letters to the Editor — 572
An Interpretation of the Effect of Piezoelectric Oscillations on the Intensity of X-ray Reflections from Quartz, *B. E. Warren*—572; Corrected Relative Intensities of the X-ray Lines in the Tantalum L Series, *Victor Hicks*—572; X-ray Reflections from Oscillating Crystals, *R. M. Langer*—573; The Enhancement of Predissociation by Collisions, *Louis A. Turner*—574; The Relative Abundance of N^{14} and N^{15}, *Harold C. Urey and George M. Murphy*—575; The Second Virial Coefficient, *J. G. Kirkwood and F. G. Keyes*—576.
Book Reviews — 578

PROCEEDINGS OF THE AMERICAN PHYSICAL SOCIETY

Pasadena Meeting, June 15–20, 1931; Minutes and Abstracts, Author Index — 579

PUBLISHED BY THE AMERICAN PHYSICAL SOCIETY
EDITORIAL OFFICE: MINNEAPOLIS, MINN.

THE AMERICAN PHYSICAL SOCIETY

OFFICERS OF THE SOCIETY

President:	W. F. G. Swann	Bartol Research Foundation, Philadelphia, Pa.
Vice-President:	Paul D. Foote	The Gulf Companies, Pittsburgh, Pa.
Secretary:	W. L. Severinghaus	Columbia University, New York City
Treasurer:	G. B. Pegram	Columbia University, New York City
Editor:	John T. Tate	University of Minnesota, Minneapolis, Minn.
Local Secretary for the Pacific Coast:	L. B. Loeb	University of California, Berkeley, Calif.

THE PHYSICAL REVIEW

Published by the American Physical Society. Executive office: University of Minnesota, Minneapolis, Minn. Two volumes annually, twelve issues per volume.

First series. From July 1, 1893, to January 1, 1913, the Review was conducted by Edward L. Nicholas, Ernest Merritt and Frederick Bedell, with the financial support of Cornell University. The first four volumes were issued annually; subsequent volumes, semi-annually; thirty-five volumes in all.

Second series. On January 1, 1913, the Review was transferred to the American Physical Society as announced on the first page of the new series which was then begun. Since then it has been conducted by a Board of Editors elected by the Society. Semi-annual volumes begin in January and July. Since July 1, 1929, the Review has been issued twice a month.

Contributors are referred to page 2 of the advertisements for further information.

Annual subscription, throughout the Postal Union, $12.00 in advance.

General index, 1893-1920, $4.00, in advance.

Back Volumes, $9.00 per volume; Back Numbers, $1.50 per copy for issues prior to July 1, 1929 (Vols. 1-33), $.75 per copy for issues subsequent thereto. Postage is free if remittance accompanies order; otherwise postage is extra. No bound volumes can be supplied. The Review offers to purchase a limited number of First Series, Vol. 1, No. 1 (at $2.00 each); Second Series, Vol. 7, No. 1, January 1916; Vol. 7, No. 2, February 1916; Vol. 7, No. 4, April 1916; and Vol. 7, No. 5, May 1916 (at $2.00 each).

Advertisements. Rates will be supplied by the Editor on request. Copy for each number must be received at Minneapolis two weeks prior to the dates of issue; old copy is used until new copy is received. Send electrotypes direct to the printers, George Banta Publishing Co., Menasha, Wis.

Discount of ten percent is allowed to members of the American Physical Society on purchase of back numbers.

Changes of Address and Complaints of failure to receive the Review, in the case of members of the Physical Society, should be addressed to the Treasurer; in the case of other subscribers, to the Editor. New copies can be sent free in response to complaint of non-delivery only if notice of non-delivery is received within three months of date of issue.

Editorial Correspondence should be addressed to the Physical Review, University of Minnesota, Minneapolis, Minn.

Entered at the post office at Menasha, Wis., as second class matter.
Acceptance for mailing at special rate of postage provided for in section 1103, Act of October 3, 1917, authorized September 6, 1926.

Second Series *August 1, 1931* *Vol. 38, No. 3*

THE
PHYSICAL REVIEW

EFFECT OF ELECTRIC FIELDS ON THE EMISSION OF PHOTOELECTRONS FROM OXIDE CATHODES

By W. S. Huxford
University of Michigan

(Received May 15, 1931)

Abstract

A study has been made of the photoelectric emission obtained at room temperature from the equipotential oxide cathodes commonly employed in radio receiving tubes. With a double monochromator, long-wave limits were determined by plotting the currents as a function of the wave-length of the incident radiation. The threshold frequencies decreased with increase in the accelerating potential according to the relation,

$$\nu = \nu_0 - bE^{1/2},$$

in which ν_0 is the "zero-field" threshold and E the electric field at the cathode surface. It is shown that the observed lack of saturation in the photo-currents may be ascribed to a decrease of work function with increase of applied field. The tendency to non-saturation is greatest for light of longest wave-length. Calculations show that the photoelectric equation of Houston satisfactorily represents the variation in numbers of emitted electrons with color of illumination, and with change of threshold. Some comparisons are made of the photo-emission and the thermionic currents obtained from the same cathode surface. There is a change in photoelectric threshold with activation. Preliminary measurements of thermionic work functions confirm the theory that in both cases the emission of electrons takes place from the outermost layers of the oxide coating.

Introduction

THE oxide-coated type of thermionic emitter is the most economical source of electrons at present available for use in commercial radio receiving tubes. Although it has been developed to a point of high efficiency in the technical laboratory, relatively little is known concerning the atomic processes which take place during the formation of the coating, and no completely satisfactory analysis of the mechanism by which electrons are released from the oxide has been made. Many investigators have studied the thermionic properties of the coating, but not a great deal of information is available concerning the photoelectric characteristics of this type of emitting element. The present paper is concerned chiefly with considerations of the surface structure of such coatings as revealed by a study of their photoelectric properties.

Results of recent investigations have raised the question as to the localization of the active elements of the coating which give rise to its high electron emissivity. The commercial form of coating is prepared from a fifty-fifty mix-

ture of barium and strontium carbonates, which, after deposition upon a metal filament, is reduced to the oxide form. It has been definitely established that when the coating becomes an active emitter, atoms (or ions) of barium and strontium are released from the oxide crystals and held in the form of "free" or adsorbed metal somewhere within the coating, or upon its outer surface. Presumably these atoms and ions constitute emission centers of low work function for electrons, but as to the exact nature of their action various investigators are not in agreement.

Lowry[1] has studied the effect of coating different metals with the same mixture and finds that the emission depends markedly upon the type of core metal used. He concludes that the thermionic efficiency is determined by the kind of surface formed at the interface between core metal and coating, and that the alkaline earth atoms which serve as active emission centers are those which are deposited upon the core metal surface. Reimann and Murgoci[2] also conclude from their experiments that the electrons are emitted from the barium metal adsorbed on the core. The results reported by Becker[3] and others,[4] on the contrary, lead to the conclusion that the alkaline earth metal is adsorbed in a layer on the superficial outer surface of the coating itself.

It was felt that an examination of the photoelectric emission from the oxide would yield results of particular value concerning the structure of its outer surface, and, by comparison with the thermionic properties of the coating, give definite information as to the activation and adsorption processes which occur.

It is a fact of common experience that well saturated electron currents cannot be obtained from an oxide coated cathode. As to the explanation of this effect, various investigators are not in agreement. Lowry[1] suggests that the process of electron diffusion through a porous coating may account for the phenomenon of non-saturation. Many writers believe that this effect in the case of composite surfaces, over and above that which may be accounted for on the basis of Schottky's electron image theory, is due to the neutralization of local surface fields by the fields applied to the cathode. Of the various hypotheses so far proposed as to the nature of these intrinsic fields, none is eminently successful in explaining the observed dependence of emission upon accelerating potential.

In order to establish a satisfactory theory, it is evident that more information on emission characteristics of composite surfaces is required. To this end, a number of data were obtained during the course of the present investigation on the photo-currents from oxide cathodes over a wide range of potentials and under various conditions of illumination. It was found that the tendency to non-saturation is particularly marked in the photo-emission as measured at room temperature, and that the effect is a function of the color of light used. It was also observed that the photoelectric threshold shifts in a

[1] E. F. Lowry, Phys. Rev. **35,** 1367–78 (1930).
[2] A. L. Reimann and R. Murgoci, Phil. Mag. **8,** 440 (1930).
[3] J. A.Becker, Phys. Rev. **34,** 1323–1351 (1929).
[4] Cf. Saul Dushman, Reviews of Modern Physics **2,** 431–441 (1930).

definite manner with applied field. On the basis of these experimental facts it is obvious that any attempt to explain the continued rise in emission with increase of accelerating potential must take into account the frequency of the incident radiation as well as the value of the applied field. It is believed that a satisfactory correlation of the effect of applied fields on saturation current values and the observed shift in long-wave limit has been obtained. In any case, the data obtained should furnish a basis for further investigations of the photoelectric properties of oxide cathodes.

Experimental Details

The coatings studied were precipitated mixtures of barium-strontium carbonates commonly used in the manufacture of commercial radio tubes. The carbonates were sprayed on treated nickel sleeves and baked for several hours in an electric oven. The coated sleeves were then mounted on a pressed seal together with grid and plate in the manner used in assembling the equipotential cathode type of radio tube, a slit being cut in the side of the plate so as to allow a beam of light to fall at normal incidence upon the cathode. The cathode lead wire was passed out through a bead on the top of the glass bulb in order to minimize leakage currents. For the emission measurements, grid and plate were joined together to form an anode. The value of the electric field at the cathode, calculated from the dimensions of cylindrical grid and cathode, is given by the relation $E = 12.3V$ volts per centimeter, where V is the value of the applied potential in volts.

A small sized bulb was used, permitting the cathode to be brought close to the exit slit of the monochromator. The assembled tube was glass-sealed onto a mercury diffusion pump and baked in an electric oven for about one hour at 400°C. All metal parts were then brought to a yellow heat by means of an induction furnace, and the tube was pumped until all traces of gaseous discharge disappeared. The cathode was held at a red heat during this treatment and as a consequence the coating was partially activated at the termination of the degassing process. A combination magnesium-barium getter was flashed over the lower portion of the glass bulb, the tube then being sealed off the pump.

The bulb was placed in a light-tight box and mounted rigidly in such a position that beams of monochromatic light were completely intercepted by the coating of the cathode. The filament could now be heated and the cathode raised to various temperatures suitable for activating the coating. Tests on tubes prepared for these studies showed no gas ion currents measureable on a galvanometer having a sensitivity of 10^{-8} amperes when thermionic currents of from 10 to 20 milliamperes were drawn from the cathode.

Voltage supply and current measurement

Voltages were supplied by two power packs joined in series, each bridged with a 3000 ohm resistance having a variable contact. Thus, potentials ranging from one to one thousand volts were available for rapid measurement. Voltage readings were made on a Weston 1500 microammeter joined in series with two 500,000 ohm wire-wound resistances having zero temperature coefficient for the range used.

Photoelectric currents were measured on a high sensitivity Leeds and Northrup galvanometer having a resistance of about 900 ohms. Two different suspensions were employed during the course of the work, the current sensitivity in both cases being of the order of 10^{-11} amperes per scale division.

Monochromator

A 400-watt projection lamp was used as source of illumination. Light from one of the tungsten filament coils of this lamp was dispersed by a Van Cittert type double monochromator having glass prisms. Any desired band of the spectrum could be selected by moving the central slit, thus making it unnecessary to alter the adjustment of the last slit or to change the position of the cathode while measuring the emission at various wave-lengths. The instrument was calibrated over the range from 4000 to 14000 Angstroms with emission lines from rare gas spectra and the mercury arc. Slit widths of from one to three tenths of a millimeter were used in the course of the work. A slit width of 0.1 mm corresponds to a band 20A wide at 5000A, and to about 280A at the 12000A setting.

Operation

Leakage currents were largely avoided by sealing the cathode lead through the top of the bulb. A "zero" reading of the galvanometer was secured with no light falling on the cathode; then, by means of a shutter, radiation was admitted to the tube and a second reading taken, the process being repeated several times for each recorded observation. A slight decrease of photo-currents with time was noted for potentials in the neighborhood of 1000 volts. The galvanometer deflection recorded was that observed about ten seconds after the light beam was admitted. The energy of the radiation over the spectral region used was determined by means of a Moll microthermopile used in conjunction with a high sensitivity Leeds and Northrup galvanometer having a resistance of fifteen ohms.

Photo-Emission from Stock Cathodes

Preliminary measurements of the photoelectric activity of the cathodes in stock radio tubes of the '27 type illustrate the method used in this work. Light from the monochromator was allowed to fall through the top of the radio bulb and strike one side of the cathode at a glancing angle. It was impossible to avoid illuminating at the same time the cathode supporting wires, so the currents observed cannot be said to originate solely in the oxide coating. In many of the tubes leakage currents were of the same magnitude as the photo-currents obtained.

The results for ten such tubes are shown in Fig. 1. The plotted currents are the *total* emissions observed at each wave-length, and *not* the emissions per unit of radiant energy. The variation in amplitude of the emission is large, and there appears to be no correlation between total photo-emission and thermionic activity of these cathodes. Subsequent results obtained with tubes in which the light beam was directed solely upon the oxide cathode showed much smaller photo-currents, so it is evident that the large variation

in amplitude of the currents obtained from the stock radio tube cathodes arises from the fact that the photo-activity observed is not merely that of the coating, but of coating plus activated cathode supporting leads.

One result is of importance. The long-wave limit as measured at a potential of 90 volts is sensibly constant, and falls at 10,400 ± 400A. The threshold of the sputtered cathode lead wires may be taken to be the same as that

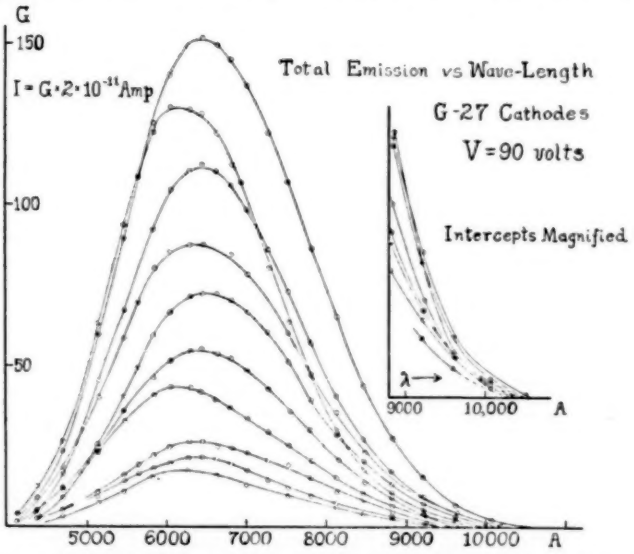

Fig. 1. Photoelectric currents obtained from the cathodes of '27, or heater type, radio receiving tubes.

of the activated grid and plate in these tubes. This threshold had previously been measured and found to lie in the region from 7500 to 8500A; hence it is believed that *the long-wave limit at* 10,400A *is fixed by a photoelectric work-function which is characteristic of the oxide coating on the cathode.* This threshold may be corrected for the effect of the applied field by a method shown in a later section. When this is done, the zero field work function of this group of well activated cathodes is found to be 1.32 ± 0.05 volts.

Variation of Photo-Emission with Activation

A study of the changes in surface structure which take place when the oxide is brought to an active state was made by obtaining the spectral sensitivity of the coating at each stage of the activation process. These tests were carried out with the specially prepared tubes in which the light beam was incident solely upon the coated portion of the cathode.

The treating-out process on the pump was carried to a point such that a few microamperes of thermionic current was obtained at normal cathode heating. After sealing off the tube and mounting it in front of the monochromator, usually no photo-emission could be detected. An activation treatment consisted in overheating the cathode for a few minutes, then dropping the filament voltage to normal value and noting the final steady value of thermionic current. When the tube was then cooled to room temperature, it was found

that a completely stable and permanent value of photo-current at any given intensity of illumination could be obtained only after the tube had remained

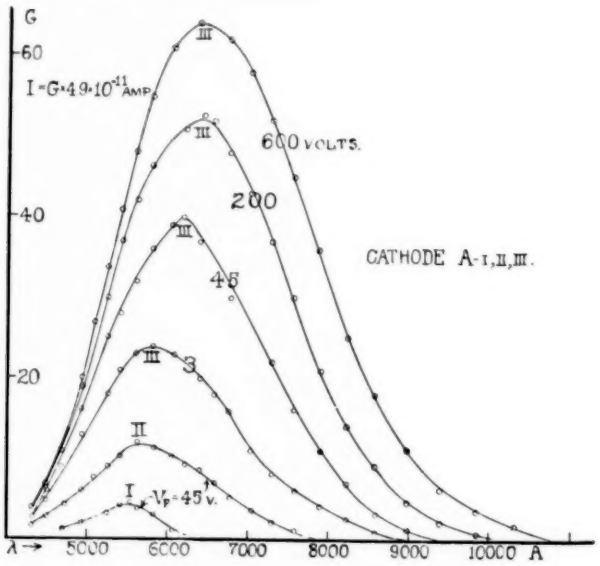

Fig. 2. Showing the variation in photo-emission with heat treatment of an oxide coated cathode.

cold for a period of from 20 to 30 hours. Presumably this action is due to a slow clean-up of gas molecules by the free barium and strontium atoms in the surface of the coating. As previously noted, the tubes failed to show detect-

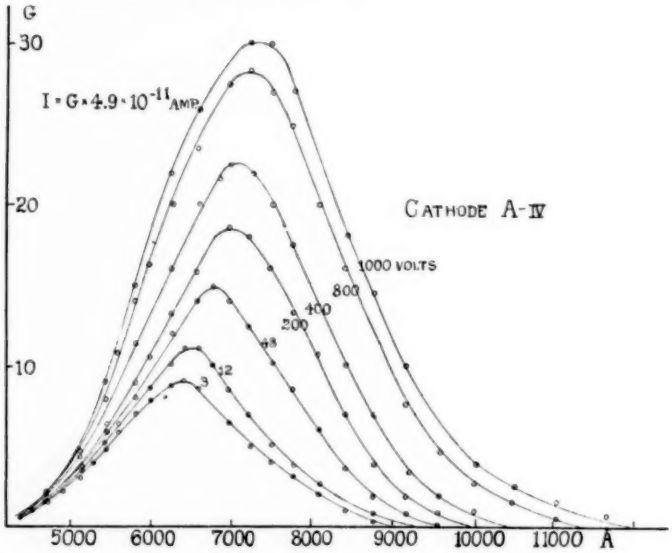

Fig. 3. Total photo-emissions from cathode *A*-IV, showing the effect of various accelerating potentials.

able gas-ion currents, indicating that the pressure was less than 10^{-7} mm of mercury.

When a stable condition of photo-activity was obtained, current measurements were taken at various wave-lengths. The process was then repeated for several activations, until the thermionic tests indicated no further gain in emission. The data obtained for the first tube, designated as cathode *A*, are shown in the graphs of Fig. 2, which indicate clearly a shift of the long wave limit towards the red end of the spectrum as the activation is carried forward. Roman numerals refer to successive activations; the plot for activation IV is shown in Fig. 3 (48 volts anode potential), and the threshold frequency for activation V (not plotted) is $3.05 \cdot 10^{14}$ sec^{-1}, $\lambda_0 = 9830$A, as measured at a grid-plate potential of 45 volts. Similar results were obtained with other cathodes.

TABLE I. *Activation data, cathode A, anode potential, 22.5 volts. Surface temperature during thermionic tests, 1120°K.*

No.	Thermionic current in milliamp.	Thresholds for $V=45$ v.	Work function at zero field*
I	10.6	$4.68 \cdot 10^{14}$ sec^{-1}	2.00 volts
II	17.0	3.82	1.64
III	21.0	3.38	1.46
IV	24.2	3.13	1.36
V	30.0	3.05	1.32

* These values for the photoelectric work function are computed on the assumption that the effect of the field is the same for low and high activations.

Table I gives the values of thermionic currents obtained after each heat treatment for cathode *A*, the corresponding threshold frequencies at 45 volts anode potential, and the photoelectric work functions reduced to zero field. We shall have occasion to refer to these data in a later section dealing with thermionic properties of the coating.

SHIFT IN LONG WAVE LIMIT WITH APPLIED FIELD

Investigations in this laboratory of the maximum excursion of the long wave limit for pure barium films have revealed a noticeable dependence of the photoelectric threshold upon the applied field. The effect is particularly striking in the case of activated oxide cathodes. Figs. 2, 3 and 4 show plots of total photo-emission in terms of galvanometer deflections for two cathodes, *A* and *B*. The light source was maintained at a constant intensity throughout. With the anode at a given potential the wave-length of the monochromatic beam was varied over the spectral region and the mean galvanometer deflection obtained for each setting of the monochromator. It is to be noted that there is a progressive shift of the maxima in the total emission, and of the long wave limits, with change of applied potential.

Fig. 2 shows the effect of the applied field in the case of cathode *A*, activation III; Fig. 3, that for the same cathode when the activation was carried one step farther. At present no theory is advanced for the decrease in amplitude of the emission in the second case. It is probably due to a change in surface structure of the oxide. The amplitude decreased still more for activation V. Fig. 4 gives the results for cathode *B* following a second heat treatment.

Fig. 5 indicates the change in threshold frequencies with applied voltage for cathode A-IV. If these threshold frequencies, determined by extrapolation, are plotted against $E^{1/2}$, where E is the field in volts per centimeter at the

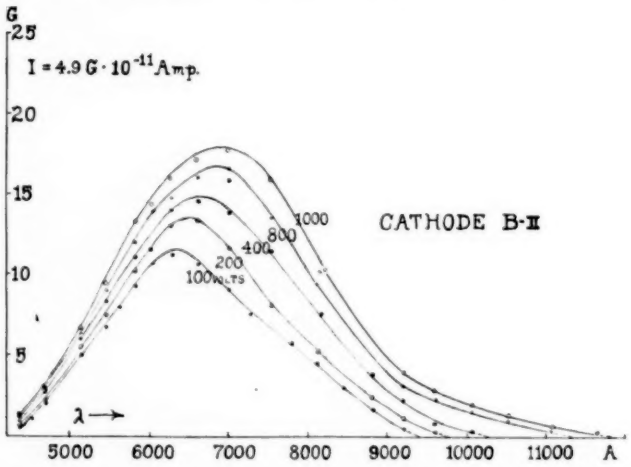

Fig. 4. Total photo-emission from cathode B after a second heat treatment, showing the effect of various accelerating potentials.

cathode, the points fall nearly on a straight line. Such plots for cathodes A and B are shown in Fig. 6. This relation suggests a change in work function due to the neutralization of image forces at the surface of the cathode. Quantitatively the effect is much too large to be explained by Schottky's electron image theory for metal surfaces.

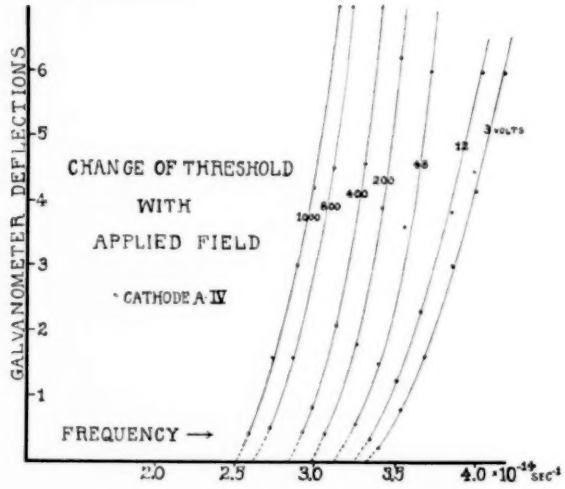

Fig. 5. The photo-currents, plotted to a large scale, as a function of frequency near the long-wave limit. Cathode A-IV.

In the present case it is inconceivable that light could penetrate through the thick coating and cause photoelectric emission from the core metal surface. Evidently the intrinsic fields which are modified by the applied field, re-

sulting in a reduction of electron work function, are due to atoms and ions of barium (or of barium and strontium) adsorbed on the outermost layers of the oxide crystals.

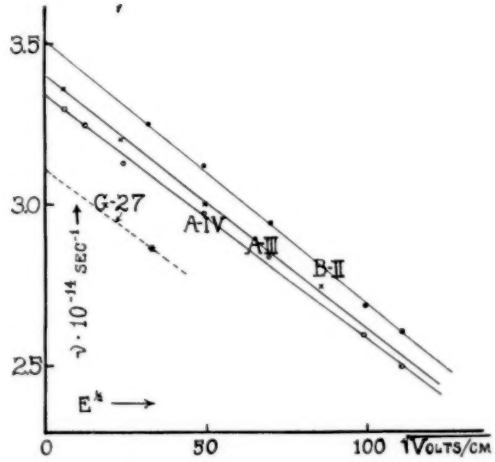

Fig. 6. Threshold frequencies, as determined by extrapolation from the type of plot illustrated in Fig. 5, are shown here plotted against the one-half power of the applied electric field. Results are shown for cathodes *A*-III, *A*-IV and *B*-II.

Comparison of Results with Theories of the Photoelectric Effect

From the plots of Figs. 2, 3 and 4 it is evident that the tendency to non-saturation of the photo-currents increases with the wave-length of incident

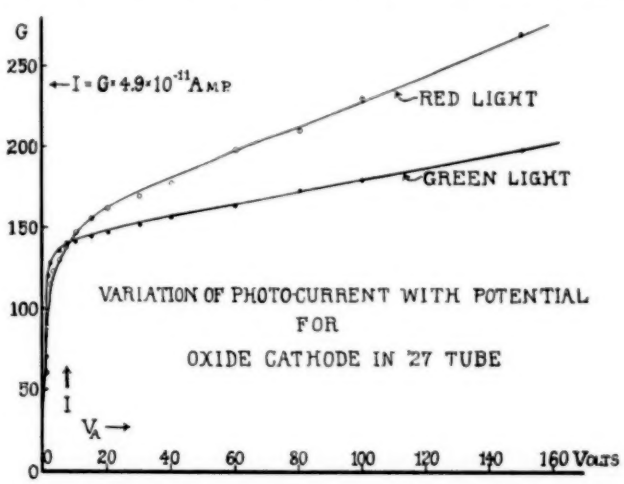

Fig. 7. Illustrating the condition of non-saturation in photo-currents from the oxide coated cathode of a stock radio tube, and dependence of the effect upon color of incident radiation. (Light intensities were adjusted to give the same photo-current at $V = 10$ volts.)

radiation. This may also be shown by plotting the current as a function of the accelerating potential for different colors of light. An example of such a plot

is illustrated in Fig. 7. The upper curve is for light from a tungsten filament focused upon the cathode of a radio tube, through a ruby glass filter; the lower curve is that obtained by using a sextant green filter.

The problem which now arises is that of determining whether or not the continued rise of current with increase of accelerating potential may be completely accounted for by a change in work function with applied field, or whether it may arise from other causes. Since the effect is dependent upon the color of light used to illuminate the emitting surface, a complete solution of the problem involves a knowledge of the dependence of emission on frequency of the incident radiation. In the discussion which follows, two theories of the photoelectric effect have been considered, one based on classical physics, the other on wave mechanics. It is assumed that the change in work function varies linearly with the one-half power of the field, and theoretical expressions are obtained giving the photo-current as a function of field and of light frequency. In order to determine which of the two equations more nearly represents the observed change of emission with field, plots are drawn up for comparison. A further test consists in calculating from the emission data the true, or zero-field, photoelectric work function of the emitting surface. When the wave-mechanical expression is used, the values are found to agree, within the limits of experimental error, with those obtained from a consideration of the long wave limits.

Compton-Richardson equation

Compton and Richardson[5] have developed an equation connecting the frequency and number of electrons emitted per unit time for light of unit intensity, of the form

$$i = k(\nu - \nu_0')/\nu^3 \tag{1}$$

where k is a constant for a given substance, ν the frequency of the incident light, and ν_0' the threshold frequency. If we assume that $\nu_0' = \nu_0 - a V^{1/2}$ is the value of the threshold for an applied field which is proportional to the accelerating potential V, we have by substitution in (1),

$$i = k(\nu - \nu_0 + aV^{1/2})/\nu^3, \tag{2}$$

in which ν_0 is the zero field threshold. Thus, when ν is held constant, i should vary linearly with the one-half power of the accelerating voltage. On the basis of observed emissions such a dependence does not satisfactorily account for the characteristic obtained. Moreover, quantitative agreement is lacking between the change in work function with applied field computed on the basis of this theory and the observed shift in the photoelectric threshold.

Houston equation

More recently theories have been developed for the dependence of photoemission upon frequency of the incident light, which are based upon wave mechanics and the newer statistical mechanics. The application of these theories to experimental results is discussed in detail in a paper by Lawrence and Linford,[6] who have measured the shift in photoelectric threshold with

[5] K. T. Compton and O. W. Richardson, Phil. Mag. **26,** 549–567 (1913).

[6] E. O. Lawrence and L. B. Linford, Phys. Rev. **36,** 482–497 (1930).

applied field for thin potassium films on tungsten. These authors give an equation derived by Houston,[6'] and based upon the previous work of Wentzel, as follows:

$$I \sim (\tilde{\epsilon}/h\nu)^{1/2}\left\{\frac{E_x^2}{\nu}\left[1+\frac{\tilde{\epsilon}}{2h\nu}\right]+\frac{E_y^2+E_z^2}{3\nu}\left[\frac{\nu-\nu_0}{\nu}\right]\right\}\left(\frac{\nu-\nu_0}{\nu}\right)^2 \qquad (3)$$

where I is the photoelectric emission at 0°K, ν is the frequency of light having electric vectors proportional to E_x, E_y, E_z, incident on a metal surface with the normal along the x-direction, ν_0 is the threshold frequency, and $\tilde{\epsilon}$ is the maximum energy of the electrons in the degenerate Fermi distribution.

Photoelectric sensitivity of the emitting surface

In order to compare the emission actually observed with that given by the above expression, considerable simplification of the equation is necessary. We consider first the variation of current with frequency of incident light, presuming the threshold to remain constant for a given applied field. If we assume a perfectly plane emitting surface, with light falling upon it at normal incidence, then $E_x=0$, and $\overline{E_y^2}=\overline{E_z^2}=$ a constant. Rewriting Eq. (3) so as to

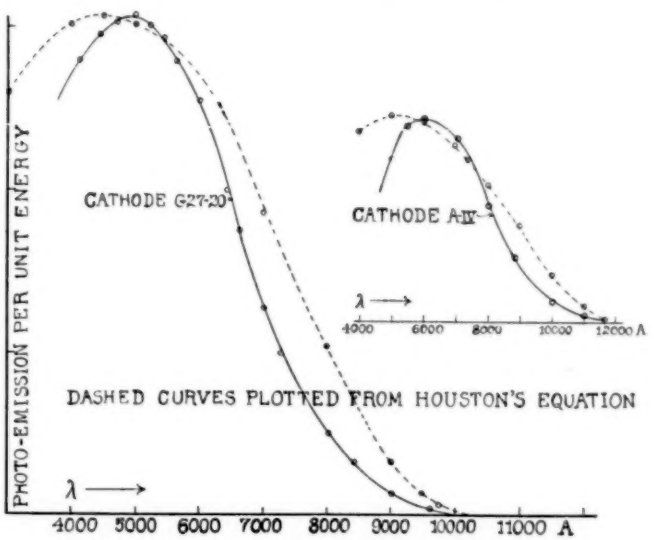
PHOTO-EMISSION PER UNIT ENERGY
CATHODE G27-20
CATHODE A-IV
λ ⟶
4000 6000 8000 10000 12000 A
DASHED CURVES PLOTTED FROM HOUSTON'S EQUATION
λ ⟶
4000 5000 6000 7000 8000 9000 10000 11000 A

Fig. 8. Comparison of the theoretical and observed photo-sensitivities of oxide cathode emitters

express I as a function of λ, and differentiating to determine the maximum in the sensitivity curve, I_{max} falls at $\lambda_{max}=\lambda_0/3$. For the Compton-Richardson equation, $\lambda_{max}=2\lambda_0/3$, in which λ_0 is the long wave limit. Plotting the observed current per unit radiant energy against wave-length, the maxima in the emissions obtained from well-activated cathodes is found to lie between these two values.

It is of interest to calculate approximately where the theoretical maximum sensitivity should occur if the light does not fall at normal incidence. The oxide surface is actually not smooth, but consists of elementary crystal sur-

[6'] Reference 6, p. 495.

faces oriented at all possible angles with respect to the direction of propagation of the incident radiation. If we may assume that in general $\overline{E_x^2} = \overline{E_y^2} = \overline{E_z^2} =$ a constant for the mean square values of components of the electric vector, then the maximum is found to lie between the limits $\lambda_{max} = \lambda_0/3$, and $\lambda_{max} = 2\lambda_0/3$. The resulting equation is too complex to permit a direct determination of λ_{max} without a great deal of labor. The easiest method of comparing theoretical and experimental results is to plot the current per unit of energy for each case, adjusting the calculated values of I so that $I = 0$ for $\lambda = \lambda_0$, and has the same value at the maximum as that shown in the experimental plot. The value assigned to $\bar{\epsilon}$ does not greatly affect the result; in the present computations $\bar{\epsilon}$ has been taken as 2.4 electron-volts, assuming that barium atoms constitute the emission centers.

Such plots are shown in Fig. 8 for the case of two cathodes that gave sufficient emission at the short wave-lengths to permit fairly accurate determinations of the observed maxima. In all cases it was found that the observed maxima occurred at longer wave-lengths than those predicted by the Houston equation. Unfortunately, in the present work, the sensitivity plots for the observed emission are least accurate in the region from 4000 to 5000A, since at this end of the spectrum both the photo-currents and the e.m.f. generated in the microthermopile are small in value, and cannot be determined with great precision. In general, Eq. (3) represents the photosensitivity of the oxide cathodes more closely than does Eq. (1).

Zero-field thresholds

Only an approximate theoretical calculation of the effect of applied fields upon the photoelectric emission is attempted in this paper. For this, simply the case in which we may assume that the light falls at normal incidence upon the cathode surface is considered in the simplification of Eq. (3). Then $E_z = 0$, $\overline{E_y^2} = \overline{E_z^2} =$ a constant, and Eq. (3) takes the form

$$I = k^3(\nu - \nu_0')^3/\nu^{9/2} \tag{4}$$

in which k is a constant and ν_0' is the effective threshold frequency. Supposing there are surface fields such that

$$\nu_0' = \nu_0 - bE^{1/2}$$

expresses the dependence of the threshold upon the applied field, E, we have, by substitution in (4),

$$I = [k^3\nu^{-9/2}](\nu - \nu_0 + bE^{1/2})^3 \tag{5}$$

in which ν_0 is the value of the threshold at zero applied field, and this, as well as the proportionality factors b and k, are constants still to be determined by comparison with experimental results.

How well Eq. (5) expresses the dependence of the current upon applied field may be determined by plotting $I^{1/3}$ against $E^{1/2}$ (or $I^{1/3}$ against $V^{1/2}$, where V is the accelerating potential). For a given color of illumination (constant ν) the graphs should be straight lines. Fig. 9b, c, d, shows such plots for cathodes *A*III, *A*IV, and *B*II. The emission values are taken from the graphs of Figs. 2, 3 and 4, the color and intensity of the light being constant for each

plot. Obviously it is not necessary to reduce the observations to photoemission per unit light intensity. Except for values of accelerating potential less than about 50 volts, the plotted points fall approximately on straight lines.

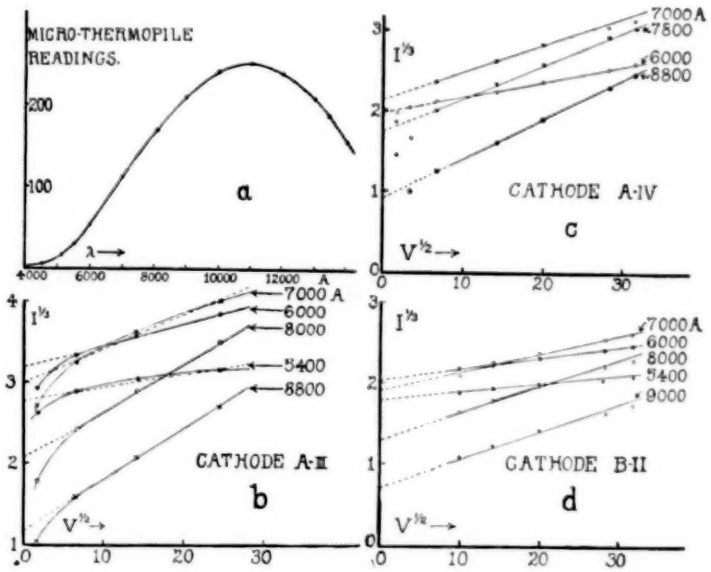

Fig. 9. (a) Microthermopile readings plotted against wave-lengths, VanCittert monochromator, using hot tungsten filament source. (b), (c), (d) $I^{1/3}$ vs $V^{1/2}$ plots for testing Eq. (5), and for determining zero-voltage "saturation" current values.

If the line which passes through most of the points be extended back until it cuts the axis of ordinates, the value of $I_0^{1/3}$ may be obtained which corresponds, for a given frequency of illumination, to the current which would result with zero applied field, were it possible to eliminate all effects of electron space charge. At zero potential, $\nu_0' = \nu_0$, and from Eq. (4) we have,

$$I_0^{1/3} = k(\nu - \nu_0)/\nu^{3/2} \text{ or } k = \frac{I_0^{1/3}\nu^{3/2}}{(\nu - \nu_0)}. \tag{6}$$

Substituting this value of k in Eq. (4) we obtain

$$(I/I_0)^{1/3} = \left(\frac{\nu - \nu_0'}{\nu - \nu_0}\right) \tag{7}$$

Eq. (7) expresses how the current I should change from its saturation value I_0, at zero field, as the effective threshold, ν_0', varies in value, when the color of the incident light is held constant. How well this equation represents observed results might be tested by using values of ν_0' and ν_0 obtained independently from considerations of the long wave limits for a given surface. This has been done and the observed changes in emission differ in magnitude from those predicted by some 15 or 20 percent.

Another mode of procedure is to obtain values for the true threshold, ν_0, directly from Eq. (7) by equating the expressions for ν_0', corresponding to a

given field, for two light frequencies, ν and ν'. Thus, omitting the intermediate steps,

$$\nu - (\nu - \nu_0)(I/I_0)^{1/3} = \nu' - (\nu' - \nu_0)(I'/I_0')^{1/3}$$

in which the primed quantities are the currents and frequency for a second color of illuminating radiation. Setting $r = (I/I_0)^{1/3}$, and $r' = (I'/I'_0)^{1/3}$, and solving for ν_0 we obtain,

$$\nu_0 = \frac{\nu'(r' - 1) - \nu(r - 1)}{r' - r}. \tag{8}$$

Table II shows the results of calculations of the zero field thresholds for three cathodes, following the method outlined above. Values of current ratios, r and r', were chosen in the range from 45 to 1000 volts anode potential. Each value of threshold shown represents the average of from 20 to 30 ν_0's calculated by using various pairs of frequency values, at various anode potentials. The maximum fluctuation from the mean is about 20 percent. Large variations may be expected, since the results depend critically upon the slopes of the lines of Fig. 9 from which the I_0's are obtained. These calculated values of zero field threshold fall below those obtained from the long wave limits (Fig. 6), but in general the agreement is satisfactory.

TABLE II. *Zero field thresholds calculated from the equation,* $\nu_0 = \dfrac{\nu'(r'-1) - \nu(r-1)}{(r'-r)}$.

	Voltage range	Range of frequencies	Average values ν_0	ν_0 from long-wave limits
Cathode *A* III	45– 600	3.75–$5.56 \cdot 10^{14}$	$3.14 \cdot 10^{14}$	$3.40 \cdot 10^{14}\ \text{sec}^{-1}$
Cathode *A* IV	48–1000	3.40–5.00	3.12	3.34
Cathode *B* II	100–1000	3.33–5.00	3.11	3.51

That one may arrive at even an approximate value of the zero field threshold of a surface from calculations based on current—potential plots and a knowledge of the frequency of the incident light, lends weight to the hypothesis that the lack of saturation in the observed photo-currents is caused by a lowering of the work function with increase of applied field. Furthermore, it appears that the form of the dependence of emission upon frequency is that given by Houston's equation. It is obvious that an attempt to apply this method to ordinary metal surfaces would fail, since the shift in threshold is small up to values of electric field which would give rise to auto-electronic currents. It should be possible, however, to apply these calculations to the changes observed with thin alkali metal films under the action of fields of the order of 10,000 to 100,000 volts per centimeter.

THERMIONIC PROPERTIES OF OXIDE CATHODES

In the course of the present investigation no extensive study of thermionic emission was undertaken. A few observations carried out at low cathode heating, and calculations based on activation tests, indicate that probably the thermionic and photoelectric work functions for these surfaces have the same value.

Thermionic work function at low temperatures

Near the close of the investigation one set of observations was taken at low temperatures to determine the Richardson line for one cathode. It is to be noted here that there are several advantages to be gained in working at low temperatures: thermionic and photoelectric emissions may be obtained under nearly the same temperature conditions with little danger of altering the surface structure of the coating by heating, and much higher potentials may be applied than at normal cathode heating. Using cathode *B*II it was found that the log i vs $V^{1/2}$ plots gave straight lines for potentials in excess of 40 volts, up to 1000 volts, over the temperature range from 370° to 530°K. It was thus possible to obtain values of the emission current at zero field for each temperature by extrapolation. The thermionic work function determined in this manner was 1.42 volts, corresponding to the zero field photoelectric value of 1.44 volts for the same surface (see Fig. 6). The agreement is well within the limits of experimental error.

Variation of ϕ and A with activation

Values of the thermionic currents measured at the same temperature for various stages of activation of cathode *A* are shown in Table I. If, for each stage, we take the thermionic work function to be identical with the zero field photoelectric value, and assume A constant, then the temperature required by the Richardson-Dushman equation,

$$i = AT^2e^{-b/T}, \tag{9}$$

is in the neighborhood of 10,000°K. The surface temperature measured by means of an optical pyrometer was 1120°K. Either, with constant value of A, the change in thermionic work function is very small, (of the order of 0.15 volt) or both A and b change with activation. We have reason to believe from the reports of other investigators on the work function of oxide coatings, that the latter is probably the case.

Espe[7] observed that while b remained fairly constant for a strontium oxide coating during activation, A increased considerably. Detels,[8] who measured the thermionic work function for various activations of barium-strontium coatings on nickel, found that both A and b decreased during activation, and that the decrease in log A was approximately proportional to that in b.

TABLE III. *Variation of A and ϕ with activation. Cathode A, heat treatments I to V. Normal test temperature = 1120°K.*

No.	i cm²	ϕ	A	ϕ^*	A^*	Values given by Detels ϕ	Values given by Detels A
I	0.0141 amp.	1.93	44.8	2.00	59.8	2.37	27.5 amp/cm² T^2
II	0.0227	1.57	.24	1.64	0.435	1.83	1.24
III	0.0280	1.39	.040	1.46	0.049	1.36	0.0373
IV	0.0322	1.29	.016	1.36	0.0207	1.36	0.0297
V	0.0400	1.24	.0116	1.31	0.0141		

* Values of ϕ and A corresponding to zero accelerating field, assuming that the variation of work function with field is not a function of the temperature. Work functions are in volts.

[7] S. Dushman, Rev. of Modern Physics **2,** 436–37 (1930).

[8] F. Detels, Jahrb. d. drathlos. Telegr. **30,** 10, 52 (1927).

Calculations based on the activation data for cathode A, assuming the photoelectric and thermionic work functions to be identical, are shown in Table III. The approximate area of the emitting surface is 0.75 cm², and the activation test temperature is taken as 1120°K. Fig. 10 shows plots of log A vs ϕ for values given by Detels and for our results. The plots nearly coincide at the higher activations. That this is more than a chance agreement is indicated by the fact that both sets of results are for barium-strontium oxide coated nickel. Moreover, our values of A are probably too high at the lower activations. The thermionic currents were measured at 22.5 volts anode potential, and it is difficult if not impossible to obtain current values extra-

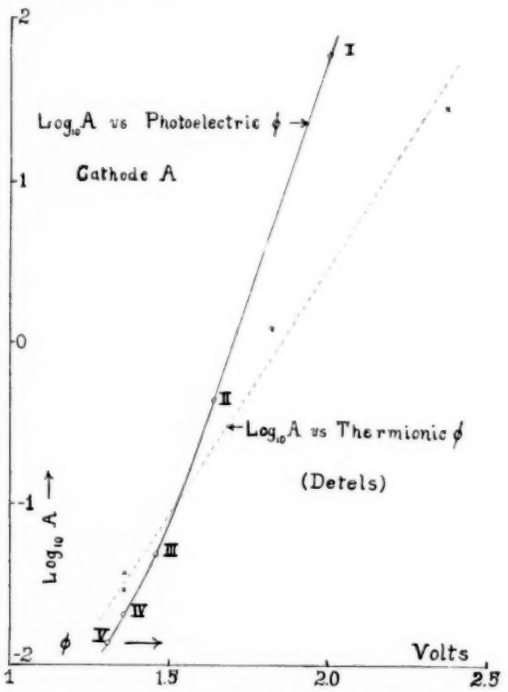

Fig. 10. The solid line represents the observed change of log A (for the thermionic emission) with photoelectric work function, ϕ, during activation of cathode A. The other points are taken from data on oxide cathodes published by Detels, for which now the values of ϕ are measured thermionic work functions, in volts.

polated to zero field at normal cathode heating. At the lower activations the emission saturates poorly, and the current values are therefore too high. As the cathode becomes activated, however, the currents exhibit better saturation, and the values obtained at III, IV and V (Fig. 10) are therefore much closer approximations to the currents which would be obtained with no accelerating field. It is believed that these results indicate a close agreement in the values of the two work functions, and show that the thermionic and photoelectric electrons originate in the same layer of adsorbed atoms.

These results are in qualitative agreement with those obtained by Becker and Mueller[9] for caesium films on tungsten, and for thoriated tungsten. These

[9] J. A. Becker and D. W. Mueller, Phys. Rev. **31**, 431–440 (1928).

investigators show that for a complete monatomic layer of caesium the currents approach metallic saturation. Also that for the log i vs $E^{1/2}$ plots, a linear relation is not found for the lower values of electric field.

In addition, it is evident from the present work that the change in work function caused by the applied field depends upon the temperature of the cathode, since our results show a continuously decreasing slope in these plots as the temperature is raised, in the case of thermionic measurements carried out at low cathode heating where anode potentials up to 1000 volts could be applied.

Summary of Results

That during the activation of an oxide cathode a photoactive surface film is formed whose work function decreases with heat treatment of the coating, is proven by the measurements described in this paper. This film, which is probably composed of barium atoms, has properties very similar to those of adsorbed films of the alkali metals. The formation process in the case of the oxides, however, is complicated by the simultaneous release of elements other than barium and strontium which are given off while the coating material is being decomposed. The photoelectric threshold shifts to longer wave-lengths as the applied field is increased, in a manner similar to that observed in the case of adsorbed alkali films. A preliminary study of thermionic properties of the coating shows that both A and ϕ decrease in value during activation.

Results obtained in the present study tend to confirm the theory that lack of saturation observed in photoelectric emission at room temperature, and in thermionic currents obtained at low cathode heating, is due to a decrease in work function with increase of accelerating potential. This contention is supported by the satisfactory agreement found between values of zero field thresholds obtained from the ν_0 vs $E^{1/2}$ plots, and those independently calculated from the observed variation of emission with applied field. For this calculation use was made of an equation recently developed by Houston for the dependence of photoelectric current per unit of radiant energy upon the frequency of incident light and the effective threshold. From the log i vs $E^{1/2}$ plots of the thermionic emission it is apparent that the applied field causes a smaller change in thermionic work function the higher the temperature.

Measurements at low temperatures of the thermionic currents from one cathode indicate good agreement between the zero field work function and the corresponding photoelectric value obtained from the long wave limits. This evidence, as well as the close agreement between the observed photoelectric work functions at various activations and the thermionic work functions for similar coatings obtained by other investigators, indicates that in both types of currents the electrons are emitted from areas of low work function which exist in the outermost surface layers of the oxide, rather than from activated layers on the surface of the core metal.

The writer takes this opportunity to express his appreciation to the Grigsby-Grunow Company of Chicago who financed this investigation, and for whom the work was carried out. He also wishes to acknowledge his indebtedness to Mr. John Hessel, who assisted in the work, and to Professor N. H. Williams, under whose supervision the investigation was conducted.

SOME PHOTOELECTRIC PROPERTIES OF MERCURY FILMS

By Duane Roller, W. H. Jordan and C. S. Woodward
Department of Physics, University of Oklahoma

(Received June 17, 1931)

Abstract

Films of very pure mercury were deposited slowly in a high vacuum on an oxidized iron plate maintained at liquid air temperature. As each film increased in thickness, the photoelectric current excited by each of the mercury arc lines 2537A, 2653A and 2700A increased from zero to a maximum value and then decreased to a final constant value. In each case the threshold wave-length at the time of maximum sensitivity was *ca.* 2750A. Its final value, that for a thick layer of mercury, was 2730 ± 15A; this did not change even when the mercury was allowed to melt, thus confirming a previous conclusion that the theshold wave-lengths for solid and liquid mercury are the same. There was no indication of a large shift in threshold wave-length at any time during the formation of the films.

THE photoelectric properties of thin films of various metals have been the subject of study for two decades[1] but determinations of the photoelectric threshold wave-lengths of films of atomic dimensions deposited slowly in a high vacuum are comparatively recent and have been confined largely to the alkali metals.[2,3,4] The characteristic feature of such an alkali metal film is that as it accumulates, the photoelectric threshold wave-length moves from the blue end of the spectrum toward the red, reaches an extreme value which for the majority of the alkali metals is in the infrared, and then recedes again to the final value characteristic of the metal in bulk.

In the present work the object has been to observe the behavior of the photoelectric current and threshold wave-length for films of mercury slowly deposited on iron in a high vacuum. Most of the photoelectric work with mercury has been confined to the liquid[5] and solid[6,7] in bulk, an exception being the work of McLennan, Hunter and McLeod[8] on the photoelectric effect of metals at the transition temperatures where they exhibit the property of superconductivity. Although the work with mercury was finally abandoned because of the unsuitableness of mercury films for the purpose of the investigation, preliminary experiments showed that the total photoelectric current from mercury deposited on glass was greater with a thin film than with a

[1] Gudden, Lichtelektrische Erscheinungen, Julius Springer (1928), Chap. 5, is perhaps the best recent summary of this work.

[2] Ives, Astrophys. J. **60,** 209 (1924).

[3] Ives and Olpin, Phys. Rev. **34,** 117 (1929).

[4] Campbell, Phil. Mag. **6,** 633 (1928); **8,** 557 (1929).

[5] Kazda, Phys. Rev. **26,** 643 (1925); Dunn, Phys. Rev. **29,** 693 (1927); Hales, Phys. Rev. **32,** 950 (1928); Roller, Phys. Rev. **32,** 323 (1928).

[6] Grutzmann, Ann. d. Physik **1,** 49 (1929).

[7] Roller, Phys. Rev. **36,** 738 (1920).

[8] McLennan, Hunter and McLeod, Roy. Soc. Canada, Trans. **24,** Sec. 3, 3 (1930).

thick one. Monochromatic radiation was not used in this work and no attempt was made to determine threshold wave-lengths.

Apparatus

The photoelectric cell was a Pyrex glass tube 3.7 cm in diameter, to the upper end of which was sealed a graded quartz-Pyrex seal containing a quartz window and to the lower end a plane Pyrex plate which formed the bottom of the cell (Fig. 1). In contact with the latter was a 3.3 cm disk of oxidized Swedish wrought iron upon which the film of mercury was allowed to deposit. This plate was maintained at 30 volts negative to ground, a potential found to be sufficient for producing a saturated photoelectric current with this cell. The anode consisted of a network of fine tungsten wire supported on a horizontal loop of 0.8 mm tungsten wire, an opening in the network being provided for illumination of the cathode. The anode was not in contact with any part of the cell except at the sealing-in point. The cell was shielded electro-

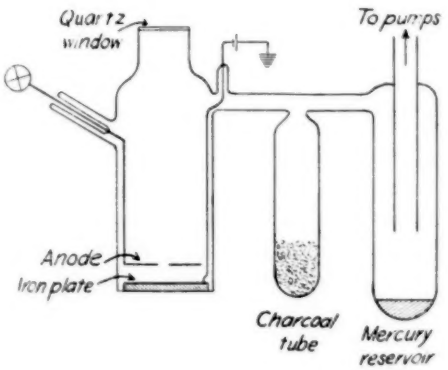

Fig. 1. Diagram of photoelectric cell.

statically by a coat of tin foil on the outside walls. The exhaust tube of the cell, to which was attached a liquid air tube containing cocoanut charcoal, was connected through a reservoir for mercury, a second liquid air trap and a mercury "cut-off" to a two-stage water-cooled mercury diffusion pump backed by a Cenco Hyvac fore-pump. The vacuum system included a McLeod gauge and a still for repeated distillation of the mercury in high vacuum. The usual precautions were taken to exclude wax and grease vapors. There was one stopcock, next to the fore-pump, but air was never admitted to the system through it.

The source of radiation was a General Electric Vapor Lamp Company horizontal-type 110-volt d.c. quartz mercury arc, enclosed in an asbestos-board housing and operated at 65 volts and 3.7 amperes. This was used in connection with a Leiss quartz monochromator and a pair of quartz lenses which formed an image of the slit 1 cm in length on the cathode of the cell. Intensity measurements of the radiation were made by means of a Burt vacuum thermocouple connected to a Leeds and Northrup high-sensitivity D'Arsonval galvanometer. Photoelectric currents were measured by a Dole-

zalek electrometer, the rate-of-charge method being used. The sensitivity of the electrometer was 2000 mm per volt at 3 m scale distance.

The foregoing description applies to the apparatus in its final form, as it was designed and completely reconstructed after extensive preliminary experiments. In the original apparatus, the metal surface in the cell, on which the mercury films were deposited, consisted of a horizontal iron disk 2.9 cm in diameter, mounted on a vertical tungsten rod sealed through the bottom of the cell. To the lower end of this rod was attached a small aluminum cylinder which could be immersed in liquid air when it was desired to cool the cathode. It was found, however, that a cathode of this type could not be cooled uniformly and that its temperature, when it was cooled, was below that of any other part of the cell, thus increasing the chance of contamination collecting on the deposited mercury. The original apparatus did not include a charcoal tube and all the preliminary observations were made with the cell attached to the pumps.

Procedure and Results

In the work with the improved apparatus, when the vacuum was as good as could be read on the McLeod gauge, the cell, charcoal tube and empty mercury reservoir were baked in ovens for 170 hours at 450, 550 and 550 degrees C, respectively, and the remainder of the glass system was heated with a torch. The highly-purified mercury[9] contained in the still was in the meantime distilled repeatedly in the high vacuum to remove occluded gases and then, with the temperature of the charcoal tube lowered to 350°C, some of this mercury was made to collect in the reservoir near the cell. The cell, charcoal tube, and reservoir were then sealed off as a unit from the remainder of the apparatus.

With the charcoal tube already in liquid air, the mercury in the reservoir was frozen by means of liquid air in order to prevent mercury from distilling over into the cell prematurely. The photoelectric cell was then immersed in liquid air up to a point on the cell walls about 2 cm above the surface of the iron cathode. As soon as the electrometer became steady, which usually required about five minutes, the liquid air was removed from the reservoir but not from the charcoal tube. About 30 minutes later the mercury depositing on the iron cathode began to exhibit a photoelectric sensitivity to the line 2537A and in approximately 110 minutes this sensitivity reached a maximum value.

Attempts had previously been made to make measurements without having a liquid air tube between the cell and reservoir and without having the mercury in the reservoir initially frozen; but the mercury then accumulated on the cathode so rapidly that the maximum sensitivity was reached within a few minutes after cooling the cell, at a time when the electrometer was still very erratic.

Measurements were made of the photoelectric current for each of the monochromator drum-settings 2537, 2653, 2700, 2752, 2804 and 2900A and

[9] Roller, J.O.S.A. **18**, 537 (1929).

for settings midway between these lines. The electrometer deflections for the drum-settings 2752, 2804 and an intermediate setting were always small and practically equal in magnitude. In the case of the lines 2537, 2653 and 2700A the results were like that shown in Fig. 2, in which the current is plotted as a function of the time elapsing after the removal of the liquid air from the reservoir.

Thresholds wave-lengths for various stages in the formation of the film were determined in the usual way by plotting the current per unit intensity of the exciting radiation as a function of wave-length. The values of these thresholds were found to be always between 2720A and 2750A, regardless of the thickness of the film. Thus they agree, within the experimental error, with the threshold values for mercury in bulk, namely 2735 ± 10A for the

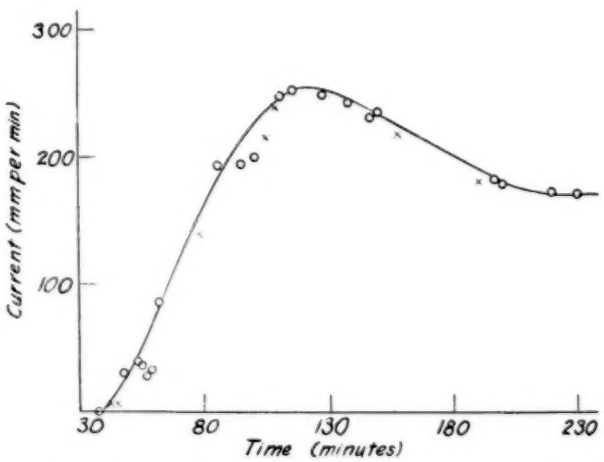

Fig. 2. Photoelectric current for the line 2653A vs. time of deposit.

liquid at room temperature[5] and 2750 ± 25 for the solid between $-190°$ C and the melting point.[7]

For any given film there was usually a progressive change in the threshold from shorter to longer wave-lengths as the time of deposit approached that corresponding to a maximum photoelectric current. At the latter time the threshold was always close to 2750A. Afterwards, while the photoelectric current was decreasing (Fig. 2), the threshold always returned to 2730 ± 15A. This final value, which was the threshold for a thick layer of mercury, did not change even when the mercury was made to melt by removing the liquid air from the cell. This confirms a previous conclusion[7] that the thresholds for solid and liquid mercury are the same.

During all of this work there was very little evidence of effects that could be attributed to contamination. Of the various contaminating substances that were likely to have been present in the cell, oxygen is believed to be the only one that will alter the long wave limit of mercury[10] and Poole[11] has con-

[10] Hales, Phys. Rev. **32,** 950 (1928).

[11] Poole, Thesis, California Institute of Technology (1927).

cluded that even oxygen is not effective unless it is in the presence of water vapor or has been exposed for some time to ultraviolet light. In view of this freedom of the cell from contamination, it would appear that the excursion of the threshold toward longer wave-lengths and the subsequent return to shorter wave-lengths as the film builds up is a true effect although it evidently is an exceedingly small one. In the case of very thin films of the alkali metals the thresholds are of the order of magnitude of 1000A farther toward the red end of the spectrum than are the thresholds for the metal in bulk.[2,3,4]

Experiments were also made with mercury condensed on the iron plate at a temperature above the freezing-point of mercury. The cell was cooled with ice and the deposit was accelerated by warming slightly the mercury reservoir with a small heating coil. At all times during the deposition of the mercury, the threshold wave-length was 2730 ± 10, which is practically the same as that for the liquid in bulk. The photoelectric current, on the other hand, increased steadily until it reached a maximum value but this was not followed by a decrease of the type observed with films deposited at the temperature of liquid air. At the end of an hour the deposit could be seen to consist of minute globules of mercury. Observations over a period of seven hours showed that these globules increased in number and slowly grew in size until they came into contact with one another and united. The unions were accompanied by slight decreases in the photoelectric current, probably due to decreases in the area of photoelectrically active metal exposed to the radiation.

In previous experiments made by one of us,[7] it was found that the photoelectric sensitivity of solid mercury in bulk was always higher than that of the liquid and this was attributed to a change in the photoelectric efficiency with change of state, due possibly to a change in the optical reflectivity. Recent experiments in this laboratory by W. Webb[12] show that when mercury is alternately frozen and melted in vacuum in such a way as to form a specular surface and under conditions unfavorable for the condensation of mercury vapor on the solid surface, then the monochromatic reflectivities for the solid and the liquid are the same for all the strong lines in the spectral region 4558–2537A. Ordinarily, however, frozen mercury presents an irregular surface that has the appearance of being a better absorber of radiation than the liquid. Whether this apparent increase in the "blackness" of the surface would account for the higher efficiency of the solid or whether there is also a change in the quantum equivalent of mercury with freezing would be difficult to determine.

[12] Not yet published.

THE EFFECT OF ADSORBED K^+ IONS ON THE PHOTOELECTRIC THRESHOLD OF IRON

By A. Keith Brewer

Fertilizer and Fixed Nitrogen Investigations, Bureau of Chemistry and Soils, Washington, D. C.

(Received May 26, 1931)

Abstract

The photoelectric emissivity of a pure iron filament, which has just previously been used as a cathode for K^+ ions, is increased directly proportional to the positive ion current, for all surfaces where the computed fraction of the surface covered is $\theta \leqq 0.03$. For larger values of θ the emissivity for λ3022 and λ3132 increases rapidly with θ while λ2804 remains proportional to θ until the fraction of the iron covered with potassium exceeds 0.08. The solution of potassium in the iron beginning above $\theta \leqq 0.03$, as well as the vaporization of potassium by the ion bombardment prevent the formation of a surface for which θ exceeds 0.10. The data have been interpreted as indicating that for $\theta \leqq 0.03$ every K^+ ion striking the iron remains on the surface as an ion, while for larger values of θ both potassium atoms and ions are present. The increase in the photoelectric current is due both to the lowering of the work function by the presence of the positive ions and to the emissivity from the adsorbed atoms.

A STUDY of the photoelectric properties of several ammonia catalysts[1] which have been used as a source of positive ions[2] has shown that it is not possible to build up anything comparable to a monomolecular layer of potassium on the surface. The threshold for most catalysts lies below 3600A, while the maximum long wave-length limit ever obtained showed a just detectable emission for λ4359. The photoelectric properties of platinum plated glass filaments[3] in which potassion ions were electrolyzed through the glass into platinum were similar in nature in that it was never possible more than just to detect emission at λ4047.

The present research was undertaken to obtain an estimation of fraction of the surface covered with potassium under conditions similar to those mentioned above, especially where potassium was deposited on the surface in the form of ions. The method employed was to study the shift in the photoelectric threshold when a known quantity of K^+ ions, as given by a measured positive ion current, was deposited on a pure iron surface.

Apparatus

The apparatus is illustrated in Fig. 1. It is essentially the same as that described in the previous papers.

[1] A. K. Brewer, J. Am. Chem. Soc. **53,** 74 (1931).
[2] C. H. Kunsman, J. Franklin Inst. **204,** 635 (1927).
[3] A. K. Brewer, Phys. Rev. **35,** 1360 (1930).

The iron filament studied was 10 cm long and 3.0 mm wide. The K^+ ion emitter was a platinum wire coated with catalyst 922 containing 0.26 percent K_2O. The filament was placed edgewise to the emitter, and with its surface perpendicular to the path of the ultraviolet light.

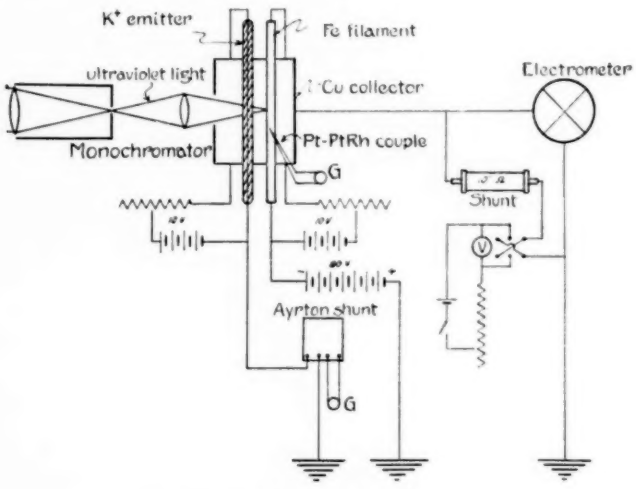

Fig. 1. Diagram of apparatus.

Method of Procedure

The iron filament was outgassed at 800°C until upon being cooled it showed a just detectable emission for λ2536, threshold being about 2575A. The potassium was deposited in the form of positive ions from the emitter, the amount of potassium being determined from the magnitude of the ion current and the time of flowing. The photoelectric emission from the filament was then read as quickly as possible. The first reading was usually taken in 30 seconds after the positive ion current was turned off; readings were taken thereafter at regular intervals until the emissivity became constant.

The emitter and the collector were maintained at zero potential at all times. The null method was used for the electrometer, the voltage necessary to be applied to the shunt to keep the electrometer at zero being read.

After the threshold had been determined the filament was glowed until the long wave-length limit again returned to 2575A. For small deposits of potassium this required about 10 minutes at 800°, but for the larger deposits it required from 30 to 40 minutes. The time could be cut in half by placing a positive potential on the filament.

Results

In using a method of this type it was first necessary to determine the amount of potassium that passed from the emitter to the filament in the form of neutral atoms. This was accomplished by heating the emitter to the highest temperatures used for a period of 10 minutes with +45 volts on the filament. The increase in the photoelectric emissivity of the iron after this treat-

ment was less than 1 percent of that which would have been observed had positive ions been drawn to the filament. The distillation of neutral atoms from the emitter to the filament, therefore, can be neglected.

The effect of the accelerating potential on the adsorption of positive ions was tested by running a known positive ion current for a given period of time with voltage on the filament varying from -22.5 to -270. The photoelectric emissivity for λ2653 was measured after each deposition of ions. No appreciable difference could be detected for voltages under 225 volts, although the ions deposited at 270 volts appeared to give a slightly lower emissivity.

The photoelectric emissivity from the potassium on iron surfaces for λ-2653 was measured at different voltages up to 225 volts. The voltage-current curve did not show complete saturation; a 30 percent uniform increase was

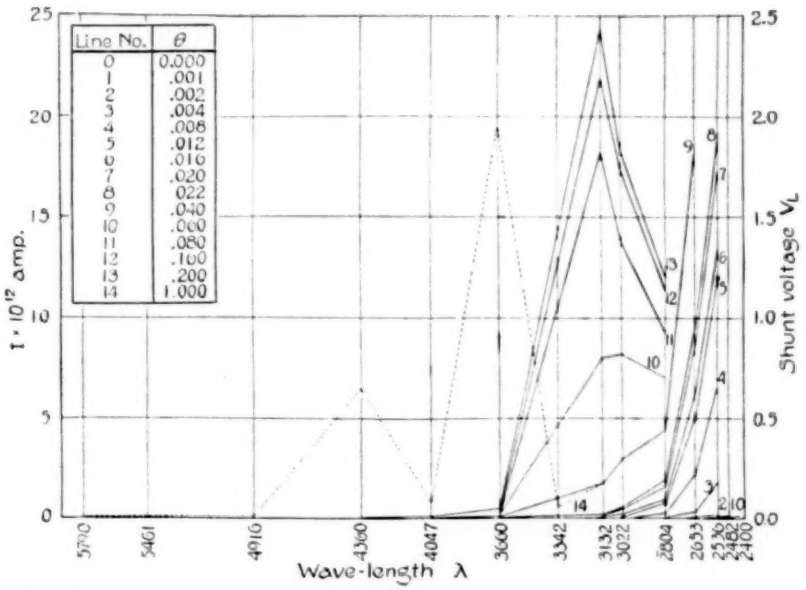

Fig. 2. The observed photoelectric current at different light frequencies for various fractions of the iron surface covered with potassium.

observed between 22.5 and 135 volts; the surface was 2 percent covered with K^+ ions.

The effect of the positive ion density on the adsorption of potassium was determined by varying both the size and the duration of the positive ion current. Identical values, to within the limits of experimental error, were obtained when the current was increased ten fold and the time cut to a tenth. Thus the rate of deposition of ions had no appreciable effect on the photoelectric emissivity.

The photoelectric emissivity for the different surfaces formed by the deposition of varying amounts of potassium ions is shown in Fig. 2. In these experiments the potential of the filament was maintained at -90 volts with respect to the collector and the emitter. The temperature of the filament was

kept at 150°C. For the sake of clearness the emissivity for the different mercury lines is plotted directly, irrespective of the intensity of the line, the observed points for a given surface being connected by straight lines to show continuity.

The column θ gives the fraction of the iron surfaces covered by potassium as computed from the positive ion current. The diameter of the K^+ ion is taken as 1.33×10^{-8} cm. Close packing of the ions is not assumed.

The results, for the most part, were very reproducible, especially for the low values of θ. This is illustrated in line 5, in which two sets of points are shown. For values of θ above 0.1, some fluctuations were observed.

A distinct difference was noted in the effect of aging on the deposits above and below $\theta = 0.04$. Below this point the emissivity increased for 5 or 10 minutes, after which it remained constant for long periods of time. For the higher values the opposite effect was observed, namely, the emissivity decreased with time, finally reaching a constant value; this is illustrated by line 13, in which the emissivity for λ2804 dropped the amount shown in 12 minutes. For ion deposits in which the computed value for θ was above 0.2, the drop in emissivity was too rapid to be measured for several minutes after turning off the positive ion current.

The fatiguing effect for the heavier deposits made it seemingly impossible to build up anything like a molecular layer on the surface. In fact a quantity of ions that should have formed two molecular layers showed but slightly greater emissivity than did a quantity capable of forming only 0.2 of a layer.

The emissivity showed an increase with temperature for all values of θ, the effect being very pronounced for those deposits showing a fatigue with time. To illustrate, a filament similar to line 10 fatigued 20 percent in 40 minutes at room temperature. When the temperature was raised to 150°C the emissivity was but 15 percent under the original, at 260° it was 3 percent under, and at 320° it was about 10 percent above. At this temperature a decreased emissivity due to evaporation from the surface set in, the emissivity decreasing slowly with time. At 400°C the photo-current fell to 40 percent of the original value in 8 minutes. The effect of temperature on the emissivity decreased with the amount of potassium on the surface; line 5, for instance, showed only a small increase below the temperature at which evaporation became appreciable.

The emissivity of pure potassium, for matter of comparison, is shown by the dotted lines. The current ordinate is 500 times that for the potassium on iron surfaces. The pure potassium surface was prepared by vaporizing metallic potassium onto a silver plate until the surface was completely covered. The tube was made entirely of Pyrex, no quartz window being used.

The long wave-length limit found for potassium was in the neighborhood of 6000A, while the maximum obtainable from the deposition of K^+ ions was about 4400A. The difference in emissivity of the two surfaces for the longer wave-length is very pronounced. This may be seen in Fig. 2 for λ3660 and for λ4360, where the emissivity for potassium is some 20,000 times that for the potassium on iron surfaces.

The effect of the fraction of the surface covered (θ) on the emissivity is shown in Fig. 3.

It will be observed that for the Hg lines λ2804, 2653, and 2536, the emissivity is proportional to the computed fraction of the surface covered under 0.08 of a molecular layer. Above this point the emissivity falls off rapidly, reaching a constant value for a surface about 0.2 covered. For the lines λ3022 and 3132, however, the emissivity increase is abnormally large. The emissivity for λ3660 was so weak at all times that the shape of the curve could not be determined.

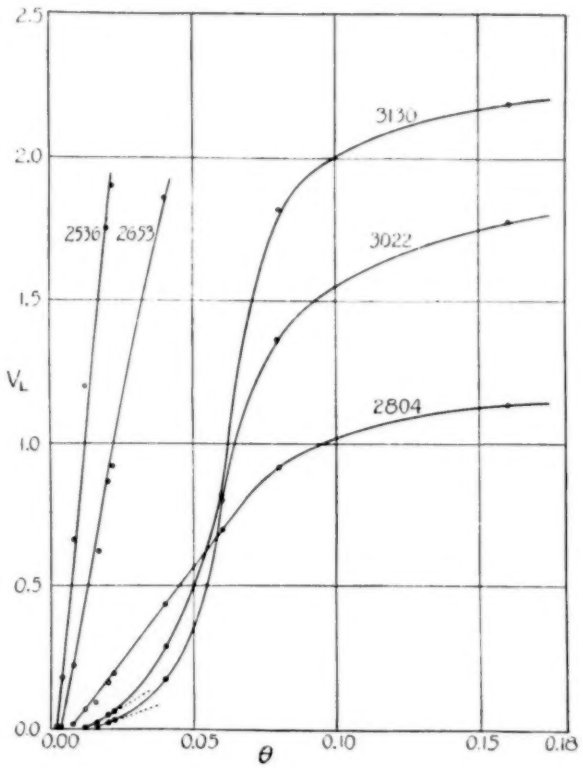

Fig. 3. The effect of the fraction of the surface covered with potassium on the photoelectric emissivity for various light frequencies. V_L = shunt voltage.

Experiments similar to those described above were made with platinum and with nickel as the filament metal. The results obtained were very unsatisfactory, except in so far as they showed clearly why so much difficulty has been experienced in the past in obtaining the work function of platinum.

Platinum was exceptionally bad in that it was exceedingly difficult to get the filament to show no shift in threshold upon further heating. After the K^+ ions were deposited on a well glowed filament the photoelectric emissivity decreased so rapidly with time that only approximate readings could be taken. Heating for hours at 1000°C failed to restore the threshold to its original value.

The results obtained with nickel were similar to those of platinum only much less pronounced. For small values of θ nickel checked iron fairly well, although it was much more difficult to remove the potassium from the surface by heat. The threshold could not be measured for the heavy deposits due to the fatiguing effect with time.

Discussion of Results

The effect of sodium vapor on the photoelectric threshold of platinum has been investigated by Ives.[4] The results show that the long wave-length limit shifts towards red as sodium is deposited on the platinum, passes through a maximum, and finally becomes constant at the threshold for pure sodium.

Becker[5] has shown that for small quantities of barium adsorbed on tungsten the ratio of adions to adatoms is large, but decreases with the amount of barium adsorbed until for a monomolecular layer only about one out of ten atoms is ionized.

These results presented in Figs. 2 and 3 are similar to those obtained by Ives in that the threshold is shifted toward the red as the amount of potassium on the surface is increased. Further, they are in accord with the postulates of Becker in that both potassium atoms and ions appear to exist on the surface.

It will be recalled that for values of $\theta \leqq 0.03$ the emissivity increased with time to a constant final value, after the positive ion current was turned off. This is evidently due to a migration of K^+ ions over the surface until a uniform distribution is established. The fact that the emissivity reached a constant value indicates that for values of θ under 0.03 the potassium is not lost to the surface either by evaporation or solution.

Line 9 of Fig. 2 is the first to show a decrease in emissivity with time; likewise it is the first to show an abnormal emissivity for λ3022 and 3132. The most probable interpretation of these facts is that for $\theta \gtreqless 0.04$ part of the K^+ ions striking the surface go over to neutral atoms in which condition they are soluble in the iron. The decrease in emissivity is not due to the evaporation of potassium since the original threshold can be restored by raising the temperature of the filament.

The effect of K^+ adions on the emissivity is shown by Fig. 3 to be proportional to the positive ion current. This indicates that for $\theta \leqq 0.03$, every ion striking the surface sticks, and that the increase in emissivity is due solely to the lowering of the work function by the adsorbed ions.

The enhancement in the emissivity for λ3022 and 3132 shown by lines 9 to 13 in Fig. 2 where $\theta \gtreqless 0.04$ must be due to some cause different from that mentioned above. The simplest interpretation of these results is that above $\theta \gtreqless 0.04$ the increased emissivity is due not only to a lowering of the work function by the adions, but also to a photoelectric emission from the neutral potassium atoms adsorbed on the surface.

[4] Ives, Astrophys. J. **60,** 209 (1920).

[5] J. A. Becker, Proc. Am. Electrochem. Soc. **55,** 153 (1929).

The failure to build up anything like a monomolecular layer of potassium by the deposition of K^+ ions is due to several causes. The dissolving of the adatoms in the iron has been mentioned. An equally important cause appears to be that while a bombarding K^+ ion hasn't sufficient energy to remove an adion, it is capable of removing an adatom. A state of equilibrium appears to be established for $\theta \gtrsim 0.08$, wherein neutral atoms are removed from the filament as fast as ions arrive.

The work function for the various ammonia catalysts is usually far above that of an iron surface 0.03 covered with potassium. It follows, therefore, that under ordinary operating conditions all potassium at the surface is ionized. The presence of potassium ions and the absence of potassium atoms is doubtless the determining factor in making these substances such excellent positive ion emitters.

The writer is especially indebted to Dr. C. H. Kunsman for his interest, and to Mr. R. A. Nelson and Mr. P. D. Kueck for their cooperation and assistance.

PHOTOELECTRIC PROPERTIES OF ZINC SINGLE CRYSTALS

By J. H. Dillon
Department of Physics, University of Wisconsin

(Received June 17, 1931)

Abstract

An experiment is described in which the photoelectric properties of outgassed single crystals of zinc were studied. After treating the emitting surfaces of a crystal with ultraviolet light and thermally evaporating some of the zinc, a stable condition was reached. In this stable condition a difference in the long wave limits of the polycrystalline surface and cleft 0001 face of approximately 260A was observed. The results are discussed with regard to possible sources of contamination and the presence of occluded gas layers.

THERE have been only a few attempts to study the photoelectric characteristics of single crystals. Of these, only that of Linder[1] merits serious consideration. He investigated the photoelectric emission from an uncleft single crystal rod of zinc. By exposing the crystal to the total radiation of a mercury arc with various orientations of the hexagonal axis with respect to the exciting light beam, he found a maximum photoelectric current with the light beam parallel to the hexagonal axis, i.e., normal to the basal (0001) plane. He further showed that the optical reflecting power of the crystal surface was sensibly uniform and hence that the observed variations in emission were due to a real dependence of the photoelectric properties upon crystal orientation. However, he did not determine the long wave limits corresponding to the various emission values, and his vacuum conditions were not of the best.

Recent photoelectric experiments have demonstrated that, with high melting point metals, reproducible results and stable characteristics can best be obtained by subjecting the metal to an extended and vigorous heat treatment under very good vacuum conditions. It is seen immediately that such a program, in the case of a single crystal of a low melting-point metal such as zinc, is possible only in a very limited sense. Furthermore, single crystals must be handled with extreme care to prevent mechanical distortion, and their growth in an outgassed state introduces difficulties not encountered in the study of polycrystalline metals. The immediate purpose of this work, then, was to outgas a crystal of zinc as thoroughly as the above limitations permit and to study its photoelectric properties by means of monochromatic light under good vacuum conditions. However, the experiment was, in a sense, more of the nature of a study of the possibilities of photoelectric work with low melting-point crystals.

[1] Linder, Phys. Rev. **30,** 349 (1927).

Growth of the Crystals

Whereas Linder used crystals made in air by the Bridgman[2] method, for this experiment a modification of the Bridgman method, previously described,[3] was developed whereby the crystals were thoroughly outgassed and grown in good vacuum. The outgassed crystals could then remain in the evacuated and sealed-off Pyrex molds until such time as they were needed.

Photoelectric Apparatus

The photoelectric tube (see Fig. 1) was of Pyrex and was connected to the vacuum system by means of a large ground joint *J* used with a slight amount of sealing wax at *p* extending down into the joint in a very thin film for only about 1 cm. This method of sealing should decrease the rate of diffusion of wax vapor very considerably. The presence of this joint was not desirable

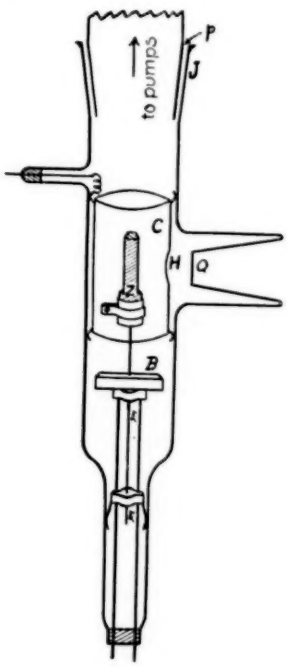

Fig. 1. Photoelectric tube.

but its use was quite necessary in order to permit transfer of the crystal from the evacuated mold to the tube with only a short exposure to the air. Light from the monochromator entered through the conically reentrant quartz window *Q*, through a hole *H* in the nickel collecting cylinder *C* which could be closed with a magnetic shutter, and thence was focussed upon the face of the zinc crystal *z*. The crystal was lightly clamped at its lower end and could be rotated about a vertical axis in the metal bearings *E* by means of a magnet operating on the soft iron bar *B*.

[2] Bridgman, Proc. Am. Acad. Arts and Sciences, **60**, 305 (1925).
[3] Dillon, Rev. Sci. Inst. **1**, 36 (1930).

The vacuum system was of Pyrex and consisted of a liquid air trap, a mercury diffusion pump backed by a Hyvac oil pump, and a McLeod gauge. The pumps were kept in operation continuously throughout the entire experiment. During this time the pressures certainly never rose above 10^{-7} mm of mercury and were considerably lower in the major part of the work.

The photoelectric currents were measured by a Compton electrometer, the quadrants of which were shunted across a high resistance of 5×10^{10} ohms. The high resistance was made by dissolving cupric oxide in soft glass and was found to be very steady after its initial fluctuation, which occupied about a week, had ceased. The electrometer and the necessary switches were inclosed in a metal shielding box through which a current of air, dried by passage through calcium chloride and a liquid air trap, could be blown. With this drying arrangement, it was possible to use the electrometer at sensitivities of 1000 to 10,000 mm per volt on the most humid summer days.

The optical system consisted of a Cooper-Hewitt quartz mercury arc operated with 80 volts across the arc, a Bausch and Lomb single monochromator, and auxiliary quartz lenses. The monochromator was carefully calibrated and studied with the purpose of learning what slit widths could be safely used. Fortunately, the long wave limit of the zinc specimens was found to lie in the region 3200A to 3700A where the mercury lines are widely spaced so that slits of width 0.3 mm which were used gave the necessary purity. Both the photoelectric current and the current from the pile were found to fall practically to zero at monochromator settings between the mercury lines 3650A, 3341A, and 3132A. This eliminated the possibility of any appreciable influence of stray light upon the long wave limit determinations.

The intensity of the light incident on the crystal was measured by a 13-junction Pt-Te vacuum thermopile connected to a Kipp Zc galvanometer. The pile was mounted directly before the exit slit of the monochromator and could be moved in and out of the light path to permit all of the light to fall either upon the crystal or upon the pile elements. The construction of the monochromator was such that the pile elements could be no closer than 12 mm to the exit slit. Hence, the receiver was large (13mm$\times$3mm) so as to intercept all of the light from the divergent cone. The variable magnetic shunt of the galvanometer was adjusted so that the critical damping resistance was equal to the resistance of the pile (44 ohms). Vacuum was maintained in the pile by means of a Hyvac oil pump giving a pressure of 10^{-3} mm of mercury.

Procedure

Before inserting the crystal for observation, the photoelectric tube, completely assembled except that the crystal was absent, was evacuated to "sticking" as indicated by the McLeod gauge which was capable of indicating pressures as low as 2×10^{-7} mm of mercury. The tube was then baked at a temperature of 400°C until the gauge indicated that the pressure was as low as before starting the furnace. The furnace was then removed and air admitted to the system. A crystal was next removed from its evacuated mold and cleft at liquid air temperature to minimize distortion. Zinc cleaves readily only

along the basal plane, which was usually nearly parallel to the axis of the cylindrical mold. Hence, only one crystal plane was available for observation. However, by taking x-ray powder spectrograms[4] it was found that a filed surface is essentially polycrystalline. Thus in addition to cleaving along the basal plane, another face parallel to it was filed at liquid air temperature so that the photoelectric properties of the basal plane could be compared with those of the polycrystalline surface. Immediately after cleaving and filing, the crystal was clamped into place in the photoelectric tube which was sealed on the system and evacuated. The total time during which the crystal was exposed to the air was usually about 20 minutes and never exceeded 40 minutes. Thus it is reasonable to suppose that very little gas would return to the volume of the metal, and that only a surface layer would result.

In an effort to remove this surface layer of gas, two methods of treatment were applied. Winch[5] and others[6] have found that a metal surface can be at least partially outgassed by irradiation in vacuum with intense ultraviolet light. This method which may be termed "ultraviolet outgassing," when applied to the zinc surfaces, produced very marked changes as will be shown later. In addition, the crystals were baked at temperatures at which a large amount of the zinc evaporated.

Results

Six zinc crystals were studied in the course of this experiment. Inasmuch, however, as none of the results from any of the crystals were discordant, only crystal #5, which was subjected to a greater variety of conditions than any of the others, will be discussed in detail. When observations on crystal #5 were first taken soon after its insertion in the tube, the photocurrents from both the polycrystal face and the cleft 0001 (Bravais indices) plane were found to decrease rapidly with time of exposure to the exciting light. This state in which the photocurrents decreased with time of exposure was never encountered with any of the other crystals. Apparently, upon treatment with the full arc, this was soon supplanted by the usual state where the photocurrents increased with time of exposure, for it was never again observed. Since, in this initial state, no dependable readings could be taken, an "ultraviolet outgassing process" was immediately begun. This was accomplished by directing the total radiation of a Cooper-Hewitt quartz mercury arc upon the face of the crystal. This process was continued for roughly 150 hours, during which time the photocurrents from both the polycrystal surface and the 0001 face increased very rapidly at first, and then more slowly approached limiting values above which further treatment caused no change. At this stage of the experiment "fatigue tests" were made at daily intervals for a week. It was found impossible to change the amount or rate of fatigue (diminution of photocurrent with time with light off) by further treatment with ultraviolet. After cutting off the light of the full arc, the photocurrents decreased quite

[4] Hanawalt, Ph. D. Thesis, University of Wisconsin (1929).
[5] Winch, Phys. Rev. **36,** 601 (1930), **38,** 321 (1931).
[6] Millikan, Phys. Rev. **29,** 85 (1909).

rapidly at first and then more slowly approached a constant and reproducible "fatigued" value (60 percent of initial value) which was attained in about eight hours. A relatively short time of exposure, 20 minutes, was required to restore the fatigued surface to the condition where the photocurrent had the maximum value. Long wave limit determinations were made for both the 0001 and the polycrystal face in the two states, the fatigued state (see Fig. 2, curves Ia and Ib) and the unstable state (see curves IIa and IIb). The long wave limit was found to be approximately the same for the two faces in both states and was roughly equal to 3400A.

After it was found that no further change in the characteristics could be produced by exposure to ultraviolet, the tube was enclosed in a furnace whose temperature was raised very slowly so as to maintain continuously a "sticking vacuum." After the furnace had been maintained for 36 hours at 260°C,

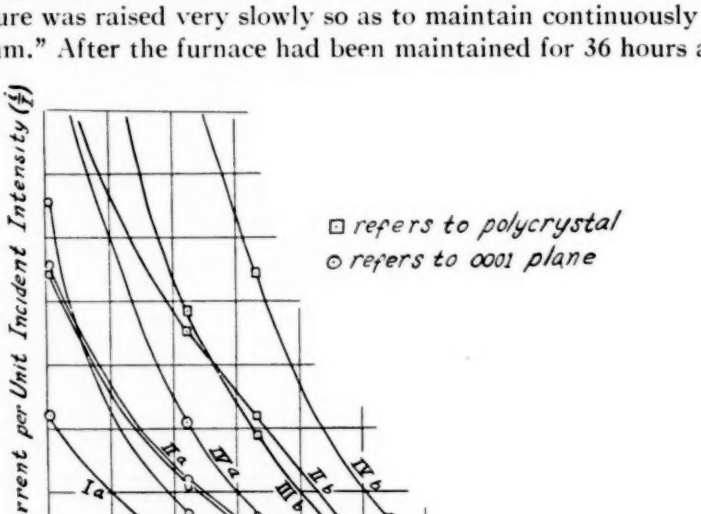

Fig. 2. Curves for crystal No. 5.

at which temperature a large amount of zinc was evaporated from the crystal, the furnace was removed and a long wave limit test was made. This revealed that the photocurrents from both faces had increased to a steady value as indicated by curves IIIa and IIIb, but the long wave limit remained at its former value for both faces. It was now found, and this is the most striking result, that exposure to ultraviolet light after distillation from the surface not only increased the photo-currents still farther but resulted in changes in λ_0 to the values 3460A for the 0001 face and 3720A for the polycrystal as given by curves IVa and IVb. Fatigue tests taken at this point showed less than 2 per cent fatigue in a period of 4 hours for both faces. Fig. 3 gives curves IVa and IVb plotted logarithmically in an attempt to determine λ_0 more accurately.

It was suggested by Dr. Roebuck that possibly the difference between the 0001 and polycrystalline faces which appeared after distillation and ultra-

violet treatment was due to the contamination of the polycrystal face by the clean file used in producing it. To check this, a third face was prepared on crystal #6 by scraping with tungsten carbide, this being the hardest substance available which could be cleaned with acids. The scraped and filed surfaces

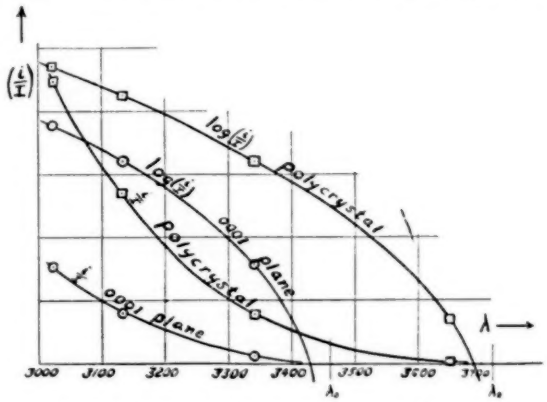

Fig. 3. Final stable state for crystal No. 5.

behaved in exactly the same way so that contamination from this source appears to be ruled out. In this case the final values of λ_0 were 3465A for the 0001 face and 3730A for the polycrystal surface.

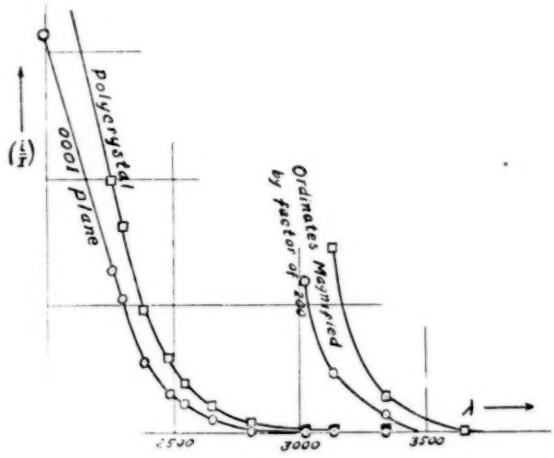

Fig. 4. Final stable state for crystal No. 6.

In addition to this direct study of λ_0, a number of curves were obtained over the entire range of wave-lengths (2000A–3800A) permitted by the monochromator. All of these curves were of the same general form as that of Fig. 4 and failed to show any kind of "selective" maximum.

Conclusions

At present no reliable value of λ_0 for zinc is to be found in the literature. Küstner,[7] Welch,[8] Lukirsky and Prilezaev,[9] Hamer,[10] Hennings,[11] and Rich-

ardson and Compton[12] have made determinations of λ_0 for zinc, but in no case were their experimental conditions good enough to warrant attaching much significance to the results. It is true that, in some cases[7, 8, 11, 12], the surface of the zinc was scraped or filed in fairly good vacuum, but no attempt was made to remove the gas from the volume of the metal. Hughes[13] determined λ_0 for zinc which had been freshly distilled in vacuum. However, he stated the pressure in the tube to be of the order of 5×10^{-4} mm, so, although his work seems superior to that of the others, it cannot be taken too seriously in the light of present day vacuum and outgassing requirements. The present experiment is, then, the first attempt to apply modern photoelectric technique to zinc in either single crystalline or polycrystalline form.

There is a possibility that the action of the intense ultraviolet light was not to outgas the metal surfaces but rather to accelerate a chemical reaction of the zinc with the residual gases in the system. The chemical compound thus formed might explain, then, the observed difference in long wave limits. However, it was observed in the case of crystal #3, which had never been exposed to intense ultraviolet light, that heating by radiation from a filament inserted in a side tube caused a large increase in the photocurrents. Crystal #5, after the first treatment with ultraviolet light, was exposed to the radiation of the filament at the same temperature for the same length of time and no measurable change in the photocurrents occurred. This would seem to indicate that the ultraviolet light actually removed gas from the surfaces.

The outgassing treatment in this experiment was, for reasons already given, less vigorous than that usually used for high melting-point polycrystals. Thus it may be argued that a really clean surface was never attained, but instead some stable intermediate state such as might exist with a monomolecular gas layer on the surface. At present, it seems impossible to refute this argument completely, although in the final state, the rate of fatigue was very small, which condition is commonly assumed to characterize a perfectly clean surface. However, the large difference in the long wave limits ($\Delta\lambda_0 = 260$Å) cannot be attributed entirely to the effect of ordinary gas layers. Of course, it is possible that the gas layers may be present on the crystal face in the form of a "gas lattice" which might have a different effect on the photoelectric properties than the layer formed on the polycrystalline surface. It seems, therefore, impossible to conclude whether the observed difference in the long wave limits for the 0001 plane and the polycrystal is due to a real dependence of the photoelectric work function upon crystal geometry or to the effect of a possible absorbed gas lattice which itself would depend on crystal structure. It is hoped that this experiment which, with its several

---

[7] Küstner, Ann. d. Physik **46,** 893 (1915).
[8] Welch, Phys. Rev. **32,** 657 (1928).
[9] Lukirsky and Prilezaev, Zeits. f. Physik **49,** 236 (1928).
[10] Hamer, Jour. Opt. Soc. Am. **9,** 251 (1924).
[11] Hennings, Phys. Rev. **4,** 228 (1914).
[12] Richardson and Compton, Phil. Mag. **24,** 575 (1912).
[13] Hughes, Phil. Trans. Roy. Soc. London **212,** 205 (1912).

limitations, nevertheless was performed as carefully as present photoelectric methods permit, will lead to further study which will give more definite information concerning the photoelectric properties of single crystals.

Quantitative comparison of these results with those of Linder seems a hopeless task, for his photoelectric emmission came from the facets or surfaces of the negative crystals, so that a given orientation of the crystal axis with respect to the exciting light beam in his experiment gives no assurance that the corresponding emission was due to the plane normal to the light beam.

R. H. Fowler[14] has developed a theory for the effect of temperature on the photoelectric sensitivity of a clean metal near the threshold. He gives a graphical method enabling the whole of the observed curves near the threshold for all temperatures to be used in determining the threshold itself thus avoiding an arbitrary extrapolation to zero current. Curves IVa and IVb were plotted in the reduced variables required by Fowler's scheme and an attempt was made to fit them to his theoretical curve. No satisfactory "fit" could be obtained and thus no conclusions could be drawn as to the true thresholds for the polycrystal and 0001 surfaces or zinc. It may be pointed out, that due to lack of data on the reflecting power of the 0001 plane of zinc, in the region 3000A–3800A, the curves IVa and IVb were not corrected for reflected light. However, the only available data on the reflecting power R of polycrystalline zinc[15] show a very slow variation of R with wave-length in this range. Hence, the lack of correlation with the theory must be due, for the most part, to the presence of some factor which is a function of frequency and which plays a more important role for zinc than for the several metals discussed in Fowler's paper.

I wish to express my appreciation of the many helpful suggestions given me by Professor C. E. Mendenhall, under whose direction this work was done, and of the assistance of Mr. C. F. DeVoe in the later stages of the experiment.

[14] Fowler, Phys. Rev., **38,** 45 (1931).
[15] Meier, Ann. d. Physik **31,** 1017 (1910).

THE FALL OF POTENTIAL IN THE INITIAL STAGES OF ELECTRICAL DISCHARGES

By J. C. Street and J. W. Beams
University of Virginia

(Received June 22, 1931)

Abstract

The fall of potential in the initial stages of condensed discharges through air, nitrogen, hydrogen and CO_2 has been studied as a function of the pressure. The experimental method consisted in measuring the magnitude and shape of the potential wave impressed upon two parallel, copper wires attached to the electrodes of the discharge. In every case the rate of potential fall was increased with increase of pressure. Over the pressure range studied (50 to 140 cm of mercury) the decrease of potential was slowest in CO_2 of the gases quantitatively studied. However, rough measurements showed the rate of fall to be very much slower in helium than in CO_2. In hydrogen a small overvoltage produced an increase in the rate of potential fall at all pressures. The results are shown to be in good agreement with Toepler's discharge law. A method is described by means of which it is possible to apply 5×10^5 volts/cm across a spark gap in air, hydrogen or nitrogen at atmospheric pressure at least 10^{-6} sec. without electrical breakdown. When such discharges once are initiated the potential falls much faster than for a static breakdown.

THE various types of electrical discharges through gases have been extensively studied in the past and remarkable progress has been made in explaining the numerous phenomena in terms of well recognized elementary processes.[1,2] However, practically all of the great mass of experimental data has been obtained in connection with discharges that had already reached a steady state and, therefore, gives little direct information about the initial stages of the discharge. This state of affairs results from the fact that in general the electrical breakdown takes place so quickly that proper apparatus with sufficient time resolving power has only within the last few years been devised. The factors, in the initial stages of the discharge, which remain to be experimentally investigated must obviously include the potential gradient in the discharge, the current density in the gas, the size and shape of the discharge together with the spectra emitted, all studied as functions of the time. Some progress has already been made in the study of the last three factors by means of Kerr cells[3,4,5] and rotating mirrors but a satisfactory direct way of measuring the actual electric field and current density throughout the discharge in such short times, does not exist, However, the cathode-ray oscil-

[1] J. J. Thomson, Conduction of Electricity through Gases, 2nd Ed. 1906; J. J. Thomson and G. P. Thomson, Conduction of Electrciity through Gases, 3rd Ed. 1928.

[2] Compton and Langmuir, Rev. Mod. Phys. **2,** 123, (1930); **3,** 190 (1931).

[3] Beams, Phys. Rev. **28,** 475 (1926); **35,** 24 (1930).

[4] Lawrence and Dunnington, Phys. Rev. **35,** 396 (1930).

[5] L. V. Hamos, Ann. d. Physik **7,** 875 (1930).

lograph[6,7] has been improved until it will give an approximation to the rate of change of potential across the discharge and, with a much less degree of precision, the rate of change of total current through the discharge. These data, though not yielding directly the electric field and current density, give valuable information from which it is possible to construct and roughly to test theories of electrical breakdown. The experimental arrangements in such cathode-ray experiments require a large amount of apparatus coupled with special technique and skill in operation. Further the oscillograph possesses inherently a certain finite capacity in its deflecting plates as well as inductance in the leads to them so that the results are often difficult to interpret. Several other methods[8,9,10] of getting the rate of fall of potential across the discharge have also been used with some success.

We have developed two comparatively simple methods of investigating the time required for the potential to fall in discharges at various pressures of the gas. The two methods supplement each other, the first giving the total length of time required for the potential across the discharge to fall to a steady value and the second giving the potential across the gap as a function of the

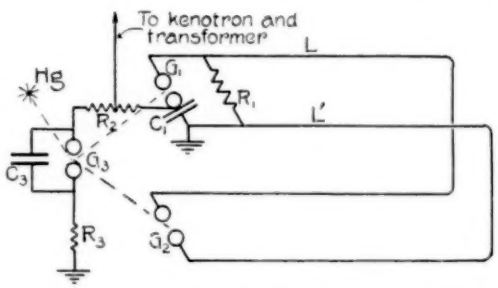

Fig. 1. Schematic diagram of apparatus used in the first experimental method.

time. Both methods are based upon the fact that a potential wave is impressed upon the lead wires during the breakdown. From a measure of the maximum potential attained between certain parts of the circuit the magnitude and shape of the potential wave could be calculated from circuital theory and thus the rate of fall of potential across the discharge secured. Somewhat similar methods have been used previously by Toepler[11] and Binder[8] but the present methods differ from theirs in some important essentials.

The first experimental arrangement is illustrated schematically in Fig. 1. The condenser C_1 of about 0.003 mf capacity, slowly charged by a transformer and kenotron, is the source of energy for the discharge to be studied at G_1. R_1 is a high resistance (about 10^5 ohms) which serves to prevent the line L from floating. The leads LL' are two straight parallel copper wires (No. 12,

[6] Dufur, Onde Elec. **2,** 19 (1923).

[7] Rogowski and Flegler, Arch. f. Elektrot. **15,** 207 (1925); Rogowski, Flegler and Tamm, Arch. f. Elektrot. **18,** 513 (1927); Beyerle, Arch. f. Elektrot. **25,** 267 (1931).

[8] See Binder, Wanderwellenvorgänge, Berlin, 1928.

[9] Lawrence and Beams, Phys. Rev. **32,** 483 (1929).

[10] Dunnington, Bul. Amer. Phys. Soc. **A2,** April 16, 1931.

[11] Toepler, Archiv. f. Elektrot. **14,** 305 (1925); **17,** 61 (1926); **18,** 549 (1927); **21,** 433 (1929).

25 cm apart). The gap G_2 (low capacity) is used as an indicator to measure the maximum potential across the ends of the wires. The condenser C_3 and gap G_3 are used in order to irradiate G_2 from a strong source of ultraviolet light, namely the discharge which occurs at G_3. For this arrangement the time lag of the indicating gap has been shown in this laboratory to be extremely short. G_1 and G_3 are set at the proper spacing in order that, when charged from the same system, they reach a breakdown field strength at the same time. Due to the irradiation from the mercury arc lamp, Hg, G_3 discharges first. G_1 (carefully shielded from Hg) is then intensely irradiated by G_3 and immediately discharges. As the breakdown in G_1 progresses, a potential wave, the shape of which is determined by the discharge characteristics of the gap, is impressed on leads LL'. (The distortion of this wave as it progresses along the wires can be computed from the known constants of the wires.) This wave travels along LL' at approximately the velocity of light until it reaches G_2 where its potential is progressively doubled at reflection. The maximum

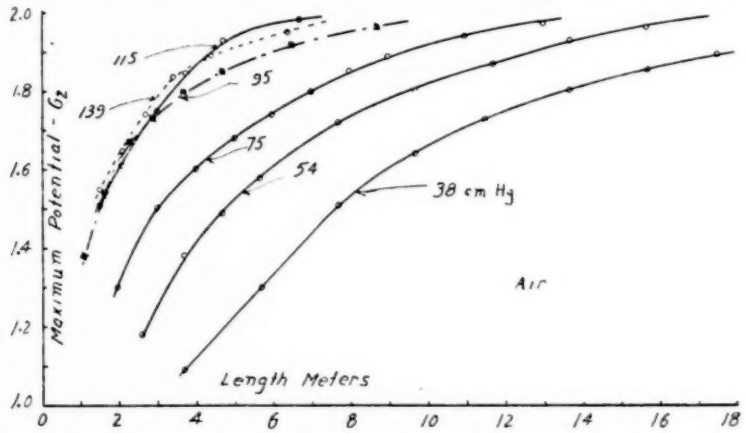

Fig. 2. Results obtained, with the first method, for air at various pressures. The maximum potential at G_2 plotted against the length of the leads LL'.

sparking width of G_2 (which is intensely irradiated from the bright spark G_3) serves as a measure of the maximum potential attained across the ends of the leads.

The curves, Fig. 2, show the values of the maximum potential at G_2 plotted against the length of LL' for various air pressures in G_1. The ordinates are reduced to a scale in which the breakdown potential of G_1 is taken as unity. When this scale is used it is found that the curves for different widths of G_1 (between 2 and 6 mm) are identical within experimental error if the air pressure surrounding G_1 is held constant.

The decrease in potential at G_2 as the leads are shortened may be qualitatively explained as follows. The reduction in maximum potential at G_2 is due to interference from the front of the wave which, after reflection there, returns to G_1, suffers a reverse reflection, and again reaches G_2 before the wave there has attained its maximum value. In order for this reversed wave to reduce the double value of the potential at the end, it is necessary that the time

length of the wave be greater than the time equivalent of twice the wire length. A careful analysis of the circuit shows that although it is possible to determine with precision the total length of the potential wave by this method, the actual potential-time curve cannot be obtained unless we know the law connecting the change of resistance in G_1 with time. The necessity for this assumption arises from the fact that the reflection coefficient at G_1 must depend upon its resistance which, in turn, is a function of the time. It will be noted from the curves that the total time required for the potential to fall to a steady value decreases with increasing pressure over the range studied. We will return to a discussion of Fig. 2 after first describing the second method.

The second method is shown in Fig. 3. The discharge at G_1 impresses an electric wave on the wires LL' in the same manner as before. It travels to the end which is closed by a heavy conductor P, suffers a reverse reflection, returns to G_1 where it is reversed again at reflection and the process repeats itself until the waves are damped out. The leads LL' were always greater

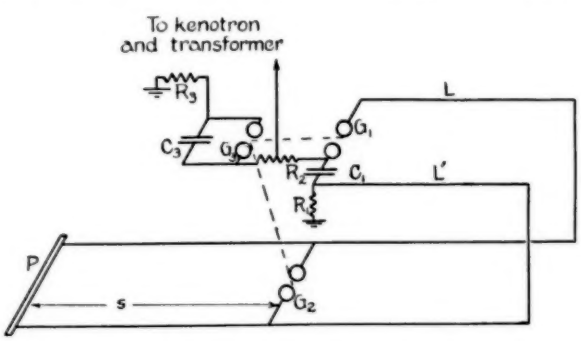

Fig. 3. Schematic diagram of apparatus used in the second method.

than half the length of the potential wave so that the resistance of G_1 could reach a low value before the first reflection occurred, thus reducing the damping. An indicating gap G_2 is placed a distance s from the closed end. This gap is irradiated from an independent discharge G_3 in the same manner as previously described. Since the time lag of G_2 is small and the damping of the oscillations not large, the sparking width of G_2 gives a direct measure of the maximum fall of potential during a time interval $2s/c$ where s is the distance of G_2 from the closed ends and c is the velocity of the electrical impulse along the wires. It may be worth while to mention our procedure in obtaining the maximum sparking potential of G_2. The transformer was adjusted so that G_1 would spark about every two seconds. The width of G_2 was then increased until sparking across it did not quite cease (one discharge across G_2 to twenty five across G_1). This point was taken as a measure of our potential. It may be significant to note that the distance necessary to widen G_2 from a condition where every spark at G_1 produced a spark at G_2 to the point where only one discharge occurred at G_2 to twenty five at G_1 was least when G_1 was in nitrogen and greatest when it was in CO_2.

Fig. 4 shows the maximum potential across G_2 plotted as a function of $2s/c$ for various pressures of air, hydrogen, CO_2 and nitrogen. It will be observed that the rate of fall of potential increases with pressure, i.e., as the pressure in G_1 is increased the electrical wave impressed upon the wire becomes steeper.

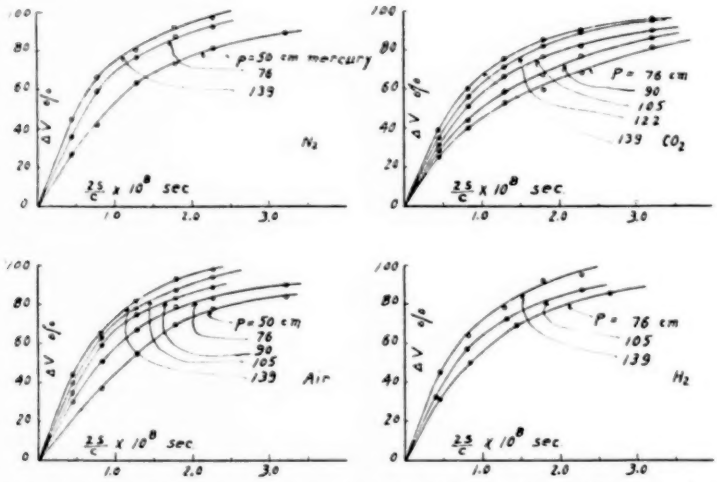

Fig. 4. Results obtained with the second method for air, CO_2, H_2 and N_2 at various pressures. The maximum potential across G_2, ΔV, plotted against the time interval $2s/c$.

Further it will be noted that for small values of $2s/c$ the ratio of the voltage across G_2 to $2s/c$ remains almost constant indicating that the potential when changing most rapidly is nearly a linear function of the time.

In formulating an analysis of the curves in Fig. 4 we were guided by the work of Toepler.[11] He has established a law for his *Gleitfunken* (surface discharge) from which it is possible to find the resistance R_t of the discharge at any time t after the beginning from the relation

$$R_t = \frac{K \cdot \delta}{\int_0^t idt} \tag{1}$$

where K is Toepler's spark constant δ the discharge length and $\int_0^t idt$ the charge which has passed during the time t. This law has been extrapolated to the case of the spark in ordinary air, and Binder[8] has obtained values for K at atmospheric pressure. Using this law of Toepler's Schilling[12] has worked out a solution for the circuit in which we are interested and shows that

$$t = \frac{K \cdot \delta}{E}\left\{\frac{V}{E-V} - \frac{1}{2} + \log\frac{2V}{E-V}\right\} = \frac{K \cdot \delta}{E} f(V) \tag{2}$$

in which t is the time and E the breakdown potential of the gap. This equation was derived on the assumption that the capacity C_1 multiplied by the

[12] Schilling, Archiv. f. Elektrot. **25**, 2, 97 (1931).

surge impedance of the leads was large in comparison to any time considered. The constants are evaluated so that t is zero when dv/dt is a maximum (coincident with the point $V=E/3$). In order to simplify the calculations the scale of E and V have been arranged so that E is 100 and accordingly the values of V are in percent. A graph of the relation is shown in Fig. 5. The values of $K\delta/E$ are obtained from Eq. (2) by first determining the values of V_1 and V_2

TABLE I. *Values of ΔV and $K\delta/E$ for air, CO_2, and N_2 at various pressures.*

Pressure cm mercury	Time interval $2s/c\times10^8$	Air ΔV percent	Air $K\delta/E\times10^9$	CO_2 ΔV percent	CO_2 $K\delta/E\times10^9$	N_2 ΔV percent	N_2 $K\delta/E\times10^9$
		($E=14.2$ kv)		($E=$—)		($E=15.1$ kv)	
50	0.45					27	2.3
	0.83	37	3.0			42	2.6
	1.29	55	2.8			63	2.2
	1.79	70	2.6			73	2.3
	2.28	78	2.5			81	2.2
	3.22	84	2.7			89	2.0
		($E=17.7$ kv)		($E=15.2$ kv)		($E=14.5$ kv)	
76	0.45	30	2.1	25	2.6	36	1.7
	0.83	51	2.0	40	2.7	59	1.6
	1.29	67	2.0	53	3.0	76	1.5
	1.79	79	1.9	59	3.5	87	1.3
	2.28	83	2.0	68	3.5	92	1.1
	3.22	90	1.8	81	3.1		
		($E=16.8$ kv)		($E=13.5$ kv)		($E=16.8$ kv)	
90	0.45	34	1.7	28	2.3	40	1.5
	0.83	59	1.6	44	2.4	60	1.6
	1.29	75	1.6	58	2.6	75	1.6
	1.79	83	1.6	67	2.8	86	1.4
	2.28	89	1.5	77	2.6	93	1.0
	3.22			86	2.2		
		($E=14.8$ kv)		($E=15.7$ kv)		($E=15.4$ kv)	
105	0.45	40	1.5	31	2.0	43	1.4
	0.83	63	1.5	51	2.0	65	1.4
	1.29	78	1.4	66	2.1	81	1.3
	1.79	87	1.3	76	2.1	92	0.9
	2.28	94	0.9	82	2.1	96	0.7
	3.22			90	1.9		
		($E=16.5$ kv)		($E=17.1$ kv)		($E=14.8$ kv)	
139	0.45	44	1.3	39	1.5	45	1.3
	0.83	65	1.4	60	1.6	66	1.3
	1.29	82	1.2	75	1.6	80	1.3
	1.79	93	0.8	85	1.5	92	0.9
	2.28	98	0.4	90	1.3	97	0.5
	3.22			96	0.9		

where $V_2-V_1\equiv\Delta V$ represents the potential measured by G_2 for each value of $2s/c$. It is easy to see that this is possible because if $(V_2-V_1)/\Delta t$ is a maximum, where $\Delta t=2s/c$, then the slopes of the curve, Fig. 5, are equal at V_1 and V_2. The values in Table I are the results of such computation for air, CO_2 and nitrogen. Those for hydrogen are in Table II. It will be observed

from the constancy of $K\delta/E$ for each pressure that the data are in fair agreement with Toepler's law, except for the larger values of ΔV. However, it should be noted that in the range where the law fails to fit, a small change in V produces a large change in $f(V)$ and the errors of observation are greatly multiplied.

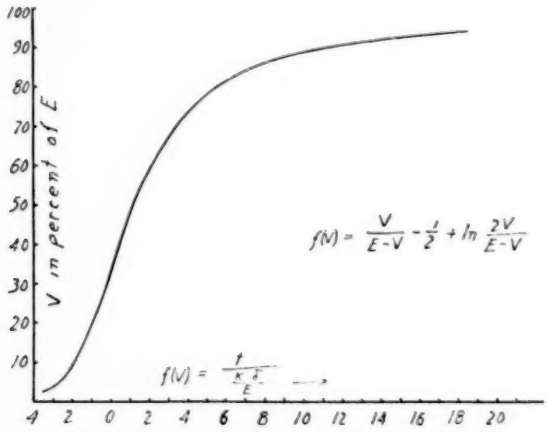

Fig. 5. Showing the variation of V with t according to Toepler's law for the case of a large condenser discharging into a long line.

From the mean values of $K\delta/E$ the variation of V with time for any pressure can be found at once by simply multiplying the scale of the absicissas ($f(V)$) in Fig. 5 by the proper value of $K\delta/E$. Fig. 6 shows such curves in-

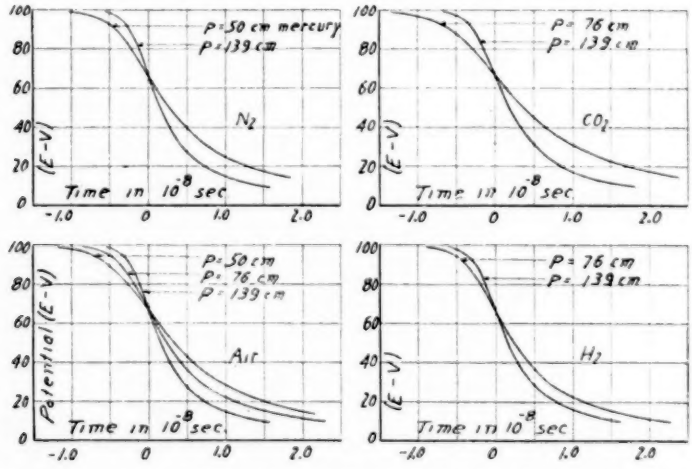

Fjg. 6. The potential across the discharge, $(E-V)$, plotted against the time for air, CO_2, H_2, and N_2 at various pressures. These curves were obtained by substituting the mean values of $K\delta/E$ from Tables I and II into Eq. (2).

verted $(E-V)$ for air, hydrogen, nitrogen and CO_2. In helium qualitative results show that the fall of potential is much slower than in air.

It will be observed from Table II that in hydrogen where the potential across the discharge is allowed to rise above the sparking voltage, that $K\delta/E$

and hence K are decreased. (These measurements could easily be obtained experimentally by the proper adjustment of the gaps G_1 and G_3.) This means that the rate of fall of potential is increased by increasing the voltage above the sparking potential before the discharge is initiated. The differences introduced are quite large and should indicate that where the potential across a gap is impressed rapidly without ultraviolet light or some agent to generate electrons in the gap to prevent time lag, the rate of fall of potential may be considerably faster. This possibly accounts in part for the range of variation

TABLE II. *Values of ΔV and $K\delta/E$ for H_2 for normal breakdown and for slight overvoltages.*

Pressure cm mercury	Time inteval $2s/c\times10^8$	H_2 ΔV percent	H_2 $K\delta/E\times10^9$	H_2 overvolted ΔV percent	H_2 overvolted $K\delta/E\times10^9$
		($E=12.3$ kv)		($E=12.6$ kv)	
76	0.46	31	2.1	39	1.6
	0.85	50	2.1	58	1.7
	1.44	69	2.1	80	1.5
	2.65	85	2.1	94	1.0
		($E=14.8$ kv)		($E=15.2$ kv)	
90	0.40	31	1.8	37	1.5
	0.74	50	1.8	57	1.5
	1.31	68	2.0	75	1.6
	2.02	81	2.0	89	1.4
	2.65	87	1.8	92	1.3
		($E=16.7$ kv)		($E=17.1$ kv)	
105	0.40	32	1.7	39	1.4
	0.81	57	1.7	63	1.4
	1.32	72	1.8	80	1.3
	2.28	87	1.6	92	1.1
		($E=16.5$ kv)		($E=17.0$ kv)	
122	0.45	43	1.4	46	1.3
	0.83	63	1.5	66	1.3
	1.29	81	1.3	82	1.2
	1.79	88	1.2	91	1.0
	2.28	92	1.1	97	0.5
		($E=18.9$ kv)		($E=19.4$ kv)	
139	0.45	45	1.3	47	1.2
	0.83	62	1.5	65	1.4
	1.29	78	1.4	81	1.3
	1.79	92	0.9	94	0.7
	2.28	95	0.8	98	0.4

found by the various investigators previously mentioned. We will describe later a method of obtaining overvoltages of many times the sparking potential and hence very rapid breakdowns.

In an attempt to analyze the results found by the first experimental method on the basis of Toepler's law we were unable to find an exact solution of the problem. However, it was found possible to obtain an approximation to the solution by a rather long and tedious method that we do not believe worth while to describe here. It will suffice to show a set of data for air at atmospheric pressure in Table III. It will be observed that the agreement is

good except for short wire lengths. This divergence, in part at least, perhaps results from the errors introduced by the time lag in the measuring gap G_2. That such errors should appear here and not (appreciably) in the second or

TABLE III. *Comparison between observed values of the maximum potential at G_2 (First Method) for air at atmospheric pressure and those calculated using Toepler's law.*

Wire length in meters	Maximum potential at the open end G_2	
	Observed	Calculated using $K\delta/E=2.0\times10^{-9}$
12	196	195
10	192	192
8	185	189
6	175	183
4	160	173

closed end method is to be expected in consequence of the difference in the multiple reflections for the two cases. The fact that the agreement between calculated and observed values is excellent for long wire lengths bears this out.

DISCUSSION

The principal possible sources of experimental error in both of the two above methods lie in the distortion of the wave as it travels along the wires and in the assumption that the sparking width of G_2 when intensely irradiated measures the maximum applied potential. Fortunately the first of these sources of error can be calculated with good approximation from well-established theory and the corrections applied when large enough to influence the results. The second difficulty, however, gives more serious trouble, but it is nevertheless possible, to investigate this source of error experimentally. In a separate set of experiments in which we measured the time lag of intensely irradiated spark gaps we found the time lag too short to affect appreciably our present results. In the second method it was possible to test directly the effect of time lag. If the capacity C_1 is increased the number of applications of the surge potential that would produce breakdown of G_2 is increased (where, for example, the first surge potential exceeded the steady breakdown value of G_2 by only a few percent). This increased number of applications of the potential should decrease the error due to time lag. Our results showed no variation with increase of C_1 above the value used in the experiment. Further, the rather rapid increase in the rate of fall of potential observed with increasing pressure indicates that the time lag is not a significant factor.

It may seem at first sight remarkable that it is possible to represent the electrical discharge phenomena in its initial stages by a relation as simple as Toepler's resistance law. More careful consideration shows, however, that the relation may be established logically as a result of the simplification introduced by the very short times involved. The discharge current arises from ionizing collisions in which both electrons and positive ions are produced. Due to the great difference in mobility between these, the current in the

initial stages of the discharge arises almost entirely from the movement of the electrons. In the short times involved there is comparatively little recombination and the positive ions move only a small distance from where they are generated. A state of ionization then exists in the discharge of an intensity proportional to the quantity of charge which has passed. Hence, to arrive at Toepler's relation it is only necessary to assume that the conductivity of the discharge is proportional to the ionization. The increase in the rate of fall of potential with increase of pressure (over the range studied) is also accounted for by the fact that the sparking potential as well as the number of molecules between the electrodes is increased. Consequently the rate of ionization should increase which, in turn, should lower k in Eq. (2). The marked lowering in every case of $k\delta/E$ for large values of ΔV in Tables I and II, indicates that the amount of ionization ceases to be directly proportional to the charge that had previously passed as the discharge approaches the arc stage.

Discharges at High Field Strengths

We shall now return to the question of obtaining a very rapid fall of potential after once the discharge is initiated. Previously, we[13] have mentioned the possibility of applying as much as 5×10^5 volts per cm for over 10^{-6} sec without electrical breakdown in air, hydrogen and nitrogen at atmospheric pressure. The gas was carefully dried and filtered and the ions kept continually removed by auxiliary fields. Fig. 7 shows a schematic diagram of such an apparatus. The gap G_3 is enclosed in either a metal chamber, or better, a large glass vessel with a cage of fine mesh brass wire screening most of the glass parts as shown by the dotted circle in the figure. The electrodes of G_3 were hard brass balls but when it is not desired to trip the spark with ultraviolet light steel balls can be used. A quartz window is so placed that G_3 can be irradiated as well as its light observed. The metal plates PP are spaced many times the distance between the electrodes in order to reduce capacity effects.

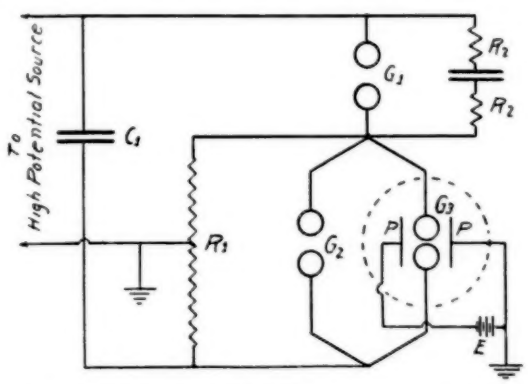

Fig. 7. Schematic diagram of the apparatus used for obtaining discharges at very high field strengths.

[13] Beams and Street, Phys. Rev. **35**, 658 (1930).

They are connected to a 200 volt vattery E and used to sweep the ions out of G_3.

The potential is slowly applied to the condensers C_1 and C_2 until G_1 breaks down. When this occurs G_2 and G_3 have approximately equal applied potentials until C_1 discharges. This time of discharge can be regulated by the size of the capacity C_1 and the resistance R_1. If ordinary unfiltered air is surrounding G_3 and all auxiliary ion sweeping removed, G_2 and G_3 have approximately the same sparking width. However, when the gas surrounding G_3 is carefully dried and filtered and a potential applied across PP to remove the ions from G_3 it was found that it was necessary to increase G_1 and G_2 to over 16 times the width of G_3 before G_3 would break down in less than 10^{-6} sec. If ultraviolet light was allowed to fall upon the cathode of G_3 it then sparked at approximately the same width as G_2 regardless of what was done to the gas. As the applied potential necessary to produce breakdown in 10^{-6} sec in G_3, when carefully swept of ions, was exceeded, even by a small amount the time between the application of the voltage and the breakdown was very much decreased. The maximum potential that could be applied across G_3 without breakdown in less than 10^{-6} sec depended upon the treatment of the surface of the electrodes. For example, a discharge in hydrogen at low pressure between the electrodes increased the maximum previous breakdown potential by almost 30 percent. Further, roughness of the electrodes, especially small microscopic projections such as develop from constant sparking, reduces the potential. If the gas is carefully removed from G_3 so that the pressure is less than 10^{-6} mm of mercury and the surge potentials applied as before, the potential necessary to break G_3 down is the same order of magnitude as with the dried filtered gas at atmospheric pressure, carefully swept free of ions.

The explanation of the fact that large fields can be impressed across a gap carefully swept of ions without breakdown seems to be that it is necessary to have an ion in the field to initiate the discharge. The drying and filtering of the air probably permit a more efficient removal of the ions by the auxiliary fields. The dependence of the maximum potential without breakdown in 10^{-6} sec, above described, upon the surface conditions of the cathode suggests that the discharge in ion-free gas is started by electrons pulled out of the cathode by the intense electric fields. When these electrons from the cathode enter the gas they become very efficient in initiating the discharge. Our measurements though only qualitative show that the rate of fall of potential is much faster than in a static breakdown. It seems that such discharges may possibly be utilized in experiments where it is necessary to produce a steep electrical wave or to give information concerning the extraction of electrons from metals by electric fields although the metal is surrounded by gases at various pressures.

THE CATHODE FALL OF AN ARC

By R. C. Mason
Research Laboratories, Westinghouse Elec. and Mfg. Co., East Pittsburgh, Pa.

(Received June 26, 1931)

Abstract

The distribution of energy of electrons at the boundary of the cathode fall of an arc is worked out for the thermionic arc and for the high field arc upon both the classical Schottky theory, and the quantum mechanical theory of high field emission. For the same value of cathode fall, the electrons from the thermionic arc have energies several volts greater than those from the high field arc. To give the positive ions necessary for space charge purposes, the cathode fall of the high field arc consequently must be several volts greater than that of the thermionic arc, if the mechanism of production of positive ions is the same in the two arcs. The minimum value of the difference in cathode fall is 4 to 6 volts. Tests are thus suggested for Langmuir's high field theory of cold cathode arcs. Data for the mercury arc indicate that electrons, in sufficient number to produce the necessary positive ions, have energies certainly less than 7 volts at the boundary of the cathode fall. Either the field theory does not apply to the mercury arc, or positive ions are produced by a cumulative process or other complicated means.

IN MANY arcs, current appears to be carried at the cathode primarily by electrons emitted thermionically. To neutralize the electron space charge, and to allow large currents to be drawn with low voltage, some positive ions must exist throughout the discharge, even near the cathode. Since the mobility of the positive ion is so small compared to the electron mobility, only a relatively small positive ion current is needed to provide the positive space charge. Chiefly, the current at the cathode is electron current. To replenish the positive ions, the electrons emitted from the cathode, acquiring sufficient energy in passing through the cathode fall, ionize the molecules of the active gas.

Such a simple theory seems plausible for normal arcs with cathodes heated from an external source, or with cathodes of refractory materials which reach a high temperature. For example, in both tungsten and carbon arcs, the cathode is at a temperature which will give a thermionic current density equal to the observed current density.[1]

When other types of arcs are observed—arcs in which the cathode temperature does not exceed a few hundred degrees—difficulties are encountered at once. Such arcs occur frequently: for example, an arc and its cathode electrode may be moved relative to each other with such velocity that the cathode never reaches a high temperature—the so-called "Stolt arc."[2,3,4] Again, in metals with high vapor pressures at moderate tempera-

[1] K. T. Compton, Trans. A.I.E.E. **46,** 870 (1927).

[2] H. Stolt, Zeits. f. Physik **26,** 95 (1924); Ann. d. Physik **74,** 80 (1924); Inaug. Dissertation, Uppsala, 1925.

[3] Slepian, Trans. A.I.E.E. **48,** 526 (1929).

[4] Seeliger and Wulfhekel, Phys. Zeits. **31,** 691 (1930).

tures, such as cadmium, mercury, etc., it is hard to believe the cathode temperature rises above a few hundred degrees. In many such "cold cathode" arcs, no appreciable purely thermionic emission can occur. How, then, is the current carried at the cathode?

Langmuir[5] first suggested that in the mercury arc electrons may still constitute the major portion of the current at the cathode, but that instead of being emitted thermionically the electrons are pulled out of the relatively cold cathode by a very high field. Later, this theory has been amplified by Compton[6] and MacKeown.[7] Though the potential drop at the cathode is only a few volts, it is conceivable that the potential is concentrated over such a small distance that the gradient may be of the order of millions of volts per cm. Such high fields are known to pull out quite high current densities of electrons.[8]

To test Langmuir's theory experimentally, though highly desirable, seems impossible to do directly. But, indirectly, a test appears possible from measurements on the cathode fall of the arc, in a manner which will be discussed below.

Magnitude of Positive Ion Current Necessary

Whatever the mechanism of freeing electrons from the cathode, a certain minimum positive ion current is necessary to neutralize the negative space charge. For this purpose, as many positive ions are needed if the electrons are pulled out under a high field as if they are emitted thermionically. The actual magnitude of the neutralizing positive ion current need not be very great—less than a thousandth part of the electron current[9] for most ions. So if the electron current density is a few thousand amps./cm^2, a positive ion current of only a few amps./cm^2 is sufficient.

It is possible, however, that many more positive ions than necessary for neutralization of electron space charge will be needed for the high field case. As Slepian and Haverstick[10] have pointed out, the high field postulated at the cathode is produced by the positive ions, and in order to have sufficiently high fields to pull out electrons, the minimum positive ion current must approach the magnitude of thousands of amperes per cm^2. If the electron field current densities are much larger than this, then, as before, the total positive ion current may be determined largely by the amount necessary for neutralization of electron space charge. If, however, the field current densities are moderate, the fraction of current carried by positive ions may be considerably larger than required for neutralization. Evidence deduced by Stern, Gossling, and Fowler[11] from cold cathode currents drawn from small wires,

[5] Langmuir, G. E. Review **26,** 731 (1923).

[6] Compton and Van Voorhis, Proc. Nat. Acad. Sci. **13,** 336 (1927). Compton, Trans. A.I.E.E. **46,** 868 (1927).

[7] MacKeown, Phys. Rev. **34,** 611 (1929).

[8] Millikan and Eyring, Phys. Rev. **27,** 51 (1926). Gossling, Phil. Mag. **1,** 609 (1926).

[9] Compton, Phys. Rev. **21,** 266 (1923); Trans. A.I.E.E. **46,** 873 (1927).

[10] Slepian and Haverstick, Phys. Rev. **33,** 52 (1929).

[11] Stern, Gossling, and Fowler, Proc. Roy. Soc. **124,** 699 (1929).

seems to show that the current densities are extremely high, though the emitting areas are very small. Whether the same conditions result in the case of the arc is, of course, uncertain; even if they do, the emitting spots may be so small, and so scattered about that a very large gross positive ion current will be needed to maintain a high average field over a large area. In any case, then, the total positive ion current required for an arc in which electrons are pulled out by a high field is at least as large as required for an arc in which electrons are emitted thermionically from a cathode maintained at a high temperature; quite possibly, the positive ion current must be much larger for the high field arc. The actual magnitude of the positive ion current density for the high field arc must be at least of the order of a thousand amps./cm^2.

Energy Distribution of Electrons—Classical Theory

The simplest hypothesis as to the production of positive ions is that electrons acquire sufficient energy in traversing the cathode fall to ionize the active gas. Then, electrons, equal in number to the positive ions necessary, must have total energies on emerging from the cathode fall at least equivalent to the ionization potential of the gas from which the positive ions are produced.

Upon the classical theory of an electron gas in a metal, in thermal equilibrium with the metal, the distribution of velocities of the emitted electrons is Maxwellian; experiment confirms the velocity distribution as Maxwellian.[12] The probability of an electron having a total energy between E and $E+dE$ as it emerges from the work function field can be shown easily to be

$$P(E)dE = \frac{e^2}{(kT)^2}\epsilon^{-eE/kT}EdE \tag{1}$$

where E is expressed in volts. The average energy of the electrons is $2\,kT$, which, at temperatures ordinarily associated with thermionic emission, is equivalent to only a few tenths of a volt. At the boundary of the cathode fall in an arc, practically all the energy of the electrons is the energy acquired from the field through which they have passed. The actual distribution in energy as secured directly from (1) is

$$f(E)dE = \frac{e^2}{(kT)^2}\epsilon^{-e(E-V_c)/kT}(E - V_c)dE \tag{2}$$

where V_c is the cathode fall. The distribution is sketched diagrammatically in Fig. 1. A certain proportion of the electrons must have energies at least as large as the ionizing potential. The shaded area in Fig. 1 is equal to the ratio of positive ion current to electron current, so it is just this fraction which must have energies greater than the ionizing potential, V_i. The diagram makes clear that

[12] Richardson and Brown, Phil. Mag. **16,** 353 (1908); Jones, Proc. Roy. Soc. **A102,** 734 (1923); Germer, Phys. Rev. **25,** 795 (1925).

$$V_c + \alpha = V_i + \beta$$

or

$$V_c = V_i + \beta - \alpha. \tag{3}$$

If a high field is applied to the cathode, the emission of electrons will be increased, according to the Schottky effect.[13] The force on the electron, due

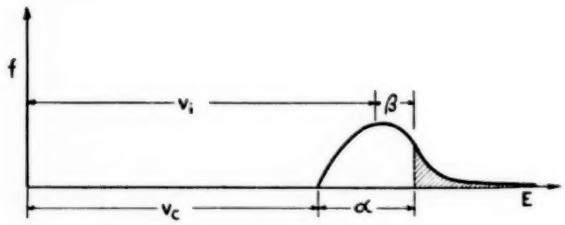

Fig. 1. Energy distribution of electrons at boundary of cathode fall, thermionic case.

to the surface field, is that of the curved line in Fig. 2, following Langmuir.[14] The external applied field is MN, shown constant for simplicity; in the case of the arc, the area OMNP is equal to the cathode fall, V_c'. If particles incident on a region of retarding force have a Maxwellian distribution of velocities, it is a characteristic of such a distribution that those particles which pass through the retarding force will also possess a Maxwellian velocity distribution with same mean energy as the incident particles. This is true regardless of the amount of work done against the field. At the point D in Fig. 2, the

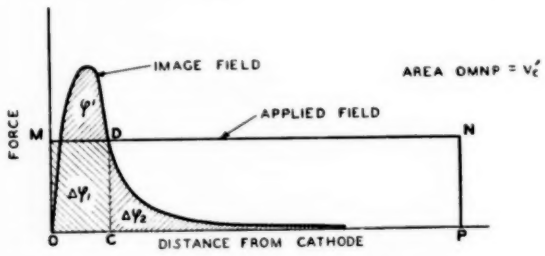

Fig. 2. Force on an electron with a high field applied.

intersection of the surface field and the applied field, the force on an electron is zero; all electrons which reach D from within the metal will escape. At D, then, the probability of an electron having an energy between E and $E+dE$ is exactly that given by Eq. (1). Beyond D, an electron gains an energy $D\,N\,P\,C - \Delta\phi_2$. But $D\,N\,P\,C = V_c' - \Delta\phi_1$, so the gain in energy is $V_c' - \Delta\phi_1 - \Delta\phi_2 = V_c' - \Delta\phi = V_c' - (\phi - \phi')$ where ϕ is the ordinary work function, and ϕ' is the effective work function under the action of the external field. $\Delta\phi$ is exactly the reduction in work function due to the Schottky effect. The distribution in energy of the electrons at the boundary of the cathode fall is changed from Eq. (2) to

[13] Schottky, Phys. Zeits. **15,** 872 (1914); **20,** 220 (1919); Ann. d. Physik **44,** 1011 (1914); Zeits. f. Physik **14,** 63 (1923).

[14] Langmuir, Trans. Am. Electrochem. Soc. **29,** 162 (1916).

$$f_1(E)dE = \frac{e^2}{(kT')^2}\epsilon^{-e(E-V_c+\Delta\phi)/kT'}(E - V_c + \Delta\phi)dE. \tag{4}$$

The function is sketched roughly in Fig. 3. No electrons have an energy less than $V_c' - \Delta\phi$. The area shaded is equal to the area shaded in Fig. 1, since the

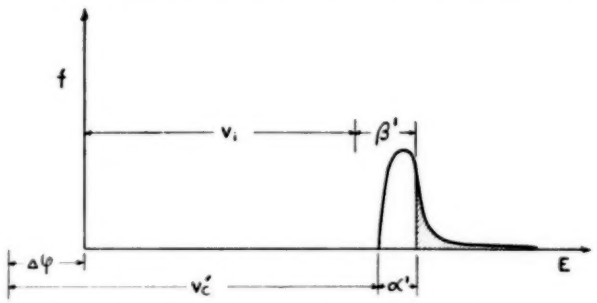

Fig. 3. Energy distribution of electrons at boundary of cathode fall, high field case, classical theory.

fraction of electrons with energy sufficient for ionization must at least be as great as in the thermionic case. As before,

$$\begin{aligned} V_c' - \Delta\phi + \alpha' &= V_i + \beta' \\ \text{or} \qquad V_c' &= V_i + \beta' - \alpha' + \Delta\phi. \end{aligned} \tag{5}$$

Since the arcs to which the high field theory are supposed to apply are those whose cathodes are at temperatures too low for thermionic emission, T' in Eq. (4) is considerably less than T in Eq. (2). So, for the same production of positive ions in the two arcs, α' must be less than α. If more positive ions have to be produced in the high field arc, as seems easily possible, α' will be decreased still further. For the last reason, β' will probably be greater than β. Therefore, V_c' must exceed V_c by at least $\Delta\phi$. The cathode fall of the high field arc must be greater than that of the thermionic arc.

An idea of the magnitude of the difference in cathode falls may be secured as follows: by Schottky's theory, the electron emission in a high field is

$$i = 60T^2\epsilon^{-e(\phi-\Delta\phi)/kT}. \tag{6}$$

If $T = 800°\text{K}$, $\phi = 4$ volts, and $\Delta\phi = 3.4$, $i = 6400$ amps/cm^2. In order to obtain current densities of a few thousand amps/cm^2, $\Delta\phi$ must approach close to the whole work function.

An estimate of α and α' comes from the probability of an electron having a velocity greater than α: from Eq. (1)

$$\begin{aligned} P(\alpha) &= \int_\alpha^\infty P(E)dE \\ &= \left(\frac{e\alpha}{kT} + 1\right)\epsilon^{-e\alpha/kT}. \end{aligned} \tag{7}$$

In the thermionic arc, take $T=3200°K$, and the following values are obtained

$$\alpha=3 \quad \text{volts}, \; P(\alpha)=2.25\times10^{-4}$$
$$\alpha=1.5 \; \text{volts}, \; P(\alpha)=2.8 \times10^{-2}$$

In the high field arc, take $T=800°K$; then

$$\alpha'=0.75 \; \text{volts}, \; P(\alpha')=2.25 \times10^{-4}$$
$$\alpha'=0.37 \; \text{volts}, \; P(\alpha')=2.8 \times10^{-2}$$
$$\alpha'=0.25 \; \text{volts}, \; P(\alpha')=0.123$$

The ratio of positive ion current to electron current in the thermionic arc is undetermined; it must be at least of the magnitude of the minimum value of $P(\alpha)$, in order to neutralize the space charge. It may be somewhat greater, if a strong positive charge exists in front of the cathode. Likewise, the value of positive ion current for the high field arc is undetermined; for electron current densities of a few thousand, $P(\alpha')$ must have about the maximum value given, in order to provide a sufficiently high field. So, α probably exceeds α' by more than a volt. How much larger β' is than β is also uncertain. It would seem though that V_c' should exceed V_c by five volts or more.

Energy Distribution of Electrons—Quantum Mechanics Theory

Though Langmuir originally offered the ordinary Schottky effect as an explanation of the origin of electrons, it is now known that, at temperatures and fields too low for the Schottky effect to play an appreciable part, quite large current densities of electrons can be secured[8]—the so-called "cold cathode" effect. Too, the classical theory of energy distribution among the electrons in a metal has been abandoned in favor of the more satisfactory theory based on Fermi statistics. Sommerfeld's development of the electron theory of metals, based upon Fermi statistics,[15] shows at temperatures sufficient for thermionic emission those electrons which have enough energy to escape possess a Maxwellian distribution of velocity, though at low temperatures there is nothing resembling a Maxwellian distribution. The theory also gives an increased mean energy to the electrons, but at the same time the work function is increased a like amount. So, for thermionic emission, the classical theory of the energy distribution of electrons still holds.

At low temperatures, where an inappreciable number of electrons have enough kinetic energy to escape through the surface forces of the metal, quantum mechanics shows that under the action of a sufficient high field, electrons will still be able to escape.[16] This can best be understood by referring to Fig. 4, partly following Nordheim.[17] On the right, the solid line represents potential energy plotted against distance from the cathode metal, upon the idealized picture of a potential barrier at the surface of the metal—the "outer" work function of Sommerfeld. The effect of the high field is to re-

[15] Sommerfeld, Zeits. f. Physik **47,** 1 (1928). See also the summary by Darrow, Rev. of Mod. Phys. **1,** 90 (1929).

[16] Fowler and Nordheim, Proc. Roy. Soc. **A119,** 173 (1928). Nordheim, Phys. Zeits. **30,** 177 (1929).

[17] Nordheim, Phys. Zeits. **30,** 180 (1929).

duce the potential beyond the barrier, finally by an amount V_c in the case of the arc. Actually, the surface field produces a gradual rise of potential corresponding to the image field over most of the range, somewhat like the dotted line. On the left of Fig. 4, as abscissa is plotted the distribution function, $N(W)$, for the *normal* components of energy of electrons incident on the metal surface against energy, in volts, as ordinate, following the probability function given by Nordheim[17]

$$N(W) = \frac{4\pi me}{h^3} kT \log (1 + \epsilon^{-e(W-\mu)/kT}) dW. \tag{8}$$

For $T=0$, the distribution follow the solid line, no electrons having energy greater than μ, the "inner" work function; at a higher temperature, the dotted line shows the distribution.

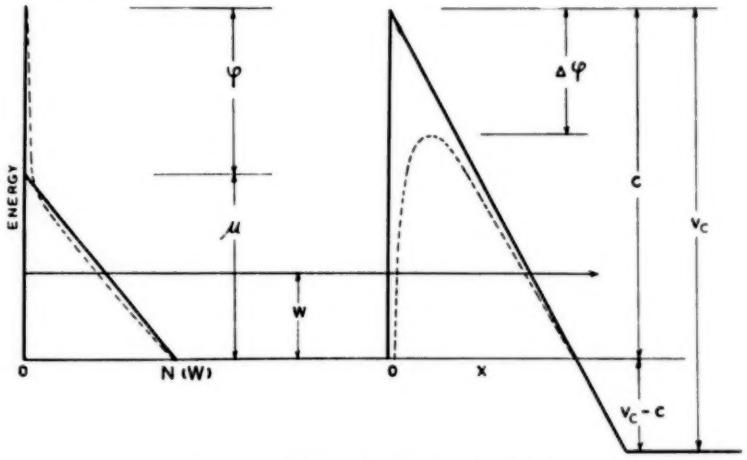

Fig. 4. Energy diagram for high field.

Quantum mechanics show that it is possible for an electron of normal energy W, much less than C, to escape from the metal, if the width of the potential barrier *through* which it must pass is not too great; that is, if the applied field is sufficiently large. Fowler and Nordheim[15] have derived an expression for such an electron emission; at $T=0$, using the idealized form of potential, they find

$$i = \frac{6.2 \times 10^{-6} \mu^{1/2}}{C\phi^{1/2}} F^2 \epsilon^{-6.8\times10^7 \phi^{3/2}/F} \tag{9}$$

i is in amps/cm^2; μ, C, and ϕ are in volts; and F is the applied field, in volts per cm. ϕ is the ordinary work function, being equal to $C-\mu$.

Now the diagram in Fig. 4 makes plain that the energy which an electron has upon emerging from the cathode fall is the sum of the normal component of energy, the components of energy in other directions, and the energy gained in the field $V_c - C$; or

$$E = V_c - C + W + \text{parallel comp. of energy.} \tag{10}$$

For ordinary thermionic emission in weak fields, the normal energy W must

be greater than C. So, by Eq. (10), all electrons emitted have energies greater than the cathode fall; the actual distribution has already been given. For zero temperature, it is a characteristic of the Fermi distribution that no electron has a total energy greater than μ. So, in the cold cathode current at $T=0$, the *maximum* value of E is $V_c-C+\mu$ or $V_c-\phi$. For temperatures above zero, but still moderate, such as occur in high field arcs, more and more electrons have energies greater than μ. The distribution of energies can be worked out approximately.

Fowler and Nordheim[16] calculate the probability of an electron with normal energy W passing through the potential barrier under an applied field F to be

$$D(W) = \frac{4[W(C-W)]^{1/2}}{C}\epsilon^{-4K(C-W)^{3/2}/3F} \tag{10}$$

where

$$K = \left(\frac{8\pi^2 m}{h^2}\right)^{1/2}$$

This holds for $W<C$.

The number of electrons in unit volume of the metal with velocity components between u and $u+du$, v and $v+dv$, $w+dw$, is[15]

$$f(u, v, w)dudvdw = \frac{2m^3}{h^3}\frac{dudvdw}{\epsilon^{[m(u^2+v^2+w^2)-2\mu]/2kT}+1}$$

where $\mu=(3n/\pi)^{2/3}h^2/8m$, and n is the number of electrons per unit volume. Take the u velocity direction normal to the surface. Then, the number of electrons incident on unit surface in unit time is

$$\nu_i = f(u, v, w)ududvdw. \tag{11}$$

The number of the above velocity class, which will be emitted is,

$$\nu_e = \nu_i D(\tfrac{1}{2}mu^2). \tag{12}$$

Substitute $u=c\cos\theta$

$$\begin{aligned} v &= c\sin\theta\cos\phi \\ w &= c\sin\theta\sin\phi \end{aligned} \tag{13}$$

where c is the magnitude of the electron velocity. Then, Eq. (12) becomes

$$\nu_{e(\theta,\phi,c)} = \frac{2m^3}{h^3}\frac{c^3\sin\theta\cos\theta d\theta d\phi dc}{\epsilon^{(mc^2-2\mu)/2kT}+1} \cdot\frac{4}{C}[\tfrac{1}{2}(mc^2\cos^2\theta)(C-\tfrac{1}{2}(mc^2\cos^2\theta))]^{1/2}\epsilon^{-4K(C-(mc^2\cos^2\theta)/2)^{3/2}/3F} \tag{14}$$

To obtain the number of incident electrons, which will later be emitted, with velocity between c and $c+dc$, Eq. (14) must be integrated from $\phi=0$ to $\phi=2\pi$; the integration for θ must be carried out in two steps. For $\frac{1}{2}mc^2<C$, θ must be integrated from 0 to $\pi/2$; for $\frac{1}{2}mc^2>C$, θ must be integrated from $\cos^{-1}(2C/mc^2)^{1/2}$ to $\pi/2$. Performing the integrations, with close approximations which are valid for strong fields and not too high temperatures, for $\frac{1}{2}mc^2<C$,

$$\nu_{e(c)} = \frac{4(2)^{1/2}\pi m^{5/2}F}{Kh^3C} \frac{\exp\left[-4K(C-mc^2/2)^{3/2}/3F\right]c^2dc}{\exp\left[mc^2-2\mu)/2kT\right]+1} \tag{15}$$

For $1/2mc^2 > C$

$$\nu_{e(c)} = \frac{8\pi m^2F}{Kh^3C^{1/2}} \frac{cdc}{\exp\left[(mc^2-2\mu)/2kT\right]+1}. \tag{16}$$

An electron of velocity c incident on the surface will have an energy

$$E = \tfrac{1}{2}mc^2 + V_c - C$$

at the boundary of the cathode fall space. Making this substitution, the number of electrons emerging from the cathode fall with a total energy between E and $E+dE$ is, for $E < V_c$

$$\nu_{e(E)} = n(E)dE = \frac{2(2)^{1/2}m^{1/2}e^{3/2}F}{h^2C} \cdot \frac{\exp\left\{\left[8(2)^{1/2}\pi m^{1/2}e^{1/2}(V_c-E)^{3/2}\right]/3hF\right\}(E-V_c+C)^{1/2}dE}{\epsilon^{e(E-Vc+\phi)/kT}+1} \tag{17}$$

and for $E > V_c$

$$n(E)dE = \frac{2(2)^{1/2}m^{1/2}e^{3/2}F}{h^2C^{1/2}} \frac{dE}{\epsilon^{e(E-Vc+\phi)/kT}+1} \tag{18}$$

where all energies are in volts. The function $n(E)$ is plotted roughly in Fig. 5, for $T=0°K$, and $T=800°K$. Only one value of field is used; the higher the

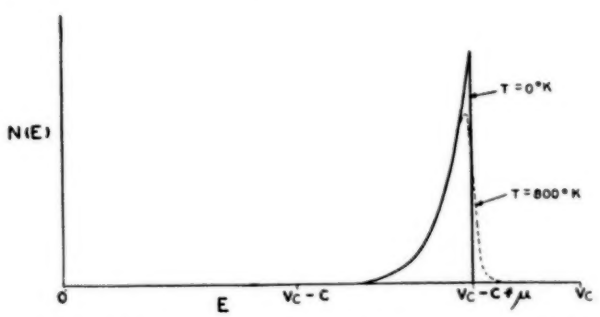

Fig. 5. Energy distribution at boundary of cathode fall for electrons emitted under influence of high field, quantum mechanics theory.

field, the greater $n(E)$, the increase being in an exponential manner. Of course, all electrons have an energy greater than V_c-C. At $T=0$, the exponential in the denominator becomes infinitely large for $E > V_c-C+\mu$, that is, $E > V_c-\phi$.

The value of field to be expected in a high field arc can be estimated by means of Eq. (9). Pairs of values of i and F, calculated from that equation are given:

$F=10^7$ volts/cm	$i=10^{-16}$ amps/cm^2
$F=5\times10^7$	$i=3.38\times10^4$
$F=10^8$	$i=3.25\times10^7$

Upon this theory, then, the field is probably of the order of 5×10^7 volts/cm. A field of this magnitude gives a reduction in work function $\Delta\phi=2.68$; the corresponding Schottky current density will be less than one ampere at low temperatures. The electrons which go over the top of the potential barrier are thus entirely negligible; only the electrons passing through the potential need be considered. Integration of Eq. (18) from V_c to ∞ gives the number of electrons with energies greater than V_c; at $T=800°K$, this number also turns out to be entirely negligible. The integration of Eq. (17) from E_1, say, to V_c, gives the effective number of electrons with energies greater than E_1. A rough approximation of this integral shows that electrons in number just beginning to be appreciable have energies greater than V_c-3 volts.

Some objection might be raised to the above calculation, since the transmission coefficient, $D(W)$, developed by Fowler and Nordheim was based upon the idealized potential barrier of Fig. 4. The actual potential curve may change $D(W)$, especially near the peak. Too, the approximations used in determining $D(W)$ break down at $W=C$. Because of the mathematical difficulties, an exact solution for $D(W)$ and determination of the energy distribution appears impossible at present. It does not seem, however, that the conclusions as to the difference in the cathode fall will be altered. A lower limit for the difference can be secured from investigating the distribution in *total* energy of the electrons incident on the inner surface of the metal, which can be calculated precisely. In Eq. (11) for the number of electrons incident on unit area per second, make the substitution of Eq. (13). Then

$$\nu_{i(c,\theta,\phi)} = \frac{2m^3}{h^3}\,\frac{c^3\sin\theta\cos\theta\,d\theta d\phi dc}{\epsilon^{(mc^2-2\mu)/2kT}+1} \tag{19}$$

To obtain the number incident with velocity between c and $c+dc$, Eq. (19) must be integrated for ϕ from 0 to 2π, and for θ from 0 to $\pi/2$. Thus

$$\nu_{i(c)} = \frac{2\pi m^3}{h^3}\,\frac{c^3dc}{\epsilon^{(mc^2-2\mu)/2kT}+1}\,. \tag{20}$$

Put $E=\frac{1}{2}mc^2$, and express energies in volts,

$$\nu_{i(E)} = N(E)dE = \frac{4\pi me^2}{h^3}\,\frac{EdE}{\epsilon^{e(E-\mu)/kT}+1}\,. \tag{21}$$

This gives the number of electrons incident per second with energies between E and $E+dE$. The function $N(E)$ is plotted in Fig. 6, for several temperatures.

The number of electrons incident on unit area per second with an energy greater than any amount, say λ, is found by integrating Eq. (21) from λ to ∞. If λ is a little larger than μ, the integration can be done easily, and

$$N(\lambda) = \frac{4\pi mekT}{h^3}\,\lambda\epsilon^{-e(\lambda-\mu)/kT}. \tag{22}$$

It will be instructive to express the number of electrons as a current. Chang-

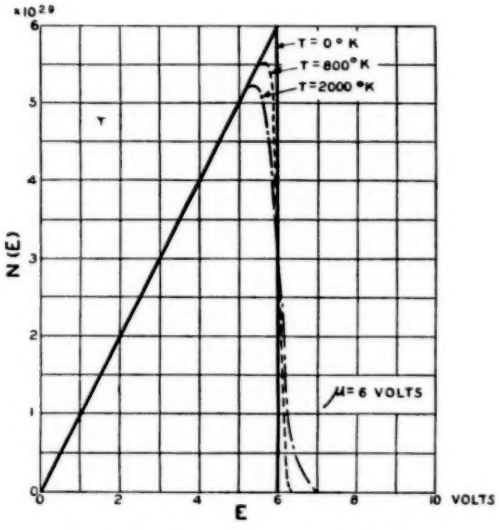

Fig. 6. Distribution in total energy for electrons incident on surface of metal.

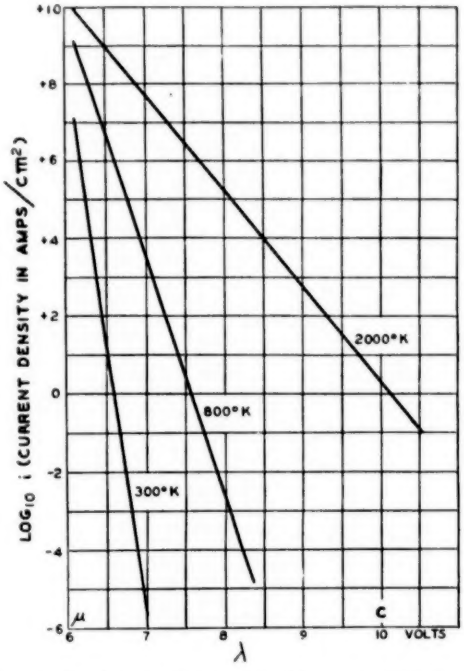

Fig. 7. Current density of electrons incident on surface of metal with total energy greater than λ.

ing to practical units, the current density of electrons incident on the metal surface with an energy exceeding λ is

$$i_\lambda = 1.3 \times 10^6 T\lambda\epsilon^{-11,600(\lambda-6)/T} \text{ amps/cm}^2 \qquad (23)$$

Log i_λ vs λ, for different T, is plotted in Fig. 7. In all the above calculations, the values $\mu = 6$, $C = 10, \phi = 4$ have been taken. If C and μ are actually higher, the effect to which attention is drawn here will be enhanced.

The emission of electrons depends on the normal component of energy, not on the total energy; so not all of the electrons with total energy λ will be emitted. Those that are emitted will have an energy at the cathode fall boundary

$$E = V_c - C + \lambda.$$

So, only a current *less* than i_λ will have energies exceeding $V_c - (C - \lambda)$. At a few hundred degrees, i_λ is in excess of a few hundred amperes only when $C - \lambda$ is greater than 2.5 to 3 volts. The emitted electron current density with energies large enough for ionization must approach a thousand amperes, in order to provide sufficient positive ions for maintenance of the high field. So, i_λ must be much larger than 1000 amps/cm^2 and hence $C - \lambda$ must be still larger than 3 volts. Since electrons sufficient to provide the necessary positive ions have energies 1.5 to 3 volts greater than the cathode fall in the thermionic arc, while they have energies less than the cathode fall in the high field arc by an amount greater than 2.5 to 3 volts, the cathode fall of the high field arc must be at least 4 to 6 volts greater than that of the thermionic arc.

Most of the above discussion has been based upon the simple theory that an electron emerging from the cathode fall of the arc must have an energy equal to or greater than the ionizing potential in order to produce a positive ion. This assumption is not necessary, however; exactly the same argument could be deduced if electrons of energy less than the ionizing potential could produce ions, as by a cumulative process. *So long as the mechanism of production of positive ions is the same in the two arcs and that mechanism depends upon electron energy, the high field arc must have a cathode fall several volts greater than a thermionic arc.*

Suggested Tests for High Field Theory

In order to determine whether Langmuir's high field theory applies to any particular arc, the cathode fall of the arc should be measured and compared with the cathode fall of a thermionic arc under the same conditions. A way of determining whether or not Langmuir's theory is true in general would be to start an arc, by high voltage breakdown, between refractory electrodes, and observe, probably by means of a cathode-ray oscillograph, if the arc voltage changed as the cathode became heated enough for considerable thermionic emission. An alternative would be to reduce the hearing current of a filament maintaining an arc, and observe if the cathode fall changed.

If in these tests, the cathode fall did not change in the passage from thermionic arc to non-thermionic arc, then it could be concluded that Langmuir's theory did not apply. The converse, however, would not necessarily prove the correctness of the Langmuir theory. Some other mechanism might give an increased cathode fall, as well as the high field mechanism.

The Mercury Arc

None of the above experiments have been carried out yet. The cathode fall of the mercury pool arc, however, has been measured recently by Killian,[18] and by Compton and Lamar,[19] and found to be about 10 volts. From this, what would one conclude about the mechanism of the mercury arc?

The temperature of the cathode spot has been variously estimated from 600°K to 2000°K. From Stark's[20] observation of a continuous spectrum at the cathode, early investigators assumed the cathode temperature to be about 2000°K. As pointed out by Compton,[6] the continuous spectrum may arise from other sources, and the actual temperature may be only 600°K. Seeliger[21] calculated the temperature of the cathode spot, from the rate of vaporization given by Guntherschulze, to be 670°K. The Brown-Boveri Company[22] have measured the temperature of a mercury arc cathode by an optical pyrometer, and found 2360°K. The cathode spot, however, was fixed by means of a tungsten rod, so the temperature may have been different from a mercury pool arc. Too, a green filter was used with the pyrometer, which seems hardly justifiable. Lubcke[23] shows that pyrometric measurements in a discharge are not at all accurate; he concludes the temperature of the cathode is not above 773°K. So, 800°K seems a safe upper limit to take for the cathode temperature.

To produce even a field of 10^6 volts/cm, a positive ion current density of 690 amps/cm^2 is necessary, according to Slepian and Haverstick's calculations.[10] To give a field of 5×10^7 volts/cm, which is necessary for large electron current densities, a positive ion current of 3.5×10^5 amps/cm^2 would be needed. It seems doubtful if surface irregularities can exist to cause a marked local multiplication of the average field. So, the positive ion current must be well above 10^3 amps/cm^2. From Fig. 7, at 800°K, an equal electron current will have energies less than the cathode fall by an amount greater than 3 volts. To produce ions at a single impact, the cathode fall would have to be over 13.4 volts, while the measured fall is only about 10 volts. If the high field does exist, an entirely negligible number of electrons have energies of 10 volts; and certainly less than a thousand amperes have energies even approaching 7 volts. One is forced to one of two conclusions, if the above temperature and cathode fall are correct: (1) the mercury arc is not a high field arc; (2) if the mercury arc is a high field arc, ionization at a single impact does not occur, and a complicated mechanism for the production of positive ions must be devised—such as cumulative ionization, attainment of high random electron velocities through scattering, etc. Since a cathode fall of 5.5 volts has

[18] Killian, Phys. Rev. **31,** 1122 (1928).

[19] Compton and Lamar, Review of paper presented before National Academy of Sciences, Washington, April 1930, printed in Science **71,** 517 (1930). Also Phys. Rev. **37,** 1069 (1931).

[20] Stark, Phys. Zeits. **5,** 51, 750 (1904).

[21] Seeliger, Phys. Zeits. **27,** 37 (1926).

[22] Brown-Boveri Review **16,** 61 (1929).

[23] Lubcke, Zeits. f. tech. Phys. **10,** 598 (1929).

been found for the low voltage mercury arc with thermionic cathode,[24] the last conclusion is not incompatible with the ideas developed in this paper.

In a very recent paper, Compton[25] has also pointed out that electrons emitted as a result of a high field have reduced energies, though he does not consider the distribution in energy in detail; and he has expressed the opinion that in the mercury arc positive ions are produced by a cumulative process.

Perhaps the same remarks concerning the existence of a high field arc may apply to the cadmium arc, and possibly also to the thallium arc, where Nottingham[26] has found the cathode fall to be very close to the ionizing potential of the cathode metal.

Conclusions

An analysis has been given, showing that the kinetic energy of an electron emitted under the action of a high field is several volts less than the energy of an electron emitted thermionically, at the end of the same applied voltage. Consequently, if the same mechanism for the production of positive ions exists in a high field arc as in a thermionic arc, the cathode fall of the high field arc must be several volts greater than that of a thermionic arc. This shows that the Langmuir high field theory of an arc should not be applied arbitrarily without considering in detail the way in which positive ions are produced. Careful study of the cathode falls of arcs, with regard to the electron energies, may afford a better understanding of the phenomena at the arc cathode.

Finally, from the measured cathode fall and cathode temperature of the mercury arc, one must conclude either that the high field theory does not apply to the mercury arc, or that ions are produced by some complicated mechanism such as cumulative ionization.

The writer gratefully acknowledges the helpful criticism and encouragement received from Dr. J. Slepian during the preparation of this paper.

[24] Compton, Trans. A.I.E.E. **46,** 868 (1927).
[25] Compton, Phys. Rev. **37,** 1077 (1931).
[26] Nottingham, Journ. Franklin Inst. **206,** 43 (1928).

AN EXPERIMENTAL TEST OF THE IONIZATION CHAMBER METHOD OF MEASURING THE RELATIVE INTENSITIES OF X-RAY SPECTRUM LINES

By Samuel K. Allison and Victor J. Andrew
University of Chicago

(Received June 12, 1931)

Abstract

A two-compartment ionization chamber has been constructed with the following properties: (1) The fraction of the x-ray energy absorbed in the front compartment could be directly measured, (2) The volume of gas from which the ionic saturation current was drawn was sharply defined, (3) Photoelectrons produced in the chamber could not reach the walls before expending their ionizing energy, (4) The direct beam entered and left the chamber through thin windows and encountered no other parts of the chamber. The relative ionization currents produced in methyl iodide, methyl bromide, argon, sulfur dioxide, and air by the α_1, β_1, γ_1, lines of the tungsten L series were measured and the ratios obtained after correction for fraction of the direct beam absorbed were found not to vary more than 2.5 percent in the first four gases. If the air values are corrected for loss through scattering, concordant results are obtained. Similar experiments have been made using the uranium L-series, where large corrections for loss through escape of fluorescent K-radiation must be made, including the case of krypton, where the K limit comes between the uranium $L\beta_1$ and $L\alpha_1$ lines. The results give strong support to the following hypothesis: The saturation current obtained from a given volume of any gas is proportional to the fraction of the x-ray beam transformed into β-rays within it, providing the β-rays come to the end of their ionizing range within the volume.

Introduction

IN ATTEMPTING to measure the relative intensity of x-ray spectrum lines by the ionization chamber method, one actually measures the ionic saturation current produced by the x-ray beam in a volume of gas bounded by the walls of the chamber. The question then arises: is this observed ionization current proportional to the intensity we wish to measure? The question becomes especially important when we wish to compare the intensities of two x-ray beams of different wave-lengths. Several investigations, designed to give an experimental answer to this question, have been carried out.[1] The method has been to measure the intensity of an x-ray beam by converting the energy into heat, and then to find the ionization produced by this beam in air. All but a negligible part of the ionization in air results from the ionizing action of photoelectrons or recoil electrons ejected by the x-rays, and by measuring the number of ions produced per second one may calculate the energy ϵ expended by a beta-ray per pair of ions formed. Although various

[1] Kulenkampff, Ann. d. Physik **79,** 97 (1926); Kircher and Schmitz, Zeits. f. Physik **36,** 484 (1926); Rump, Zeits. f. Physik **43,** 254 (1927); Auren K. Vetenskapsakad, Nobelinst. Medd. 6, **13,** 1 (1927); Steenbeck, Ann. d. Physik **87,** 811 (1928); Crowther and Bond, Phil. Mag. **6,** 401 (1928).

researches give values of ϵ for air which differ somewhat, they all show that ϵ is independent of wave-length over the range investigated, or from about 0.5 to 1.5 A.U. This question of the variation of ϵ with λ is vital to the ionization measurement of the intensities of x-ray beams of different wave-lengths. The result that ϵ is constant may be stated in the following form: the relative intensity of two x-ray beams of different wave-length is correctly given by the relative ionic saturation currents produced in air in an ionization chamber in which all of the x-ray energy is transformed to beta-ray energy in air, and the beta-rays produced come to the end of their ionizing range before reaching the boundaries.

Another type of problem which involves similar considerations is the experimental determination of the efficiency of production of fluorescent radiation, in which the intensities of the primary and secondary x-rays, necessarily of different wave-lengths, must be measured.[2] (These considerations do not apply to the direct method of counting the relative number of double and single tracks in a Wilson chamber.) The experiments of Martin, and of Compton have an especially important bearing on the results to be reported here. It seems quite obvious from the quantum theory that the fraction w_k of a number of atoms ionized in the K shell which return to their normal state by a process involving the emission of K series characteristic radiation is independent of the wave-length of the primary beam which produced the ionization. Martin and Compton find by experiment that such is the case, on the assumption that the energy spent in producing a pair of ions is the same for the primary and fluorescent x-rays. We may then conclude from their experiments that if ϵ varies with the wave-length, then w_k, the fluorescence yield,[3] varies with the primary wave-length, and because such a variation of w_k is highly improbable, the experiments furnish evidence of the constancy of ϵ. The assumption of the constancy of ϵ is set forth very clearly in the paper of Martin, who used oxygen gas in his ionization chamber.

It is not always practicable to use such light gases as air and oxygen in ionization chambers because of the small fraction of the primary beam absorbed in a chamber of convenient length, and the resultant loss of intensity. In Compton's work on w_k, methyl bromide was used, and such gases as argon, methyl iodide, and krypton have also been used in various researches involving intensity measurements. When such gases are used, the possibility arises that fluorescent x-rays excited in the gas may reach the boundaries of the space from which the ionic saturation current is being drawn without being absorbed. Martin has derived equations expressing the corrections to be applied when fluorescent radiation is produced, and used them for the calculation of w_k from measurements of the ionization relative to air of the heavier gases, as reported by other investigators. Compton has also derived such equations, and applied them to his work with methyl bromide. In certain of the experiments reported here, these corrections are given a rather severe

[2] Harms, Ann. d. Physik **82,** 87 (1926); Balderston, Phys. Rev. **27,** 696 (1926); Martin, Proc. Roy. Soc., Lond. **A115,** 420 (1927); Compton, Phil. Mag. **8,** 961 (1929).

[3] Auger, Ann. d. Physique **6,** 183 (1926).

test, and their derivation will accordingly be reviewed. The development of the equations follows closely the method given by Compton.[2]

Derivation of Corrections to Observed Ionization Currents

Consider a cylindrical volume of gas, of length l and radius r. The beam of x-rays enters at the center of one end of the cylinder and traverses the volume along the axis of the cylinder. In the following calculations the cross-section of the beam is not limited by the area of the opening of the ionization chamber, but is supposed to be small compared to πr^2. We can speak of the power, P, of the beam of x-rays entering the chamber. The x-rays may interact with the gas in the chamber in three ways, (1) The ejection of photoelectrons, (2) The classical scattering, and (3) The Compton scattering. We shall simplify the problem at once by assuming that the Compton effect plays no significant part in the process. This assumption is justifiable in the experiments reported here, but of course would not be valid over all wave-length ranges with all gases. Another simplifying assumption which we shall make is that the diameter of the chamber is sufficiently great so that the photoelectrons come to the end of their ionizing range within the gas. In the present experiments it was not difficult to construct the ionization chamber so that this condition was fulfilled. The amount of the energy of the primary beam absorbed in the chamber per second is

$$P(1 - e^{-\mu l}) \equiv PF \tag{1}$$

where μ is the absorption coefficient of the gas for the wave-length of the primary beam. If appreciable amounts of fluorescent or scattered secondary x-rays of sufficient hardness to reach the walls are produced, the power PF is not all expended in producing ions. We shall proceed to set up expressions for the power lost through these secondary x-rays. We shall first treat of the losses through fluorescent radiation. If ν be the frequency of the primary x-ray beam, the number of quanta absorbed per second is $PF/h\nu$. The number of atoms ionized in the K shell per second will be

$$\frac{PF}{h\nu} \cdot \frac{\tau_k}{\mu} \tag{2}$$

where τ_k is the absorption coefficient of the gas corresponding to frequency ν for the ejection of photoelectrons from the K level. The L and softer fluorescent radiations are completely absorbed in the gas in all cases reported here, so that it will not be necessary to consider them. The number of atoms ionized in the K-level per second which recombine by processes involving the emission of K-series x-ray lines is

$$\frac{PF}{h\nu} \cdot \frac{\tau_k}{\mu} w_k \tag{3}$$

where w_k is the fluorescent yield for the K-series as defined by Auger.[3] Let f_i be the fractional part of the total number of quanta emitted having the fre-

quency ν_i of the ith line of the K-series, then the power escaping from the chamber in the form of K-series radiation from the gas may be written

$$\frac{PF}{h\nu}\frac{\tau_k}{\mu}w_k\sum_i f_i h\nu_i e^{-\tau_i r} = w_k PF\frac{\tau_k}{\mu}\lambda\sum_i\frac{f_i}{\lambda_i}e^{-\tau_i r} \tag{4}$$

where τ_i is the fluorescent absorption coefficient of the gas for the ith line of its own K-series, and r is the effective path length of the radiation in the gas before reaching the walls. In an ionization chamber in which $l \gg r$, and in which the absorption of the primary beam is not so pronounced that it is almost all absorbed before penetrating a distance short compared with r into the gas, we may as a first approximation identify r of Eq. (4) with the radius of the chamber.

X-ray energy which has been scattered from the primary beam may also reach the walls before its energy has been expended in the production of ions, and the rate of such loss may be written

$$\frac{\sigma}{\mu}PFe^{-\tau r} \tag{5}$$

where σ is the scattering coefficient of the gas for the primary wave-length, and τ is the absorption coefficient for fluorescent processes for the primary wave-length. In the experimental arrangement to be described later, these secondary x-rays actually reached the metal walls of the chamber, and ejected photoelectrons from them, some of which went back into the gas volume and produced ionization. This effect is not taken into consideration in the equations, and the results show that it must introduce a correction to relative intensities which is less than 2 percent in the wave-lengths studied. Combining Eqs. (1), (4), and (5), we have

$$I = cPFR \tag{6}$$

where

$$R = 1 - \frac{\tau_k}{\mu}w_k\lambda\sum_i\frac{f_i}{\lambda_i}e^{-\tau_i r} - \frac{\sigma}{\mu}e^{-\tau r}. \tag{7}$$

In this expression, I is the ionic saturation current, and c is a constant for the gas which is inversely proportional to ϵ, where ϵ is the energy spent in producing a pair of ions.

If we are comparing the intensities of two lines α and β, we have

$$\frac{P_\alpha}{P_\beta} = \frac{I_\alpha F_\beta R_\beta}{I_\beta F_\alpha R_\alpha} \tag{8}$$

if ϵ is independent of λ, as discussed in the first section. For convenience, we shall write Eq. (8) in the following form

$$P_{\alpha\beta} = I_{\alpha\beta}F_{\beta\alpha}R_{\beta\alpha}. \tag{9}$$

Experimental Procedure and Apparatus

An experimental test of the adequacy of Eq. (9) for relative intensity measurements has been carried out as follows. X-ray beams of constant relative intensity and different wave-length were obtained by using lines in the *L*-series spectrum as diffracted by a calcite crystal from an x-ray tube run at constant voltage and current. Observations were taken on the relative ionic saturation currents resulting from these lines when absorbed in an ionization chamber filled in turn with as many different gases as could be conveniently obtained. The corrections of Eq. (9) were applied and the *P* ratios calculated, with a view to finding out if any variations occurred from gas to gas.

The x-ray tube was of the type previously described by Allison.[4] The equipment for generating the high voltage included a 5 kva 540 cycle generator driven by a 8.5 H.P. synchronous motor with a small d.c. exciter connected in the same shaft. This low voltage 540 cycle current was stepped up

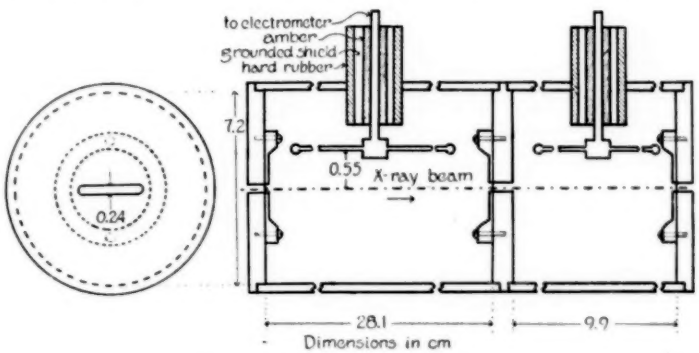

Fig. 1. Diagram of apparatus.

to x-ray voltages in an appropriate transformer, rectified by kenetrons, and smoothed by a condenser of 0.1 microfarad capacity. The high voltage could be read directly from a specially constructed electrostatic voltmeter, the smallest division on the scale of which corresponded to 297 volts in the region between 30 and 40 kv. Half of a division could easily be read so that at 30 kv the voltage could be kept constant to 150 volts or 0.5 percent. The calculated ripple was 0.3 percent at 5 m.a. and 30 kv.

The x-ray beam left the tube through an aluminium window 1.65×10^{-3} cm thick. Its angular divergence was limited by two slits, 25.4 cm apart and each 0.0114 cm wide so that the angular spread of the beam was about 3 minutes of arc. A vertical stop 4 mm high was put in the path of the beam at a point 38 cm from the target of the tube. The distance from the target of the tube to the rear window of the compound ionization chamber was 88 cm. The distance in air traversed by the x-rays before entering the front compartment of the ionization chamber was 37 cm.

The construction of the ionization chamber is of special interest in this investigation, and is shown in Fig. 1. It consisted of two compartments, one

[4] Allison, Phys. Rev. **30**, 245 (1927), Fig. 1.

behind the other. The front compartment (28.1 cm long) was used to measure the ionic saturation currents. The rear compartment was used to measure the F-values directly, since in some of the cases they could not be computed with sufficient accuracy from the tables of absorption coefficients. The collecting electrodes in the front and rear chambers could be alternately connected to the Compton electrometer used. The rear chamber was filled with methyl bromide gas at about 74 cm pressure throughout the whole period of the experiments. Let i_0 be the ionization current in the rear chamber when the front chamber is evacuated, and i the corresponding current when the front chamber contains the gas to be tested. Then,

$$F \equiv 1 - e^{-\mu l} = (i_0 - i)/i_0 \tag{10}$$

and

$$F_{\beta\alpha} = \frac{(i_{0\beta} - i_\beta) i_{0\alpha}}{(i_{0\alpha} - i_\alpha) i_{0\beta}} . \tag{11}$$

From Eq. (11) it is seen that the F-values were obtained directly from observations of ionization currents, and their values obtained in this way are independent of the accuracy of tables of absorption coefficients, or of measurements of the length of the ionization chamber, or of manometric measurements of the pressure of the gas in it.

The diameter of the chamber must be great enough so that ejected photoelectrons come to the end of their ionizing range within the gas. In the experiments reported here, the longest range photoelectrons were those ejected by the uranium $L\gamma_1$ line (0.6136A) in argon. Information on the length of path may be obtained from results of C. T. R. Wilson.[5] The length of path x is roughly given by

$$x = V^2/b$$

where V is the energy of the electron in kilovolt equivalents, and b is a constant. Wilson's results lead to the value of 4.41×10^2 for b in air at atmospheric pressure if x is in centimeters. b is proportional to the density so that in argon at atmospheric pressure b is 6.1×10^2. The quantum voltage of $UL\gamma_1$ is 20.1 kv, hence if one of the outer electrons of the argon atom is ejected (binding energy negligible), x is 0.66 cm. The diameter of the chamber was 7.2 cm, hence in the most unfavorable case the ionization was confined to a narrow bundle down the axis of the chamber.

The x-ray beam entered the front compartment through a window 0.24 cm wide and 2.54 cm high, covered with cellophane 7.6×10^{-3} cm thick in the case of the tungsten L-series experiments, and with aluminium 1.65×10^{-3} cm thick in the experiments with the uranium L series. The window through which the beam left the front chamber was similar in size to the one previously described and covered with mica 1.3×10^{-3} cm thick. The rear window of the rear compartment was covered with a thicker piece of cellophane and was used in sighting through the chamber to adjust it relative to the spectrometer.

[5] Reported in A. H. Compton, X-rays and Electrons p. 256.

The chamber was constructed of brass, which was nickel plated inside to reduce chemical action with the gases. The collecting electrodes were steel rods 1.59 mm in diameter; the length of the rod in the front chamber was 24.8 cm, so that its ends were roughly 1.6 cm from the ends of the front compartment. Connection to these collecting electrodes was made through amber insulators set in through the walls of the chamber and protected by grounded guard rings in the usual manner. The entire walls of the chamber were charged to 277 volts. Between 177 and 277 volts the ionization currents obtainable from a constant x-ray input did not vary by more than 0.5 percent, hence it was judged that saturation had been reached.

A Compton electrometer, mounted over the axis of the spectrometer, was used. The electrometer had a sensitivity of 580 divisions per volt on a scale 96 cm distant. The current through the x-ray tube was adjusted until the strongest line ($L\alpha_1$) gave a rate of deflection of about 8–9 mm per second. The rates of deflection observed varied between this and the base-line rates which were of the order of 0.1 mm per second.

Adjustments and Method of Taking Readings

The ionization chamber was mounted on the arm of a Bragg type spectrometer, in such a way that it could be rotated about a vertical axis through its center. The usual adjustments of the ionization spectrometer were made. The x-ray tube was mounted on a carriage which could be moved in a direction perpendicular to the line joining the centers of the slits, and by observing the ionization currents for a constant spectrometer setting during this translation the center of the tube window could be found. It was also desirable that the beam pass through the centers of the ionization chamber slits. This was accomplished by rotating the ionization chamber about a vertical axis through its center until the ionization curves obtained from the front and rear compartments as the chamber was swung about the axis of the spectrometer with the crystal stationary had a common center. When this had been found, the ionization chamber arm was placed at its angular position locked to the crystal table through a set of 2 to 1 gears, so that the chamber necessarily followed the reflected beam. The height of the beam was observed by turning the ionization chamber to the position corresponding to zero glancing angle, removing the crystal, and placing a fluorescent screen behind the rear window of the chamber. The height of the x-ray tube and of the slit limiting the vertical spread of the beam was adjusted until the fluorescent screen showed that the beam left the rear window of the chamber at its center in the vertical direction.

Two different targets were used, tungsten and uranium, and in each case the $L\alpha_1$, $L\beta_1$ and $L\gamma_1$ lines were selected for the test, these being the strongest lines in the three groups of greatest wave-length separation. Before beginning the experiments on tungsten, for instance, the spectrum in the vicinity of these lines was investigated and the angular settings found on the scale of the spectrometer corresponding to the tips of the peaks, and to convenient adjacent points on the base-line of the general radiation. The front chamber

was then filled with the gas to be tested and the pressure noted on the manometer. The voltage on the x-ray tube was set to the value adopted for the spectrum in question (30 kv for tungsten, 41.2 for uranium), and the electron current was brought to a value which in preliminary trials had been shown to give adequate ionization currents, as previously mentioned. The collecting

TABLE I. *A. Comparison of $L\alpha_1$ and $L\beta_1$ lines of tungsten.*
$\lambda L\alpha_1 = 1.473$A
$\lambda L\beta_1 = 1.279$A

Gas	Pressure	No. of trials	$I_{\alpha\beta}$	$F_{\beta\alpha}$	$R_{\beta\alpha}$	$I_{\alpha\beta}F_{\beta\alpha}$	$I_{\alpha\beta}F_{\beta\alpha}R_{\beta\alpha}$
CH_3I	20.49cm	7	1.614	0.997	1.00	1.609	1.609
CH_3Br	75.00	3	1.623	0.995	1.00	1.615	1.615
Argon	69.43	3	1.715	0.953	1.00	1.632	1.632
SO_2	72.99	4	1.759	0.914	1.00	1.607	1.607
Air	74.30	7	2.421	0.702	.98	1.70	1.66

B. Comparison of $L\alpha_1$ and $L\gamma_1$ lines of tungsten.
$\lambda L\alpha_1 = 1.473$A
$\lambda L\gamma_1 = 1.095$A

Gas	Pressure	No. of trials	$I_{\alpha\gamma}$	$F_{\gamma\alpha}$	$R_{\gamma\alpha}$	$I_{\alpha\gamma}F_{\gamma\alpha}$	$I_{\alpha\gamma}F_{\gamma\alpha}R_{\gamma\alpha}$
CH_3I	20.49cm	7	6.97	0.991	1.00	6.91	6.91
CH_3Br	75.00	3	7.20	0.950	1.00	6.84	6.84
Argon	69.43	3	8.07	0.833	1.00	6.72	6.72
SO_2	72.99	4	8.64	0.791	1.00	6.83	6.83
Air	74.30	7	16.34	0.450	.950	7.35	7.0

TABLE II. *A. Comparison of $L\alpha_1$ and $L\beta_1$ lines of uranium.*
$\lambda L\alpha_1 = 0.9087$A
$\lambda L\beta_1 = 0.7185$A

Gas	Pressure	No. of trials	$I_{\alpha\beta}$	$F_{\beta\alpha}$	$R_{\beta\alpha}$	$I_{\alpha\beta}F_{\beta\alpha}$	$I_{\beta\alpha}F_{\beta\alpha}R_{\beta\alpha}$
CH_3I	20.07 cm	4	3.19	.820	1.00	2.61	2.61
Argon	74.74	3	4.05	.631	.99	2.56	2.53
Krypton	10.10	4	1.65	2.55	.621	4.22	2.62
CH_3Br	14.26	6	2.89	.801	1.15	2.32	2.66

B. Comparison of $L\alpha_1$ and $L\gamma_1$ of uranium.
$\lambda L\alpha_1 = 0.9087$A
$\lambda L\gamma_1 = 0.6136$A

Gas	Pressure	No. of trials	$I_{\alpha\gamma}$	$F_{\gamma\alpha}$	$R_{\gamma\alpha}$	$I_{\alpha\gamma}F_{\gamma\alpha}$	$I_{\alpha\gamma}F_{\gamma\alpha}R_{\gamma\alpha}$
CH_3I	20.07	4	12.8	0.668	1.00	8.56	8.56
Argon	74.74	3	18.6	.463	.98	8.60	8.43
Krypton	10.10	4	6.22	2.04	.675	12.7	7.56
CH_3Br	14.26	7	10.7	.634	1.22	6.78	8.27

electrode of the front compartment was connected to the electrometer, and the ionic saturation currents observed for the base-line near $L\gamma_1$. The spectrometer was then set at an angle 15 seconds of arc less than that which had previously been determined as the peak for $L\gamma_1$, and moved in 15 second steps over the top of the peak. The maximum ionization current observed

was taken as the uncorrected value of the line intensity. This was repeated for the $L\beta_1$, and $L\alpha_1$ lines. By subtracting the base-line readings, a set of I-values was obtained. The electrometer was then connected to the rear compartment, and the same set of readings taken, giving a set of i-values. A set of i_0-values was then obtained by a third repetition of the readings with the front compartment evacuated. From the i and i_0-values, the F-values were calculated from Eq. (11), and thus the IF-values obtained.

Results

The results are shown in Tables I and II. Some remarks on the various processes taking place in the ionization chamber follow.

Tungsten lines in CH_3I.

The wave-lengths of the lines are all between those of the K and L absorption limits of iodine, so that the L-series of iodine (2.5 to 3.2A) was the hardest fluorescent radiation emitted. The scattering is negligible in comparison with the fluorescent absorption. The soft fluorescent rays were all absorbed before reaching the walls of the chamber, hence R is unity, and the P ratios, which in general are IFR, (Eq. (9)), in this case are simply IF.

Tungsten lines in CH_3Br.

The wave-lengths of the lines lie between the K and L-limits of bromine and the situation is similar to the previous case of CH_3I.

Tungsten lines in argon.

The quantum voltage of the lines is sufficient to excite the K-series of argon. Two facts, however, contribute to keep R very near unity. w_k is small, about 0.07, and the argon K-series (about 4A) is highly absorbed on its way to the walls of the chamber.

Tungsten lines in SO_2

The case is somewhat similar to argon in that the sulfur K-series wave-lengths may be excited but as in argon, do not escape to the walls. The scattering coefficient is negligible in comparison with the total absorption coefficient at these wave-lengths.

Tungsten lines in air.

No fluorescent wave-lengths of sufficient hardness to reach the walls are excited. The loss through scattering is appreciable, making R less than 1. See Table III.

In the results with the tungsten spectrum, it is seen that the corrected intensity ratios ($I_{\alpha\beta}F_{\beta\alpha}R_{\beta\alpha}$) are constant to about 1.5 percent, and the $I_{\alpha\gamma}F_{\gamma\alpha}R_{\gamma\alpha}$ ratios constant to within 2.5 percent, in the first four gases. In air slightly higher values are obtained, perhaps due to the uncertainty of the scattering correction. The experimental errors, calculated from the least squares formula as applied to the deviations of the I ratios obtained in various trials, run about 1 percent in the $\alpha\beta$ comparison, and 1.5 percent in the $\alpha\gamma$ ratio, where the weakness of the γ_1 line with respect to the background reduces the accuracy. In air the experimental errors are roughly twice the

above, since F becomes an important factor, which cannot be determined more accurately than I. The tungsten lines covered the wave-length range from 1.095 to 1.473A; the measurements could be extended downward to 0.6136A by using the uranium L-series.

Uranium lines in CH_3I.

The conditions here correspond to the tungsten lines in CH_3I. The fluorescent radiation produced is not sufficiently penetrating to reach the walls and scattering is negligible.

Uranium lines in argon.

The K-series of argon can be emitted, but the previous comments on argon still are valid for fluorescence. The scattering becomes appreciable here, hence R is less than 1. See Table III.

Uranium lines in krypton.

Here we have an interesting case where large deviations from the P ratios given by CH_3I and argon would be expected if the theory were inadequate. The K absorption limit of krypton (0.864A), lies between the $L\beta_1$ and $L\alpha_1$ lines of uranium. The gas is practically transparent to $L\alpha_1$ and opaque to $L\beta_1$. This unusual condition makes the F factor large, and greater than 1, whereas in all the other cases it is less than 1. The product IF, listed in column 7 of the tables, may be considered as the ionization current ratio which would be observed if the entire primary beam were absorbed in a chamber of this diameter. In Table II it is seen that in the case of krypton the IF value is farther from the P-value obtained from argon and CH_3I than is the I-value alone. This discrepancy is clearly due to the excitation of fluorescent radiation by the $L\beta_1$ and $L\gamma_1$ lines of uranium, and the escape of this radiation from the regions from which the saturation current is drawn. The calculated R factor, however, is just the correct one to bring the P ratio in line with the other gases, and gives us great confidence in our analysis of the processes occurring in the ionization chamber.

Uranium lines in CH_3Br.

Here again we have a case of unusual interest, in that although all the uranium lines considered lie on the short wave-length side of the bromine K absorption, $UL\alpha_1$ lies within 1 percent of the limit. The wave-lengths are, $UL\alpha_1$, 0.90874A; Br K-limit, 0.91809A. The photoelectrons ejected from the K-levels of bromine by the $UL\alpha_1$ line have a velocity of only 140 volts, whereas the photoelectrons ejected in all the other cases reported here have velocities of a different order of magnitude, ranging from those ejected by the $UL\beta_1$ line from the K level of krypton (2890 volts) to those ejected from the outer layers of the argon atom by $UL\gamma_1$ (20,100 volts). It was at first thought that this experiment would detect a variation of ϵ, if it existed, since ϵ at 140 volts may conceivably be different from ϵ at the higher range specified above. Further consideration, however, showed that a variation of ϵ would have no measurable effect, since the larger part of the ionization is produced by electrons ejected by internal transitions of the second kind. Thus from 100

atoms of bromine ionized in the K shell by the x-ray beam, there appear 100 photoelectrons, each of only 140 volts energy, but from roughly 44 of these 100 atoms there will appear an Auger electron of approximately $(\nu_K - 2\nu_L)$ or 10,200 volts energy, the ionization from which will entirely mask any due to the photoelectrons. Again we find that our correction formulae are adequate to derive from the observed I ratios, P ratios which agree with those obtained in other gases.

The probable error in the experimental determination of the I-values in the uranium spectrum was calculated from the usual formula.[6] This gave probable errors of about 1 percent in both the $\alpha\beta$ and $\alpha\gamma$ comparisons. In the F-value determinations, the probable error for $F_{\beta\alpha}$ was about 2 percent; for $F_{\gamma\alpha}$ about 4 percent. The experimental errors in the IF-values, and therefore in the P ratios then should be on the order of 3 percent for the $\alpha\beta$ comparison and 5 percent for the $\alpha\gamma$ ratio. The observed deviations in Table II for the $\alpha\beta$ ratio are within 5 percent, and within 3.5 percent for the $\alpha\beta$ ratio. It may therefore be stated that the deviations in the P ratios are such as may be accounted for by the probable errors in the experimental determinations of the I and F factors.

Some apparently anomalous results were obtained by investigating the uranium lines in the chamber when filled with CH_3Br at 74 cm pressure. Under these conditions the $I_{\alpha\beta}$ and $I_{\alpha\gamma}$ were 2.27 and 6.51, respectively. $I_{\alpha\beta}F_{\beta\alpha}$ was found to be 2.26 and $I_{\alpha\gamma}F_{\gamma\alpha}$; 6.41. The R-values, calculated from the radius of 3.4 cm used in all other cases gave $R_{\beta\alpha}=1.11$; $R_{\gamma\alpha}=1.17$, hence P ratios of 2.51 and 7.50 were obtained. These definitely disagree with those of Table II. The explanation of this undoubtedly lies in the fact that r in Eq. (7) is really a function of wave-length and pressure for a given gas. Thus in CH_3Br at 74 cm pressure, 50 percent of $UL\alpha_1$ is absorbed in the first 1.9 cm of path length in the chamber. The effective path length r which fluorescent radiation must travel to reach the walls is clearly less than the radius of the chamber, and different from the appropriate r value for $UL\gamma_1$ rays which penetrate 4.1 cm before being half absorbed. The proper value of r for

TABLE III. *Quantities used in computation of R values. (Eq. (7)).*

Gas	Target	τ_k/μ	τ_i/ρ		r/cm	w_k	f_i			σ/ρ		
			$K\alpha_{1,2}$	$K\beta_1$			$K\alpha_2$	$K\alpha_1$	$K\beta_1$	$L\gamma_1$	$L\beta_1$	$L\alpha_1$
Air	Tungsten	—	—	—	3.4	—	—	—	—	0.31	0.34	0.38
Argon	Uranium	—	—	—	3.4	—	—	—	—	0.44	0.51	0.64
CH_3Br	Uranium	0.85	21	15	3.4	0.565	0.298	0.582	0.116	—	—	—
Krypton	Uranium	0.85	30	21	3.4	0.587	0.298	0.582	0.116	—	—	—

Remarks on sources for data:
The value of τ_k/μ was obtained from Richtmyer and Warburton, Phys. Rev. **22,** 539 (1923).
The values of τ_i/ρ were computed from tables in A. H. Compton's "X-rays and Electrons."
w_k was obtained from A. H. Compton Phil. Mag. **8,** 961 (1929).
f_i values were computed from data on the relative intensity of K-series x-ray lines by H.-T. Meyer, Wissenschaftliche Veröffentlichungen aus dem Siemens-Konzern **7,** 108 (1929).
Scattering coefficients were computed for argon and air for the authors by E. O. Wollan of this laboratory from data reported in his paper (Phys. Rev. **37,** 862 (1931)).

[6] For instance, Birge, Phys. Rev. Suppl. **1,** 1 (1929) p. 5–6.

a given wave-length in this case would be obtained by a rather complicated integration, and has not been attempted, but the deviations are in the right direction to be explained by the effect suggested. This illustrates a pitfall which should be avoided in intensity measurements.

Table III shows the values of the quantities entering Eq. (7) which were used in the calculation of the R-values, and gives the sources from which data were obtained. As a by-product of these experiments, it was possible to calculate the absorption coefficients of the gases used. It must be emphasized again that the validity of the conclusions drawn from these experiments does not depend on the accuracy with which these absorption coefficients are given. (Table IV.) The various gases were obtained from commercial sources and

TABLE IV. *Absorption coefficients of various substances used in intensity measurements.*

λ	μ/ρ							μ	
	CH_3I	Krypton	CH_3Br	Argon	Air	SO_2	Al	Mica	Cellophane
1.473A			51	84	8.3	40	44	123	12
1.279	149		40	55	5.6	28	29		5.5
1.095	106		26	37	3.4	18	20		4.9
.9087	64	24	115	26			10	26	
.7185	34	79	62	13			5.4	13	
.6136	22	59	40	8.9			3.4		

no attempt at purification was made. Although these gases have been widely used in ionization chambers, no data on their absorption coefficients, except for heterogeneous beams, are available.[7]

DISCUSSION

From the results given in Tables I and II, we conclude that ionic saturation currents, corrected by the formulae given in this paper, are a reliable measure of the relative intensities of x-ray spectrum lines, even when these lines lie near critical absorption limits of the gas, and excite fluorescent radiation. Measurements of the relative intensities of the L-series lines of uranium at 52.8 kv[8] and of tungsten at 20 kv[9] have been reported. When the results reported here are corrected for the length of path in air and aluminium between the x-ray tube and the ionization chamber, and brought to the voltages used by Allison and Jönsson respectively, agreements within 10 percent are found.[10] The work of Hicks[11] has shown that if agreements to better than

[7] International Critical Tables, Vol. VI p. 16.

[8] Allison, Phys. Rev. **32,** 1 (1928).

[9] Jönsson, Zeits. f. Physik **36,** 426 (1926).

[10] The present results on tungsten, corrected for absorption in air and in the windows, and expressed at 20 kv instead of the 30 kv at which they were measured, give the $\alpha_1:\beta_1:\gamma_1$ ratios as 100:43.7:9.1; Jönsson found 100:40.8:7.2. The present uranium results, corrected for absorption and brought to 52.8 kv give the $\alpha_1:\beta_1:\gamma_1$ ratio as 100:36.7:10.9; Allison found 100:40.5:9.7.

[11] Hicks, Phys. Rev. **36,** 1273 (1930). Hicks found the relative intensities in the tantalum L spectrum for lines of large wave-length separation to differ markedly from the results obtained

10 percent are to be expected, the coefficient of reflection of the calcite crystal used must be measured for the various wave-lengths. We do not, therefore, wish to stress our results as the relative intensities of the lines until the crystal used has been calibrated.

---

by Jönsson in the adjacent element tungsten. Hicks also reports a qualitative trial on tungsten and states that his apparatus gave results similar to his tantalum measurements and disagreeing with those of Jönsson. The measurements reported in this paper support those of Jönsson and correspondence with Dr. Hicks has disclosed a source of error in his measurements which affected the results on lines of large wave-length separation. This error arose from the construction of his ionization chamber, which permitted the absorption of the lines in a layer of gas directly behind the window of the chamber without the ions produced being measured by the electrometer. This same source of error undoubtedly entered in the earlier experiments of Allison and Armstrong also (Phys. Rev. **26,** 714 (1925). This correction is discussed more fully by Dr. Hicks on page 572 of this issue.

IONIZATION OF HELIUM, NEON, AND ARGON

By R. L. Womer
Washington University, Saint Louis

(Received June 12, 1931)

Abstract

The finding of extra ionization potentials in mercury and potassium vapors, and more recently in nitrogen and carbon monoxide, suggested the problem of examining the ionization curves for helium, neon, and argon in the region of their normal ionization potentials. A modified form of the Hertz space charge method was used. Results with this apparatus have shown that, over the voltage ranges examined, there is only one ionization potential for each of the gases helium, neon, and argon.

Introduction

THE results of various investigations by electron impact, revealing the presence of several extra ionization potentials in mercury vapor, have been summarized by Smith.[1] Lawrence's and Edlefsen's[2] study of the ionization of potassium vapor by ultraviolet light has shown an extra-ionization potential in this vapor. This result has been verified by Hughes and Van Atta,[3] using electrons as the ionizing source. More recently Smith[4] has reported the finding of these extra-ionization potentials in nitrogen and carbon monoxide.

In a study of ionization efficiencies by electron impact, Smith[5] observed that in the cases of helium, neon, and argon, the ionization efficiency is a smoothly increasing function of the voltage in the neighborhood of the ionization potentials. It was deemed worth while, however, to make a careful examination of these gases over the voltage ranges just mentioned, with the idea of finding any discontinuities in the ionization curves that might have escaped previous observers.

Apparatus and Results

The experimental tube used in this work was very similar in principle to that used by Hughes and Van Atta[3] in their study of potassium vapor. Electrons from the outer filament, however, were accelerated into an enclosed nickel cylinder through a narrow slit in a nickel shield, placed just outside a gauze-covered opening in the side and near the end of the cylinder. A hairpin type filament was mounted inside and near the opposite end of the cylinder in a manner described by Foote and Mohler.[6] Both filaments were of 4 mil tungsten.

[1] P. T. Smith, Phys. Rev. **37,** 808 (1931).
[2] E. O. Lawrence and N. E. Edlefsen, Phys. Rev. **34,** 1056 (1929).
[3] A. L. Hughes and C. M. Van Atta, Phys. Rev. **36,** 214 (1930).
[4] P. T. Smith, Phys. Rev. **36,** 1293 (1930).
[5] P. T. Smith, 170th Meeting of the American Physical Society, April, 1931.
[6] P. D. Foote and F. L. Mohler, Phys. Rev. **26,** 195 (1925).

The electrical circuit was essentially the same as that of Hughes and Van Atta.[3] Two potentiometers provided variable accelerating voltages between the outer filament and the slit, and the slit and cylinder respectively. In most of the work the field between the shield and cylinder was kept constant, the varying field being applied between filament and shield. This method gave an electron current to the cylinder that was practically independent of the accelerating voltage. This electron current was always small (a small fraction of a percent) as compared to the space charge limited current between the hairpin filament and the cylinder.

Gas pressures were used which were sufficiently high to insure that practically all the electrons entering the cylinder from the outer filament suffered

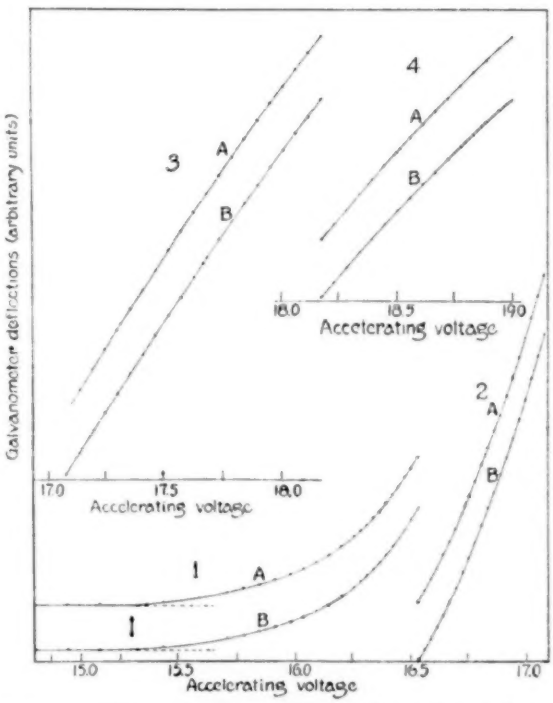

Fig. 1. *A* and *B* denote different runs. The zeros of the ordinates for parts 1, 2, 3 and 4 are displaced so as to allow a better representation of results.

a collision. The necessary pressures were calculated from Normand's[7] data. The gases were allowed to flow into the apparatus through a small capillary and were pumped out through small holes, the effective number of which could be regulated by a mercury cut-off arrangement. Using this "flow method," a wide range of pressures could be obtained in the apparatus.

The helium was purified by twice passing it over charcoal immersed in liquid oxygen. The neon and argon were supplied as spectroscopically pure, and were used directly from their containers. An ionization potential test, however, revealed the presence of a slight trace of argon in the neon. This did not affect the results in neon, except in a quantitative sense.

[7] C. E. Normand, Phys. Rev. **35**, 1217 (1930).

Mercury vapor was kept out of the apparatus by means of mercury traps immersed in a mixture of dry ice and *n*-butyl alcohol. The experimental tube was outgassed before each series of readings.

The accompanying curves (Fig. 1) show typical results in argon. The deflections of the balanced galvanometer are plotted as functions of the accelerating voltages between the outer filament and the cylinder. The voltage at which ionization commenced was arbitrarily taken as the normal ionization potential for the gas, this being a standard to which the other voltages were referred. The curves are seen to be absolutely smooth throughout the range studied, which is characteristic of some thirty curves taken in argon.

The curves for helium and neon are very similar in shape to those shown for argon. They display the same smoothness throughout. Over twenty curves were run in each of these two gases under varying conditions of gas pressure, ionizing electron current, and space charge limited current.

The slow increase in ionization, starting at the ionization potential, is not a real effect, but is due to the thermal distribution of velocities of the ionizing electrons emitted from the outer filament. Velocity distribution curves, plotted to the correct voltage scales, were found to fit closely the ionization curves over a range of about a volt above the potentials of the three gases.

The conclusion to be drawn from this work is that there are no extra-ionization potentials in helium, neon, or argon. In the case of helium it is believed that any ionization potentials separated by 0.3 volts could be detected. A separation of 0.12 volts for ionization potentials in neon and argon could be observed. The voltage ranges examined are as follows:

Helium	24.5–29.8 volts
Neon	21.5–26.0 volts
Argon	15.3–19.0 volts

The writer wishes to thank Dr. A. L. Hughes, under whose direction this problem was undertaken, for the many helpful suggestions that made possible the completion of this work.

THE INFRARED SPECTRUM OF SN I

By H. M. Randall and Norman Wright
University of Michigan
(Received June 12, 1931)

Abstract

An open arc of 80 amperes between a carbon rod and tin pool has been used as source, and observations have been made using a grating spectrometer and thermopile. The wave-lengths of forty-five new lines of the tin arc spectrum in the region from 1μ to 3μ have been measured, and rough determinations of the relative intensities of the strong lines have been made. Nine energy levels of the $5s^25p6p$ configuration have been found, which with the one found by Green and Loring complete the set. Three of the four levels of the $5s^25p(^2P_{1/2})4f$ set have been found, and the fourth, 3_3, has been accounted for as lying too close to 4_2 for resolution. With the fixing of these levels all the strong infra-red lines have been classified. The finding of the levels $5p(^2P_{1/2})4f4_2$ and $5p(^2P_{1/2})5f4_2$ has made possible a good determination of the absolute term values.

THE tin atom in its lowest state has the electron configuration $5s^25p^2$ which gives rise to five low energy levels. The next higher groups of levels from which transitions can be made to the low levels are those due to the configurations $5s^25p6s$ and $5s^25p5d$. The relative term values of these levels have been well established by the work of McLennan, Young, and McLay,[1] Sponer,[2] and Zumstein.[3] A tentative classification of the levels was made by Sur.[4] Later Back[5] and Green and Loring[6] observing Zeeman effects corrected and practically completed the classification. A study of the spectrum of SnII by Green and Loring[6] showed the separation of the $5s^25p^2P_{\frac{1}{2},1\frac{1}{2}}$ levels to be 4252 cm^{-1}.

Another configuration of the neutral tin atom, $5s^25p6p$, gives rise to ten levels which of course cannot combine with the levels of the normal configuration $5s^25p^2$ but which can combine with the levels of both the $5p6s$ and $5p5d$ configurations. These ten levels should be divided into two groups, a group of four levels with $J=0, 1, 1, 2$ built upon the $5p^2P_{1/2}$ state of SnII, and above these by roughly the SnII ^2P separation a group of six levels with $J=0, 1, 1, 2, 2, 3$ built upon the $5p^2P_{1\frac{1}{2}}$ state of SnII. Green and Loring using the infra-red lines measured by Randall[7] found only the $5p(^2P_{1/2})6p3_1$ (designated $^3P_1$) level of this set. The purpose of this work was to re-investigate the region of the tin arc spectrum from 0.8μ to 1.3μ observed by Randall and to extend the measurements to 3μ in the hope of finding more of these levels.

[1] J. C. McLennan, J. F. T. Young, and A. B. McLay, Trans. Roy. Soc. Canada Sec. III, 57 (1924).
[2] H. Sponer, Zeits. f. Physik **32,** 19 (1925).
[3] R. V. Zumstein, Phys. Rev. **27,** 150 (1926).
[4] N. K. Sur, Zeits. f. Physik **41,** 791 (1927).
[5] E. Back, Zeits. f. Physik **43,** 309 (1927).
[6] J. B. Green and R. A. Loring, Phys. Rev. **30,** 575 (1927).
[7] H. M. Randall, Astrophys. J. **34,** (1911).

Experimental

The source of radiation was an open air arc, a pool of molten tin in a carbon or iron cup forming the cathode and a carbon stick the anode. The current was taken from a 250 volt d.c. motor-generator and maintained at an average of 80 amperes. The nitrogen, oxygen, and carbon lines which come out strongly at a current of 125 amperes could not be detected at 80 amperes. The only impurity which gave lines of observable intensity was potassium which was present in the carbons.

The spectrometer employed in this work is a grating instrument that has been in use in this laboratory for many years. It was recently described by Ingram[8] in his work on carbon and nitrogen. The thermopile and thermorelay were also described by him. For this work a Michigan grating, of echelette type, ruled by Barker on a nickel surface, gave very good intensity throughout the spectral region covered. It was ruled with 14400 lines per inch. With the slit width used a spectral range of 10A at 1.5μ was transmitted. The smallest separation resolvable was probably about 15A. The method of setting upon lines for measurement was that described by Randall.[7] The error in the measurements is roughly within 2A.

Since the deflection of the galvanometer as any particular line was observed varied greatly depending on the level of the tin in the pool, the gap length, etc., the relative intensities of a number of the stronger lines were obtained in the following manner. The arc would be struck and allowed a few seconds to become steady after which the instrument would be turned in succession over two adjacent lines and back again, the galvanometer deflection in each case being noted. The arc would then be shut off, the whole process having required about one minute. Then one of these lines and its other neighbor would be selected and the process repeated. The ratios of the deflections for adjacent lines were then computed. Taking a deflection of 2000 mm as average for the line λ11457A, the corresponding deflections for the other lines were found using these ratios. The deflections calculated in this manner are in italics in Table I. For adjacent lines the ratio of the intensities as given should not be in error by more than 15 percent. The intensities not in italics in the table are merely rough averages of the galvanometer deflections taken at different times.

Sn I Wave-lengths and Assignments

Table I is a list of the newly measured infrared wave-lengths together with the previous measurements of Randall. Some photographic lines measured by Walters[9] which have been classified in this work are added at the end of the table. Table II gives the classified levels of Sn I. Levels found in this work are marked by asterisks.

The levels sought, i.e. those of the $5p6p$ configuration, were all found. The positions of two of these levels, $5p6p6_3$ and $5p6p9_0$, were based on but one combination each; the justification of this will be seen in what follows. The

[8] S. B. Ingram, Phys. Rev. **34**, 421 (1929).
[9] F. M. Walters, Bur. Stand. J. 411 (1921).

TABLE I.

Wave-lengths (I. A.)	Wave-numbers (vacuum)	Int.	$\nu_{calc} - \nu_{obs}$	Assignments
24740.0	4041.0	40		
24329.0	4109.2	40	0.5	$6s^1P_1^0 - 6p3_1$
22999.0	4346.8	30		
22133.5	4516.8	40	1.9	$6p10_1 - 7s^1P_1^0$
21688.0	4609.6	80	1.4	$6p8_2 - 7s^3P_2^0$
20863.5	4791.8	400	1.2	$6p4_2 - 7s8_1^0$
20624.0	4847.4	200	1.6	$6p3_1 - 7s7_0^0$
20596.2	4854.0	70	1.8	$6p3_1 - 7s8_1^0$
17809.3	5613.5	100	2.5	$6p3_1 - 5d10_1^0$
17746.5	5633.4	70	1.7	$6p2_0 - 5d10_1^0$
17200.0	5812.4	40	1.0	$6p5_1 - 7s^3P_2^0$
17021.7	5873.3	100	1.7	$6p1_1 - 7s7_0^0$
17002.3	5880.0	200	1.8	$6p1_1 - 7s8_1^0$
16383.0	6102.2	70	1.2	$6p5_1 - 7s^1P_1^0$
15795.5	6329.2	30	−0.2	$6p1_1 - 5d9_2^0$
15751.5	6346.9	70		
15637.0	6393.3	100		
15586.0	6414.2	50		
15466.0	6464.0	300	1.2	$6p4_2 - 5d11_3^0$
15369.0	6504.9	100		
15057.0	6639.7	100	2.3	$6p1_1 - 5d10_1^0$
15020.0	6656.0	130		
14799.0	6755.4	60		
14670.0	6814.8	100		
14484.0	6902.3	100		
13610.0	7345.5	*1440*	0.9	$6s^1P_1^0 - 6p5_1$
13462.0	7426.3	*3780*	0.2	$6s^3P_1^0 - 6p1_1$
13351.0	7488.0	30	0.0	$5d1_2^0 - 7p4_2$
13322.7	7504.0	70	0.5	$5d10_1^0 - 4f5_2$
13083.3	7641.2	*675*	1.8	$6p3_1 - 6d1_2^0$
13020.3	7678.3	*1870*	0.0	$5d4_3^0 - 4f2_4$
13022.0*				
13002.1	7689.0	200	0.5	$5d4_3^0 - 4f4_2$
12983.5	7700.0	*1870*	0.0	$6s^3P_0^0 - 6p1_1$
12982.9*				
12936.0	7728.2	30		
12890.3	7755.7	*890*	0.8	$5d3_1^0 - 4f4_2$
12847.0	7781.3	*160*		
12790.0	7816.4	*370*	1.1	$5d9_2^0 - 4f5_2$
12535.3	7975.2	*845*	−0.6	$6s^3P_2^0 - 6p5_1$ and
			2.9	$6s^1P_1^0 - 6p7_2$
12336.0	8104.1	*330*	−0.6	$5d2_2^0 - 4f1_3$
12316.6	8117.0	*1110*	4.0	$5d2_2^0 - 4f4_2$
12056.3	8292.2	30		
12010.1	8324.0	*480*	1.2	$6p4_2 - 6d4_3^0$
11935.4	8376.2	*2540*	0.0	$6s^3P_2^0 - 6p6_3$
11935.3*				
11854.4	8433.4	*1060*	0.0	$6s^3P_1^0 - 6p2_0$
11853.3*				
11827.5	8452.6	*960*	−0.1	$6s^3P_1^0 - 6p3_1$
11827.2*				
11742.1	8515.3	*2580*	0.0	$6s^3P_1^0 - 6p4_2$
11741.9*				
11693.8	8549.2	*250*	−0.5	$6s^1P_1^0 - 6p8_2$ also Potassium

TABLE I (*Continued*)

Wave-lengths (I. A.)	Wave-numbers (vacuum)	Int.	$\nu_{calc} - \nu_{obs}$	Assignments
11671.6 11672.6*	8565.2	*760*	−0.2	$5d1_2^0 - 4f1_3$
11652.0	8579.8	125	2.7	$5d1_2^0 - 4f4_3$
11617.7 11618.0*	8605.0	*2000*	1.4	$6s^3P_2^0 - 6p7_3$
11533.3	8668.1	30	0.9	$6p1_1 - 6d1_2'$
11457.5 11457.3*	8725.7	*2000*	0.3	$6s^3P_0^0 - 6p3_1$
11340.0 11339.4*	8816.3	*170*		
11279.5 11279.2*	8863.2	*560*	0.0	$6s^1P_1^0 - 6p9_0$
11216.8	8912.8	80		
11194.1 11194.0*	8931.0	*700*	0.0	$6s^1P_1^0 - 6p10_1$
10942.0	9136.6	30	−0.6	$6p1_1 - 6d3_1^0$
10895.1 10896.0*	9176.0	*540*	1.0	$6s^3P_2^0 - 6p8_2$
10809.5 10808.8*	9248.6	*110*		
10705.0	9338.9	30	1.6	$5d5_2^0 - 4f5_2$
10457.1 10458.6*	9560.4	*250*	−1.1	$6s^3P_2^0 - 6p10_1$
9852.1 9852.5*	10147.4	125		
9808.7*	10192.3	—	−0.3	$5d4_3^0 - 5f4_2$
9746.0*	10257.9	40	1.1	$5d3_1^0 - 5f4_2$
9414.9*	10618.6	30	4.9	$5d2_2^0 - 5f4_2$
9018.9**	11084.8	(1)	0.2	$5d1_2^0 - 5f4_2$
8552.6**	11689.1	(7)30	0.0	$6s^3P_1^0 - 6p5_1$
8391.3**	11913.9	(2)	−2.4	$5d4_2^0 - 4f5_2$
8357.03**	11962.7	(4)	−0.1	$6s^3P_0^0 - 6p5_1$
8345.38**	11979.4	(1)	−1.1	$5d3_1^0 - 4f5_2$
8114.06**	12320.9	(7)	0.0	$6s^3P_1^0 - 6p7_2$
8100.42**	12341.7	(2)	1.3	$5d2_2^0 - 4f5_2$
7808.25**	12803.4	(1)	1.1	$5d1_2^0 - 4f5_2$
7754.94**	12891.5	(2)	−0.1	$6s^3P_1^0 - 6p8_2$
7685.29**	13008.3	(1)	−0.1	$6s^1P_1^0 - 4f4_2$
6444.83**	15512.0	(2)	−1.3	$6s^1P_1^0 - 5f4_2$
6149.67**	16256.6	(6)	0.1	$6s^3P_1^0 - 7p4_2$
5801.79**	17231.3	(1)	−1.1	$6s^1P_1^0 - 4f5_2$
5761.77**	17351.0	(2)	0.0	$6s^3P_1^0 - 4f4_2$
2148.71	46524.8	(3)	−0.8	$5p^{23}P_1 - 7s7_0^0$

* Previous measurements of Randall[7]
** Measurements of Walters[9]

level $5p6p6_3$ was expected to combine strongly with $5p6s^3P_2^0$. Also $5p6p9_0$ was expected to combine with $5p6s^1P_1^0$ but with less intensity. However there remained still to be classified, including the above two lines, six fairly strong infrared lines as well as several others of somewhat smaller intensity.

In order to account for the rest of these strong lines the levels of the configuration $5p(^2P_{1/2})4f$ were then sought. There were to be expected four of these levels with $J=2, 3, 3, 4$ which should combine with the $5p(^2P_{1/2})5d$ set to give eleven lines. Also transitions from the $5p4f$ set to the $5p6s$ set are possible by two-electron jumps. These four $4f$ levels were expected to lie fairly close together.

A level was found having the relative term value 52265.5 cm^{-1} and $J=2$ which combines with all four of the $5p(^2P_{1/2})5d$ levels to give infrared lines. It also combines with $5p6s^3P_1^0$ and $5p6s^1P_1^0$ giving photographically measured lines. Another level having $J=2$ and relative term value 54768.0 cm^{-1} was found which also combines with the four $5p(^2P_{1/2})5d$ levels and with $5p6s^1P_1^0$. These levels were assumed to be the $5p(^2P_{1/2})4f4_2$ and $5p(^2P_{1/2})5f\ 4_2$ respectively. Fitting these two levels to a Rydberg series assigns to them the absolute term values 6926.5 cm^{-1} and 4424.0 cm^{-1}. As is to be expected these term values are quite hydrogenic being equal to $R/(3.980)^2$ and $R/(4.980)^2$ respectively. The absolute term value of the lowest level of SnI thus becomes 59192.0 cm^{-1}, a value 498 cm^{-1} smaller than that given by Green and Loring.

The calculated frequencies of the combinations of the $5p4f\ 4_2$ level with $5p6s^3P_1^0$, $5p6s^1P_1^0$, and $5p5d\ 3_1^0$ are in good agreement with the observed frequencies. In the case however of the combinations of $5p4f\ 4_2$ with $5p5d\ 1_2^0$ and $5p5d\ 2_2^0$ the calculated frequencies are a few units higher than the observed values. This points definitely to the fact that the $5p4f\ 3_3$ level must lie several units below $5p4f\ 4_2$ so that combinations of both these levels with a single $5p5d$ level give lines so close as to be unresolved with the apparatus used. The $5p4f\ 1_3$ level was found by means of its combinations with $5p5d\ 1_2^0$ and $5p5d\ 2_2^0$. Its combination with $5p5d\ 4_3^0$ gives a calculated frequency so close to the strong line $\nu 7678$ cm^{-1} that it is undoubtedly obscured by it. The $5p4f\ 2_4$ level was expected to lie close to the other $4f$ levels and to combine with $5p5d\ 4_3^0$ to give a quite strong line. The only unclassified line which fulfills these conditions is $\nu 7678$ cm^{-1} and so it may safely be assigned this origin. This fixes the term value of $5p4f\ 2_4$ at 6937.7 cm^{-1}.

There now remained two unclassified strong lines, $\nu 8376$ cm^{-1} of strength 2540 and $\nu 8863$ of strength 560. As there apparently remained but the two possible origins, viz, the previously mentioned $5p6s^3P_2^0-5p6p\ 6_3$ and $5p6s^1P_1^0-5p6p\ 9_0$, the lines were given these respective classifications thus fixing the values of the $5p6p\ 6_3$ and $5p6p\ 9_0$ levels.

Another high level was found (term value 2704.5 cm^{-1}, designation $5p(^2P_{1\frac{1}{2}})4f\ 5_2$ which combines with the four $5p(^2P_{1/2})5d$ levels and with $5p6s^1P_1^0$. Obviously this is one of the $5p(^2P_{1\frac{1}{2}}4f$ levels since its separation from the mean of the $5p(^2P_{1/2})4f$ levels is very close to the $5s^25p^2P_{\frac{1}{2},1\frac{1}{2}}$ separation of SnII, and since it also combines with several of the $5p(^2P_{1\frac{1}{2}})5$ levels to give observed infrared lines.

TABLE II. *Term Values of Sn I.*

Normal $5s^25p^2$	$^3P_0$ 59192.0	$^3P_1$ 57500.0	$^3P_2$ 55764.0	$^1D_2$ 50578.5	$^1S_0$ 42029.0
$5s^25p(^2P_{\frac{1}{2}})6s$	$^3P_0^0$ 24551.0	$^3P_1^0$ 24277.5	$5s^25p(^2P_{1\frac{1}{2}})6s$	$^3P_2^0$ 20563.0	$^1P_1^0$ 19934.7
$7s$				6775.	6485.
$5s^25p(^2P_{\frac{1}{2}})6p$	1_1 16851.0*	2_0 15844.1*	3_1 15825.0	4_2 15762.2*	
$7p$	8436.0	8347.6	8078.5	8021.0*	
$5s^25p(^2P_{\frac{1}{2}})5d$	$^3D_2^0$ 1_2^0 15509.0	$^3F_2^0$ 2_2^0 15047.5	$^3D_1^0$ 3_1^0 14683.0	$^3F_3^0$ 4_3^0 14616.0	†
$6d$	8182.	8029.	7715.	7437.	
$5s^25p(^2P_{1\frac{1}{2}})6p$	5_1 12588.4*	6_3 12187.2*	7_2 11956.6*	8_2 11386.0*	9_0 11071.5* 10_1 11003.7*
$5s^25p(^2P_{1\frac{1}{2}})5d$	$^1D_2^0$ $^3D_3^0$		$^3P_1^0$	$^3P_2^0$ $^3P_1^0$	$^1F_3^0$ $^1P_1^0$ †
and	5_2^0 6_3^0	7_0^0	8_1^0	9_2^0 10_1^0	11_3^0 12_1^0
$5s^25p(^2P_{\frac{1}{2}})7s$	12045. 11704.	10976.*	10969.2	10522. 10209.	9297. 9065.
$5s^25p(^2P_{\frac{1}{2}})4f$	1_3 6944.*	2_4 6937.7*	3_3 —	4_2 6926.5*	
$5f$				4424.0*	
$5s^25p(^2P_{1\frac{1}{2}})4f$	5_2 2704.5*				

† Old Notation * New Levels

The levels designated in this work as $[5p(^2P_{1/2})7s$ and $5p(^2P_{1\frac{1}{2}})5d]8_1^0$ and 10_1^0 were given the designations $5p(^2P_{1/2})7s\,^3P_1^0$ and $5p(^2P_{1\frac{1}{2}})5d\,^3P_1^0$ respectively by Green and Loring while Back classified them in the reverse order. In cases such as this when the levels of two odd or two even configurations intermingle there is no real significance in assigning a level either to one or to the other of the configurations since in a manner of speaking it belongs to both. Even the g-sum rule no longer holds in such cases, and no considerations of positions of levels or of intensities of lines can be made criterions for the assignment of the level to a particular one of the configurations.

The only new level of odd configuration found in this work is that designated $[5p(^2P_{1/2})7s$ and $5p(^2P_{1\frac{1}{2}})5d]7_0^0$, which lies quite close to the 8_1^0 level of this set.

ON THE HYPERFINE STRUCTURE OF HEAVY ELEMENTS

By G. Breit
Department of Physics, New York University

(Received June 26, 1931)

Abstract

The ordinary theory of hfs splitting is incomplete for two reasons in the case of heavy elements. (1) When the electron is close to the nucleus its velocity is high. Nonrelativistic approximations to Dirac's equation become meaningless. (2) The probability of the electron being sufficiently close to the nucleus to interact with it at all may be appreciably different for different components of the same multiplet. General relativistic formulas (12), (12″) are derived for single electron spectra. Quantitative estimates are made for the specific case of the Tl lowest p term. The nonrelativistic approximations with the same $\overline{r^{-3}}$ for $p_{1/2}$ and $p_{3/2}$ are found to give values of $(\Delta\nu)p_{1/2}/(\Delta\nu)p_{3/2}$ which are too small by a factor of about $3.4=2\times1.7$. The factor 2 is attributable to relativistic corrections. The estimated factor 1.7 is due to the higher energy of the $p_{3/2}$ level which decreases the chance of the electron to be close enough to the nucleus to interact with it. Comparison with the observations of John Wulff on Tl I shows that even the corrected value of $(\Delta\nu)p_{1/2}/(\Delta\nu)p_{3/2}$ is too small by a factor of 2. A qualitatively similar disagreement exists for Bi I. The observed hfs of these elements is therefore not accounted for by the theory of a nuclear magnetic moment.

ACCORDING to the recent theoretical analysis of Goudsmit[1] the hyperfine structure of Bi and Tl is in disagreement with simple theoretical expectations. The outstanding final result is that the hfs splitting of a $p_{3/2}$ single electron state is anomalously small in comparison with the hfs splitting of a $p_{1/2}$ state. There are two omissions in the simple theory used by Goudsmit: (1) the electron is treated nonrelativistically, and (2) the difference in energy of the two p states is neglected i.e. the spin orbit coupling giving rise to doublet structure is supposed to be small. For heavy atoms both omissions may be expected to be of importance. The approximations involved in the nonrelativistic treatment amount to a neglect of higher powers of αZ where α is the fine structure constant and Z is the atomic number. For Tl $\alpha Z=81/137.3$ and is not small. As a result the $p_{1/2}$ state is somewhat similar to an s state and is subject to a large splitting. The difference in energy of $p_{3/2}$ and $p_{1/2}$ is also large being of the order of 0.9 volt. The necessity of considering these effects has been pointed out in a recent letter to the Physical Review.[2] In the present note a quantitative estimate of their influence is made for the case of Tl.

The splitting ratio $(\Delta\nu)p_{1/2}/(\Delta\nu)p_{3/2}$ as given by the simple nonrelativistic theory is found to be too small. The relativistic corrections close to the nucleus increase the ratio by a factor of 2. In addition there is a further increase of the ratio by a factor of approximately 1.7. This is due to the higher energy

[1] S. Goudsmit Phys. Rev. **37,** 663 (1931).
[2] Breit, Phys. Rev. **37,** 1182 (1931).

of $p_{3/2}$ which makes it easier for the valence electron to escape from the inner shell. The proper function is depressed by approximately $(1.7)^{1/2}$ in the region of its first four half waves. Both effects owe their origin to the same cause: the large value of αZ. The first effect is due to an essential difference in the radial distribution of "current density" of the two p states at distances of the order of 0.02 to .005 of a Bohr radius (0.528A). The second is due to differences in radial distribution on the periphery of the atom, which affects the magnitude of electron currents close to the nucleus without affecting their distribution.

The simple nonrelativistic theory gives therefore a too small value of $(\Delta\nu)p_{1/2}/(\Delta\nu)p_{3/2}$ by a factor of about 3.4. A deliberately wrong way of treating the proper function in the neighborhood of its last and most important maximum gives about 4.4 for the same factor. This deliberately wrong calculation affects the nuclear g factor by a factor of about 5. It is believed therefore that the results are fairly independent of possible inexactness in the computation of the proper functions as long as one is primarily interested in the comparison of the $p_{1/2}$ and $p_{3/2}$ splittings.

The experiments of Wulff[3] indicate that the disagreement with the nonrelativistic formulas is by a factor of about 7. On making a correction for the effects discussed here there remains a discrepancy between theory and experiment by a factor of $7/3.4=2$. The splitting of the $p_{1/2}$ level is twice as large in comparison with that of $p_{3/2}$ as it should be according to the theory of a fixed magnetic moment of the nucleus. In order to account for Wulff's results it seems necessary to consider other types of interaction. Of the two states the $p_{1/2}$ is the more penetrating. Qualitatively the anomaly is such as though at close distances from the nucleus the interaction between the nucleus and the electron became greater than it should be on the hypothesis of a nuclear magnetic moment.

General Relativistic Treatment

We suppose for the present purpose that the nucleus is a rigid point charge of electrostatic charge Ze and magnetic moment

$$g\mu_0 \boldsymbol{I}$$

where $\mu_0=eh/4\pi mc$ is the Bohr magneton. The angular momentum is $\boldsymbol{I}$ in units $h/2\pi$. The factor g is a pure number which may be called the Landé g-factor for the nucleus. The magnetic moment $\boldsymbol{I}$ may be represented by a matrix. The maximum proper value of a component of $\boldsymbol{I}$ is denoted by i. The interaction energy of the electron with the nucleus is

$$+\frac{e}{c}\boldsymbol{\alpha}\cdot g\mu_0 r^{-3}[\boldsymbol{r}\times\boldsymbol{I}]. \tag{1}$$

Here $\boldsymbol{\alpha}=(\alpha_1, \alpha_2, \alpha_3)$ is the vector composed of the first three of Dirac's α's.

[3] John Wulff, Zeits. f. Physik **69**, 70 (1931).

The charge of the electron is taken to be $(-e)$. The angular momentum of nucleus and electron together is

$$\boldsymbol{F} = \boldsymbol{J} + \boldsymbol{I} \tag{2}$$

where $\boldsymbol{J}$ is the angular momentum of the electron alone. In the usual notation the maximum proper values of components of $\boldsymbol{F}$ and $\boldsymbol{J}$ are written f, j. The interaction energy (1) is of the form

$$\boldsymbol{A}\cdot\boldsymbol{I} \tag{1'}$$

with $\boldsymbol{A}$ involving only the electron variables. The first order perturbation in the energy is

$$\Delta w = (\boldsymbol{AJ})_j[f(f+1) - i(i+1) - j(j+1)]/[2j(j+1)]. \tag{3}$$

Here $(\boldsymbol{AJ})_j$ is the value of any diagonal element in the matrix $\boldsymbol{AJ}$ in that part of it which belongs to the quantum number j. We have

$$\boldsymbol{A} = (ge\mu_0/c)r^{-3}[\boldsymbol{\alpha}\times\boldsymbol{r}]. \tag{4}$$

In order that (3) should hold it is sufficient that the commutation relations

$$[J_x, A_x] = 0, \quad [J_x, A_y] = iA_z \text{ etc.}$$

be satisfied. This is the case. The substitution of Landé's cosine into the classical precession formula made in (3) is therefore justified whenever the hfs splitting is small in comparison with the multiplet structure.

Nonrelativistically

$$(\boldsymbol{AJ})_j = 2g\mu^2_0 l(l+1)\overline{(r^3)} \tag{5}$$[4]

where l is the azimuthal quantum number. The relativistic value of $(\boldsymbol{AJ})_j$ can be obtained by direct calculation. It is much simpler however to avoid such rather complicated calculations by determining only the form of $(\boldsymbol{AJ})_j$ and then fixing the factor by comparison with (5).

The separation of angles from the radial distance for Dirac's equation in a central field has been made by Dirac and Darwin. We find it convenient to use the radial functions denoted by Gordon as ψ_1, ψ_2. In order to distinguish them from the components of the wave-function $\Psi = (\psi_1, \psi_2, \psi_3, \psi_4)$ we call them ϕ_1, ϕ_2. The ψ_μ in terms of the ϕ_1, ϕ_2 may be written as

$$= \frac{1}{r}(i\phi_1\rho_3,\ i\phi_1\rho_4,\ \phi_2\tau_3,\ \phi_2\tau_4) \tag{6}$$

where $\rho_3=\rho_1-\tau_1$, $\rho_4=\rho_2-\tau_2$, $\tau_3=\rho_1+\tau_1$, $\tau_4=\rho_2+\tau_2$ and ρ_1, ρ_2, τ_1, τ_2 are angular functions used by Weyl. The important thing for us is not the form of the functions ρ, τ but the fact that they enter Ψ as shown in (6). The differential equations satisfied by ϕ_1, ϕ_2 may be mentioned at this point for future reference. They are

[4] Pauling and Goudsmit, McGraw Hill, 1930. p. 225. The present derivation of the relativistic result is an almost exact parallel of a short derivation of (5) given by the writer (Phys. Rev. **37**, 51 (1931). The $\overline{\boldsymbol{A}}$ of the present text corresponds to $g\mu_0\overline{\boldsymbol{A}}$ of the just mentioned note.

$$\frac{d\phi_1}{dr} - \frac{j'\phi_1}{r} = [(2\pi/\Lambda)(1 - E/mc^2) + V]\phi_2$$
$$\frac{d\phi_2}{dr} + \frac{j'\phi_2}{r} = [(2\pi/\Lambda)(1 + E/mc^2) - V]\phi_1 \tag{7}$$

$j' = -1, 1, -2$, etc. for s, $p_{1/2}$, $p_{3/2}$, . . . where $\Lambda = h/mc$ is the Compton wavelength, E is the energy and V is the potential energy.

In order to find $(\boldsymbol{AJ})_j$ it is sufficient to find the diagonal matrix element of $\boldsymbol{A}$ corresponding to the magnetic quantum number $m = j$. If this matrix element be called a then $(\boldsymbol{AJ})_j = (j+1)a$. To find a we must integrate $\Psi^*(\alpha_1 y - \alpha_2 x)\Psi$ over the whole configuration space. An inspection of (6) and the matrices α_1, α_2 shows that the summation over the spin variables brings in a common factor $\phi_1\phi_2/r^2$. The radius r is contained in this combination only. Besides there is also a factor involving the polar angles which gives rise on integration to a number depending on l, j but not on a. Thus $(\boldsymbol{AJ})_j$ is $C(l, j)\int_0^\infty \phi_1\phi_2 r^{-2}dr$. The function $C(l, j)$ may be determined by comparison with (5). The radial properties of the proper function are contained in (5) only in $\overline{(r^{-3})}$. We look, therefore, for a connection between $\overline{(r^{-3})}$ and $\int_0^\infty \phi_1\phi_2 r^{-2}dr$. This is given by the two Eqs. (7). We multiply the first by ϕ_1, the second by ϕ_2 and add, thus eliminating V. The result we divide by r^2 on both sides and obtain

$$(4\pi/\Lambda)\phi_1\phi_2/r^2 = (1/2r^2)\frac{d(\phi_1^2 + \phi_2^2)}{dr} + (j'/r^3)(\phi_2^2 - \phi_1^2).$$

By partial integration

$$(4\pi/\Lambda)\int_0^\infty (\phi_1\phi_2/r^2)dr = (4\pi/\Lambda)\int_0^{r_0} (\phi_1\phi_2/r^2)dr - (\phi_1^2 + \phi_2^2)_{r_0}/(2r_0^2)$$
$$+ \int_0^\infty [(j'+1)\phi_2^2 - (j'-1)\phi_1^2]r^{-3}dr \tag{8}$$

where r_0 is arbitrary. We now consider (8) for a light atom where the relativistic corrections are not important. We may then choose such a value for the so far arbitrary r_0 that the value of the first two terms on the right side of (8) is small in comparison with the last. This may be done for anything but s terms. For these the second term approaches a constant value also in the nonrelativistic case and the last term vanishes because $j' = -1$ and ϕ_1 is small. In the limit $c \to \infty$ for anything but s terms the right hand side of (8) is therefore $(j'+1)\overline{(r^{-3})}$ with the normalization

$$\int_0^\infty (\phi_1^2 + \phi_2^2)dr = 1. \tag{9}$$

Since $C(l, j)$ does not involve α we may replace $\overline{(r^{-3})}$ in (5) by

$$\overline{(r^{-3})} \to [(4\pi/\Lambda)/(j'+1)]\int_0^\infty (\phi_1\phi_2/r^2)dr. \tag{10}$$

The combination which occurrs in (5) is

$$l(l+1)\overline{(r^{-3})} \rightarrow (4\pi j'/\Lambda)\int_0^\infty (\phi_1\phi_2/r^2)dr. \tag{11}$$

The replacement (10) has no meaning for s terms ($l=j'+1=0$). Formula (5) with the substitution (11) is correct however also in this case.[5]

Combining (3), (4), (11) we have

$$\Delta w = 4\pi j' g\mu_0^2[f(f+1)-j(j+1)-i(i+1)]\int_0^\infty \phi_1\phi_2 r^{-2}dr/[\Lambda j(j+1)] \tag{12}$$

with the radial function normalizing condition (9). For practical applications it is convenient to express all lengths in terms of

$$a_H = h^2/(4\pi^2 me^2). \tag{13}$$

We then have on letting $\mu_0^2/a_H^3 = R_\infty\alpha^2/2 = 2.909\ \text{cm}^{-1}$

$$\Delta w = 2.909g\frac{l(l+1)}{j(j+1)}[f(f+1)-j(j+1)-i(i+1)]\overline{\left(\frac{a_H}{r}\right)^3} \tag{12'}$$

nonrelativistically. On the other hand if in formula (12) and the normalizing condition (9) we use a_H as the unit length the factor

$$4\pi g\mu_0^2/\Lambda \rightarrow R_\infty ag = 799g\text{cm}^{-1} = 0.434(1840g)\ \text{cm}^{-1}. \tag{12''}$$

Numerical Calculations

To start with the central field of Thomas and Fermi[6] was used. On trying it we find that it must be modified somewhat to bring about agreement with the experimentally known energies. The field is changed so as to agree with the term value of $p_{1/2}$ and it then is found by numerical trial to agree also with the energy of $p_{3/2}$. We first explain the method of calculation for a given field.

The same units as those used by Fermi[7] are employed.

$$r = (h^2/8\pi^2 me^2)x = a_H x/2$$
$$-\eta = (h^2/8\pi^2 me^4)E = E/(4R_\infty).$$

The unit of length is 1/2 of the Bohr radius and the unit of energy is 4 times the Rydberg constant. Here E is the term value energy. The total energy is

$$mc^2 - 4R_\infty\eta.$$

In these units in terms of the central field function denoted by Fermi as ϕ the Eqs. (7) become

[5] This may be found by means of (8) remembering that nonrelativistically $(r^{-3}(l+1)=2\pi\psi^2(0)$ where ψ is Schroedinger's function normalized so as to have $\int_0^\infty 4\pi\psi^2(r)r^2dr=1$.

[6] L. H. Thomas, Proc. Cambridge Phil. Soc. **23,** 542 (1927); Fermi, Zeit. f. Physik **48,** 73 (1928).

[7] Fermi, Zeit. f. Physik **49,** 550 (1928).

$$\frac{d\phi_1}{dx} - \frac{j'\phi_1}{x} = \alpha[\eta - (1/x)\{1 + (Z-1)\Phi(\gamma x)]\phi_2$$
$$\frac{d\phi_2}{dx} + \frac{j'\phi_2}{x} = (1/\alpha)[1 - \alpha^2\eta + (\alpha^2/x)\{1 + (Z-1)\Phi(\gamma x)\}] \tag{14}$$

where $\gamma = (16(Z-1)/9\pi^2)^{1/3}$, Z is the atomic number and $\alpha = 2\pi e^2/hc$. For small values of the argument $\gamma x (\gamma x < 0.3)\Phi$ may be approximated by

$$\Phi(\gamma x) = 1 - \gamma x$$

In this region it is convenient to use the variable

$$y = Zx \tag{15'}$$

in terms of which (14) becomes

$$\frac{d\phi_1}{dy} - \frac{j'\phi_1}{y} = \left(b - \frac{a}{y}\right)\phi_2$$
$$\frac{d\phi_2}{dy} + \frac{j'\phi_2}{y} = \left(c + \frac{a}{y}\right)\phi_1 \tag{15}$$

where

$$a = \alpha Z,\ b = (\alpha/Z)[\eta + \gamma(Z-1)]$$
$$c + b = 1/a \tag{15''}$$

Eqs. (15) are exactly of the form occurring in the problem of the Coulomb field.[8] The solution of (15) may be put into the following form

$$\phi_1 = b^{1/2}(\sigma_1 - \sigma_2),\ \phi_2 = c^{1/2}(\sigma_1 + \sigma_2);$$
$$\sigma_1 = c_0^{(1)} e^{-z} z^\rho F(1 - n', 2\rho + 1, 2z);\ F(\alpha, \beta; x) = 1 + \frac{\alpha}{1!\beta}x + \frac{\alpha(\alpha+1)}{2!\beta(\beta+1)}x^2 + \cdots$$
$$\sigma_2 = c_0^{(2)} e^{-z} z^\rho F(-n', 2\rho + 1, 2z);$$
$$z = (bc)^{1/2}y,\ \rho = +(j'^2 - a^2)^{1/2} \tag{16}$$
$$n' = -B - \rho,\ A = (a/2)[(b/c)^{1/2} + (c/b)^{1/2}]$$
$$B = (a/2)[(b/c)^{1/2} - (c/b)^{1/2}]$$
$$\frac{c_0^{(1)}}{c_0^{(2)}} = \frac{j' + A}{B - \rho} = \frac{\rho + B}{-j' + A} = \frac{n'}{j' - A}.$$

It is seen from (15″) that b depends for its existence on the variation of the function Φ with distance i.e. on the rate of change of the effective charge for the potential. It is this variation that gives rise to $\gamma(Z-1)$ in the expression for b. The quantity η is negligible in comparison being of the order of 0.1 while $\gamma(Z-1) \leqq 200$. Although b is not very small we obtain a rough approximation by letting $b = 0$ in (15). Then we obtain simple solutions

[8] W. Gordon, Zeits. f. Physik **48**, 11 (1928); C. G. Darwin, Proc. Roy. Soc. **A118**, 654 (1928).

$$\phi_1 = J_{2\rho}(2(acy)^{1/2})$$
$$a\phi_2 = (j' - \rho)J_{2\rho}(2(acy)^{1/2}) + (acy)^{1/2}J_{2\rho+1}(2(acy)^{1/2}) \tag{16'}$$

where the J_m are Bessel functions of order m.

These approximate solutions have been used[2] for a preliminary estimate of the difference between $p_{1/2}$ and $p_{3/2}$ terms. Although (16′) is a sort of an approximation an examination of the numerical values makes it validity somewhat questionable. In the present case

$\gamma = 2.4334$, $a = 0.58994$, $b = 0.01751$, $c = 1.6776$
For $p_{3/2}(j' = -2)$, $\rho = 1.911$ and $n' = 0.946$
For $p_{1/2}(j' = +1)$, $\rho = 0.8074$ and $n' = 2.050$

The number $n' + \rho$ corresponds to the total quantum number of an electron moving in the field of charge Ze. In our case $n' + \rho = 2.86$. The proper function of the valence electron near the nucleus is therefore such as though there were no screening but as if the electron had an energy

$$mc^2 - \frac{RZ^2}{(2.86)^2}$$

i.e., roughly as if it were an unscreened M electron. Setting $b = 0$ amounts to letting $n' + \rho = \infty$. For this reason b was taken into account in one case by means of (16) and in another by a somewhat different but mathematically equivalent expansion. The results were checked numerically by using the expressions for $d\phi_1/dy$, $d\phi_2/dy$ which follow from the differential equations and then computing $\int d\phi_1/dydy$, $\int d\phi_2/dydy$ by Simpson's rule. The integrals $\int_0^\infty \phi_1\phi_2 r^{-2}dr$ have then been also computed by Simpson's rule. The integrand became relatively small for values smaller than those corresponding to $\gamma x < 0.3$ and of the order of $\gamma x = 0.2$.

Formulas (16) contain an arbitrary factor which may be determined only by continuing the solution for larger r and determining the normalization. It is not important to continue the solution very exactly particularly where the functions are relatively small. These regions give a negligible contribution to the normalization integral and only a small one to the effective value of $\overline{r^{-3}}$. The method of Kramers-Wentzel-Brillouin[9] was used. Since in the present instance we are concerned with solving two simultaneous differential equations a slight modification of the method had to be made. Eqs. (14) are of the form

$$\frac{d\phi_1}{dx} - \frac{j'\phi_1}{x} = (b - v)\phi_2; \quad \frac{d\phi_2}{dx} + \frac{j'\phi_2}{x} = (c + v)\phi_1. \tag{17}$$

Eliminating ϕ_1 and making the substitution

$$\phi_2 = (c + v)^{1/2}\chi_2$$

[9] H. A. Kramers, Zeits. f. Physik **39**, 828 (1926); G. Wentzel, Zeits. f. Physik **38**, 518, (1926); L. Brillouin, C. R. July (1926).

we obtain the differential equation satisfied by χ_2

$$\frac{d^2\chi_2}{dx^2} + f^2\chi_2 = 0$$

$$f^2 = (v-b)(c+v) - \frac{j'(j'+1)}{x^2} - \frac{j'(dv/dx)}{x(c+v)} + \frac{(d^2v/dx^2)}{2(c+v)} - \frac{3(dv/dx)^2}{4(c+v)^2}. \quad (17')$$

Here the first two terms are exactly as though we were dealing with Schroedinger's nonrelativistic equation. The third and fourth represent the main part of the interaction of the electron spin with the electric field of the nucleus. The last term is an unimportant correction. We have then in the region $f^2>0$

$$\phi_2 = [(c+v)/f]^{1/2} \cos\left\{\int f dx + \text{const.}\right\} \quad (17'')$$

a constant multiplier to be determined from normalization being understood.

The approximate solution (17″) applies in the region $f^2>0$. It has been used from somewhat beyond the first maximum of ϕ_2. It was joined to the power series (16) at the maximum of $[f/(c+v)]^{1/2}$. For the calculation of $\int_0^{r_0}\phi_1\phi_2 r^{-2}dr$ however the power series was used. The electron states in question are p states with total quantum number 6. Therefore ϕ_2 has 5 maxima and minima between $r=0$ and ∞. Solution (17″) applies reasonably well between the first and the last maximum. From there to $r=\infty$ it was joined to an exponential function by the device due to Kramers[10] which in our case consists in making

$$(c+v)^{1/2}f^{-1/2}\cos\left\{\int_r^{r_2} f dx - \pi/4\right\} (r<r_2) \quad (18')$$

join to the function

$$(\tfrac{1}{2})(c+v)^{1/2}|f|^{-1/2}\exp\left\{-\int_{r_2}^{r}|f|\,dx\right\} (r>r_2). \quad (18'')$$

Here $f=0$ at $r=r_2$

The value of $\int f dx$ from the first to the last maximum was made $(4+1/4)\pi$ in agreement with Kramers' half quantum number quantization rule. Neither (18′) nor (18″) represent the transition region around $f=0$ satisfactorily. The well-known confluent hypergeometric function solution was used here. The constant factor by which it should be multiplied was determined by making it join and coincide with (18″) for large x.

Instead of using (18′), (18″) another deliberately rougher method was also tried. The phase integral was made to have the value $9\pi/2$, the limits of integration being from the first maximum to the point $f=0$. The function ϕ_2 then vanished at this point and was broken off from there on. This amounts to treating the electron classically at large distances. The ratio of the nor-

[10] See also Zwaan Utrecht Dissertation, 1929.

malization integrals was found to be roughly the same as in the more exact calculation but their values were quite different. The comparison of the two methods indicates that an absolute calculation of the g factor is more difficult than a test of its constancy.

A serious limitation on the accuracy of these calculations is the lack of knowledge of the central field. The potential function $\Phi(\gamma x)$ is multiplied throughout by $Z-1=80$ which makes an accurate knowledge of Φ important. Fermi's table for Φ was tried first. The phase integral for $p_{1/2}$ was found to be $>9\pi/2$. The field was then changed so as to have it purely Coulomb and due to a single charge e from a certain point on. The amount $(Z-1)\Phi$ at this point was subtracted from the potential for smaller values of x. Recomputing the phase integral for a few such trial fields a field giving the desired value of the phase integral was found. The phase integral for $p_{3/2}$ was then computed and was found to give the same result. This indicates that the field used was not very bad for the present purpose. A summary of the main results of the calculation follows.

$\gamma=2.4334$, $\xi=\gamma x$. From $\xi=12$ field is purely Coulomb

	$p_{1/2}$	$p_{3/2}$
Experimental	$\eta=0.11223$	$=0.09448$
First maximum of	$f^{1/2}(c+v)^{1/2}\phi_2$	
at	$y=4.4$	5.2
	$\int_{y=4.4}^{\xi=2} f dx = 0.707$	$\int_{y=5.2}^{\xi=2} f dx = 0.431$
Roots	$\xi \leqq 0.30, 0.9, 2.1, 4.8$	$\xi \leqq 0.35, 0.98, 2.2, 5.3$
	$\int_0^\infty \phi_2^2 d\xi = 31.3$	53.2
	$\xi_0 = 0.2$	0.3
	$\frac{4\pi}{\Lambda(j'+1)} \int_0^{\xi_0} \phi_1\phi_2 r^{-2} dr = 28.8 a_H^{-3}$	$8.3 a_H^{-3}$
	$\frac{4\pi}{\Lambda(j'+1)} \int_{\xi_0}^\infty \phi_1\phi_2 r^{-2} dr = 0.7 a_H^{-3}$	$0.7 a_H^{-3}$
	$\frac{4\pi}{\Lambda(j'+1)} \int_0^\infty \phi_1\phi_2 r^{-2} dr = 29.5 a_H^{-3}$	$9.0 a_H^{-3}$.

Using Wulff's observed value of $(\Delta\nu)p_{1/2}=0.727$ cm^{-1} and $i=1/2$, 1840 $g \leqq 2.9$. From the splitting of $p_{3/2}$ however 1840 $g \leqq 1.4$.

Calculations with the phase integral adjusted to be $9\pi/2$ gave a ratio of $4\pi/\Lambda(j'+1)\int_0^\infty \phi_1\phi_2 r^{-2} dr$ for $p_{1/2}$ to $p_{3/2}$ of about 4.4. The only difference from the preceding solution is in the normalization factors which in this case give rise to a factor of roughly 2. The qualitative reason for this factor (1.7 by the more accurate calculation) if that the electron has a higher energy in the $p_{3/2}$

state so that it escapes vigorously from the inner shells of the atom. The relativistic corrections consisting in the use of $\int_0^\infty \phi_1\phi_2 r^{-2}dr$ are seen also to lead to a correction by about a factor of 2. This may be also verified analytically by the more easily handled solutions in terms of Bessell functions (16′) and leads to approximately the same result. It is felt that the above considerations are sufficiently independent of the special assumptions made about the nature of the central field. It is quite possible that the ratio of the values of $4\pi/\Lambda(j'+1)\int_0^\infty \phi_1\phi_2 r^{-2}dr$ for the two p terms is somewhere between 3 and 4 but it appears impossible that it should be as large as 7. For Bi I, according to Goudsmit[1] we would have to account for a factor of more than 10. On applying the corrections worked out here there remains a discrepancy by a factor of roughly 3. In both cases $(\Delta\nu)p_{1/2}/(\Delta\nu)p_{3/2}$ is anomalously great. This suggests that at close distances the nucleus binds the electron to the nuclear spin axis more tightly than the magnetic doublet model would lead one to suppose.

The writer is very grateful to Dr. F. W. Doermann for his help with some of the numerical calculations.

THE EFFECT OF HYPERFINE STRUCTURE ON THE POLARIZATION OF CADMIUM RESONANCE RADIATION

By Allan C. G. Mitchell
Bartol Research Foundation of the Franklin Institute
(Received June 8, 1931)

Abstract

The polarization of cadmium resonance radiation (λ3261) has been calculated assuming that cadmium is composed of two kinds of isotopes having a nuclear moment $i=0$ and $i=1/2$ respectively. The ratio of the isotopes of nuclear moment $i=1/2$ to $i=0$ was taken from the hyperfine structure data on cadmium as measured by Schüler and Keyston. The percentage polarization to be expected for "broad" and "narrow" line excitation and for different orientations of electric vector and magnetic field are given and comparison is made with Soleillet's experiments.

THAT hyperfine structure can affect the polarization of resonance radiation was shown by MacNair and Ellet[1] in the case of the 2537A line of mercury. In this way they were able to explain the fact that mercury resonance radiation, in the absence of a magnetic field, is only 90 percent polarized instead of 100 percent which one would expect from the Zeeman levels of a line $(2^3P_1-1^1S_0)$ showing no hyperfine structure. More recently Ellet[2] has calculated theoretically the polarization to be expected for certain thallium lines taking into account the known hyperfine structure exhibited by these lines.

Schüler and Keyston[3] measured the hyperfine structure of the sharp triplet in cadmium $(2^3S_1-2^3P_{0,1,2})$. They found that their results could be explained on the assumption that of the various isotopes of cadmium those of even atomic weight have no nuclear moment $(i=0)$ and those of odd atomic weight have a nuclear moment $i=1/2$. The isotopes having no nuclear mo ment give rise to an unshifted hyperfine-structure component while those having a nuclear moment show shifted components. By measuring the relative intensities of the several components, they were able to obtain the abundance ratio of the isotopes of even to those of odd atomic weight.

Applying these considerations to the resonance line of cadmium $(2^3P_1-1^1S_0)$ at λ3261, one would expect to obtain three hyperfine-structure components—$(2^3P_{f=1}\rightarrow 1^1S_{f=0})$ for the isotopes with $i=0$; $(2^3P_{f=3/2}\rightarrow 1^1S_{f=1/2})$ and $(2^3P_{f=1/2}\rightarrow 1^1S_{f=1/2})$ for the isotopes of $i=1/2$. Here, as is customary, $f=i+j$. The hyperfine structure of this line has been measured by Wood[4] and Schrammen,[5] who found only two components. Since with the sources they used it was hard to obtain the 3261A line entirely free from self reversal, it is possible that one of the components may have been missed.

In order to calculate the polarization of cadmium resonance radiation the Zeeman diagrams for the three hyperfine-structure components must be

[1] W. MacNair and A. Ellett, Phys. Rev. **31,** 180 (1928).
[2] A. Ellett, Phys. Rev. **35,** 588 (1930).
[3] Schüler and Keyston, Zeits. f. Physik **67,** 433 (1931).
[4] R. W. Wood, Phil. Mag. **2,** 611 (1926).
[5] A. Schrammen, Ann. d. Physik **83,** 1161 (1927).

drawn. For low magnetic fields when the Zeeman separation is small compared to the hyperfine structure separation, the three components may be treated as three separate lines. The levels for the three components in question are given in Fig. 1. The figures under each Zeeman component give the intensity of each component, while the greek letters and the figures directly under them represent the transition probabilities. The component A, due to isotopes with $i=0$ shows the usual cadmium-like Zeeman pattern, while the components a and b due to isotopes with $i=1/2$ are sodium-like. The *a priori* weights of $a:b$ are as 2:1 which follows from the sum rule and has been shown experimentally by Schüler and Keyston[3] for the line 4678A ($2^3S_1-2^3P_0$) which should have the same structure as 3261. The *a priori* weight of the component A is taken as 3 on the same scale and the intensities of each component are so chosen that the chance of leaving any given magnetic level shall

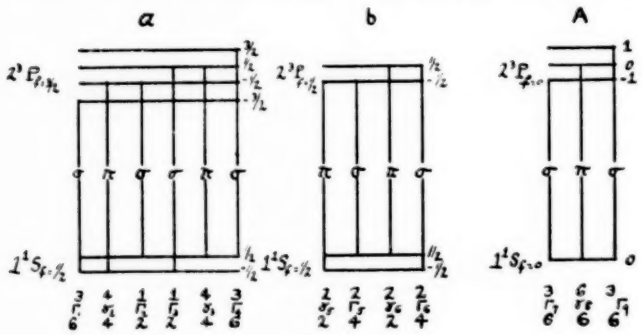

Fig. 1.

be the same for all levels. This is equivalent to the assumption that all the upper magnetic levels of all the hyperfine structure components have the same mean life.

In calculating the polarization, let I_a, I_b, I_A be the intensity of the hyperfine structure component a, b, and A in the source, and N_1, N_2 the relative numbers of isotopes having $i=1/2$ and $i=0$ respectively. Suppose the exciting light beam approaches the resonance tube from the Y direction and observations of the resonance radiation are made along Z. Let the electric vector of the incident light wave make an angle θ with a magnetic field applied to the resonance tube anywhere in the $X-Y$ plane. Let ξ and η be the intensities of the components of the resonance radiation along and perpendicular to the magnetic field respectively. Van Vleck[6] has given formulae for ξ and η in the case of single lines under various excitation conditions. The formulae for a single hyperfine structure component are

$$\xi = CI \sum_i \frac{\gamma_i}{\gamma_i + \Gamma_i} \left\{ \gamma_i \cos^2\theta + \tfrac{1}{2}\Gamma_i \sin^2\theta \right\} \tag{1}$$

$$\eta = \tfrac{1}{2}CI \sum_i \frac{\Gamma_i}{\gamma_i + \Gamma_i} \left\{ \gamma_i \cos^2\theta + \tfrac{1}{2}\Gamma_i \sin^2\theta \right\} \tag{2}$$

where C is a constant and I the intensity of the exciting light beam.

[6] J. H. Van Vleck, Proc. Nat. Acad. Sci. **11**, 612 (1925).

For the case of hyperfine structure under consideration the intensity of the resonance radiation is proportional to the relative intensity of the hyperfine structure components in the source and to the relative number of isotopes of the two kinds present in the resonance tube. Eqs. (1) and (2) will now become

$$\xi = k \sum_j N_j I_j \sum_i \frac{\gamma_i}{\gamma_i + \Gamma_i} \{\gamma_i \cos^2\theta + \tfrac{1}{2}\Gamma_i \sin^2\theta\} \tag{3}$$

$$\eta = \tfrac{1}{2} k \sum_j N_j I_j \sum_i \frac{\Gamma_i}{\gamma_i + \Gamma_i} \{\gamma_i \cos^2\theta + \tfrac{1}{2}\Gamma_i \sin^2\theta\} \tag{4}$$

where $\sum_i$ is to be taken over all the Zeeman transition probabilities of a given component and $\sum_j$ means

$$N_1 I_a \sum_i (\quad)_a + N_1 I_b \sum_i (\quad)_b + N_2 I_A \sum_i (\quad)_A$$

Now the polarization P is defined by

$$P = \frac{\xi - \eta}{\xi + \eta}.$$

On substituting the values of γ_1, Γ_1 from Fig. 1 in (3) and (4) and carrying out the indicated summation one finds

$$P = \frac{(2I_a N_1 + 3I_A N_2)(\cos^2\theta - \tfrac{1}{2}\sin^2\theta)}{2I_a N_1(5/3\cos^2\theta + 7/6\sin^2\theta) + I_b N_1 4/3 + 3I_A N_2(\cos^2\theta + \tfrac{1}{2}\sin^2\theta)} \tag{5}$$

Schüler and Keyston measured the relative intensities of the hyperfine structure components for the 4675A line of cadmium and found

$$\frac{I_a + I_b}{I_a + I_b + I_A} = 0.23 \tag{6}$$

from which it follows, since $I_a = N_1$, $I_b = N_1$, $I_A = 3N_2$, that

$$N_2 = 3.34 N_1. \tag{7}$$

Several interesting cases arise for computation. The source may be one which gives broad lines, due to high temperatures, such that $I_a = I_b = I_A$; or it may be a low temperature source giving hyperfine structure lines with relative intensities as given by (6). The incident beam may be polarized in the X direction and the resonance lines may be in a zero magnetic field. This case, due to spectroscopic stability, is the same as if the resonance tube were in a weak magnetic field parallel to X so that $\theta = 0$. The incident light may be unpolarized and the resonance tube in a weak magnetic field parallel to Y so that $\theta = \pi/2$. The results for the various cases are given in Table I.

TABLE I.

	$\theta = 0$	$\theta = \pi/2$
Broad Lines	81.9%	69.4%
Narrow Lines	96.4%	93%
Experiment (λ3261)	73%[A]	85$\pm$8%[B]

Comparison with Experiment

The polarization of the resonance line λ3261 in cadmium has been measured by MacNair[7] and Soleillet.[8] The experiments of the former were made with rather high vapor pressures of cadmium so that some depolarizing effect had undoubtedly set in. Soleillet measured the polarization in a zero magnetic field with exciting light polarized parallel to X, and used low vapor pressures. At temperatures of 170°C and 115°C he found the polarization to be constant and equal to 73 percent. Since the 2^3P_1 state of cadmium has a long mean life the polarization of the resonance radiation is greatly affected by weak magnetic fields, of the order of 0.01 gauss. As it is difficult to make the resonance tube free from magnetic fields to this extent he also repeated the experiment in a magnetic field parallel to the incident light beam, and also in a zero field. In these experiments, the exciting light was unpolarized. In both cases he found 85 percent polarization. The experimental conditions for the second set of experiments seems to have been much better than in the first, the resonance tube always being attached to the pumps instead of sealed off as in the former case.

In a zero magnetic field it is clear that the Zeeman separation is small compared to that of the hyperfine structure. For the case of a magnetic field parallel to Y of the order of 50 gauss (Soleillet's field was probably about this strong), the Zeeman separation is of the order of 2×10^{-3} cm^{-1} while that of the hyperfine structure is about $(50\text{–}100)\times10^{-3}$ cm^{-1} so that the assumptions used in the present calculation probably hold.

The ratio of the hyperfine-structure components in the source is, of course, not known, and the measurements are difficult to carry out so that no exact agreement can be expected. If, as one might expect, a source which will excite resonance radiation is more nearly a "narrow line" than a "broad line" source, the agreement with Soleillet's second experiment is quite satisfactory.[9] The fact that the results of Soleillet's second experiment lie between the theoretical values for "broad" and "narrow" lines while those of his first experiment are always too low, is probably due to having less gas in the resonance tube, so that less depolarization by collision occurred, and to better neutralization of stray fields.

The writer is indebted to Professor G. Breit for his criticism of this work.

[7] MacNair, Phys. Rev. **29,** 766 (1927).

[8] P. Soleillet; A. Compt. Rend. **185,** 198 (1927); B, ibid. **187,** 212 (1928).

[9] The effect of nuclear spin, of course, is to decrease the value of the percentage polarization below that of 100 percent to be expected for cadmium resonance radiation if there were no nuclear spin. The fact that the percentage agreement between the 85 percent (experiment) and 93 percent (theory) seems good and the difference between 100 percent and the above values gives a large percentage error between theory and experiment does not seem significant, on account of the uncertainties of the experiments as pointed out above. What is of interest, however, is that the observed polarization lies between the theoretical values for the two types of sources and that its value is certainly not as great as 100 percent.

ABSORPTION LINE WIDTH IN SODIUM VAPOR

By S. A. Korff
Palmer Physical Laboratory, Princeton University

(Received May 8, 1931)

Abstract

Spectrograms of the D lines of sodium in absorption were obtained and measured on a densitometer, thus determining an optical constant which was uncertain in former work. Absolute contours in terms of transmitted intensity against wave-length were obtained. Possible sources of error were studied in detail. The observed contours were compared with the classical formula. The contours were found to have the theoretical inverse square variation of opacity with wave-length distance from resonance; they showed the theoretical variation of width with the square root of the number of atoms in the line of sight, and the 2:1 ratio between the two D lines. The width of the lines was, however, about five times that which classical radiation damping accounts for. A detailed further experimental study of this discrepancy is planned.

General

IN PREVIOUS[1] experimental tests made in this laboratory of the classical equations for the widths of absorption lines as produced by a radiation damping, a certain optical constant k was left undetermined. Designate by ψ the ratio I/I_0 of transmitted to incident intensity. Then $\psi = e^{-Kz}$ where K is the opacity coefficient of the vapor and z is the length of the column of vapor in centimeters. The previous measurements of line width were made by eye, and indicated that ψ had a constant value, defined as e^{-k}, at the observed "edge" of all lines (with a given spectroscope) but failed to determine the value of k. The experiments determined instead a parameter $a/k^{1/2}$, where a theoretically is $2e^2/3mc^2$, or 1.88×10^{-13} cm, the classical "electromagnetic radius of the electron," where e and m are its charge and mass, and c is the velocity of light. The observations showed that this parameter $a/k^{1/2}$ was a constant for lines of different widths; and that *if* a had the above theoretical value, k had to be of the order 0.05.

This result meant that what the eye called the "edge" of the absorption line corresponded to a point on the contour (Fig. 1C) where 0.95 of the incident light was transmitted; which was described as "surprisingly high." In the present work the actual value of k was determined with a densitometer and found to be about 1.4, representing an edge contrast of 0.2. In consequence the experimental value of a is indicated as about 5 times larger than the above theoretical value of 1.88×10^{-13} cm.

Experimental Procedure

To study absolute contours of the D lines in absorption the following procedure was employed. A 2000 watt projection bulb was used as a source. The

[1] S. A. Korff, Phys. Rev. **33**, 584 (1929); **34**, 457 (1929); J. Q. Stewart, and S. A. Korff, Phys. Rev. **32**, 676 (1928); A. S. Fairley, Astrophys. J. **67**, 114 (1928).

light from this was passed through a Pyrex tube into which sodium had been distilled in vacuum. The sodium was purified by repeated distillation and freed from occluded gas by long pumping, before the tube was sealed off from the vacuum system. The McLeod gauge read 10^{-5} millimeters or less when the tubes used were sealed off. Two different tubes gave consistent results. The tube was mounted within an electric furnace 35 cm in length equipped with Pyrex windows, so that its temperature could be kept throughout at a known value. Tubes of length $z = 25.5$ and 10.5 cm were used. The temperature was determined with a mercury thermometer on which the temperature could be read with accuracy to less than a degree. The readings of the thermometer were verified with boiling mercury (357°C) and melting ice. Temperatures from 200°C to 320°C were employed. The light was focused on the slit of a spectrograph, which had 14,000 line grating and a lens of 312 cm focal length (Littrow mounting). Wratten and Wainright Process panchromatic plates were selected because of uniform sensitivity, good contrast, small grain size and clear emulsion. A typical plate is reproduced in Fig. 3 showing the D lines in absorption at various temperatures (vapor densities) and the calibrating wedge.

The plates were calibrated by using an Eastman wedge and screens. With the furnace cold, and hence D lines absent, the continuous background was photographed on the plate. Then a wedge, of known transmission coefficient per mm from a fiducial mark and calibrated rate of variation of transmission coefficient (prepared and calibrated by Eastman Kodak Co. Research Laboratories) was put directly in front of the plate against the emulsion, and another exposure taken of identical length on a different portion of the plate. The wedge was long and consequently put with the direction of varying transmission along the direction of varying frequency in the spectroscope, in the plane of dispersion of the instrument. In employing this procedure, two sources of error must be considered. The black body radiation curve of the filament gives a varying amount of energy with wave-length in this region. A simple computation from Planck's law will show that this variation is small over a range of 50 Angstrom units, the approximate effective length of the wedge. Similarly the variation in sensitivity of the emulsion over a region of 50 Angstrom units in this region is small. It was found observationally that it made no difference whether the dense end of the wedge was toward red or toward violet.

The plate thus prepared had on it an absolute intensity calibration from the wedge alone and this sufficed for an absolute determination of line contour. Tests were made to determine whether scattering of light by the wedge was significant. The result showed that the difference in question was within the errors of observation.

The plates were next examined with a densitometer and absolute contours in percent of transmitted intensity vs. wavelength obtained. With the densitometer any point on the line could be matched with a point on the wedge photograph, the corresponding transmission coefficient of the sodium vapor being then equal to that of the wedge. The densitometer was similar to the

one described by Harrison[2] and had a slit 0.01 mm wide almost in contact with the emulsion of the plate. The photograph of the wedge was first run over the densitometer, and the transmission read on the calibration curve of the wedge and plotted against densitometer deflections. Thus the characteristic (calibration) curve of the plate was obtained. A typical resulting calibration curve is shown in Fig. 1B.

Next, records of the absorption lines were obtained and plotted as densitometer deflections against wave-lengths giving curves as shown in Fig. 1A. Since from the characteristic curves the transmitted intensity corresponding to any given densitometer deflection was known, the absolute contour is at once obtained in transmission percent plotted against wave-length. A typical absolute curve is shown in Fig. 1C. The calibration of the motion of the plate

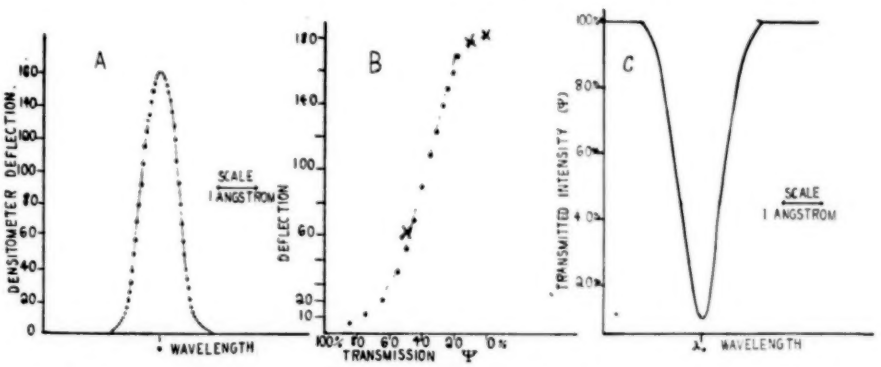

Fig. 1. Curve *A* shows a typical densitomer tracing of a spectrogram of one *D* line. Curve *B* shows a typical plate characteristic calibration curve. Curve *C* shows an absolute line-contour obtained from curves *A* and *B*.

on the densitometer in angstroms was obtained by taking the distance between the centers of the *D* lines as 5.967 angstroms (Fowler).

Optical Sources of Error

In work on the widths of spectral lines it is well known that any feature of the apparatus used which tends to broaden or confuse the image of the line on the photographic plate must be considered. In particular (a) the effects of the limited resolving power of the grating, (b) the slit width, of spectrograph and densitometer, (c) the circle of confusion due to possible departure from exact focus, (d) the creeping of the image on the sensitised film and (e) the departure from theoretical perfection of lens and grating, all contribute to this effect.

(a) The grating had 14000 lines per inch, the lens diameter was 65 mm, and the spectroscope was operated in the 2nd order, giving a theoretical resolving power of approximately 70,000. Hence at about 6000 Angstroms the minimum resolvable separation between two close lines according to Lord Rayleigh's well-known criterion is 6/70 A or 0.05 mm on the plate (the dispersion being 1.7 angstrom units per mm).

[2] G. R. Harrison, J. Opt. Soc. Am. **10**, 151 (1925).

The effect of limited resolving power on the contour of theoretical absorption lines was made the subject of a numerical computation by Mr. R. King of this laboratory. The computations show that the spectroscope will throw a small amount of light into the center of the line (10 percent for a line one "resolving power," or in this spectroscope 0.1 angstrom units in apparent width, eye estimate, 2 per cent for a line 0.5 A wide, less for wider lines). This accounts for some of the observed light at the center (see absolute contours, curve C, Fig. 1). The effect is less elsewhere on the contour, but would result in a slight lessening of the slopes and broadening of the shoulders.

(b) As the distance from the spectrograph slit to the collimating lens of the Littrow mounting was of course equal to the distance from the lens to the plate, the size of the slit image on the plate was equal to the slit width. This was observed with a microscope and adjusted to 0.01 mm. The densitometer slit was adjusted to the same width. Since the other smearing effects were large compared to this there was no object in making either of these widths smaller.

(c) The ratio (f) of the focal length to aperture of the collimating lens was 3120/65 mm, or 49.4. If x is the distance from the lens to the plate, and dx is the uncertainty in position of the lens as regards focus, then the diameter of the circles of confusion with a perfect lens will be dx/f. The value of dx was obtained by photographing the spectrum of an arc while changing the focus by small amounts, and examining the spectra with a microscope to pick out the narrowest and sharpest line. Near exact focus a small variation in x was found to make no appreciable difference in apparent sharpness of focus and the center of the region was selected as being most probably the exact focus. The width of the region, 1 mm, was then assigned as dx, leading to a value of 0.02 mm for dx/f, as an upper limit of the error thus produced.

(d) The spreading of the images on the emulsion was tested by putting an opaque flat object of known dimensions in front of the plate and exposing to parallel light. Various exposures were made with varying conditions of development and the resulting plates were measured and compared with the object. These tests showed that the creeping of the image was small compared to 0.02 mm, (the focus error) except at large overexposures. No spectrograms of the D lines were overexposed.

(e) The smearing effect due to the departure from exact mathematical perfection of the grating and lens was believed to be within and masked by the sum of the other broadening effects since the narrowest lines photographed were well defined. Lines were not photographed below 0.12 angstroms in width, while the sum of the effects a, b and c tabulated above was of the order 0.08 mm, corresponding to 0.10 angstroms.

Reduction of Observations

The value of n, the number of atoms per cubic centimeter, was taken from a table given by Fairley.[1] This table had been computed from the vapor pressure formula of Edmondson and Egerton,[3] their Eq. (3):

[3] W. Edmondson, and A. Egerton, Proc. Roy. Soc. **A113,** 530 (1927); H. Rowe, Phil. Mag. **3,** 538 (1927); W. Rodebush, and E. G. Walters, J Am. Chem. Soc. **52,** 2654 (1930).

$$\log p = -5573.2/T + 9.7255 - 0.6794 \log T \quad (1)$$

where p is the pressure in mm and T the absolute temperature. The computation of vapor density from vapor pressure was made through the equation:

$$n = n_0 273p/760T \quad (2)$$

where n is the number of atoms per cc, n_0 is the Loschmidt number (Birge's value), p the pressure in mm (from Eq. (1)), and T the absolute temperature. Experimental values of the vapor pressures are tabulated by Rowe and others.[3] The experimental points fall on the theoretical Eq. (1) within the experimental error.

The classical n corresponds to the quantum theoretical nf, the "number of equivalent classical oscillators." In accordance with well-known relations, the value $\frac{1}{3}$ is assigned to the f for D_1 and $\frac{2}{3}$ to the f of D_2. Define $N = nfz$, z being the tube length, so that N is the number of active atoms per square centimeter column in the line of sight. The values of N were tabulated for each spectrogram. For each value of ψ a value of Kz was obtained from the equation $\psi = e^{-Kz}$. For the various values of ψ the width $2\Delta\lambda$ as measured in angstrom units on the contours was squared and multiplied by Kz, then it was divided by N and a set of values of a constant called A (see Eq. (4)) was obtained. Table I shows a typical computation.

TABLE I.

Plate	Temp °C	D line	$N\times10^{14}$	ψ	Kz	$(2\Delta\lambda\times10^{-8})$	$4A\times10^{-30}$
11	220	2	0.51	0.8	0.22	0.6	0.16
		1	0.26	0.8	0.22	0.5	0.22
		2	0.51	0.6	0.5	0.4	0.16
		1	0.26	0.6	0.5	0.3	0.18

CONTOURS

To obtain a single contour from all observations the values of $\Delta\lambda$ were next reduced using the following equation:

$$\Delta\lambda_0 = \Delta\lambda(N_0/N)^{1/2}$$

where $\Delta\lambda_0$ is the reduced width, $\Delta\lambda$ is the observed width, N is the corresponding observed number of atoms in the line of sight, and N_0 is a standard number of atoms. A value N_0 was selected in about the middle of the range of N (7.6 and 3.8×10^{14}). Then the observed values of $\Delta\lambda$ and N were substituted in the equation and a set of values of $\Delta\lambda_0$ obtained. Four such sets were obtained, one for each of the values of ψ used in Table I (0.8, 0.6, 0.4, 0.2). The values for D_1 and D_2 were separated, and the results averaged, giving the following contours:

ψ	$\Delta\lambda_0$ for D_1	$\Delta\lambda_0$ for D_2
0.8	1.9	2.4
0.6	1.35	1.65
0.4	0.95	1.35
0.2	0.62	0.84

The values of D_2 are plotted as circles in Fig. 2. They constitute an average line contour embodying all the observed points.

A theoretical contour corresponding to this case is shown as a solid line in Fig. 2. It is obviously inadequate to account for the observed width. Crosses indicate the same theoretical contour with the constant adjusted, which is seen to fit the observed reduced points well, except at the shoulders.

If $\Delta\lambda^2$ is plotted against $-\log \psi$ a straight line should result. This is indeed the case for the reduced values tabulated above. It was found that for higher values of ψ (i.e., 0.95 and up) there was a slight departure from this straight line. Harrison[4] has shown that this type of departure is often observed in such contours, and may be ascribed to a small zero point error; and that multiplying I_0 by a factor of about 1.05 will bring the points into line. This correction is of importance only at the extreme shoulders of the line.

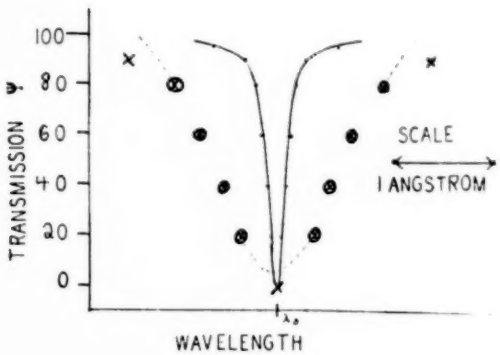

Fig. 2. Full line is theoretical contour. Circles represent reduced values from all observations. Crosses represent theory with adjusted constant about 5 times larger.

The effect on the contours produced by this error is shown by the broken line in Fig. 2, where the slopes at the extreme shoulders are seen to be too steep. The broken line at the center of the contour indicates the error produced by scatteri g of light due to dust etc. on the grating, any stray light, and resolving power effects discussed above under section (a) in the paragraph on optical sources of error.

Theory

Stewart[5] following Lorentz generalized the opacity coefficient from the Rayleigh form. His Eq. (6) is

$$Kz = \frac{3\pi}{2} Na^2(\lambda/\Delta\lambda)^2 \tag{3}$$

where K is the Rayleigh opacity coefficient, z the length of the column of vapor, N or nfz the number of active atoms per square centimeter column in

[4] G, R. Harrison, Phys. Rev. **25** 778 (1925).

[5] J. Q. Stewart, Astrophys. J. **59,** 30 (1926) and J. Opt. Soc. Am. **11,** 581(1925); H. A. Lorentz, Proc. Amsterdam Acad. **8,** 591 (1905); W. Voigt, Münch. Ber. P603 (1912).

the line of sight, a the "radius of the electron" ($2e^2/3mc^2$ or 1.88×10^{-13} cm), λ the wave-length of resonance and $\Delta\lambda$ the wave-length distance from resonance to the point of opacity K. The restriction on Eq. (3) is that $\Delta\lambda$ be large compared to a, i.e., the equation breaks down when within 10^{-4} anstrom of resonance.

This equation may be written:

$$\begin{aligned} Kz &= AN/(\Delta\lambda)^2 \\ &= \log\psi = \log(I/I_0) \end{aligned} \tag{4}$$

thus defining A as $A=3\pi a^2\lambda^2/2$. Substituting the values $\lambda=5890\times10^{-8}$ cm, and $a=1.88\times10^{-13}$ cm, we obtain

$$\begin{aligned} A &= 5.79\times10^{-34} \\ &= Kz(\Delta\lambda)^2/N. \end{aligned} \tag{5}$$

As was shown above, the value of A given by the contours was $5.32\pm0.5\times10^{-32}$. Eq. (4) gives a theoretical value 92 ± 24 times too small. It is obvious from Eq. (5) that the only quantity in the definition of A not directly known is "a," which is therefore determined by this evaluation of A. The value of "a" is found to be 1.81×10^{-12} cm, or 9.6 ± 1.2 times larger than classical theory predicts. Work on the effects of pressures (see below) showed that about half of this discrepancy was due to pressure broadening, leaving a residual discrepancy of about 5. Thus the widths are about 5 times greater than classical theory predicts.

The values of $10^{-32}A$ were next averaged in several ways in an attempt to discover any systematic departures from Eq. (5).

It was found that the value of A was independent of the vapor pressure, or of N. The average value of $10^{-32}A$ for all vapor pressures greater than about 10^{15} atoms in the line of sight was 4.47 while the value for all less was 5.42, the difference being within the probable error.

It was found that the value of A was the same for the two D lines. The 2 to 1 value of the "f's" of the two D lines had been put into the value of N as explained above, and hence the constancy of A for the two D lines means that their ratios were observed to be 2:1, or that their widths were as $2^{1/2}$:1 or 1.4:1. In this case the average value of A for D_1 was 4.78 while that for D_2 was 5.48, again within the limits of the probable error.

Similarly for the long and short tubes, the values of A were 5.48 and 4.93 respectively. This is a further check of the independence of A and N.

To determine whether A was independent of $\Delta\lambda$, the values of A were averaged for all values of $\Delta\lambda$ greater than 1 angstrom, and for all less. The A's were found to be 5.27 and 5.19 respectively.

To determine whether A was independent of ψ, the values of A were averaged for all values of ψ, giving for $\psi=0.8$, $A=5.85$; $\psi=0.6$, $A=5.35$; $\psi=0.4$, $A=5.20$; the low value for $\psi=0.2$, $A=3.50$ may be attributed to experimental error since there were only 5 observations of this value of ψ, and they were made in a region of less sensitivity.

Measurements of Widths by Eye

The spectrograms of the D lines in absorption at various vapor densities were then examined under a miscroscope-comparator, and the "widths" of the absorption lines measured by setting crosshairs on what appeared to be their edges. This method involves of course the "constant" of the eye in choosing the edge. Fig. 3 shows a typical spectrogram, showing how the width varies as the number of atoms in the line of sight is increased.

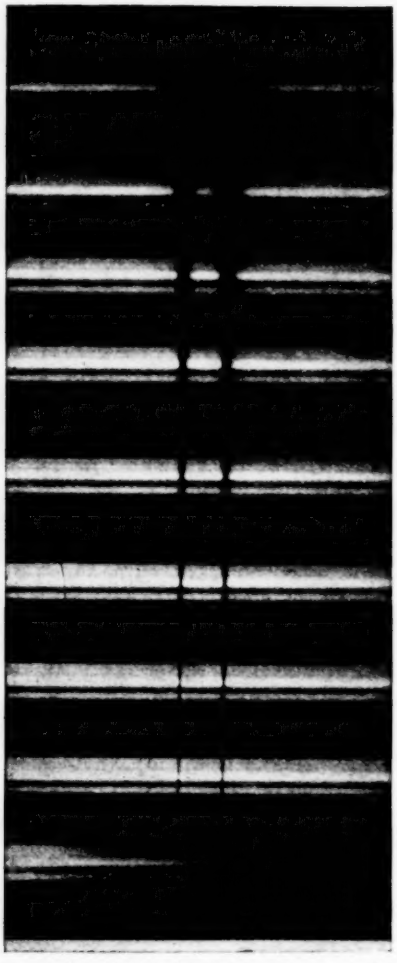

Fig. 3. Spectrogram of the D lines in absorption at various vapor densities. Calibrating wedge shown at bottom.

The lines were found to conform to the form of Eq. (3). But k $(=Kz)$ was defined in terms of ψ, whence for any given ψ now determined on the absolute contour, k can be computed. When this is done, k is found not to be 0.05 but about 1.4. In other words, when the crosshairs of the microscope were set on the "edge" of the line, the point where they were set is shown by the densitometer to be the point where 20–30 percent of the light of the con-

tinuous background is transmitted. This is not surprising when we consider that 20–30 percent of a given amount of light produces much more than 20–30 percent of the density that the full light does, since the density is exponentially related to the intensity. Thus the anomalous value of k which in previous[1] work was described as "surprisingly large" is explained.

An "artificial line" was made by Mr. Green of this laboratory which matched a theoretical contour (Eq. (4)) by stretching threads on a frame at varying lateral distances from each other. When this device was observed from a distance, with a white surface behind it, the conclusion was that the "observed width" corresponded to a ψ of only about 0.2, thus confirming the above conclusion.

Discussion

The possibility of residual gas broadening the lines through "pressure broadening" was next considered. To investigate this, an absorption tube was constructed and left attached to the vacuum system and McLeod gauge. Sodium was introduced into a side tube, and after five or six redistillations, driven slowly into the absorption tube. During the distillation the pumps were kept running, the tube was baked out, and following each distillation the portion of the side tube which had contained the sodium was sealed off. The McLeod gauge gave the residual gas pressure after this treatment as of the order 10^{-5} mm. The D lines were next examined in absorption. Then argon was admitted in controlled amounts keeping the temperature constant, and the D lines were observed for varying argon pressures. Argon had no effect on the eye widths of the D lines until the pressure had risen to 0.8 mm. After this point the well known pressure broadening set in, and for higher argon pressures the lines were observed correspondingly wider. This gives an optical "interaction-radius" for the argon-sodium combination as of the order of 10^{-7} cm.

The widths for zero pressure broadening for argon pressures less than 0.8 mm were then compared with the theoretical widths. It was found that they were 5.0 ± 0.75 times wider than the theoretical widths.

It was found that a pressure of 8 mm of argon made the same twice as wide as 0.8 mm the sodium density being constant. The tubes used in the contour work were next examined with a high frequency coil, and the discharge inside indicated that a residual gas pressure in all cases of less than 8 mm was present. This represented gas which had ben given off by the sodium after the tube had been sealed off. Comparing widths between the more carefully evacuated tube and the tubes used in the contour work it was found that the former gave widths 1.9 times smaller. Accordingly it seems that pressure broadening accounts for a factor of about two in the discrepancy of ten (observed width to classical width) described above, but seems not to be capable of accounting for the remaining factor of five. Further close investigation is planned.

This tentative conclusion is to order of magnitude in agreement with recent work of Minnaert[6] on the Fraunhofer lines, where he finds that also in

[6] A. Minnaert, Naturwiss. **9**, 211 (1931).

this case the lines are wider than the theory demands. It is difficult, however, to reconcile these results with those of Minkowsky[7] who found widths agreeing with classical theory.

SUMMARY

The classical theory gives correctly the variation of width with the square root of the number of atoms in the line of sight. The decrease of opacity with the inverse square of the wavelength distance from resonance called for by Eq. (3) gives theoretical contours of the correct shapes to match the observed lines. The 2:1 relation between the D lines is found to hold accurately.

The value of the constant "a" is found to be $9.5 \pm 1.2 \times 10^{-13}$ cm, or 5.0 ± 0.75 times larger than the theoretical value, 1.88×10^{-13} cm. The absorption lines are found to be about 5 times wider than the theory predicts. This constant factor is the only point where theory and experiment differ.

The author wishes to express his appreciation to Professor J. Q. Stewart for his continuous interest and criticism during the progress of the work, to Professors L. A. Turner and H. N. Russell for helpful advice in the preparation of this paper, and to Dr. J. C. Boyce for advice concerning vacuum technique.

It is planned to continue the work with the aid of more powerful instruments.

[7] R. Minkowsky, Zeits. f. Physik **36**, 839 (1926) and **55**, 16 (1929).

SELECTIVE THERMAL RADIATION OF COLORED AND PURE FUSED QUARTZ

By R. W. Wood
Johns Hopkins University
(Received June 22, 1931)

Abstract

Thermal radiation of fused quartz.—The peculiarity of pure fused quartz in that it does not visibly radiate at all until its temperature nears the fusion point is explained by the displacement, with increasing temperature, of the ultraviolet absorption band toward the visible.

Selective thermal emission of neodymium oxide dissolved in quartz.—Quartz-neodymium rods, containing neodymium oxide were prepared. When heated they emit a radiation consisting of seven distinct bands. The wave-lengths of the centers of the bands are 8730, 8270, 7504, 6717, 5944, 5340, 4570A. Absorption measurements show bands in the same positions. A method for preparing the neodymium-quartz is described.

IF A thin rod of very pure fused quartz, containing no small particles of foreign matter, is heated in the flame of a bunsen burner, there is practically no emission of light, in conformity with Kirchhoff's law, which predicts that an absolutely transparent body will not radiate, no matter how high its temperature.

However, small specks of impurities embedded in the quartz glow brilliantly, and at one time I was of the opinion that minute air bubbles were also luminous. More careful observations show, however, that this was a mistake, and that, if any luminous bubbles appear, they shine only by reflecting the light radiated by solid particles. If quartz is heated in the oxy-coal-gas flame, it becomes vividly incandescent. The blue white luminosity fades away on removal from the flame without passing through the orange and red stages exhibited by practically all substances shining by thermal radiation.

This indicates clearly that quartz exhibits selective thermal radiation because of the circumstance that, at high temperatures the ultraviolet absorption band migrates towards the region of longer wave-lengths. Radiations in the violet and near ultraviolet preponderate owing to the higher value of the absorption coefficient in this region.

This selective emission was clearly brought out by a spectrogram made in the following way: a fragment of graphite was placed in a small quartz capillary tube and the tube was fused down to a cylindrical rod, with the graphite at its center. The rod was mounted vertically, and heated with a blast lamp operated by only sufficient oxygen to bring the graphite to a bright yellow heat. An image of the glowing fragment was focussed on the center of the slit of a quartz spectrograph, and a series of exposures made with increasing oxygen supply to the flame. When the rod reached full incandescence and was just beginning to soften, it was apparent that its image on the slit was much

whiter than that of the graphite fragment. Also the spectrogram showed that while the graphite was the brighter in the red and yellow region the radiation from the rod was more intense in the violet and ultraviolet as is shown by Fig. 1. This might at first sight be interpreted as short wave-length luminescence since no substances can emit a more intense thermal radiation in any region of the spectrum than a black body. The real explanation appears to be that the graphite is at a slightly lower temperature than the quartz owing to its more rapid dissipation of energy in the form of long wave radiation. Its temperature is not necessarily that of the quartz, depending upon the rate at which energy can be fed in from the quartz in comparison to the rate at which it is lost by radiation. Owing to its low emissivity fused quartz appeared to be the ideal solvent for oxides of the rare earths for exhibiting sharp bands of emission. It is well known that these oxides exhibit more or less conspicuous maxima of emissivity corresponding in spectral distribution to the absorption

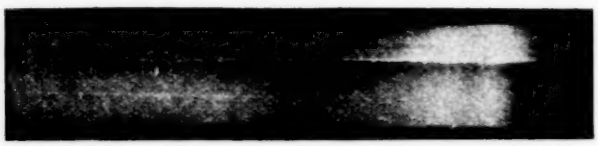

Fig. 1.

bands, but there is always a good deal of continuous spectrum as well. In the case of black or brown oxides, such as that of neodymium, it is obvious that little or no selective emission will be observed. Erbium oxide, which is nearly white, shows the phenomenon well, but there is much continuous spectrum which would probably be absent if a sufficiently thin layer could be employed. After a little experimenting I succeeded in getting a very satisfactory solid solution of neodymium oxide in fused quartz, a pyrosal as the physical chemists would term it.

This was drawn out into thin rods and fibers which when heated in the flame of a bunsen burner and viewed through a direct vision prism exhibited a most beautiful discontinuous spectrum consisting of a red, and orange-yellow and a green band, separated by perfectly dark in intervals.

The spectrum of one of these rods was photographed from the ultraviolet region to the extreme infrared as reached with a meocyanine plate, with a comparison spectrum of neon or neon and argon. The wave-lengths at the center of the bands are given in the Table I.

TABLE I.

λ	Wave-number	λ	Wave-number
8730	114516	5944	168190
8270	120886	5340	187214
7504	133296	4570	219381
6717	148835		

Fig. 2, number 3, gives a very good idea of the complete emission spectrum. This was made with a Bausch and Lomb one-prism spectrograph, suitable color filters being employed to compensate for the variable spectral sensibility of the neocyanine plate. The 8730 band shows faintly at the extreme right. The 5340 and 4570 bands at the lift merge into one another. There is also indication of a band of still shorter wave-length, but its center cannot be easily determined. Spectrum number 4 was taken with a larger prism spectrograph, a panchromatic plate and no filter compensation, and number 2 with a dicyanine plate.

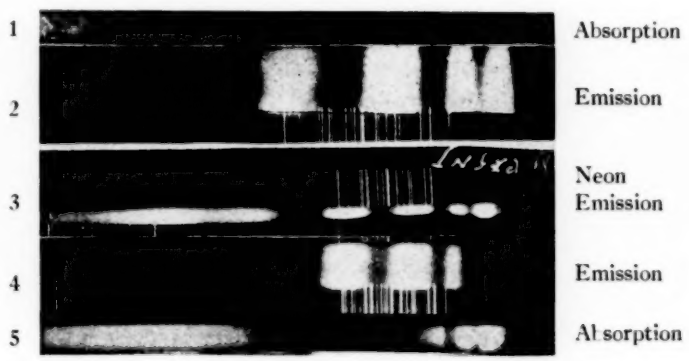

Fig. 2.

The absorption of the neodymium quartz was next investigated. Its absorption coefficient is so low, thin rods appearing perfectly transparent, that an estimated layer of about two centimeters thickness would be required. Having no facilities for preparing a large mass of the material, I drew out a large fused bead into a rod 2 cm long by 1 mm in diameter. This was mounted in a horizontal position by passing it through holes in two pieces of asbestos board with the light of a distant mazda lamp focussed on one end of the rod. The other end, imprisoned by total reflection which was of considerable intensity, was focussed on the spectrograph slit. During the exposure the quartz rod was heated to a temperature sufficient to cause the emission of a feeble yellow light. It is important to secure a record of the absorption at a temperature not far from that at which the emission spectrum was secured, since the absorption bands all move toward the region of longer wave-lengths with rising temperature.

The absorption spectra, secured in this manner are reproduced in coincidence with the emission spectra at the top and bottom of the figure.

Attempts to color quartz with other substances were not very successful. Oxides of nickel and manganese refused to dissolve. A light blue quartz was however obtained with cobalt, and a very beautiful demonstration was made with a fiber the upper part of which is colored with cobalt and the lower with neodymium. The two can hardly be distinguished by the eye, but when we heat it in a flame and view it through a direct vision prism we see a contin-

uous spectrum supported on three colored pedistals of green, yellow and red, respectively.

A few words as to the preparation of the quartz may be of help to any wishing to prepare specimens for demonstration. Neodymium oxide can be prepared from the neodymium ammonium nitrate, obtainable from the Welsbach Light Company of Gloucester City, Pennsylvania, by precipitating the oxalate with oxalic acid, and heating the dried precipitate after washing in a platinum crucible to a white heat with constant stirring.

A speck, the size of a pinhead is introduced into the middle of a quartz tube, of say, 3 mm external and 1 mm internal diameter. The spot containing the oxide is fused in the oxy-coal-gas flame, and twisted and drawn out over an oven again. The rapid twisting of the fused bead, combined with drawing out and reforming into a bead, eventually gives a homogeneous mass. In the earlier stage we find the bead filled with spiral streaks of a bluish color. After the bead is uniform it is drawn out into a thin rod or fiber, of say, 0.5 mm diameter, and bent at a right angle to the rod which serves as a support for holding it vertically in the bunsen flame.

A CANONICAL TRANSFORMATION AND THE VIBRATIONS OF A LOADED STRING

By R. B. Lindsay
Brown University

(Received June 22, 1931)

Abstract

The classical method of discussing the transverse motion of a finite string of negligible weight fastened at the ends with tension τ and loaded with particles of equal mass m, equally spaced at distances a is that in which the Lagrangian equations for a system of n degrees of freedom are set up and integrated by means of determinant analysis. In the present paper it is shown that if we denote the coordinate and conjugate momentum of the sth particle by q_s, p_s, we can find a function $S(q_s, Q_s)$ defining a canonical transformation to the set Q_s, P_s, which transforms the Hamiltonian of the dynamical system (neglecting dissipation) into the particularly simple linear form $H=\Sigma_{s=1}^{n}\omega_s P_s$. The ω_s are the characteristic frequencies of the loaded string (multiplied by 2π), and the usual solution is then obtained very easily from the fact that the P_s, Q_s are action and angle variables. The initial conditions are discussed. The transition to the case of the continuous string is made by finding the transformation functional S analogous to S and the corresponding canonical transformation. The wave mechanics quantization of the loaded string is carried through, the quantized energy values appearing in the form $E=\Sigma_{s=1}^{n}(n_s+\frac{1}{2})h\omega_s/2\pi$.

THE classical method of treating the transverse motion of a finite string of negligible mass fastened at the ends with tension τ and loaded with particles of equal mass m spaced at equal distances a is due to Lagrange.[1] The set of particles is considered as a dynamical system of n degrees of freedom and the equations of motion in Lagrangian form are set up and solved by determinant analysis. The first task of the present paper is to show that the problem can be handled very directly by means of a canonical transformation.

Let the displacement coordinate of the j-th particle be q_j and its conjugate momentum be p_j. We shall neglect dissipation. The Hamiltonian then has the form

$$H = 1/2m \cdot \sum_{j=1}^{n} p_j^2 + \tau/2a \cdot \sum_{j=1}^{n+1}(q_j - q_{j-1})^2 \qquad (1)$$

where, since the string is fastened at the ends, $q_0 = q_{n+1} = 0$. The motion of the system is given by the canonical equations

$$\frac{\partial H}{\partial q_j} = -\dot{p}_j, \quad \frac{\partial H}{\partial p_j} = \dot{q}_j \qquad (j = 1, 2, \cdots n). \qquad (2)$$

[1] Rayleigh, Theory of Sound, Vol. I, para. 120.

We now seek a transformation p_j, $q_j \rightarrow P_j$, Q_j and $H \rightarrow K$ such that the new canonical equations are

$$\frac{\partial K}{\partial P_j} = \dot{Q}_j, \quad \frac{\partial K}{\partial Q_j} = -\dot{P}_j. \tag{2'}$$

Such a transformation is called *canonical*. Our particular aim, of course, is to find such a transformation that the new Hamiltonian has a very simple form. The transformation is defined by the so-called transformation or substitution function S, from which we have (if, as in the present case, it is chosen as a function of the Q_j and q_j)

$$\frac{\partial S}{\partial q_j} = p_j, \quad \frac{\partial S}{\partial Q_j} = -P_j. \tag{3}$$

For the sake of illustration let us confine our attention for the moment to the case of a single particle performing simple harmonic motion. It is well known that if

$$S = m\omega/2 \cdot q^2 \cot Q, \tag{4}$$

where ω is a parameter, the transformation so defined leads to a particularly simple Hamiltonian. In fact, we have at once from Eqs. (3)

$$p = m\omega q \cot Q$$

and

$$P = m\omega/2 \cdot q^2 \csc^2 Q$$

whence it follows that

$$q = (2/m\omega)^{1/2} \cdot P^{1/2} \cdot \sin Q \tag{5}$$

$$p = (2m\omega)^{1/2} \cdot P^{1/2} \cos Q. \tag{6}$$

In this case the Hamiltonian, which is

$$H = 1/2m \cdot p^2 + \frac{\kappa}{2} \cdot q^2 \tag{7}$$

(where κ is the stiffness coefficient) transforms into

$$K = \omega p \tag{8}$$

where $\omega = (\kappa/m)^{1/2}$. The canonical Eqs. (3) yield at once

$$P = \text{const.}, \quad Q = \omega t + \beta \tag{9}$$

and the resulting value of q which gives the solution to the problem is

$$q = (2/m\omega)^{1/2} P^{1/2} \cdot \sin(\omega t + \beta), \tag{10}$$

$\omega/2\pi$ appearing as the frequency of the motion.

We look for a generalization of the transformation function (4) which will transform H in the general case (i.e., that of Eq. (1)) into a linear function of the P_j. This proves to be of the form

$$S = \sum_{k=1}^{n} (m/2)^2 \omega_k^2 \cot Q_k \Big(\sum_{s=1}^{n} a_{sk} q_s \Big)^2 \tag{11}$$

where the ω_k form a set of parameters and

$$a_{sk} = 2/(m(n+1)\omega_k)^{1/2} \cdot \sin sk\pi/(n+1). \tag{12}$$

For on assuming (11) we have

$$\frac{\partial S}{\partial q_j} = p_j = 2 \sum_{k=1}^{n} (m/2)^2 \omega_k^2 \cot Q_k \cdot a_{jk} \Big(\sum_{s=1}^{n} a_{sk} q_s \Big), \tag{13}$$

and

$$-\frac{\partial S}{\partial Q_j} = P_j = (m/2)^2 \omega_j^2 \csc^2 Q_j \Big(\sum_{s=1}^{n} a_{sj} q_s \Big)^2. \tag{14}$$

Hence

$$\sum_{s=1}^{n} a_{sk} q_s = \frac{2(P_k)^{1/2}}{m\omega_k} \sin Q_k \tag{15}$$

whence on resubstitution into Eq. (13) there results

$$p_j = \sum_{k=1}^{n} m\omega_k a_{jk} (P_k)^{1/2} \cos Q_k. \tag{16}$$

Solving the set of simultaneous Eqs. (15) using the relations

$$\begin{aligned} \sum_{s=1}^{n} a_{sk} a_{sj} &= 2/m\omega_k, \text{ for } j = k \\ &= 0, \qquad \text{for } j \neq k \end{aligned} \tag{17}$$

and the equivalent relations

$$\begin{aligned} \sum_{s=1}^{n} a_{ks} a_{js} \omega_s &= 2/m \text{ for } j = k \\ &= 0 \quad \text{for } j \neq k \end{aligned} \tag{17'}$$

we obtain the q_j in terms of the Q_k, P_k as follows:

$$q_j = \sum_{k=1}^{n} a_{jk} (P_k)^{1/2} \sin Q_k. \tag{18}$$

Substitution of (16) and (18) into Eq. (1) then reveals that $H(p, q) \rightarrow K(P, Q)$, where[2]

$$K = \sum_{j=1}^{n} \omega_j P_j \tag{19}$$

[2] Further identities besides (17) and (17') needed for the demonstration of (18) are

$$\sum_{j=1}^{n} a_{jk} a_{j+1,k} = \frac{2}{m\omega_k} \cos \frac{k\pi}{n+1} \quad \text{and}$$

$$\sum_{j=1}^{n} a_{jk} a_{j+1,l} = -\sum_{j=1}^{n} a_{j+1,k} a_{jl}.$$

provided that

$$\omega_j = 2(\tau/ma)^{1/2} \cdot \sin j\pi/2(n+1). \tag{20}$$

The canonical Eqs. (3) then yield at once

$$P_j = \text{const.}, Q_j = \omega_j t + \beta_j \tag{21}$$

in which the β_j are arbitrary constants. The solution to the problem then appears in the usual form

$$q_j = \sum_{k=1}^{n} a_{jk}(P_k)^{1/2} \cdot \sin(\omega_k t + \beta_k), \tag{22}$$

where the ω_k appear as the characteristic frequencies (multiplied by 2π, of course). The constants P_k and β_k are determined by the boundary conditions. Let the initial displacement of the j-th particle be q_j^0, and obtain

$$q_j^0 = \sum_{k=1}^{n} a_{jk}(P_k)^{1/2} \sin \beta_k.$$

Multiplying through by a_{js} and summing over all j, there results

$$\sum_{j=1}^{n} q_j^0 a_{js} = 2/m\omega_s \cdot (P_s)^{1/2} \sin \beta_s \tag{23}$$

by virtue of the relations (17). Performing the same operation for the initial momenta we get

$$\sum_{j=1}^{n} a_{js} p_j^0 = 2(P_s)^{1/2} \cos \beta_s. \tag{24}$$

The elimination between (23) and (24) gives

$$P_s = m^2\omega_s^2/4 \cdot \left(\sum_{j=1}^{n} a_{js} q_j^0 \right)^2 + 1/4 \cdot \left(\sum_{k=1}^{n} a_{js} p_j^0 \right)^2 \cdot \tag{25}$$

while

$$\tan \beta_s = m\omega_s \cdot \frac{\sum_{j=1}^{n} a_{js} q_j^0}{\sum_{j=1}^{n} a_{js} p_j^0} \cdot \tag{26}$$

Incidentally we note of course that Eqs. (23)–(26) hold for q_j, p_j in general if we replace β_s by Q_s. We shall utilize this fact in the definition of the normal coordinates. (See the later section on the quantization of the loaded string.)

It may be of some interest to consider for a moment more closely the connection between the P_s and the initial distribution. Let us take but a single illustration and suppose that $P_s\omega_s = C$ where C is a constant (same for all s). This corresponds, of course, to equipartition of energy among the various

possible modes of oscillation, and for ω_s small and C large is approximately equivalent to the Planck quantum distribution based on the Boltzmann statistics. The latter is of course in the form (for the *average* energy corresponding to frequency $\nu_s = \omega_s/2\pi$)

$$E_s = h\nu_s/e^{h\nu s/C} - 1 \tag{27}$$

and for C large enough this reduces to the equipartition case

$$E_s = C. \tag{28}$$

Let us assume that all the particles have zero initial displacement, i.e., $q_j^0 = 0$ for all j. We may then determine the p_j^0 to satisfy (28). In fact from (16)

$$p_j^0 = 2(mC)^{1/2}/(n+1)^{1/2} \cdot \sum_{k=1}^{n} \sin \frac{jk\pi}{n+1} \cdot \tag{29}$$

From the summation formula

$$\sum_{k=1}^{n} \sin k\theta = \sin (n+1)\theta/2 \cdot \sin n\theta/2 \cdot \csc \theta/2$$

there results at once

$$\begin{aligned} p_j^0 &= 2(mC/(n+1))^{1/2} \cdot \cot j\pi/2(n+1), \text{ for } j \text{ odd} \\ &= 0, \text{ for } j \text{ even}. \end{aligned} \tag{30}$$

We thus obtain the interesting result that for equipartition, if $q_j^0 = 0$ for all j, the even numbered particles have $p_j^0 = 0$ as well. The p_j^0 for j odd decrease as j increases from 1 to n.

The above is merely an illustration. More general considerations are attended with considerable mathematical difficulties.

Extension to the Continuous String

The preceding analysis is easily extended to the case of the continuous string. We let $x = ja$, where $(n+1)a = l$, the length of the string. Then $j\pi/n+1 = \pi x/l$. And as $n \to \infty$ and $m \to 0$, $m(n+1) \to M$, where M is the mass of the whole string. We therefore have

$$a_{jk} \to a_k(x) = 2/(M\omega_k)^{1/2} \cdot \sin k\pi x/l \tag{31}$$

and our transformation (18) becomes in the limit

$$q_j \to q(x) = \sum_{k=1}^{\infty} a_k(x)(P_k)^{1/2} \sin Q_k. \tag{32}$$

Introducing now the generalized Lagrangian functional, we have

$$L = \tfrac{1}{2} \int_0^l \left\{ M/l \cdot (\dot{q}(x))^2 - \tau \left(\frac{\partial q}{\partial x} \right)^2 \right\} dx, \tag{33}$$

and we define the conjugate to $q(x)$ as

$$p(x) = \frac{\delta L}{\delta \dot{q}(x)}$$

where the notation implies what may be called the functional derivative of L with respect to $\dot{q}(x)$.[3] It then follows that

$$\begin{aligned} p(x) &= M/l \cdot \dot{q}(x) \\ &= M/l \cdot \sum_{k=1}^{\infty} \omega_k a_k(x) (P_k)^{1/2} \cdot \cos Q_k, \end{aligned} \tag{34}$$

since in the limit we may set $p_j/m \to \dot{q}(x)$. The ω_k are still to be considered parameters to be evaluated presently. Corresponding to the transformation function (11) for the loaded case we now have for the continuous string the *transformation functional*

$$S = \sum_{k=1}^{\infty} (M/2l)^2 \omega_k^2 \cot Q_k \left\{ \int_0^l a_k(x) q(x) dx \right\}^2. \tag{35}$$

We have indeed the following

$$\frac{\partial S}{\partial Q_k} = - (M/2l)^2 \omega_k^2 \csc^2 Q_k \left\{ \int_0^l a_k(x) q(x) dx \right\}^2. \tag{36}$$

Now from (31) and (32) there follows

$$\int_0^l a_k(x) q(x) dx = \int_0^l a_k(x) \left\{ \sum_{j=1}^{\infty} a_j(x) (P_j)^{1/2} \sin Q_j \right\} dx. \tag{37}$$

But we recall that

$$\begin{aligned} \int_0^l \sin j\pi x/l \cdot \sin k\pi x/l \cdot dx &= l/2 \quad \text{for } k = j \\ &= 0 \quad \text{for } k \neq j \end{aligned}$$

with similar results for the cosine in place of the sine. Therefore

$$\int_0^l a_k(x) q(x) dx = \frac{4}{M\omega_k} \cdot \frac{l}{2} (P_k)^{1/2} \sin Q_k \tag{38}$$

and hence on substitution

$$\frac{\partial S}{\partial Q_k} = - P_k. \tag{39}$$

[3] See F. Möglich, Ann. d. Physik **2**, 676 (1929); Also: R. B. Lindsay, Proc. Nat. Acad. Sci., July, 1931.

Moreover forming the functional derivative we have

$$\begin{aligned}\frac{\delta \boldsymbol{S}}{\delta q(x)} &= 2\left(\frac{M}{2l}\right)^2 \sum_{k=1}^{\infty} \omega_k^2 \cot Q_k \cdot a_k(x) \int_0^l a_k(x) q(x) dx \\ &= p(x)\end{aligned} \tag{40}$$

by Eq. (34). Hence $\boldsymbol{S}$ appears as the generalization of S, with Eqs. (39) and (40) the analogue of Eq. (3). The Hamiltonian functional is now

$$\boldsymbol{H} = \tfrac{1}{2} \int_0^l \left\{ \frac{l}{M} \cdot (p(x))^2 + \tau \left(\frac{\partial q}{\partial x}\right)^2 \right\} dx, \tag{41}$$

and the substitution of (32) and (34) into this expression yields at once

$$\boldsymbol{H} = \sum_{k=1}^{\infty} \omega_k P_k = E \tag{42}$$

where now we must have, however,

$$\omega_k = k\pi(\tau/Ml)^{1/2}. \tag{43}$$

The latter are the natural frequencies (multiplied by 2π) of the finite continuous string of mass M, length l and stretched with tension τ. We have thus expressed the total energy of the continuous string as well as that of the loaded string as the sum of the contributions due to the individual frequencies.[4]

The Quantization of the Loaded String

The discussion in this paper is in a form appropriate for the treatment of the problem of the quantized motion of the loaded string. Thus we can quantize at once by the method of the older quantum theory in setting

$$\oint P_j dQ_j = n_j h \tag{44}$$

n_j being any positive integer. The P_j and Q_j are angle and action variables and hence we have

$$P_j = n_j h / 2\pi \tag{45}$$

and the quantized energy values are

$$\begin{aligned}E &= \sum_{j=1}^{n} n_j h \omega_j / 2\pi \\ &= \sum_{j=1}^{n} n_j h \cdot \nu_j\end{aligned} \tag{46}$$

[4] Cf. the more elaborate treatment of Möglich, reference 3.

with $\nu_j = \omega_j/2\pi$. This result, of course, does not agree with the quantization on the basis of wave mechanics. The latter can be carried out as follows.[5] We first separate the variables in terms of the normal coordinates ϕ_s defined as follows. In fact, recalling Eqs. (15) and (16) we have

$$\begin{aligned} \sum_{j=1}^{n} a_{js} q_j &= 2/m\omega_s \cdot (P_s)^{1/2} \sin Q_s \\ \sum_{j=1}^{n} a_{js} p_j &= 2(P_s)^{1/2} \cdot \cos Q_s \end{aligned} \tag{47}$$

from which by the elimination of Q_s we have

$$P_s = m^2\omega_s^2/4 \cdot \left(\sum_{j=1}^{n} a_{js} q_j \right)^2 + \tfrac{1}{4} \cdot \left(\sum_{j=1}^{n} a_{js} p_j \right)^2 \tag{48}$$

whence the energy is given by

$$\begin{aligned} K &= \sum_{s=1}^{n} \omega_s P_s \\ &= \sum_{s=1}^{n} \omega_s/4 \cdot \left\{ m^2\omega_s^2 \left(\sum_{j=1}^{n} a_{js} q_j \right)^2 + \left(\sum_{j=1}^{n} a_{js} p_j \right)^2 \right\} \\ &= E. \end{aligned} \tag{49}$$

The energy is thus represented in terms of a sum of squares and we are led to define the normal coordinate ϕ_s as follows

$$\begin{aligned} \phi_s &= 1/(m(n+1)\omega_s)^{1/2} \cdot m\omega_s \sum_{j=1}^{n} a_{js} q_j \\ &= 2/(m(n+1)\omega_s)^{1/2} \cdot (P_s)^{1/2} \sin Q_s. \end{aligned} \tag{50}$$

It then follows that

$$\begin{aligned} \dot{\phi}_s &= 2/(m(n+1)\omega_s)^{1/2} \cdot \omega_s (P_s)^{1/2} \cos Q_s \\ &= 1/(m(n+1)\omega_s)^{1/2} \cdot \omega_s \sum_{j=1}^{n} a_{js} p_j. \end{aligned} \tag{51}$$

Substituting from (50) and (51) into (49) we have

$$K = m(n+1)/4 \cdot \sum_{s=1}^{n} \{ \phi_s^2 + \omega_s^2 \phi_s^2 \} \tag{52}$$

where the ω_s are given as in Eq. (20).

[5] The quantization of the continuous string has been carried through by Möglich (reference 3, p. 697) in a much more elaborate treatment. It is felt however that the special case of the loaded strong has some interest in itself.

The Schrödinger equation in normal coordinates now becomes[6]

$$\frac{\partial}{\partial\phi_1}\left\{\sum_{s=1}^{n}\phi_{1q_s}^2\cdot\frac{\partial\psi}{\partial\phi_1}+\sum_{s=1}^{n}\phi_{1q_s}\phi_{2q_s}\cdot\frac{\partial\psi}{\partial\phi_2}+\cdots+\sum_{s=1}^{n}\phi_{1q_s}\phi_{nq_s}\cdot\frac{\partial\psi}{\partial\phi_n}\right\}$$
$$+\ \cdot\ \cdot\ \cdot\ \cdot\ \cdot\ \cdot\ \cdot\ \cdot\ \cdot\ \cdot\ \cdot\ \cdot\ \cdot$$
$$+\frac{\partial}{\partial\phi_n}\left\{\sum_{s=1}^{n}\phi_{1q_s}\phi_{nq_s}\cdot\frac{\partial\psi}{\partial\phi_1}+\cdots+\sum_{s=1}^{n}\phi_{nq_s}^2\cdot\frac{\partial\psi}{\partial\phi_n}\right\} \tag{53}$$
$$+\frac{8\pi^2m}{h^2}(E-V)\psi=0,$$

where $\phi_{jq_s}=\partial\phi_j/\partial q_s$. The calculation of the latter quantities is easy to make from (50). Thus, recalling Eq. (12)

$$\phi_{jq_s}=2/(n+1)\cdot\sin sj\pi/(n+1). \tag{54}$$

Then

$$\sum_{s=1}^{n}\phi^2{}_{jq_s}=4/(n+1)^2\cdot\sum_{s=1}^{n}\sin^2 sj\pi/(n+1) \tag{55}$$
$$=2/(n+1)$$

while

$$\sum_{s=1}^{n}\phi_{jq_s}\phi_{kq_s}=4/(n+1)^2\cdot\sum_{s=1}^{n}\sin js\pi/(n+1)\cdot\sin ks\pi/(n+1)=0 \tag{56}$$

(See Eq. (17).) The wave equation then becomes

$$\sum_{s=1}^{n}\frac{\partial^2\psi}{\partial\phi_s{}^2}+(n+1)/2\cdot\frac{8\pi^2m}{h^2}(E-V)\psi=0. \tag{57}$$

The potential energy V is

$$V=(n+1)\tau/a\cdot\sum_{s=1}^{n}\phi_s{}^2\sin^2 s\pi/2(n+1). \tag{58}$$

Substituting into (57) we have

$$\sum_{s=1}^{n}\frac{\partial^2\psi}{\partial\phi_s{}^2}+(n+1)/2\cdot\frac{8\pi^2m}{h^2}\left\{\sum_{s=1}^{n}E_s-\frac{m(n+1)}{4}\sum_{s=1}^{n}\omega_s{}^2\phi_s{}^2\right\}\psi=0 \tag{59}$$

which is easily separable into individual equations of the form

$$\frac{\partial^2\psi}{\partial\phi_s{}^2}+(n+1)/2\cdot\frac{8\pi^2m}{h^2}\left\{E_s-\frac{m(n+1)}{4}\omega_s{}^2\phi_s{}^2\right\}\psi=0. \tag{60}$$

The eigenwerte are, of course,

$$E_s=(n_s+\tfrac{1}{2})h\nu_s \tag{61}$$

[6] Sommerfeld, Wellenmechanischer Ergänzungsband, p. 146.

and the total quantized energy is

$$E = \sum_{s=1}^{n} E_s = \sum_{s=1}^{n} (n_s + \tfrac{1}{2}) h\nu_s \tag{62}$$

with n_s any positive integer.

It is interesting to note that if in the equation

$$\sum_{s=1}^{n} \omega_s P_s = E \tag{63}$$

we consider P_s (in line with the suggestion of Eq. (52)) as replaced by the operator

$$P_s \cdot \equiv \left\{ -\frac{h^2}{4\pi^2 m(n+1)\omega_s} \frac{\partial^2}{\partial \phi_s^2} + \omega_s \frac{m(n+1)}{4} \phi_s^2 \right\}. \tag{64}$$

the equation

$$(\sum \omega_s P_s - E)\psi = 0 \tag{65}$$

at once becomes the Schrödinger equation in the form (59). This operator interpretation materially simplifies the problem of quantization of the loaded string.

THE MOTION OF A DIRAC ELECTRON IN A MAGNETIC FIELD*

By L. D. Huff
California Institute of Technology, Pasadena

(Received June 17, 1931)

Abstract

Solutions of the Dirac wave equation representing a free electron moving in a uniform magnetic field are obtained. The functions are similar to those obtained by Landau and by Uhlenbeck and Young as solutions of the Schrödinger equation. A wave packet is constructed representing a beam of electrons passing through a slit. The results agree with the classical predictions to terms of the order of the de Broglie wave-length of the electron divided by the radius of curvature of its classical path. For experimental cases this ratio is of the order 10^{-5} to 10^{-10}. Hence it is concluded that the difference between magnetic deflection measurements of e/m and other determinations cannot be explained as a quantum effect.

A NUMBER of papers[1,2,3,4] have recently appeared treating the motion on an electron in a magnetic field on the basis of quantum mechanics. The purpose of these investigations was to see if the difference in the values of the specific charge of the electron[5] obtained by deflection and by spectroscopic experiments could be explained as a quantum effect. Recent experimental work on free electrons by Perry and Chaffee[6] and by Kirchner[7] give values for the ratio e/m very close to the spectroscopic values. However, neither of these experiments involved deflections in a magnetic field so that a quantum mechanical effect might still be present in the magnetic measurements. In fact, Kirchner suggests that Page's investigation might explain the difference between his own results and the older ones of Wolf.[8]

Page[1] obtains solutions of the Schrödinger equation representing a free electron in a magnetic field. He shows that the mean radius of the electron's path for each of these solutions is less than the classical radius given by $r = mvc/eH$, except that for one solution his mean radius is equal to the classical. He concludes that if a beam of electrons passing through a slit is represented by a combination of his solutions the average radius of curvature of the paths of the electrons will be less than that calculated by the classical formula and that the difference is of the right order of magnitude to explain the observed

* Reported at the Pasadena meeting of the American Physical Society, June, 1931.
[1] L. Page, Phys. Rev. **36,** 444 (1930).
[2] G. E. Uhlenbeck and L. A. Young, Phys. Rev. **36,** 1721 (1930).
[3] M. S. Plesset, Phys. Rev. **36,** 1728 (1930).
[4] E. H. Kennard, Proc. Nat. Acad. **17,** 58 (1931).
[5] R. T. Birge, Phys. Rev. Sup. **1,** 47 (1929).
[6] Charlotte T. Perry and E. L. Chaffee, Phys. Rev. **36,** 904 (1930).
[7] F. Kirchner, Phys. Zeits. **31,** 1073 (1930).
[8] F. Wolf, Ann. d. Physik **83,** 849 (1927).

discrepancy in e/m. However, he does not show that a finite beam of electrons can be represented by such a combination of his solutions and in particular he ignores a whole set of solutions of this equation obtained by letting his quantum number m take on negative values. For these solutions the mean radius is *greater* than the classical radius. Hence, his work cannot be considered conclusive. Plesset[3] used a second order relativistic wave equation and carried out calculations similar to those of Page. The above remarks apply to his work as well.

Uhlenbeck and Young[2] used a different form of solution of the Schrödinger equation, which was first given by Landau.[9] They calculated the distance which a beam of electrons incident normally would penetrate into a magnetic field and obtained the classical result.

Kennard[4] showed that in any electromagnetic field the center of gravity of a wave packet obeying the Schrödinger equation would move according to classical laws. From this he concluded that the classical expression could be used whenever an experiment consisted in measuring a mean position of a large number of electrons. He was not able to extend his results to the Dirac wave equation.

In the present work the Dirac equation for the electron is used. Solutions for a homogeneous magnetic field are obtained which are analagous to the solutions used by Uhlenbeck and Young. From these solutions a wave packet is constructed which represents a beam of electrons passing through a slit into a magnetic field. The motion of this packet is studied.

Solutions in the Magnetic Field

We shall use the linear Hamiltonian for the electron in the form given in Dirac's quantum mechanics.[10]

$$\{W/c + (e/c)A_0 + \rho_1[\boldsymbol{\sigma}\cdot(\boldsymbol{p} + (e/c)\boldsymbol{A})] + \rho_3 mc\}\psi = 0. \tag{1}$$

For a uniform magnetic field H in the z-direction we can write

$$A_0 = 0,\ A_z = 0;\ A_x = -\tfrac{1}{2}Hy;\ A_y = \tfrac{1}{2}Hx.$$

Putting $w = eH/2c$, Eq. (1) becomes

$$\{W/c + \rho_1[\sigma_x(p_x - wy) + \sigma_y(p_y + wx) + \sigma_z p_z] + \rho_3 mc\}\psi = 0.$$

We shall find solutions of this equation which are much like those used by Uhlenbeck and Young.[2,9] To do this put

$$\psi = e^{i(w/k)xy}e^{i(\eta/k)y}\phi(x). \tag{2}$$

k is Planck's constant divided by 2π. Assuming that ψ is independent of z.

The equation for ϕ is

$$\left\{\frac{W}{c} + \rho_1[\sigma_x p_x + \sigma_y(2wx + \eta)] + \rho_3 mc\right\}\phi = 0. \tag{3}$$

[9] L. Landau, Zeits. f. Physik **64,** 629 (1930).

[10] P. A. M. Dirac, Quantum Mechanics, Oxford University Press (1930).

We see that the solution for any value of η can be obtained from that for $\eta=0$ by replacing x by $(x+\eta/2w)$. That is

$$\phi_\eta(x) = \phi_{\eta=0}\left(x+\frac{\eta}{2w}\right).$$

Writing out the component equations for the case $\eta=0$

$$\begin{aligned}
\left(\frac{W}{c}+mc\right)\phi_1 + \frac{k}{i}\frac{d\phi_4}{dx} - i2wx\phi_4 &= 0\\
\left(\frac{W}{c}+mc\right)\phi_2 + \frac{k}{i}\frac{d\phi_3}{dx} + i2wx\phi_3 &= 0\\
\left(\frac{W}{c}-mc\right)\phi_3 + \frac{k}{i}\frac{\partial\phi_2}{dx} - i2wx\phi_2 &= 0\\
\left(\frac{W}{c}-mc\right)\phi_4 + \frac{k}{i}\frac{d\phi_1}{dx} + i2wx\phi_1 &= 0.
\end{aligned} \tag{4}$$

Eliminating ϕ_1, between the first and last of the above gives

$$\frac{d^2\phi_4}{dx^2} + \frac{1}{k^2}\left((W^2/c^2) - m^2c^2 + 2wk - 4w^2x^2\right)\phi_4 = 0.$$

Or putting $\xi=2x(w/k)^{1/2}$ and

$$\nu = \frac{1}{4wk}(W^2/c^2 - m^2c^2) = \frac{1}{4wk}p^2$$

where p is the total momentum, we obtain

$$\begin{aligned}
\frac{d^2\phi_4}{d\xi^2} + (\nu + \tfrac{1}{2} - \tfrac{1}{4}\xi^2)\phi_4 &= 0\\
\frac{d^2\phi_1}{d\xi^2} + (\nu - \tfrac{1}{2} - \tfrac{1}{4}\xi^2)\phi_1 &= 0.
\end{aligned} \tag{5}$$

We recognize the first of these as the equation for D_ν given in Whittaker and Watson, Modern Analysis.[11] The second is the equation for $D_{\nu-1}$. Comparing the first of Eqs. (4) with the second recurrence formula for the D_ν's given in Whittaker and Watson

$$D_\nu'(\xi) + \tfrac{1}{2}\xi D_\nu(\xi) - \nu D_{\nu-1}(\xi) = 0$$

we find that if

$$\phi_4(x) = aD_\nu(\xi) \tag{6}$$

[11] Whittaker and Watson, Modern Analysis, Cambridge University Press, Fourth Edition (1927).

then

$$\phi_1(x) = i\frac{((W/c) - mc)}{2(kw)^{1/2}} aD_{\nu-1}(\xi).$$

It can be shown in a similar manner that

$$\begin{aligned} \phi_2 &= iC((W/c) - mc)\phi_4 \\ \phi_3 &= iC((W/c) + mc)\phi_1. \end{aligned} \tag{7}$$

The condition that the z- component of the current be zero at $x=0$ makes C real, and if C is real $S_x=0$ for any value of x.

We can write the solutions

$$\begin{aligned} \psi_1 &= e^{i(w/k)xy}e^{i(\eta/k)y}\phi_1\left(x+\frac{\eta}{2w}\right) \\ \psi_2 &= e^{i(w/k)xy}e^{i(\eta/k)y}iC\left(\frac{W}{c}-mc\right)\phi_4\left(x+\frac{\eta}{2w}\right) \\ \psi_3 &= e^{i(w/k)xy}e^{i(\eta/k)y}iC\left(\frac{W}{c}+mc\right)\phi_1\left(x+\frac{\eta}{2w}\right) \\ \psi_4 &= e^{i(w/k)xy}e^{i(\eta/k)y}\phi_4\left(x+\frac{\eta}{2w}\right) \end{aligned} \tag{8}$$

where the ϕ's are given by (6). We might point out that if $\lambda=h/p$ is the de Broglie wave-length and $r=cp/eH$ is the radius of the classical circle then

$$\pi r = \nu\lambda.$$

Hence ν is the number of de Broglie wave-lengths in a classical half circle. Uhlenbeck and Young found that $\pi r=(\nu+\frac{1}{2})\lambda$ when Schrödinger's equation is used instead of Dirac's.

The Solutions in Free Space

Put $p^2=p_1^2+p_2^2=W^2/c^2-m^2c^2$ where p_1 and p_2 are the momenta in the x and y-directions. The monentum in the z-direction is considered zero. Then for field free space we expect solutions of the form $e^{i/k(p_1x+p_2y)}$. The following set of solutions was found:

$$\begin{aligned} \psi_1 &= \frac{p_1 - ip_2}{(W/c) + mc} A_4 e^{i/k(p_1x+p_2y)} \\ \psi_2 &= A_2 e^{i/k(p_1x+p_2y)} \\ \psi_3 &= \frac{p_1 - ip_2}{(W/c) - mc} A_2 e^{i/k(p_1x+p_2y)} \\ \psi_4 &= A_4 e^{i/k(p_1x+p_2y)} \end{aligned} \tag{9}$$

where A_2 and A_4 are arbitrary constants.

If we consider the functions (9) as representing a beam moving in the $+x$ and $+y$-directions, we can find the representation of a similar beam moving in the $-x$ and $+y$-directions by using different constants B_2 and B_4 and by replacing p_1 by $-p_1$.

Matching Solutions

Let us suppose that we have a uniform magnetic field of strength H in the z-direction for all positive values of x, and that for x negative the field is zero. We wish to match solutions of the type (8) with those of type (9) for $x=0$. We see first that $p_2=\eta$ in order that the solutions be equal for all values of y. We suppose that in the free space there is both an incident beam (p_1 positive) and an emergent beam (p_1 negative). Setting the sum of these solutions equal to the functions in the field with $x=0$ gives

$$\begin{aligned}
&\frac{-p_1(A_4-B_4)+ip_2(A_4+B_4)}{(W/c)+mc}=\phi_1(p_2/2w)\\
&A_2+B_2=iC((W/c)-mc)\phi_4(p_2/2w)\\
&\frac{-p_1(A_2-B_2)+ip_2(A_2+B_2)}{(W/c)-mc}=iC((W/c)+mc)\phi_1(p_2/2w)\\
&A_4+B_4=\phi_4(p_2/2w).
\end{aligned}\tag{10}$$

Solving for the B's in terms of the A's gives

$$\begin{aligned}
B_4&=\gamma A_4\\
B_2&=\gamma A_2
\end{aligned}\tag{11}$$

where

$$\gamma=\frac{1-ip_2/p_1+\dfrac{(W/c)+mc}{p_1}\dfrac{\phi_1(p_2/2w)}{\phi_4(p_2/2w)}}{1+ip_2/p_1-\dfrac{(W/c)+mc}{p_1}\dfrac{\phi_1(p_2/2w)}{\phi_4(p_2/2w)}}.\tag{12}$$

Since the ratio ϕ_1/ϕ_4 is pure imaginary from Eqs. (6) we see that γ is a number divided by its complex conjugate and hence $|\gamma|=1$. Also since D is even or odd according as ν is even or odd, one of the functions ϕ_1, ϕ_4 is odd, the other even. Hence, their ratio is odd. Hence, if we change the sign of p_2, γ becomes $1/\gamma$. That is

$$\gamma(p_1,-p_2)=\frac{1}{\gamma(p_1,p_2)}=\gamma^*(p_1,p_2).\tag{13}$$

Having obtained these solutions we will use them in several ways. We will first consider an infinite beam incident normally and later will construct a wave packet.

Distribution of Current in the Field for an Infinite Incident Beam

Let us find the current densities inside the field for the case $p_2=0$. From Dirac:

$$-S_z = \psi^*\alpha_z\psi = \psi_1^*\psi_4 + \psi_2^*\psi_3 + \psi_3^*\psi_2 + \psi_4^*\psi_1$$
$$= (1 + C^2p^2)(\phi_1^*\phi_4 + \phi_4^*\phi_1) = 0.$$

Since the product $\phi_4^*\phi_1$ is pure imaginary from (6) and hence $\phi_1^*\phi_4 = -\phi_4^*\phi_1$. Similarly, $-S_y = \psi^*\alpha_y\psi = -i(1+C^2p^2)(\phi_4^*\phi_1 - \phi_1^*\phi_4)$.

If we use our expressions for the &'s in terms of the D's we have

$$S_y = (1 + C^2p^2)\frac{(W/c) - mc}{(kw)^{1/2}} aa^*D_\nu D_{\nu-1}. \tag{14}$$

Since $D_{\nu-1}$ and D_ν are successive solutions of the Weber equation (5), they have a different number of zeros between $x=0$ and $x=0$. (There are no zeros for $x>r$.) Therefore, S_y is negative for some values of x. In fact, the distance between successive regions of negative S_y is of the order of λ, the de Broglie wave-length. This is apparently an effect of spin since Uhlenback and Young found an expression for S_y which is always positive.

Let us find the average x-coordinate of the current, defined by

$$\bar{x} = \frac{\int_0^\infty xS_y dx}{\int_0^\infty S_y dx}.$$

Classically $S_y = 2I/(r^2-x^2)^{1/2}$ and $\bar{x} = \pi v/4$.

In evaluating $\bar{x}$ using the quantum mechanical expressions we shall need the integrals

$$\int_0^\infty D_\nu D_{\nu-1}d\xi \quad \text{and} \quad \int_0^\infty D_\nu D_{\nu-1}\xi d\xi.$$

We shall evaluate these integrals for ν even. The methods are much the same for ν odd and the final value of $\bar{x}$ is exactly the same.

By multiplying the first of Eqs. (5) by $D_{\nu-1}$, the second by D_ν and subtracting and then integrating we find

$$\int_0^\infty D_\nu D_{\nu-1}d\xi = [D_\nu(0)]^2 = \left(\frac{\Gamma(\tfrac{1}{2})2^{\nu/2}}{\Gamma(\tfrac{1}{2} - \tfrac{1}{2}\nu)}\right)^2. \tag{15}$$

Using the recurrence formulae we find

$$\int_0^\infty \xi D_\nu D_{\nu-1}d\xi = \tfrac{1}{2}\int_0^\infty [D_\nu]^2 d\xi = \tfrac{1}{2}(2\pi)^{1/2}\nu!. \tag{16}$$

Putting into our expression for $\bar{x}$

$$\bar{x} = \tfrac{1}{4}\left(\frac{k}{w}\right)^{1/2} \frac{\left[\left(\frac{\nu}{2}\right)!\right]^2}{\nu!} 2\nu(2\pi)^{1/2}.$$

By using Stirling's formula

$$n! = (2\pi n)^{1/2}\left(\frac{n}{e}\right)^n$$

we obtain

$$\bar{x} = \frac{\pi}{4} r$$

the classical value. Hence the result agrees with the classical value to the extent that Stirling's formula holds. The error in Stirling's formula is of the order $1/\nu$ and since ν is of the order 10^8 to 10^{10} this deviation is entirely negligible. The same results is obtained if we use Uhlenbeck and Young's solutions of the Schrödinger equation.

By using a Wentzel-Brillouin-Kramers[2,12] approximation near $x = r$ (See Uhlenbeck and Young) ϕ_4 and ϕ_1 can be expressed in the form:

$$\omega\left\{2\nu^{-2/3}\left(1 \pm \frac{1}{2\nu}\right)^{2/3}\left(1 - \frac{x}{r(1 \pm \frac{1}{2}\nu)^{1/2}}\right)\right\}. \tag{17}$$

The plus sign being used for ϕ_4 and the minus for ϕ_1 we find that the last maximum of S_y is between

$$x = r(1 + \tfrac{1}{2}\nu^{-2/3} + \tfrac{1}{4}\nu^{-1}) \quad \text{(maximum of } \phi_4)$$

and

$$x = r(1 + \tfrac{1}{2}\nu^{-2/3} - \tfrac{1}{4}\nu^{-1}) \quad \text{(maximum of } \phi_1)$$

and the current will fall to 0.001 times its maximum value in going a distance of the order $3/2r(\nu)^{-2/3}$.

We have found that if an experiment consists of measuring the *average* x coordinate of the current the difference between classical and quantum mechanical results will be of the order of 1 part in ν while if the *maximum* x coordinate is used the difference will be of the order 1 part in $\nu^{2/3}$. In either case it is too small to observe.

Two Incident Beams

We shall combine two incident beams such as those found above Eqs. (9), with momenta p_1, p_2 and $p_1 - p_2$. The constants A_2 and A_4 will be the same for both beams. This is the first step in the construction of a wave packet. It will be simpler to make a wave packet from these solutions than from the original solutions (9).

We find for the combined beams

$$\psi_{i1} = \psi_1(p_1, p_2) + \psi(p_1, -p_2) = \frac{-2A_4 e^{ip_1x/k}}{\frac{W}{c} + mc}\left\{p_1 \cos\frac{p_2y}{k} + p_2 \sin\frac{p_2y}{k}\right\}.$$

Put $\tan\epsilon = p_2/p_1$. Then

$$\begin{aligned}
\psi_{i1} &= \frac{-2A_4 p e^{ip_1x/k}}{\frac{W}{c} + mc}\cos\left(\frac{p_2y}{k} - \epsilon\right) \\
\psi_{i2} &= 2A_2 e^{ip_1x/k}\cos\frac{p_2y}{k} \\
\psi_{i3} &= \frac{-2A_2 p e^{ip_1x/k}}{(W/c) - mc}\cos\left(\frac{p_2y}{k} - \epsilon\right) \\
\psi_{i4} &= 2A_4 e^{ip_1x/k}\cos\frac{p_2y}{k}.
\end{aligned} \tag{18}$$

Now let us find the functions representing the emergent beams. Put $\gamma = e^{i\delta}$. Then

$$\begin{aligned}
B_4(p_1, p_2) &= \gamma A_4 = A_4 e^{i\delta} \\
B_4(p_1, -p_2) &= \gamma A_4 = A e^{-i\delta}
\end{aligned}$$

and similar expressions for B_2. We obtain

$$\begin{aligned}
\psi_{e1} &= \frac{2A_4 p}{(W/c) + mc}\, e^{-ip_1x/k}\cos\left(\frac{p_2y}{k} + \delta + \epsilon\right) \\
\psi_{e2} &= 2A_2 e^{-ip_1x/k}\cos\left(\frac{p_2y}{k} + \delta\right) \\
\psi_{e3} &= \frac{2A_2 p}{(W/c) - mc}\, e^{-ip_1x/k}\cos\left(\frac{p_2y}{k} + \delta + \epsilon\right) \\
\psi_{e4} &= 2A_4 e^{-ip_1x/k}\cos\left(\frac{p_2y}{k} + \delta\right).
\end{aligned} \tag{19}$$

For p_2 small compared to p_1 the emergent beam is displaced along the y-axis a distance $k\delta/p_2$. Hence, we wish to find δ.

Using Eqs. (6) we find

$$\frac{(W/c) + mc}{p_1}\,\frac{\phi_1(p_2/2w)}{\phi_4(p_2/2w)} = i(\nu)^{1/2} p/p_1\,\frac{D_{\nu-1}[(p_2/p)2\nu^{1/2}]}{D_\nu[(p_2/p)2\nu^{1/2}]} \tag{20}$$

To evaluate δ we must make some approximations. Two independent approximations are involved. We assume that p_2 is small compared to p_1, and

the ν is large compared to 1. Let us consider the differential Eq. (5) for the D_ν. If ν is large compared to 1 and ξ is small compared to $2(\nu)^{1/2}$ we see that an approximate solution can be obtained in the form

$$D = a \cos ((\nu)^{1/2}\xi + \alpha).$$

Let us again consider the case ν even, then D_ν is an even function and $D_{\nu-1}$ an odd one and we can write

$$\begin{aligned} D_\nu &= a \cos (\nu)^{1/2}\xi \\ D_{-1} &= b \sin (\nu)^{1/2}\xi. \end{aligned} \tag{21}$$

Using Whittaker and Watson's expressions for D_ν we can show that

$$\lim_{\xi \to 0} \frac{D_{\nu-1}(\xi)}{\xi D_\nu(\xi)} = -1.$$

Hence for small ξ

$$\frac{(\nu)^{1/2} D_{\nu-1}(\xi)}{D_\nu(\xi)} = -\tan (\nu)^{1/2}\xi. \tag{22}$$

A better approximation can be obtained by using the Wentzel-Brillouin-Kramer's method[12]

$$D_{\nu-1}(\xi) = \frac{-a}{\left[1 - \dfrac{\xi^2}{2(2\nu-1)}\right]^{1/4}} \sin \tfrac{1}{4}\left\{\xi(2(2\nu-1) - \xi^2)^{1/2} + 2(2\nu-1)\sin^{-1}\frac{\xi}{2(\nu-\frac{1}{2}))^{1/2}}\right\}$$

and

$$D_\nu(\xi) = \frac{a}{\left[1 - \dfrac{\xi^2}{2(2\nu+1)}\right]^{1/4}} \cos \tfrac{1}{4}\left\{\xi(2(2\nu+1) - \xi^2)^{1/2} + 2(2\nu+1)\sin^{-1}\frac{\xi}{2(\nu+\frac{1}{2})^{1/2}}\right\}.$$

These hold for considerably larger values of ξ than do Eqs. (21). If we assume ν is large compared to 1, but do not restrict ξ we obtain

$$\frac{(\nu)^{1/2} D_{\nu-1}(\xi)}{D_\nu(\xi)} = -\tan \tfrac{1}{4}\left\{\xi(4\nu - \xi^2)^{1/2} + 4\nu \sin^{-1}\frac{\xi}{2(\nu)^{1/2}}\right\}. \tag{23}$$

Put this expression equal to $-\tan \sigma$ when $\xi = (p_2/p)2(\nu)^{1/2}$. We see that if we expand the argument in terms of ξ and neglect terms of higher order than the 1st, Eq. (23) reduces to (22). This expansion will be considered later.

[12] G. Wentzel, Zeits. f. Physik **38**, 518 (1926); L. Brillouin, C. R. Juli, (1926); H. A. Kramers, Zeits. f. Physik **39**, 828 (1926).

Using Eq. (23) we obtain

$$e^{i\delta} = \frac{1 - i(\tan\epsilon + \sec\epsilon\tan\sigma)}{1 + i(\tan\epsilon + \sec\epsilon\tan\sigma)}.$$

Hence

$$-\tan\frac{\delta}{2} = \tan\epsilon + \sec\epsilon\tan\sigma = \frac{\sin\epsilon\cos\sigma + \sin\sigma}{\cos\epsilon\cos\sigma}.$$

Now $\tan\epsilon = p_2/p_1$ and if p_2 is very small compared to p_1, ϵ is a very small angle. If we neglect ϵ altogether we obtain too small a value for $-\tan\delta/2$ since we decrease the numerator and increase the denominator of the fraction. On the other hand, if we *decrease* the denominator by subtracting $\sin\epsilon\sin\sigma$ and decrease the numerator only by a second order term in by multiplying the last term by $\cos\epsilon$ we obtain

$$-\tan\frac{\delta}{2} = \frac{\sin\epsilon\cos\sigma + \cos\epsilon\sin\sigma}{\cos\epsilon\cos\sigma - \sin\epsilon\sin\sigma} = \tan(\sigma + \epsilon).$$

Neglecting ϵ altogether gives

$$-\tan\frac{\delta}{2} = \tan\sigma.$$

Hence, we can say

$$\sigma < -\frac{\delta}{2} < \sigma + \epsilon. \tag{24}$$

All the above arguments hold for $\cos\sigma$ negative if we interchange the words decrease and increase.

Now let us evaluate σ.

$$\sigma = \tfrac{1}{4}\left(\xi(4\nu - \xi^2)^{1/2} + 4\nu\sin^{-1}\frac{\xi}{2(\nu)^{1/2}}\right).$$

Expanding in powers of $\xi/2(\nu)^{1/2}$ gives

$$\sigma = 2\nu\left\{\frac{\xi}{2(\nu)^{1/2}} - \frac{1}{6}\left(\frac{\xi}{2(\nu)^{1/2}}\right)^3 + \cdots\right\}.$$

Putting $\xi = (p_2/p)2(\nu)^{1/2}$ gives

$$\sigma = 2\nu\frac{p_2}{p}\left\{1 - \frac{1}{6}\left(\frac{p_2}{p}\right)^2 + \cdots\right\}. \tag{25}$$

If p_2 is so small compared to p that the square of p_2/p may be neglected we have

$$\sigma = 2\nu\frac{f_2}{p}.$$

Now $\sin \epsilon = p_2/p$. Hence ϵ is small compared to σ in the same way that 1 is small compared to ν. Since we have already neglected terms of the order $1/\nu$ we shall neglect ϵ compared to σ. This gives

$$\delta = -2\sigma = -4\nu p_2/p. \tag{26}$$

Neglecting the ϵ in expressions (18) and (19) we see that the wave functions are the same for the incident and emergent beams except for (1) the negative signs on ψ_1 and ψ_3 and in the exponent which make the currents be in opposite directions and (2) the phase angle δ in the cosines. Hence, if y_i is the maximum of the incident beam and y_e the maximum of the emergent beam then

$$y_e - y_i = -\frac{k}{p_2}\delta.$$

Putting in the value of from (26) gives

$$y_e - y_i = \frac{4\nu k}{p} = \frac{2\nu\lambda}{\pi} = 2r. \tag{27}$$

We have neglected terms of the order $1/\nu$ hence this result may be in error by a term of order λ. Hence to within distances of the order of a de Broglie wave-length the maximum of the emergent beam will be displaced just twice the radius of the classical circle from the maximum of the incident beam.

Construction of a Wave Packet

The functions we have been considering had a cosine dependence on y and hence extending an infinite distance in both directions. However, by using a Fourier integral over such solutions we can find functions which are negligibly small except in the region: $-\Delta y \leqq y \leqq \Delta y$. These will be of the form:

$$\Psi_{i1} = \int_0^{p_2} \frac{-2A_2(p_2)p}{(W/c) + mc} e^{ipx/k} \cos\frac{p_2 y}{k} dp_2 \tag{28}$$

Where P_2 is the maximum value of p_2,

With similar expressions for $\Psi_{i2}, \Psi_{i3}, \Psi_{i4}$. A_4 is considered a function of p_2. Since each component here will give an emergent beam of the form (17) we can write the functions for the total emergent beam

$$\Psi_{e1} = \int_0^{p_2} \frac{2A_4(p_2)p}{(W/c) + mc} e^{-ip_1x/k} \cos\left(\frac{p_2 y}{k} + \delta\right) dp_2. \tag{29}$$

We have shown that for p_2 sufficiently small δ/p_2 is independent of p_2. Hence the incident beam is reproduced at a distance $y_e - y_i = -k\delta/p_2$ above the point of incidence. This means that if we pass electrons through a slit into a magnetic field they will come out at a distance $2r$ away, the uncertainty being of the order of a de Broglie wave-length.

The functions in the field will be of the form

$$\Psi_1 = e^{iwxy/k} \int_{p_2}^{p_2} e^{i\eta y/k} \phi_1\left(x + \frac{\eta}{2w}\right) d\eta \tag{30}$$

and similar expressions for Ψ_2, Ψ_3, Ψ_4, where the A's and ϕ's are connected by the relations (10).

We can now dispense with the device of a field ending abruptly at $x=0$ since the functions (30) will represent a packet of the same form even though the field extends beyond the slits at $x=0$ and hence the functions will have the same form at this point. The use of such a discontinuous field is merely a convenient way of studying the solutions at $x=0$.

We must now examine how small we can make Δy. We want P_2/p to be small compared to unity. At the same time we can conclude either from the theory of Fourier integrals or from Heisenberg's uncertainty relation that:

$$\Delta y \frac{P_2}{k} \approx 1.$$

Hence $\Delta y p/k$ must be large compared to one or Δy is large compared to λ.

$$\Delta y \gg \frac{k}{p} \approx \lambda.$$

This is usually true since a slit 0.1 mm wide would be a very narrow one while λ is of the order of 1 Å. Hence $\Delta y/\lambda \approx 10^6$. This means also that the uncertainties introduced by the approximations used will be small compared to the uncertainties coming from a finite slit width. Hence, when applied to the motion of an electron in a magnetic field quantum mechanics will give the same results as classical for the value of the ratio e/m.

In conclusion, the author wishes to thank Dr. W. V. Houston, who directed this research, for continued advice and encouragement during its development.

PICTORIAL REPRESENTATIONS OF THE DIRAC ELECTRON CLOUD FOR HYDROGEN-LIKE ATOMS

By H. E White
University of California, Berkeley

(Received June 4, 1931)

Abstract

Previous attempts to represent graphically the Schrodinger *electron cloud* for hydrogen-like atoms have been so successful that similar graphical representations have been looked for on the Dirac theory. With a single electron specified on Dirac's theory by a set of four wave functions instead of one, the *probability density* $\Psi\Psi^* = \psi_1\psi_1^* + \psi_2\psi_2^* + \psi_3\psi_3^* + \psi_4\psi_4^*$ is treated by considering, as on the Schrodinger theory, the independent angular and radial factors separately. Tables and graphs are given for $\Psi\Psi^*$ as a function of θ alone. The graphs are compared with and shown to correspond closely to the space quantization of the classical electron orbits. Graphs representative of $\Psi\Psi^*$ as a function of r alone are given and compared with the electron-nucleus distances of the corresponding electron orbits. The radial and angular factors are brought together by means of a mechanical device described previously,[1] which when photographed represents closely the *electron-cloud* $\Psi\Psi^*$. Photographs are given for the states $1^2S_{1/2}$, $2^2P_{1/2,\ 3/2}$ $3^2D_{3/2,\ 5/2}$ $4^2F_{5/2,\ 7/2}$, and $5^2G_{7/2}$, with $m = \pm\frac{1}{2}, \pm\frac{3}{2}, \cdots \pm j$

PREVIOUS attempts to represent graphically the solutions of the Schrodinger wave-equation for hydrogen-like atoms have been so successful that similar attempts have been made to represent the solutions of the Dirac electron in the same way. The graphical comparisons of the classical electron orbits, including electron spin, with the *probability density* $\Psi\Psi^*$ as given by Dirac's theory is to say the least interesting and informing.

It is well known that on Dirac's theory a single electron in a central force field is specified by a set of four wave-functions, ψ_1, ψ_2, ψ_3, and ψ_4 instead of one as in the case of the Schrodinger theory.[2] With each wave-function properly normalized the probability density $P = \psi\psi^*$ is given by

$$\psi\psi^* = \psi_1\psi_1^* + \psi_2\psi_2^* + \psi_3\psi_3^* + \psi_4\psi_4^* \tag{1}$$

For given allowed values of the so called azimuthal quantum number l and the magnetic quantum number $m = u + \frac{1}{2}$ there are two sets of solutions[3,4,5] according to whether the inner quantum number $j = l + \frac{1}{2}$, or $j = l - \frac{1}{2}$,

$$\left.\begin{aligned} \psi_1 &= -iM_\theta P_{l+1}^{u} \cdot M_r F_l \\ \psi_2 &= -iM_\theta P_{l+1}^{u+1} \cdot M_r F_l \\ \psi_3 &= (l+u+1) M_\theta P_l^{u} \cdot M_r G_l \\ \psi_4 &= -(l-u) M_\theta P_l^{u+1} \cdot M_r G_l \end{aligned}\right\} \quad j = l + \tfrac{1}{2} \tag{2}$$

$$\left.\begin{aligned} \psi_1 &= -i(l+u) M_\theta P_{l-1}^{u} \cdot M_r F_{-l-1} \\ \psi_2 &= i(l-u-1) M_\theta P_{l-1}^{u+1} \cdot M_r F_{-l-1} \\ \psi_3 &= M_\theta P_l^{u} \cdot M_r G_{-l-1} \\ \psi_4 &= M_\theta P_l^{u+1} \cdot M_r G_{-l-1} \end{aligned}\right\} \quad j = l - \tfrac{1}{2} \tag{3}$$

[1] White, Phys. Rev. **37**, 1416 (1931).
[2] See Darwin, Proc. Roy. Soc. **A118**, 654, 1928.
[3] Gordon, Zeits. f. Physik **48**, 11 (1928).
[4] Hartree, Proc. Cam. Phil. Soc. **25**, 225 (1929).
[5] Roess, Phys. Rev. **37**, 532 (1931).

In this form each wave-function in polar coordinates is written as the product of two functions one of which gives ψ as a function of the angles ϕ and θ alone and the other gives ψ as a function of r alone. M_θ and M_r are the angular and radial normalizing factors respectively. The spherical harmonics $P_l^u(\phi, \theta)$ are defined, in a convenient form,[6] by

$$P_l^u = (-1)^u(l+u)!\sin^{-u}\left(\frac{d}{d\cos\theta}\right)^{l-u}\frac{(\cos^2\theta-1)^l}{2^l\cdot l!}\cdot e^{im\phi}. \tag{4}$$

The radial functions F and G are functions of the electron nucleus distance alone and are given by

$$F_l^2 = \frac{N-p-n_r}{N+p+n_r}(\sigma_1-\sigma_2) \tag{5}$$

$$G_l^2 = (\sigma_1+\sigma_2) \tag{6}$$

where

$$\sigma_1 = (N+l+1)r^{p-1}e^{-kr}{}_1F_1(-n_r, 2p+1, 2kr) \tag{7}$$

$$\sigma_2 = -n_r r^{p-1}e^{-kr}{}_1F_1(-n_r+1, 2p+1, 2kr) \tag{8}$$

and

$$n_r = n-l-1 = \text{radial quantum number.} \tag{9}$$

$$p = [(l+1)^2-\alpha^2]^{1/2} \tag{10}$$

$$N = [n_r^2+(l+1)^2+2pn_r]^{1/2} \tag{11}$$

$$k = 1/a_1N,\ a_1 = .528A.U.,\ \alpha^2 = 5.30\times 10^{-5} \tag{12}$$

where a_1 is the radius of the first Bohr orbit, and α is the fine structure constant. The functions ${}_1F_1$ are of the form of series

$${}_1F_1(a, b, c) = 1+\frac{a}{b\cdot 1!}c+\frac{a(a+1)}{b(b+1)\cdot 2!}c^2+\frac{a(a+1)(a+2)}{b(b+1)(b+2)\cdot 3!}c^3\cdots \tag{13}$$

which terminate for negative values of a.

The angular factor P_θ.

With two sets of four wave-functions the solutions and hence the *probability density* $\psi\psi^*$ must be divided into two parts one for $j=l+\frac{1}{2}$ and one for $j=l-\frac{1}{2}$. Corresponding to given n, l, and j there are $2j+1$ magnetic states for which the magnetic quantum number m takes values from $m=+j$ to $m=-j$. Hartree has shown[4] that for given n, l, and j the magnetic states with equal but opposite m have the same *probability density*, (or *charge distribution* as it is called by Hartree). He has also shown that the angular *charge distribution* for two electrons with the same n, j, and m and $l=j\pm\frac{1}{2}$ is the same. As an example of these two theorems the *angular charge distributions* for the magnetic states $m=\pm 3/2$ for a ${}^2P_{3/2}$ term are not only the same but are also identical with the two magnetic states $m=\pm 3/2$ of the ${}^2D_{3/2}$ term. It should be pointed

[6] The spherical harmonics expressed in this form, with the exponent $(l-u)$ was suggested to the author by Professor Kramers since it requires fewer differentiations than the form often used.

out that the *radial charge distributions* of the ^2P and ^2D terms are different. With this simplification of the problem the *charge distributions* need be determined for $j=l+\frac{1}{2}$ and positive m only.

For $j=l+\frac{1}{2}$ the *probability density* $\psi\psi^*$ on the Dirac theory is written

$$\psi\psi^* = P_\theta \cdot P_r = M_\theta^2[P_{l+1}^u P_{l+1}^{u*} + P_{l+1}^{u+1} P_{l+1}^{u+1*}] \cdot M_r^2[F_l^2 + G_l^2]. \tag{14}$$

The first part of the solution is a function of the angles ϕ and θ alone.

$$P_\theta = M_\theta^2[P_{l+1}^u P_{l+1}^{u*} + P_{l+1}^{u+1} P_{l+1}^{u+1*}] \tag{15}$$

where the angular normalizing factor in the form given by Roess[5] is

$$M_\theta^2 = [4\pi(l+u+1)!(l-u)!]^{-1}. \tag{16}$$

From Eqs. (4) and (15) it may be seen that the angle ϕ occurs in each polynomial in the form of an exponential $e^{im\phi}$ and is always to be multiplied by its complex conjugate $e^{-im\phi}$ giving a constant for all m values. Exactly this same result is obtained on the Schrodinger theory, which indicates that

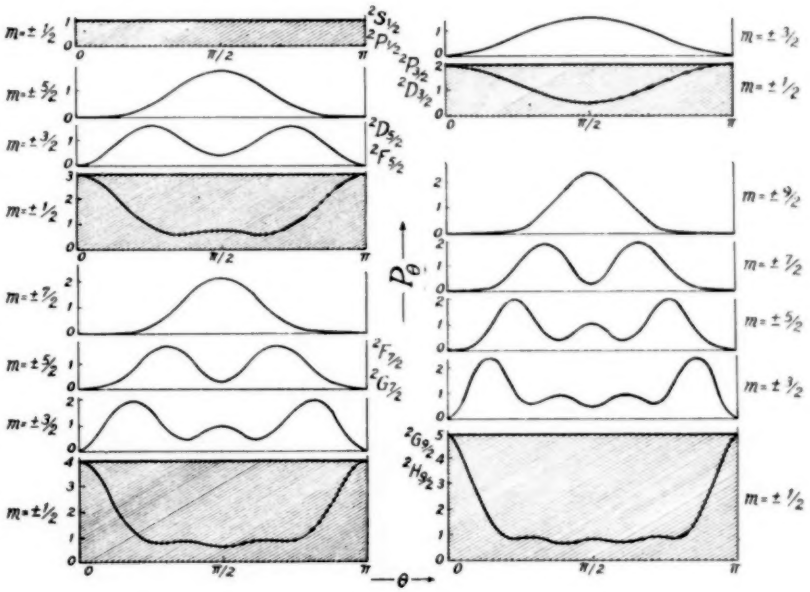

Fig. 1. The angular factor, P_θ, of the probability density $\Psi\Psi^*$ plotted as a function of the angle θ. The shaded areas indicate the spherical symmetry presented by half a main Smith-Stoner subgroup of electrons.

the *probability density* is symmetrical about the ϕ (magnetic) axis for all states. Leaving out the factor $1/4\pi$ in the normalizing factor M_θ^2, the *probability density* P_θ for a number of states is given in Table I and shown graphically in Fig. 1.

Hartree has shown[4] that for electrons with the same n, l, and j, the *probability density* summed over the states $m=+\frac{1}{2}$ to $m=+j$ presents *spherical symmetry*. In this case *spherical symmetry* is shown by

$$\sum_{m=+1/2}^{m=+j} P_\theta = \text{constant} \tag{17}$$

given in the last column of Table I, and graphically by the shaded areas under the straight lines in Fig. 1. Since the *probability density* for negative m states is the same as that for the corresponding positive m states the sum of the *probability densities* for all negative m states is also a constant. This result as shown by Hartree means that each half of a *Main-Smith-Stoner* subgroup of

TABLE I. *The Probability density as a function of the angle* θ.

Energy States	j	m	P_θ	$\sum_{m=+\frac{1}{2}}^{m=+j} P_\theta$
$^2S_{1/2}$ or $^2P_{1/2}$	1/2	1/2	1	1
$^2P_{3/2}$ or $^2D_{3/2}$	3/2	3/2 1/2	$3/2\sin^2\theta$ $1/2\ (3\cos^2\theta+1)$	2
$^2D_{5/2}$ or $^2F_{5/2}$	5/2	5/2 3/2 1/2	$15/8\sin^4\theta$ $3/8\sin^2\theta(15\cos^2\theta+1)$ $6/8\ (5\cos^4\theta-2\cos^2\theta+1)$	3
$^2F_{7/2}$ or $^2G_{7/2}$	7/2	7/2 5/2 3/2 1/2	$35/16\sin^6\theta$ $5/16\sin^4\theta\ (35\cos^2\theta+1)$ $15/16\sin^2\theta(21\cos^4\theta-6\cos^2\theta+1)$ $1/16\ (175\cos^6\theta-165\cos^4\theta+45\cos^2\theta+9)$	4
$^2G_{9/2}$ or $^2H_{9/2}$	9/2	9/2 7/2 5/2 3/2 1/2	$315/128\sin^8\theta$ $35/128\sin^6\theta(63\cos^2\theta+1)$ $140/128\sin^4\theta(45\cos^4\theta-10\cos^2\theta+1)$ $60/128\sin^2\theta(147\cos^6\theta-105\cos^4\theta+21\cos^2\theta+1)$ $30/128\ (147\cos^8\theta-214\cos^6\theta+98\cos^4\theta-12\cos^2\theta+3)$	5

electrons presents a *probability density* spherically symmetrical about the nucleus. In this connection one of the consequences of the Dirac theory is that a single p electron or two similar p electrons, depending on whether $j=\frac{1}{2}$ or $j=3/2$ respectively, present spherical symmetry. Not only are all S states spherically symmetrical, as on the Schrodinger theory, but also all one electron systems having but one valence electron and that electron in a $^2P_{\frac{1}{2}}$ state, eg., the normal states of B, Al, Ga, In, Tl.

If angular coordinates are used when plotting P_θ a number of interesting correlations with the classical orbits may be made. Such angular curves are shown in Fig. 2, for s, p, d, and f electrons. There are in general use four well known classical models which may be compared with the *probability density* figures. These models which will here be called (a), (b), (c), and (d) have the same total quantum number and azimuthal quantum numbers as follows;

$$\text{(a) } l,\ \text{(b) } l^* = [l(l+1)]^{1/2},\ \text{(c) } l+\tfrac{1}{2},\ \text{(d) } l+1=k \tag{18}$$

Above and below each density figure in Fig. 2, the corresponding classical orbits are shown oriented in each case according to model (b). On this model

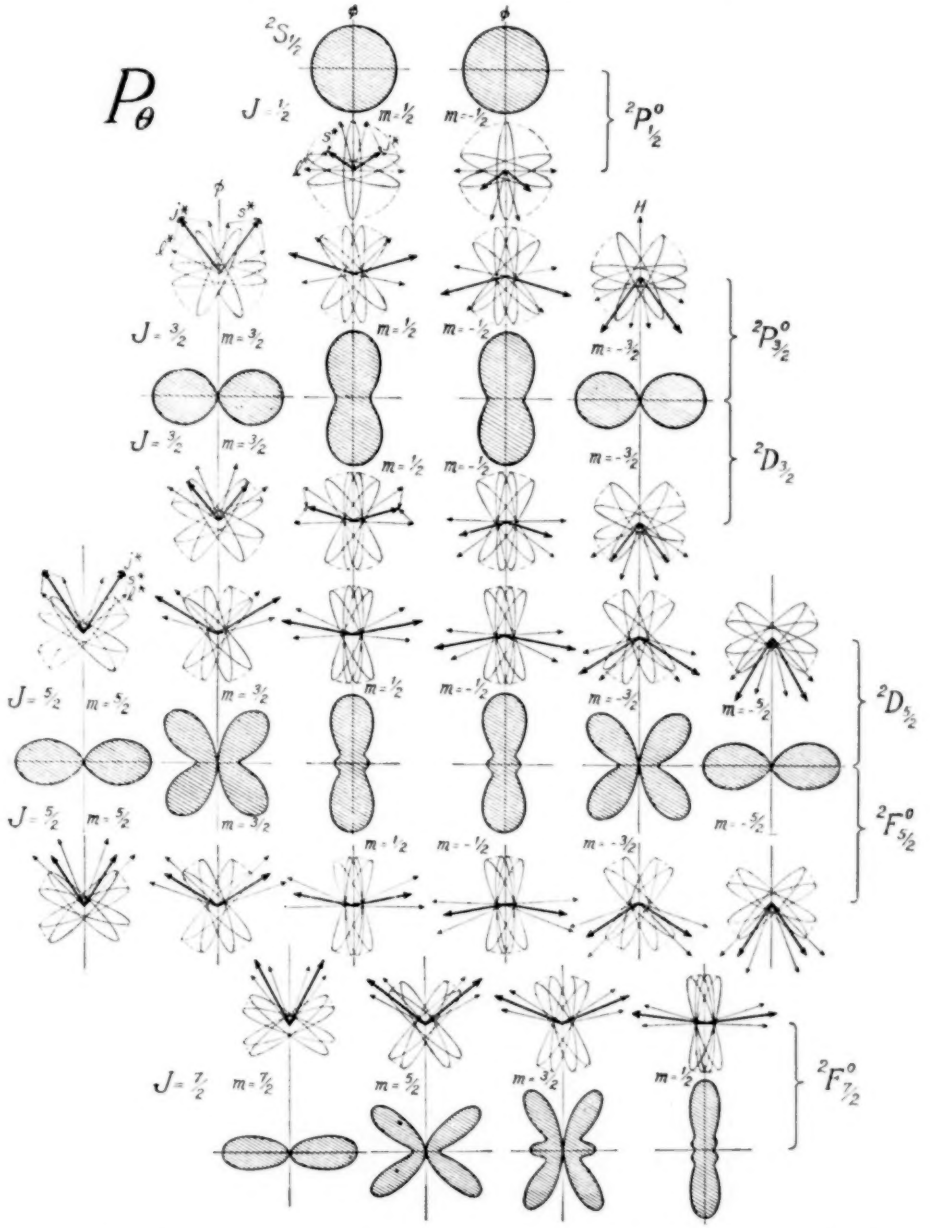

Fig. 2. The angular factor, P_θ, of the probability density $\Psi\Psi^*$ plotted in angular coordinates. Above and below the quantum mechanical electron distributions the corresponding classical electron orbits are shown oriented in each case according to the model l^*, s^*, j^* and m.

the angular momentum vectors $l^* = [l(l+1)]^{1/2}$ and $s^* = [s(s+1)]^{1/2}$ are combined to form the resultant $j^* = [j(j+1)]^{1/2}$, j^* in turn being so oriented that

its projection m on the ϕ (*magnetic*) axis takes half integral values $m = \pm\frac{1}{2}$, $\pm 3/2$, $\pm 5/2$, $\cdots$ $\pm j$. It may be seen from the figures that in the precession of l^* about j^* and the simultaneous precession of j^* about the ϕ axis the electron orbit fills out a figure in space not greatly unlike that of the quantum mechanics. The density curves are symmetrical about ϕ. The orbit normal l^* is shown for the four positions it may take when in the same meridian plane, the plane of the paper. In order to illustrate an orbit rather than its straight line projection the orbit plane is tipped slightly out of the normal to l^*. While the classical models (a), (c), and (d) may also be compared with the probability curves of Fig. 2, model (b) is in general in good agreement, as is also model (a). It should be pointed out that the electron is not confined to the shaded areas in each probability figure but that the magnitude of a line joining the center and any point on the curve is a measure of the electrons probability of being found in the direction of that line. From the physical standpoint it is interesting that P_θ becomes zero for values of $\theta = 0$ and π only. The electron can pass therefore from any region to another without going through a node of zero probability. This is also true for the radial factor as will be shown.

The radial factor P_r.

For $j = l + \frac{1}{2}$ the *probability density* factor P_r Eq. (14), is

$$P_r = M_r^2(F_l^2 + G_l^2). \tag{19}$$

The radial normalizing factors M_r^2 have been given by Roess[5] as

$$M_r^2 = \frac{(N + p + n_r)(2k)^{2p+1}\Gamma(2p + n_r + 1)}{n_r!2N[\Gamma(2p + 1)]^2[(N + l + 1)^2 + n_r(n_r + 2p)]} \tag{20}$$

which from tables of the gamma function are readily evaluated. The radial function F_l^2 as compared with G_l^2 is extremely small and for hydrogen is of the order of magnitude of the square of the fine structure constant, α^2. If α is set equal to zero throughout the radial equations, the gamma functions become simple factorials, F_l^2 becomes zero and, P_r reduces to the radial factor of the Schrodinger theory[1] $[R_{n,l}]^2$.

Since the radial densities on the Schrodinger and Dirac theories are so nearly identical it is difficult to graphically show the difference between the two, however, by splitting up $M_r^2(F_l^2 + G_l^2)$ into the two factors $M_r^2F_l^2$ and $M_r^2G_l^2$ curves may be given for each on different scales. In Fig. 3, for example curves for the $4^2P_{3/2}$ state are drawn. The factors $M_r^2G_l^2$ and $M_r^2F_l^2$ are shown by the dotted lines in the top and middle figures respectively. Multiplying by $4\pi r^2$ the *density distribution* curves, shaded areas, are obtained. The essential feature of so representing the *density distribution* is to show that the two zero points of each curve, other than those at $r = 0$ and $r = \infty$, occur at different values of r. While the resultant curve, $4\pi r^2\ M_r^2(F_l^2 + G_l^2)$, in the bottom figure is almost identical with the top figure for $4\pi r^2M_r^2G_l^2$ it does not come to zero at the two points near $r = 6$ and near $r = 14$. (The difference at these two points only has been exaggerated in the bottom figure.) The slight

shift in the *probability density*, due chiefly to the addition of the F function produces the fine-structure shift of the hydrogen energy levels.[3] The classical $4p$ electron orbit is shown in the last figure of Fig. 3, using model (c), Eq. (18). As in the case of the Schrodinger theory the *density distribution* differs greatly

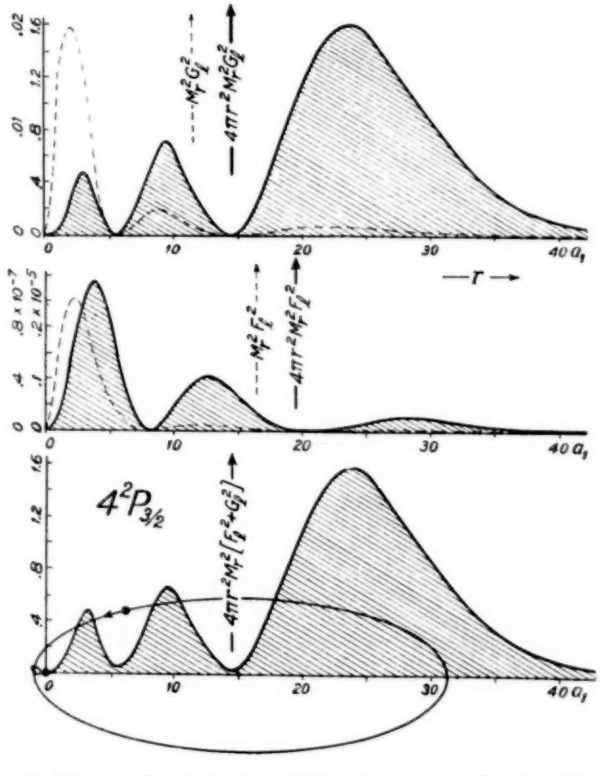

Fig. 3. The radial factor, P_θ, of the probability density $\psi\psi^*$, for the $4^2P_{3/2}$ state. The chief spin correction $4\pi r^2 M_r^2 F_l^2$ (middle figure) added to the almost Schrodinger distribution $4\pi r^2 M_r^2 G l^2$ (top figure) gives the Dirac distribution, in the lower figure.

from zero only within the electron-nucleus distance of the corresponding classical orbits. Model (b), Eq. (18), gives closely the same orbit and electron-nucleus distances as model (c).

The probability density $\psi\psi^*$.

Attempts to bring together the probability factors P_θ and P_r into one single picture for $\psi\psi^*$ have been somewhat successful. Preliminary attempts to produce a three dimensional model which will represent as closely as possible $\psi\psi^*$ has resulted in a mechanical device described in a previous paper.[1] With this mechanical device photographs have been made which represent the Dirac electron-cloud for a number of the simpler hydrogen states. The photographs shown in Fig. 4, were taken from the equatorial plane of the cloud so that the ϕ (*magnetic*) axis is vertical and in the plane of the paper. While these photographs were made to represent the electron-cloud and not

simply cross-sections the latitude lost in photo-copying and printing almost makes them cross-sections. The states represented are given beneath each figure. Since states with negative m values are identical with the corresponding positive m states only one picture is given for $+m$ and $-m$. The electron-cloud for states given in brackets are so nearly like the figures given for unbracketed states that the difference is not distinguished in such a photograph. The scale for each state is given beneath each symbol in angstrom units.

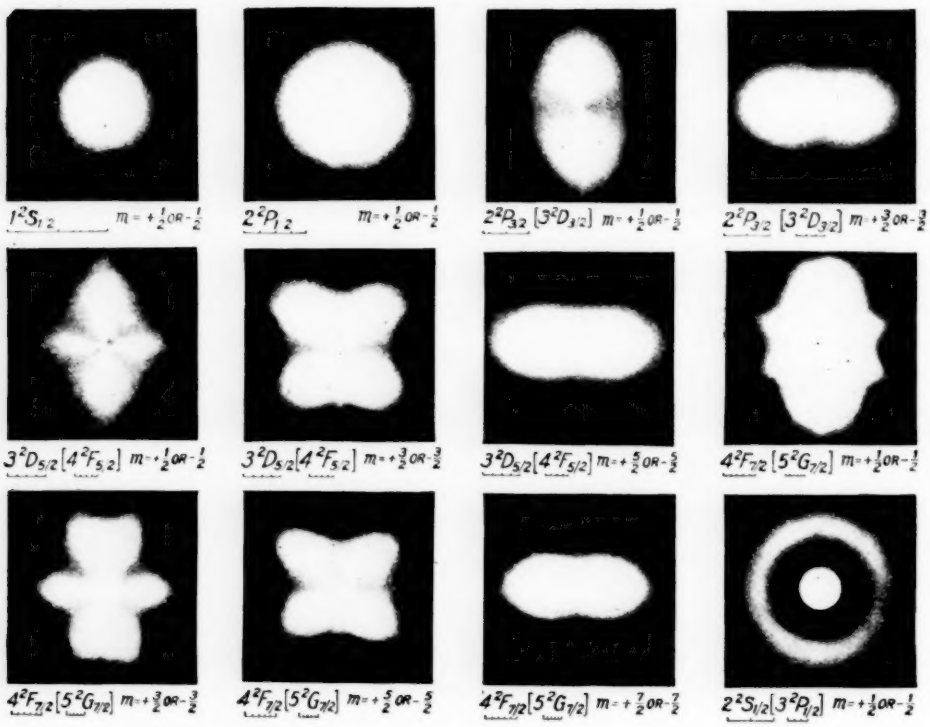
$1^2S_{1/2}$ $m=+\frac{1}{2}$ OR $-\frac{1}{2}$
$2^2P_{1/2}$ $m=+\frac{1}{2}$ OR $-\frac{1}{2}$
$2^2P_{3/2}$ $[3^2D_{3/2}]$ $m=+\frac{1}{2}$ OR $-\frac{1}{2}$
$2^2P_{3/2}$ $[3^2D_{3/2}]$ $m=+\frac{3}{2}$ OR $-\frac{3}{2}$
$3^2D_{5/2}[4^2F_{5/2}]$ $m=+\frac{1}{2}$ OR $-\frac{1}{2}$
$3^2D_{5/2}[4^2F_{5/2}]$ $m=+\frac{3}{2}$ OR $-\frac{3}{2}$
$3^2D_{5/2}[4^2F_{5/2}]$ $m=+\frac{5}{2}$ OR $-\frac{5}{2}$
$4^2F_{7/2}[5^2G_{7/2}]$ $m=+\frac{1}{2}$ OR $-\frac{1}{2}$
$4^2F_{7/2}[5^2G_{7/2}]$ $m=+\frac{3}{2}$ OR $-\frac{3}{2}$
$4^2F_{7/2}[5^2G_{7/2}]$ $m=+\frac{5}{2}$ OR $-\frac{5}{2}$
$4^2F_{7/2}[5^2G_{7/2}]$ $m=+\frac{7}{2}$ OR $-\frac{7}{2}$
$2^2S_{1/2}[3^2P_{1/2}]$ $m=+\frac{1}{2}$ OR $-\frac{1}{2}$

Fig. 4. Photographs representing the Dirac electron-cloud for a number of the simpler hydrogen-like states made by means of photographing a mechanical model. The ϕ (magnetic) axis is vertical and in the plane of the paper. The scale for each state is given beneath each symbol in angstrom units.

Graphical comparisons of the classical electron orbits, without spin, have shown that the electron path closely follows the *probability density* $\psi\psi^*$ on Schrodingers theory.[1] Introducing the electron spin into the classical model, the orbit, in weak field, no longer precesses about the ϕ axis but about the spin and orbit resultant j, and j in turn precesses about ϕ. Corresponding to this change in space quantization is the change in the θ factor of the *probability density* $\psi\psi^*$ brought about by introducing the spin through Dirac's theory. Radially, however, little change has occurred in either the orbital model or the quantum mechanical model $\psi\psi^*$.

THE TEMPERATURE VARIATION OF THE ELECTRIC MOMENT OF ETHYLENE CHLORIDE

By C. T. Zahn
Palmer Physical Laboratory, Princeton University

(Received June 24, 1931)

Abstract

Observations of the molecular polarization of ethylene chloride vapor have been made over a temperature range from 32° to 270°C and over a considerable pressure range at each temperature. These observations show a definite departure from the Debye theory, since the Debye function plotted against temperature gives a definitely curved line. The data might be explained as approximately consistent with an electric moment of value zero and a value of the constant part of the polarization equal to about twice that of the optical refractivity; but for reasons discussed this interpretation is disregarded. It seems necessary to assume that the electric moment varies with temperature, as suggested by Eucken and Meyer. This was to be expected as a result of the hindrance of free rotation due to the interaction of the two atomic groups rotating around the single bond between the two carbon atoms. The possibility of the existence of disturbing effects such as association and adsorption is discussed, but is shown to be improbable, if not untenable, The values of the electric moment are then calculated by the use of a value for the constant part of the polarization, 23.9 cm^3, determined by C. S. Hitchcock from the solid state. In the observed temperature interval the electric moment increases with the temperature from 1.1 to 1.5×10^{-18} c.g.s.e.s. u.; whereas the value calculated by Meyer for truly free rotation is 2.4×10^{-18}. This suggests that the rotation is considerably hindered; and in fact the results are entirely in accord with the predictions of Eucken and Meyer. The interaction energy may, however, be sufficiently great that it may be necessary, in order to obtain an accurate theory of this effect, to take into consideration the quantum theory rather than the classical theory of Meyer. The interpretation of other observations, of Meyer and of Sänger, is discussed with reference to certain inconsistencies which have been observed.

THE phenomenon of free rotation around single bonds in complex molecules has received considerable attention recently in connection with dipole moments calculated from Debye's equation. The effect of such rotations on observed moments has been discussed by Højendahl, Hückel, Ebert, Williams, Eucken and Meyer, and others.[1] Particularly, Højendahl has pointed out that the two rotating parts of a molecule may interact with one another and therefore cause a partial hindrance of the free rotation. Williams, and Eucken and Meyer have shown that, if the rotation is truly free, the observed moment is to be regarded as the square root of a random average of the square of the moment, over all possible values of the rotational angle.

[1] Højendahl, Studies of Dipole-moment. Copenhagen 1928, and Phys. Zeits. **30,** 391 (1929) W. Hückel, Zeits. f. Phys. Chem. (B) **2,** 451 (1929); L. Ebert, Leipziger Vorträge 1929. Hirzel 1929, page 44; J. W. Williams, Zeits. f. Phys. Chem. **138,** 75 (1928); Eucken and Meyer, Phys. Zeits. **30,** 397 (1929); C. T. Zahn, Phys. Rev. **37,** 1516 (1931). An excellent résumé of this subject has been given by H. Sack, Ergebnisse der Exakten Naturwissenschaften, Band VIII, 337 (1930).

Eucken and Meyer have also pointed out that, if there is sufficient interaction between the two mutually rotating dipoles, one should expect the observed moment to differ from this random root mean square value and possibly to vary with the temperature. For example, this possibility was discussed for the cases of the COOH group and for ethylene chloride.

Several observers have made experiments to determine whether such a temperature variation actually exists in the observable interval. Meyer[2] has determined the molecular polarization of ethylene chloride in benzene and hexane solutions. In benzene the calculated electric moment is practically constant, 1.83×10^{-18}; whereas in hexane the moment is considerably smaller and varies from 1.26 to 1.42×10^{-18} in the temperature interval from $-75°$ to 40°C. If the rotation were truly free the value 2.4×10^{-18} should be expected from a calculation after the manner of Eucken and Meyer, based on the addition of vector moments characteristic of the individual chemical bonds and the method of random averaging over the rotational angle. Meyer interpreted these results as indicating an actual temperature variation of electric moment.

Now it is well known that calculations of electric moment from the interpolated values of molecular polarizations of solutions are subject to the following possible errors. (1) Since the concentration of the solute in the liquid state is large compared to that in the gaseous state, there is the possibility of association of the solute molecules both with one another and with the solvent molecules. (2) Since the Debye theory applies rigorously only to the gaseous state, there has always existed the possibility that the strong innermolecular field could be different from the Lorentz value $4\pi P/3$. (3) There is also the possibility of the formation of adsorbed layers on the condenser plates, which have been observed even in the gaseous state. Nevertheless, in many cases the experiments on solutions have led to very nearly the same values as those on the gaseous state. The customary test for the validity of the former values has been to determine the moment in several different solvents. If there is agreement between the various values so obtained it seems reasonable to assume that the values are the true non-associated molecular moments. In fact, it is just such cases, where different solvents have led to different values of the electric moment, which have also shown the most marked disagreement with the moments obtained from experiments on the gaseous state. For example, this has been borne out particularly clearly in the case of the fatty acids. Wolf[3] has given the value 1.21 for the moment of formic acid and values around 0.8×10^{-18} for several of the higher members of the series. Also Smyth[4] has made experiments on solutions of acetic acid in benzene and in ether. The observations on the benzene solutions were in general abnormal and led to a value of the electric moment around 0.7×10^{-18}; whereas those on the ether solutions were normal and indicated a moment of 1.40×10^{-18}. On the other

[2] L. Meyer, Zeits. f. Phys. Chem. (B) **8,** 27 (1930).

[3] K. L. Wolf, Phys. Zeits. **31,** 227 (1930).

[4] C. P. Smyth and H. E. Rogers, Jour. Amer. Chem. Soc. **52,** 1824 (1930).

hand experiments by the author[5] on acetic acid vapor led to an even higher value. These latter experiments indicated also what was *originally* interpreted to be a temperature variation of electric moment from 1.4 to 1.7×10^{-18} in the interval from 300° to 500°K. Later experiments on formic and propionic acid vapors[6] have made it seem highly probable that this temperature variation really does not exist, but that the effect is due to a considerable amount of association. If this interpretation is correct, the moments are approximately 1.51 for formic acid, 1.73 for acetic acid, and 1.74×10^{-18} for propionic acid. All of these values are considerably higher than those of Wolf, and the value for formic acid relative to that of the other members of the series is even reversed.

Since no association of ethylene chloride in the gaseous state has been reported from vapor density measurements or otherwise, it was thought that it might not exist to an appreciable extent, and that it would be particularly easy to determine whether or not the temperature variation reported by Meyer is a bona fide non-associated molecular effect. For this reason the following measurements on ethylene chloride vapor were undertaken. In the meantime Sänger[7] published the results of similar experiments. The interpretations of these and other experiments have led to inconsistencies.[8] Sänger's experiments indicate normal behavior according to the Debye theory, but lead to a value of the constant part of the polarization almost twice that of the optical refractivity. His calculated value of the electric moment is 1.1×10^{-18}. Since he obtains different values of the polarization for two different densities, he believes his results are somewhat falsified by association, and that the true value should lie between 1.2 and 1.4×10^{-18}. On the other hand Meyer's values of molecular polarization from the liquid state are considerably higher than those of Sänger and consequently lead to higher values of the electric moment, 1.83 in benzene and 1.26 to 1.42×10^{-18} in hexane. He does not believe that Sänger's assumption of association is valid for his own experiments, since he thinks the amount of association necessary to explain the observed difference in polarization is too great. Sänger suggests that part of the discrepancy in the two experiments may be due to adsorption on the condenser plates. This *might* be greater in the liquid state and therefore give higher values for the molecular polarization. But in this latter case the effect of a given percentage adsorption should be less than in the gaseous state, since the amount of solute is actually measured by weighing. Then any effect here must be due entirely to a change in the property of the molecule on adsorption. In the gaseous state the density value is obtained from a measurement of the pressure and temperature of the vapor and does not therefore include the increase in average density due to the adsorption.

[5] C. T. Zahn, Phys. Rev. **35,** 1047 (1930).

[6] C. T. Zahn, Phys. Rev. **37,** 1516 (1931).

[7] R. Sänger, Phys. Zeits. **32,** 21 (1931).

[8] L. Meyer, Phys. Zeits. **32,** 260 (1931); R. Sänger, Phys. Zeits. **32,** 414 (1931).

Experimental Results and Interpretations

The experiments[9] here described were made over a temperature and pressure range as large as feasible. The pressure curves are of particular interest in connection with the possibility of association or adsorption. They are, however, not conclusive in this connection, since apparently linear pressure curves have previously lead to false interpretations, as in the case of acetic acid vapor.[6] The large observed temperature range from 305° to 543°K enables one to obtain a better test of the Debye equation than was possible in the previous experimental interval 333° to 453°K. The experimental conditions for these experiments were as good as any ever obtained by the author, as regards both steadiness of the electric circuits and reproducibility. A relatively large range of pressure was also studied; for the lower temperatures it was possible to approach saturation in order to search for a curvature effect due to possible association or adsorption. All of the pressure curves of electric

Table I. *Ethylene chloride.*

T°K	P	PT	max. p (cm Hg)	$\mu\times10^{18}$ c.g.s.e.s.u.
304.95	49.47	15086	7	1.12
341.03	51.92	17706	37	1.24
376.25	52.54	19768	74	1.32
419.00	52.74	22098	68	1.40
456.96	52.48	23981	68	1.45
479.82	51.87	24888	49	1.48
484.82	51.74	25085	58	1.48
543.66	50.74	27585	59	1.54

polarization were so perfectly linear that it is to no purpose here to record the data for the individual pressures. The data for the different temperatures are shown in Table I. In order to determine the molecular polarization, P, the pressures were corrected for departures from the ideal gas values before plotting the pressure curves. For this purpose the van der Waals constants were used as described in a previous article.[9] From the table it is seen that the values of P vary relatively slightly (about 10%), having a maximum around 150°C. The curves obtained by plotting P and PT against T (shown in Fig. 1) show a definite departure from the Debye theory.

Purified ethylene chloride was obtained by fractional distillation of a specimen from the Eastman Kodak Company, both at room pressure and under its own pressure.

Now even if one supposes that the curvature of PT is due to experimental error (about 3 percent) and passes a straight line approximately through the observed values, the resulting values of the constant polarization, A, and the electric moment, μ, are unreasonable, as was the case for Sänger's value of A. Actually this straight line passes almost through the origin (a rough estimate gave even a small negative intercept), and the electric moment has a value

[9] For experimental methods see previous articles: Phys. Rev. **24** 400 ;1924); Phys. Rev. **35,** 848 (1930).

zero. On the other hand the value of A is equal to about 52 cm³, which is more than twice the value of the optical refractivity, with which it should agree to within probably about a 10 percent difference due to infrared terms. The molecular refractivity of ethylene chloride is about 21 cm³ and if one were to add 10 percent in order to estimate the value of A, one would obtain a value of 23. This is in approximate agreement with a recent value of A, 23.9, obtained by C. S. Hitchcock from measurements of electric polarization in the solid state. Apart from the above mentioned curvature of the Debye line, it does not seem possible that the moment is zero, and that the atomic polarization in the gaseous and liquid states is of the same order as that of the electronic polarization, while that in the solid state is of the ordinary order of magnitude, 10 percent of the refractivity.

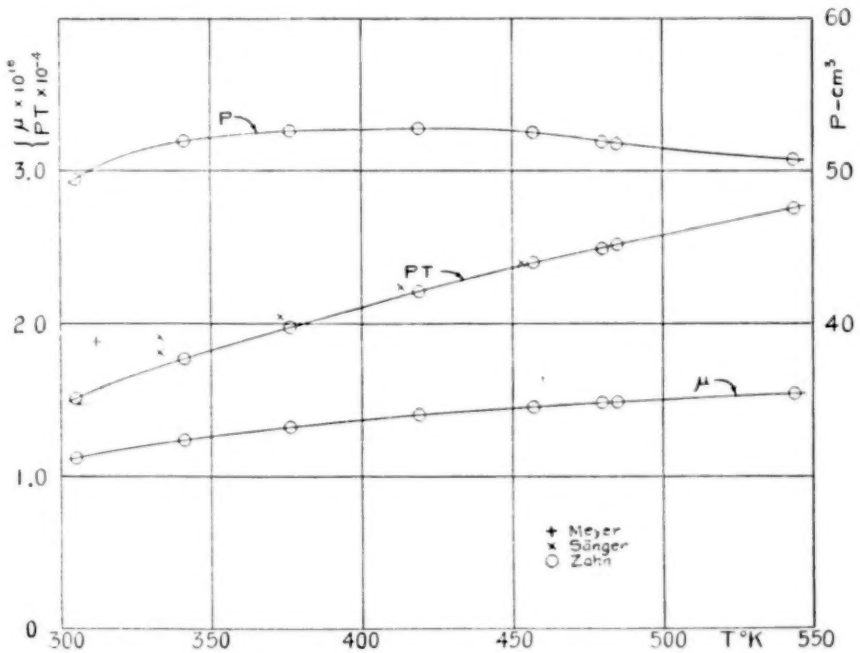

Fig. 1.

Disregarding this possibility, one is left to conclude that the electric moment actually increases with the temperature in accord with Meyer's suggestion, unless one supposes that the experimental data are falsified by either adsorption or association. Considering the value of P at the high temperatures to be free from error, the possibility that the effect is due chiefly to adsorption is excluded by the fact that such an effect should give abnormally high values at the *low* temperatures, whereas the reverse is true. The question of association is more difficult. First of all one must make a plausible assumption as to the effect of association on P. As a fair approximation one can assume that A is doubled on association into double molecules. This gives a value 47.8, which is very little smaller than the value of total P observed at

the lowest temperature. As regards the change in electric moment on association one could assume either (1) that the moment is reduced to zero, or (2) that the moment of the double molecule has some value different from zero, probably of the order of that of the single molecule. For case (1) it would be necessary to assume a very large and seemingly improbable amount of association in order to explain the observed data. For case (2) the association would lead to abnormally large values of P at *low* temperatures, which is again in contradiction to the observed facts. In this connection it is hoped that in the near future measurements of the refractivity of ethylene chloride vapor will be made in this laboratory in order to determine in what amount, if any, associated molecules are present.

All of the above assumptions regarding plausible sources of error can therefore be said to lead to contradictions; and it seems necessary to assume a temperature variation of electric moment, which has been expected for some time to exist in certain molecules. There is, in fact, a further argument in favor of this conclusion. All of the experiments of the various observers mentioned above lead to values of electric moment considerably lower than that corresponding to truly free rotation, 2.4×10^{-18}. For example, by assuming Hitchcock's value for A the present data show a variation of electric moment from 1.1 to 1.5×10^{-18}. The largest value reported is that of Meyer for the benzene solution, 1.83×10^{-18}. These values of moment indicate that the rotation is not truly free. Neither is it completely hindered; for then the moment should be zero. Now since the actual observed data correspond to the intermediate case, it seems very probable that a temperature variation should be observable in such a large range of temperature as 250°C. One could, of course, raise the objection that these low values may be due to distortions of the two rotating parts; but this would require a strong interaction, which would probably lead back to the necessity of hindered rotation and consequent temperature variation of electric moment.

Finally there seems to be no plausible way to avoid making the assumption that the electric moment of ethylene chloride varies with temperature. In fact, the observations here described present no objections to this conclusion. Still it remains to discuss the observations of other experimenters. If one accepts the proposed interpretation of the data here given, it would seem that the interpretations of both Meyer and Sänger are in part correct. As regards the observations of Meyer, since his values of moment differ widely for the two different solvents, benzene and hexane, there is probably some effect present tending to give abnormally high values of P, and even in the hexane solution. For example, a similar situation was found for the fatty acids as mentioned above. Still the temperature variation of the moment reported by Meyer exists, but because of the disturbing effect, to a different degree from that given by him. With the uncertainties mentioned his results could hardly be considered as conclusive evidence in favor of such a temperature variation. Whether or not these high values are due to association, adsorption, or to a misapplication of the Debye theory, it is difficult to say. It would seem, as Meyer has pointed out, that too great a degree of associ-

ation is necessary to explain them, and similarly for adsorption. The following suggestion is here offered: that the innermolecular forces in the liquid state may be of such a nature as to shift the potential energy function (as dependent upon rotational angle) and thereby produce a change in the rotational hindrance and a change in the actual observed electric moment.

While Sänger's experiments cover a considerable range of temperature, they are practically all made at the same density. One observation at a different density was made and this was not in agreement with the other at the same temperature. Inasmuch as the author has over a considerable range of temperature and pressure found no such disagreement, it seems that this effect must not be real. Sänger's value of P at the highest temperature is in almost perfect agreement with that here observed (see Fig. 1). His two values at the lowest temperature differ by about the same amount as one of them differs from the author's. If this disagreement is to be explained by some effect such as mentioned in connection with the observations of Meyer, this effect must be either association or adsorption, since the innermolecular field is almost negligible in the vapor state. Association seems to be excluded by the previous discussion of the author's results. Adsorption may exist in both Sänger's and the present results, but if this is the case, it must exist to a smaller extent in the latter. Furthermore in the present experiments no evidence of adsorption was detected, at least as a departure from the linearity of the pressure curves. However, if Sänger's data were used to calculate the electric moment as in the present case, one would obtain a temperature variation of electric moment, but the values of the moment would be somewhat different.

MAGNETIZATION AND THE MAGNETO-CALORIC EFFECT

By Francis Bitter
Westinghouse Research Laboratories, East Pittsburgh, Penn.

(Received June 17, 1931)

Abstract

Definition of the effect.—The magneto-caloric effect is defined as the reversible evolution of heat accompanying a change in the magnetization of a ferromagnetic substance, in contradistinction to the irreversible evolution of heat referred to as hysteresis.

Assumption regarding the mechanism of magnetization.—In two previous notes it was suggested that ferromagnetic substances are spontaneously magnetized in small regions containing roughly 10^5 atoms. Here the following points are briefly discussed: (1) the formation of these units, called blocks; (2) the interactions of these blocks to form clusters, which probably give rise to the Barkhausen effect; (3) the changes that take place in the neighborhood of the Curie point; (4) the changes that take place during magnetization.

The Magneto-caloric effect.—The essential result of the above discussion is that a sudden change in the applied field will produce changes in the energy of every block. The new energy distribution is not stable, and equilibrium is reached by means of an adiabatic diffusion process resulting from thermal agitation, which brings with it a reversible change in temperature. The mechanism is illustrated by means of a simple model.

The effect under certain simple conditions.—If the strains due to magneto-striction, stray internal fields, and the effect of crystal orientation are negligible, the magneto-caloric effect is amenable to calculation. It is pointed out under what experimental conditions such neglects are justifiable.

The interpretation of the experiments of Weiss and Forrer on Nickel.—A detailed comparison is undertaken between experimental observations of the magneto-caloric effect in nickel in high fields and the theoretical predictions based on the assumption that the effect is due to processes involving Weiss' molecular field. The agreement is satisfactory at temperatures not too near the Curie point. Too little is known about the nature of the magnetic transformation to permit a quanitative analysis to be made there.

Magnetization and the magneto-caloric effect in single crystals.—Akulov's static theory of the magnetization curve of single crystals predicts the absence of a magneto-caloric effect due to rotation of the regions of spontaneous magnetization, i.e., the work done in rotating the magnetization of such a region is equal to its change in potential energy, and therefore there can be no change in heat content. Experimentally this relation is approximately satisfied for iron and nickel, and less well for cobalt. If, in the case of cobalt, the discrepancy is real, a magneto-caloric effect of the order of 0.03°C is to be expected. The magnetization curves for crystals of nickel and cobalt on the basis of Akulov's theory are calculated. It is pointed out that experiments on the magneto-caloric effect of single crystals would be of great help in determining the mechanism of magnetization.

EVER since the introduction by Weiss of the molecular field to explain the spontaneous magnetization of ferro-magnetic substances, it has been difficult to understand how a substance in which such a field acts may be de-

magnetized. Weiss himself suggested that the regions of spontaneous magnetization did not necessarily include the whole of a sample. It was suggested that crystal grains had natural boundaries at which to assume abrupt changes. This was not entirely satisfactory, as similar results had to be explained in single crystals. Recently Sizoo[1] has suggested that the "Lockerstellen," spontaneous imperfections in crystals, suggested by Smekal to explain chiefly mechanical and electrical properties, might somehow be connected with the breaking up of the regions of spontaneous magnetization. And more recently, the author has suggested[2] that the block theory of Zwicky might have considerable bearing on this problem. Whatever the cause, it seems very probable that ferromagnetic bodies are composed of permanently magnetized regions of some sort, and that the macroscopic effects observed are due to their interactions—thermal, mechanical, magnetic, etc. The problem is enormously complicated by the fact that besides having to account for the effect of one region on the next by means of its magnetization, magnetostriction, etc., accidental strains and impurities having a large influence on the magnetic properties must be taken into consideration. For instance, Yensen[3] has shown that the hysteresis loss of iron-silicon alloys can be halved by reducing the carbon content from 0.008 percent to 0.004 percent. Similarly some materials, permalloy for instance, may have a wide range of magnetic properties, depending on their previous thermal and mechanical treatment. It is quite evident, then, that the detail in the arrangement of ferromagnetic atoms is of great importance in determining some of the properties of the substance which they make up, and until such detail can be put into a theory, only a very rough agreement with experiment is to be expected. The best procedure for establishing a theory seems therefore to consist of showing that it contains mechanisms capable of describing a large number of phenomena, and that the order of magnitude of the various calculated effects is reasonable. Once such evidence for some group of initial assumptions is amassed, it may be possible to work out the detail of a more quantitative procedure. The following article is part of a preliminary program to discover whether a block theory is capable of describing ferromagnetic phenomena in general, and if so, to discover as many of the properties of such blocks as possible.

Definition of the Magneto-caloric Effect

When a ferromagnetic substance is subjected to a cyclic magnetization process, the temperature gradually rises due to the existence of hysteresis. In other words, the work done on the sample in taking it through a cycle appears as heat. If, however, the change is not cyclic, so that the magnetic as well as the thermal energy may have changed, no statement can be made relating the change of temperature to the work done without a knowledge of the detail of the magnetization process. This evolution of heat in a part of a magnetic cycle was first observed by Weiss and Piccard[4] and later investigated

[1] G. J. Sizoo, Physica **10,** 1 (1930) (in Dutch).

[2] F. Bitter, Phys. Rev. **37,** 91 (1931).

[3] T. D. Yensen, Trans. A.I.E.E. **43,** 145 (1924).

[4] P. Weiss and A. Piccard, Journal de Physique **7,** 103 (1917). C. R. **166,** 352 (1928).

more fully by Weiss and Forrer.[5] They discovered that in addition to the gradual increase in temperature due to hysteresis, there exists a *reversible* change in temperature. Thus they found that magnetizing a piece of nickel raised its temperature, but that demagnetizing it *lowered* its temperature. This reversible effect they called the magneto-caloric effect, and in this article the name will be used in this sense, rather than to designate any change in temperature accompanying magnetization. Subsequent experimenters working on the change of temperature with magnetization observed only hysteresis losses, and the magneto-caloric effect was not further studied until 1929 when Ellwood[6] investigated its detail with much more sensitive apparatus than that used in previous experiments. Both the results of Weiss and Forrer, and of Ellwood will be discussed further on.

Assumptions Regarding the Mechanism of Magnetization

If we are to discuss the magneto-caloric effect, we must first have some notion of what goes on within a piece of iron, for instance, while it is being magnetized. In accordance with the introductory remarks, we will assume our sample, which may be called iron for the sake of definiteness, to be permanently magnetized in small regions. The magnetization of each region is a function of the temperature as given by the Weiss-Heisenberg theory,[7] and the energy is a function of the orientation of the magnetization with respect to the field and the crystal axes as given by Powell.[8]

The only reasonable estimate it has so far been possible to make of the size of these regions at room temperatures is by means of the law of approach to saturation. In an extended investigation Weiss and Forrer[9] found that the intensity per unit mass at a temperature T and in a field H is given in terms of the saturation intensity by the expression

$$\sigma_{H,T} = \sigma_{\infty,T}\left(1 - \frac{a}{H}\right) \tag{1}$$

where a is a constant. Now the potential energy of a block may be written in the form: (1) a term depending on the crystal orientation, (2) a term depending on the irregular field produced by the neighboring blocks, (3) a term depending on the mechanical distortion, and (4) on the external field. For sufficiently large fields the first three terms may be neglected, and we have for the potential energy of a block simply $\mu H \cos\theta$, where μ is the magnetic moment, and θ is the angle between μ and H. But it is known that the magnetization of a group of dipoles having such a potential energy function is given by

[5] P. Weiss and R. Forrer, Ann. d. Physique **5,** 153 (1926).

[6] W. B. Ellwood, Nature **123,** 797 (1929); Phys. Rev. **36,** 1066 (1930).

[7] W. Heisenberg, Zeits. f. Physik **49,** 619 (1928). Probleme der Modernen Physik, edited by P. Debye, p. 114, Hirzel, 1928. F. Bloch, Zeits. f. Physik **57,** 545 (1929), **61,** 206 (1930). Or for a more simple treatment see: E. C. Stoner, Proc. Leeds Phil. Soc. **2,** 56 (1930).

[8] F. C. Powell, Proc. Roy. Soc. **A130,** 167 (1930).

[9] P. Weiss and R. Forrer, Ann. d. Physique **12,** 279 (1929).

$$\sigma_{H,T} = \sigma_{\infty,T}\left(\coth x - \frac{1}{x}\right)$$
$$x = \mu H/KT \tag{2}$$

which reduces, for large values of x, to

$$\sigma_{H,T} = \sigma_{\infty,T}\left(1 - \frac{1}{x}\right) = \sigma_{\infty,T}\left(1 - \frac{KT/\mu}{H}\right) \tag{3}$$

or comparing (1) and (3), we see that $a = KT/\mu$. But $\mu = \sigma_{\infty,T} m$ where m is the mass of a block. Or, introducing N, the number of particles per block, we have $N = m/M$ (M = atomic weight) and consequently $a = KT/\sigma_{\infty,T} NM$ or

$$N = \frac{KT}{aM\sigma_{\infty,T}}. \tag{4}$$

With the help of Eq. (4) it is possible to estimate the number of particles per block, but it is necessary to emphasize that this is only an estimate, and may be a very poor one in cases where there happen to be large local internal fields, or blocks having special shapes rendering the internal fields particularly effective, or perhaps impurities and strains that would invalidate the simple expression $\mu H \cos\theta$ for the energy. In fact, Weiss himself found that two samples of nickel did not follow Eq. (1), but in view of the many substances (including some samples of nickel) that did, and in view of Kapitza's experiments[10] on iron and nickel which are quite compatible with Eq. (1), it seems reasonable to assume that Eq. (1) is experimentally true and may provisionally be interpreted by Eq. (2). From Weiss' data, the block sizes given in Table I are obtained. The general indication of this calculation is that the magnetized units contain in the neighborhood of 100,000 atoms. These estimates are probably significant only as to order of magnitude.

TABLE I. *Estimate of the number of atoms cooperating to form a spontaneously magnetized region. Weiss' experimental data on the approach to saturation are used in Eq. (4). The values chosen for "a" are the average of Weiss' actual observations for each substance.*

Substance	a	$\sigma_{\infty}T$	M	N
Iron	6	217	56	350,000
Nickel	8.5	56	59	900,000
Magnetite $FeO \cdot Fe_2O_3$	17	920	33	48,000
Iron Sesquioxide Fe_2O_3	132	76	34	70,000
Fe_2B	255	160	40	15,000
Cementite Fe_3C	460	135	44	9,000
Fe+Co in all proportions	8	210	57	280,000

Before going on to a discussion of the magnetic properties of blocks of this size, it may be well to say a few words about their physical significance, and the factors which determine their existence. Consider, to begin with, a geometrically perfect ferromagnetic lattice near the absolute zero, and con-

[10] P. Kapitza, Proc. Roy. Soc. **A131,** 243 (1931).

sider two possible configurations; in one it is uniformly magnetized; and in the second its two halves are uniformly magnetized in opposite directions. In the first case let the energy be E. In the second case it will be $E+\sigma S-\int f dv$ where σS represents the increase in energy due to the formation of a surface, and $-\int f dv$ represents the decrease in magnetic energy due to changes in the magnetic field. It may happen that the second state represents a lower energy than the first, in which case it may be expected to occur. In calculating the probability of its occurrence, it is of course necessary to take into consideration the entropy, or the number of ways in which a given final state can be produced. So it is easy to see that even a perfect crystal may break up into smaller regions of spontaneous magnetization. If the magnetic energy plays a large part in determining this breaking up, one will expect the size and shape of the regions to depend markedly on the external field.[11] In contradistinction to this model, consider now the same metal bereft of its ferromagnetism. Zwicky[12] has shown that the perfect crystal need not represent the most stable grouping of atoms, but that a secondary structure may appear. This secondary structure manifests itself by the contraction of certain planes at more or less regular intervals. Although it is not possible at present to state definitely that any given ferromagnetic substance has this or that block structure, still it must be borne in mind that quite independently of the tendency to form blocks resulting from magnetic considerations, certain prescribed blocks may already be there to determine the extent of the regions of spontaneous magnetization. In the latter case the size and shape of the blocks may be quite independent of the state of magnetization and more or less independent of the temperature. It is interesting to note that blocks of the order of magnitude of those deduced in Table I are distinctly comparable to those with which Zwicky's work is concerned. Because blocks of the order of magnitude of those deduced in Table I seem to be of the right size to account for magnetic phenomena over a wide range of temperatures and magnetizations, and would therefore seem to be very stable, we shall here assume the second hypothesis, that the block sizes and shapes are determined by energies other than magnetic. If this is true, it follows that a group of such blocks can change its resulting magnetization only by a rotation of the direction of magnetization of the individual blocks, rather than by the growth of one block at the expense of another through atomic jumps or rotations along an interface.

Assuming, then, that a piece of iron consists of spontaneously magnetized blocks approximately cubic in shape and containing roughly 10^5 atoms, we proceed to enumerate some of the expected properties of iron. Let us assume for simplicity that the internal magnetic fields are negligible. Later on we shall drop this assumption, and show the consequences that follow. Such conditions would exist only just below the Curie point where the spontaneous magnetization (and hence the magnetic moment of each block) is small. Under these circumstances each block will resemble a saturated piece of iron, and we

[11] Concerning this type of block, see J. Frenkel and J. Dorfman, Nature **126,** 274 (1930).
[12] F. Zwicky, Helvetica Physica Acta **3,** 269 (1930).

may write its energy as a function of the direction of magnetization just as we would for a magnetically saturated macroscopic sample. Akulov[13] writes for the energy E_p of a cubic crystal

$$E_p = K_0 + 2K(s_1^2 s_2^2 + s_2^2 s_3^2 + s_3^2 s_1^2) \tag{5}$$

where s is a unit vector in the direction of magnetization having components s_1, s_2, s_3 along the rectangular axes perpendicular to the (100), (010), and (001) planes. Or, introducing polar coordinates for which $s_1 = \sin\theta \sin\phi$, $s_2 = \sin\theta \cos\phi$, $s_3 = \cos\theta$, the above expression reduces to

$$E_p = K_0 + \frac{K}{4}\left\{\tfrac{1}{2}(\tfrac{3}{4} - \cos 2\theta + \tfrac{1}{4}\cos 4\theta)(1 - \cos 4\phi) + (1 - \cos 4\theta)\right\} \tag{6}$$

K is a constant which Akulov interprets as being due to a quadrupole moment. More recently Powell[8] has shown that equivalent espressions can be obtained without assuming quadrupole moments by taking into consideration the interaction between "the effective electrons and the atoms to which they belong." In practice K must be evaluated by comparison with experiment. If a magnetic field is present, a term $-I_W H \cos\psi$ where ψ is the angle between I_W and H, must be added. I_W is the magnetization of a block as given by the Weiss-Heisenberg theory. By way of illustration a few curves have been plotted. If H is in a (100) plane, parallel to a (100) direction, the energy as a function of the direction of magnetization in this plane is given by

$$E_p(100) - I_W H \cos\theta$$

or, putting $h = 4I_W H/K$, we have for the energy per cm³

$$E_p = [-\cos 4\theta - h\cos\theta]\frac{K}{4} + \text{const.} \tag{7}$$

Similarly, if H is in a (100) plane parallel to a (110) direction, the corresponding expression becomes

$$E_p(100) - I_W H \cos(\theta + \pi/4)$$

or

$$E_p = [-\cos 4\theta - h\cos(\theta + \pi/4)]\frac{K}{4} + \text{const.} \tag{8}$$

In Figs. 1 and 2 are plotted Eqs. (7) and (8) for $h = 0, 2, 5, 10$. It is assumed that $K > 0$. If $K < 0$, Eq. (7) represents magnetization in a (110) and Eq. (8) in a (100) direction. The full expressions for any directions of magnetization in any field are somewhat more complicated than (7) and (8), chiefly because of the simultaneous occurrence of both θ and ϕ. Knowing the function E_p, or potential energy of a block for any direction of magnetization in any field, we may write for the probability f of finding a block magnetized in the direction θ, ϕ in the prescence of any external field $\exp(-E_p/KT)$ *provided we have an equilibrium distribution*. Knowing this distribution function, the mag-

[13] N. S. Akulov, Zeits. f. Physik **54,** 582 (1929). See also G. S. Mahajani, reference (18).

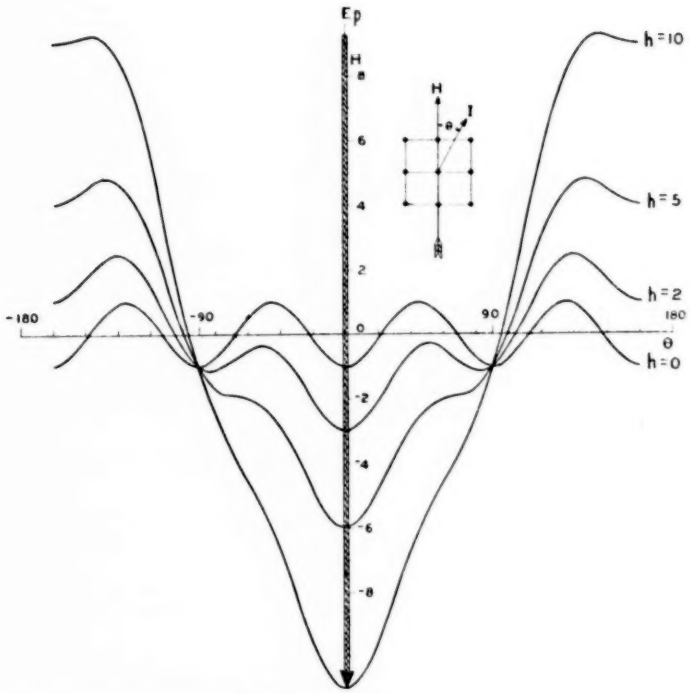

Fig. 1. The potential energy of a cubic crystal as a function of direction of magnetization in a (100) plane for various values of the external field which is proportional to h and is applied in a direction of easy magnetization (along a cube edge in iron).

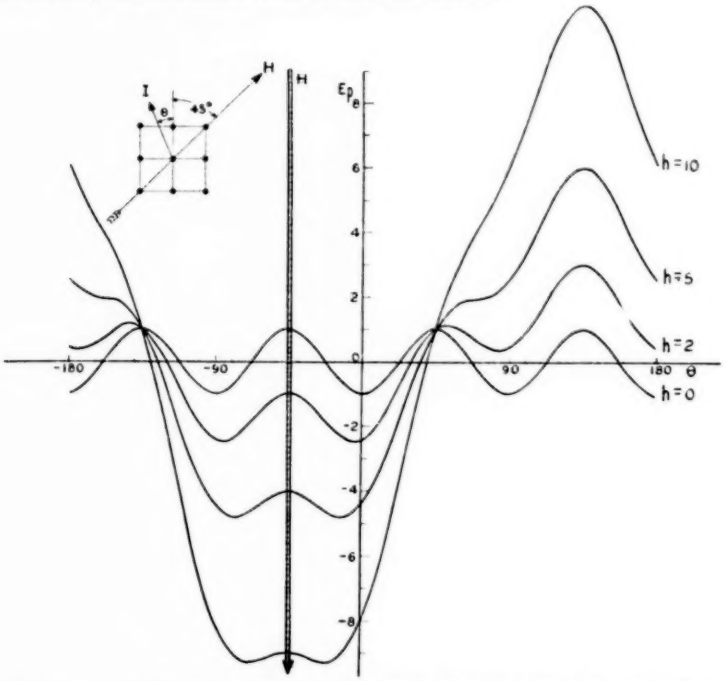

Fig. 2. The same as in Fig. 1, except that the field is applied in a direction of difficult magnetization. If the substance is iron, the figure represents conditons for H parallel to a (110) direction.

netization I and energy U of a macroscopic sample follow directly. The integrals will in general have to be evaluated by graphical methods. The chief point of interest, however, lies in the degree of approach to equilibrium in any special case. It is clear that the above expressions for E_p, and consequently also for I and U are single-valued functions of H. In other words, the material will not show hysteresis as long as equilibrium conditions are maintained. Just when equilibrium conditions are to be expected is determined by the following conditions. Suppose we apply a very large field to a substance, so that the potential energy curve becomes similar to that shown in Fig. 1 for $h=10$. If h is sufficiently large, most of the blocks will be magnetized in the direction $\theta=0$, and the distribution function will have a sharp maximum at this point. Suppose now the field is reduced so that the potential energy curve is that corresponding to $h=5$ in Fig. 1. A new distribution must set in. This new distribution must be created by a process of thermal diffusion. A closer inspection shows that the diffusion process is probably governed by a diffusion equation of the type

$$a\nabla\cdot(f\nabla E_p)+b\nabla^2 f=\frac{\partial f}{\partial t} \tag{9}$$

where a and b are constants. Physically this equation states that diffusion is determined by the concentration gradient and the potential forces, and that for equilibrium these two factors must just cancel each other. Without attempting even an approximate solution of Eq. (9) we may predict certain properties of its solutions in view of its physical content as described in the previous sentence. Suppose that for $t=0$ we have $h=5$, (see Fig. 1) and that the minimum is still deep enough so that most of the blocks are magnetized in the direction $\theta=0$. At the time $t=0$, h is changed from 5 to 0. Evidently the particles must diffuse to the right and left, at first rapidly, and then more slowly as the distribution becomes more uniform. Whether any appreciable number will get over the maxima at $\theta=\pm 45°$ will depend on the height of these maxima with respect to KT. If $E_p/KT\gg 1$ f will always be almost zero here. Hence there can be no gradient to speak of, and so very few particles will go from one minimum to the next. But E_p is directly proportional to the volume of a block. Thus we may say that if the blocks are large we would expect most of them to stay in the minimum $\theta=0$ even when $h=0$, whereas if they are small, we would expect a rapid distribution among the four minima at $\theta=0, \pm 45°$, and 180°. In the first case there would be a large remanence, and in the latter none. A more detailed discussion of this aspect of the problem will appear elsewhere. Emphasis is desired here only on the nature of the physical processes that are assumed to take place during magnetization. It should be pointed out that the presence of strains will greatly modify the potential function E_p, and consequently the detail of the magnetization process. Becker[14] discussed the effect of uniform strains on E_p for a saturated crystallite, but beside these, the strains due to the magneto-striction of each block must eventually be taken into consideration. The fact that unstrained single crystals show very little if any hysteresis would indicate that the blocks

are small. Rough estimates[15] of how small they must be in order to account for this lead to sizes comparable with those deduced in Table I.

In order to approximate actual conditions more closely we must now consider the effect of the internal magnetic field. A detailed discussion of this subject would take up too much space to be considered in this article, and we shall therefore confine ourselves to a qualitative discussion. The field inside a spherical cavity in a magnetized medium is $4\pi I/3$. Hence we may write approximately for the magnetic energy of a block $\mathfrak{y}\cdot(\boldsymbol{H}+4\pi\boldsymbol{I}/3)$, and neglecting the term depending on crystal structure (see Eq. (6)), and neglecting strains, the magnetization of a group of blocks is given by

$$I = I_W\left(\coth x - \frac{1}{x}\right) \tag{10}$$

$$x = \frac{\mu}{KT}\left(H + \frac{4\pi}{3} I\right). \tag{11}$$

Spontaneous magnetization will occur, according to this equation, if $dI/dx < I_W/3$ or from Eq. (11) if

$$\frac{dI}{dx} = \frac{3KT}{4\pi\mu} < \frac{I_w}{3}$$

or in other words if

$$T < \theta_f = \frac{4\pi\mu I_w}{9K}. \tag{12}$$

Now if $\mu = I_W v$ where $v \sim 10^{-18}$ cm^3 this gives $\theta_f \sim (4\pi \times 10^{-18}/9 \times 1.37 \times 10^{-16})$ $(I_W)^2 \sim 0.01(I_W)^2$ so that even if I_W is only about 500, θ_f is a high temperature. Actually, for most ferromagnetic substances at room temperature, I_W is greater than 500, so that we may conclude that the blocks are magnetically coupled to one another and the magnetization of each tends to be more or less parallel to that of its neighbors. The presence of homogeneous strains, and the energy due to crystal structure, both of which factors were neglected above, would have served chiefly to determine the direction of spontaneous magnetization of such a group of blocks.

We saw that the Curie point of a group of blocks, θ_f, was proportional to $(I_W)^2$, the square of the intensity of magnetization of each block. Let θ_p be the Curie temperature of a spontaneously magnetized block as given by the formulae

$$\frac{I_W}{I_0} = \tanh \frac{\mu_B N_W I_W}{KT}$$

$$\theta_p = \frac{\mu_B N_W I_0}{K}$$

where $I_0 = I_W\big]_{T=0}$ and N_W is the Weiss molecular field constant.

[14] R. Becker and M. Kersten, Zeits. f. Physik **64,** 660 (1930); R. Becker, Zeits. f. Physik **62,** 253 (1930).

[15] F. Bitter, Phys. Rev. **37,** 1176 (1931).

As we approach the Curie temperature from below we have at every temperature T a value of I_W determining θ_f. In other words

$$\theta_f\Big]_T = \frac{4\pi v}{9K} I_W{}^2\Big]_T$$

and the group of blocks will break up when $T=\theta_f$ or

$$\theta_f = \frac{4\pi v}{9K} I_W{}^2\Big]_{T=\theta_f}$$

Experimentally the magnetic transformation takes place in two stages. At a temperature θ_f the magnetic poperties undergo a marked change, and at the tmperature θ_p there is a change in energy content corresponding to the change in energy of spontaneous magnetization of each block $-\frac{1}{2}N_W I_W{}^2$. In general these temperatures are only a few degrees apart. We shall assume that the experimentally observed temperatures θ_f and θ_p correspond to the theoretical temperatures deduced above. In order to determine the order of magnitude of the blocks that would give small values for $\theta_p-\theta_f$, we may write

$$\frac{\theta_f}{\theta_p} = \frac{4\pi\mu_W I\big]_{T=\theta_f}/9K}{N_W\mu_B I_0/K}$$

or

$$\frac{\mu}{\mu_B} = \frac{9N_W}{4\pi}\,\frac{\theta_f}{\theta_p}\,\frac{I_0}{I_W\big]_{T=\theta_f}}$$

where μ_B is a Bohr magneton, and μ is the magnetic moment of a block. μ/μ_B is of the same order of magnitude as the number of atoms per block. It is not desired at this point to attempt accurate estimates of block sizes, but rather to discover whether ferromagnetic phenomena in general are explicable in terms of blocks containing roughly 10^5 atoms, or in other words that the assumption of such blocks leads to no obvious inconsistences. With this in mind we may put

$$N_W \sim 10^4;\ \frac{\theta_f}{\theta_p} \sim 1;\ \frac{I_0}{I_W\big]_{T=\theta_f}} \sim 10$$

and find that $\mu/\mu_B = 10^5$ in satisfactory agreement with the numbers in Table I. The phenomena near the Curie point will be discussed more fully elsewhere, but it may be stated in advance that there seems to be some hope of describing, with the help of this block model, the changes that take place.

Evidently this spontaneous coupling of the blocks will not cover an entire sample, for by breaking it up it is possible to reduce the total magnetic energy, and such a breaking up process may be expected to go on until clusters of blocks, or Barkhausen units, as they might be called, of a given size are formed. Just as there is an optimum size, so there will be an optimum shape, probably one that is more or less elongated in the direction of magnetization. When an external field is applied to a sample, the total field acting on a group will be approximately $(H+cI)$ where c depends on the shape of the group

and is very small for elongated shapes, so that we may conclude that practically only the external field acts on the Barkhausen units.

In an unmagnetized sample these Barkhausen units will be magnetized in the various directions of easy magnetization (see the last section for further details), for instance in iron in the directions (± 100), (0 ± 10), (00 ± 1). Because of their size, they will be very little influenced by temperature. (We saw[15] that the energy of the blocks as their direction of magnetization changes, varies by an amount of the same order of magnitude as KT. Since the Barkhausen units contain thousands or millions of blocks, the above statement seems amply justified.) That is, temperature agitation will not be able to boost them out of the directions of easy magnetization, though it will, in general, determine the relative concentrations in the various directions of easy magnetization. If, now, we apply a small field to the above iron crystal in the (100) direction, a Barkhausen unit magnetized in the (-100) direction will no longer be stable, but will jump into the (100) direction. The relative numbers in these directions will be given (in the absence of hysteresis) by the usual exponential function $e^{\pm \mu_{BU} H/KT}$. μ_{BU} is the magnetic moment of a Barkhausen unit. From the initial slope of the ideal magnetization curve the size of μ_{BU} may be estimated, and it turns out to be of the same order of magnitude as actually observed Barkhausen units. As Akulov[16] has shown, once this initial process is complete, the rotation of the magnetization of the Barkhausen units sets in. This is further discussed in the last section. From the preceding it is clear why Akulov is able to develop so satisfactory a theory without considering internal fields or temperature.

According to what has been said, the magnetization process may be conceived as follows:

1. Small blocks containing approximately 10^5 atoms are permanently magnetized in accordance with the Weiss-Heisenberg theory, the energy as a function of direction of magnetization being determined by Powell's crystalline field, by the presence of strains, and by the internal and external magnetic field.

2. At room temperature these blocks become spontaneously magnetized in clusters, which probably give rise to the Barkhausen effect, and are here called Barkhausen units.

3. Magnetization consists of two processes, a rotation of the magnetization of the Barkhausen units as a whole, and the rotation of magnetization of individual blocks separately. The Barkhausen units will occupy only positions of minimum potential energy; one might say they are too large to execute Brownian movements. The blocks, on the other hand, are small, and so capable of picking up enough thermal energy to "push" them into regions other than minima of potential energy.

4. A change in field will produce two principal changes—a change in the position of the potential energy minima, and a consequent change in the direction of magnetization of each Barkhausen unit, and secondly a tendency to redistribute the number of Barkhausen units in the various minima. This

[16] N. S. Akulov, Zeits. f. Physik **67,** 794 (1931).

latter process, called by Akulov[16] "Schrumpfprozess" is possible if the potential walls between minima are low enough to let blocks pass. If they are very high, as in strained material, the blocks cannot pass, there is no "Schrumpfprozess," and so the material exhibits hysteresis. Akulov[16] has shown that these two mechanisms suffice to give an approximate theory of the magnetization of single crystals of iron. In the last section of this paper his theory is applied to nickel and cobalt. The block theory gives an explanation of his Schrumpfprozess, and the elongated shape of the Barkhausen units explains why he was able to neglect the internal fields.

5. The final approach to saturation is due to the final alignment of the blocks composing the Barkhausen units.

6. As the temperature approaches the Curie point the Barkhausen units become smaller, and break up at $T=\theta_f$. At $T=\theta_p$ the magnetization of each block disappears.

7. Three arguments are adduced in favor of assuming blocks containing about 10^5 atoms, (a) an argument based on the law of approach to saturation, (b) an argument based on the absence of remanence in single crystals, and (c) an argument based on the small observed values of $\theta_p-\theta_f$.

The Mechanism of the Magneto-Caloric Effect

The magneto caloric effect is of course, governed by thermodynamic principles. If a certain amount of work dW is done in changing the total energy of a system by dU, and if this change occurs adiabatically, then $dU=dW$. If the total energy of the system is of two kinds, potential, and thermal, we can write $dU=dE_p+dQ$ and solving for dQ, obtain

$$dQ = dW - dE_p. \tag{13}$$

Consequently, in order to calculate dQ, it is necessary and sufficient that we know the work done and the change in the potential energy. But Eq. (13) can of course throw no light on the detail of such a process, and it is the purpose of this section to illustrate, on the basis of what might be called a kinetic theory as opposed to a thermodynamic theory, how such a change takes place.

To study the mechanism of the magneto-caloric effect, let us consider first a very simple mechanical system which will later be shown to possess certain similarities to a ferromagnetic substance. This system consists of a large number of particles in thermal equilibrium, having one degree of freedom each, namely x. They are contained between the limits $x=0$ and $x=1$. $f(x)dx$ is the probability of finding a particle between x and $x+dx$. The particles are subjected to a force such that their potential energy at a point x is $\phi(x)$. Then it follows that when equilibrium has set in

$$f(x) = Ae^{-\phi(x)/KT}$$

where A is determined by the equation

$$\int_0^1 f(x)dx = 1$$

At some particular instant let $\phi_1(x) = x$. This function, and the corresponding distribution function f_1 are drawn in solid lines in Fig. 3. KT was chosen equal to unity. The total potential energy in this state is E_1

$$E_1 = N \int_0^1 \phi_1(x) f_1(x) dx.$$

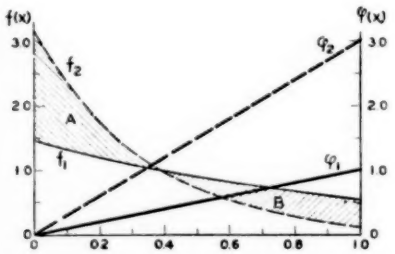

Fig. 3. If $f(x)dx$ represents the number of particles between x and $x+dx$, and $\phi(x)$ is the potential energy of a particle at the point x, then $f(x) = \text{const}\ e^{-\phi(x)/KT}$ at equilibrium and the figure shows $f(x)$ for two values of $\phi(x)$. If ϕ_1 is discontinuously changed to ϕ_2, the particles represented by region B will move to region A and so lose potential energy and gain thermal energy. If ϕ_2 changes to ϕ_1 the reverse processes take place. The reversible temperature changes are analogous to those occurring in the magneto-caloric effect.

N is the total number of particles. Now suppose the external field is suddenly changed so that the potential becomes $\phi_2(x) = 3x$. This change will result in the establishment of a new total potential energy E_1^1

$$E_1^1 = N \int_0^1 \phi_2(x) f_1(x) dx$$

and the amount of work done is obviously $E_1^1 - E_1$. The distribution f_1 is, however, no longer stable, and will change and gradually become f_2

$$f_2 = A_2 e^{-\phi_2(x)/KT}.$$

ϕ_2 and f_2 are drawn in dotted lines in Fig. 3. The energy in this state is

$$E_2 = N \int_0^1 \phi_2(x) f_2(x) dx.$$

If the change in potential energy from E_1^1 to E_2 proceeded adiabatically, this must have been compensated by a change in the thermal energy of the system.

$$-\Delta Q = E_2 - E_1^1.$$

In words, we can say that the number of particles represented by the area B in Fig. 4 have dropped from a region of higher potential to the area A which is at a lower potential, and have given up the energy of their "fall" in the form of heat. If now we change the field back again so that the potential becomes ϕ_1 again, the same processes will take place in the reverse order, only instead of "falling," the particles will be "lifted" by temperature agitation from the

region A at low potential to the region B at high potential, and so convert a certain amount of thermal energy ΔQ into potential energy. It should be noted that the amount of heat evolved in going from state 1 to state 2 depends on the path taken. For, if we proceed first from ϕ_1 to some ϕ_0, and wait until equilibrium sets in,, and then to ϕ_2, the total heat evolved will be

$$N \int_0^1 \phi_0(f_1 - f_0)dx + N \int_0^1 \phi_2(f_0 - f_2)dx$$

instead of

$$N \int_0^1 \phi_2(f_1 - f_2)dx$$

which is the expression ΔQ above for the heat evolved in going from state 1 to state 2 in a single step. To see that these expressions are not equal, subtract the second from the first. The result is

$$N \int_0^1 \phi_0(f_1 - f_0)dx - N \int_0^1 \phi_2(f_1 - f_0)$$

which is obviously not zero. Similarly the heat evolved in the changes $\phi_1 \rightarrow \phi_0 \rightarrow \phi_2$ depends on whether or not the change $\phi_0 \rightarrow \phi_2$ was made after the equilibrium distribution f_0 had been established. Still again, the heat evolved in the change $\phi_1 \rightarrow \phi_2$ will depend on whether this change was instantaneous, and the diffusion actually took place in the field ϕ_2, or whether $\phi_1 \rightarrow \phi_2$ was gradual. Briefly the results are:

1. If the slope of the potential energy curve is suddenly increased, a rise in temperature follows.

2. If the slope of the potential energy curve is suddenly decreased, a drop in temperature follows.

3. The change in temperature accompanying a change in the applied field depends not only on the initial and final states, but also on the particular way in which the field is varied.

The Effect at High Temperatures in the Absence of Distortions

The analogy between the system discussed in the last section and a ferromagnetic body consists of the fact that in both cases a large number of particles strive toward an equilibrium distribution in a variable external field. In a piece of iron, the direction of magnetization of the atoms, the blocks, and the Barkhausen units are in thermal interaction, and the total magnetic energy is determined by the distribution of their angular coordinates. Here the problem is complicted by the fact that in addition to the potential in the external field the interaction of the various particles has to be considered. In accordance with what has been said in a previous section, the factors that have to be taken into account are: the crystal structure, the permanent distortions of the lattice, the distortions due to the varying magnetostriction in adjacent parts of the lattice magnetized in different directions, the stray magnetic fields, the externally applied magnetic field, and of course the degree

of magnetization of each block if the applied fields are sufficiently strong to affect this. An accurate description of these various factors is not possible, and we shall consider under what conditions sufficient simplifications may be made to allow a more or less quantitative treatment. To begin with by assuming large crystal grains in a well-annealed material possessing no magnetostriction the complications due to strains are avoided. And further, by limiting the discussion to large fields, or to temperatures so high that KT is large compared to the variations in potential due to crystal structure (see Fig. 1, $h=0$), the complications arising from expressions similar to Eq. (5) are avoided. And if this high temperature is also near the Curie point where the intrinsic magnetization of each block is small, there will be no internal stray fields to consider. Internal fields will also be negligible if the regions of permanent magnetization are elongated, as is the case at low temperatures, where Barkhausen units of this form predominate, as pointed out in a previous section. Under this conditions, the energy of a block may be written simply*

$$-\mu H\cos\theta-\tfrac{1}{2}n\sigma_W{}^2m$$

where σ_W is the intensity of magnetization per unit mass of a block as accounted for by the Weiss-Heisenberg theory. The distribution of orientations of block moments is then given by the Langevin theory, and the energy per unit mass is

$$-\sum\mu H\cos\theta Nf(\theta)-\tfrac{1}{2}n\sigma_W{}^2.$$

where the summation extends over all the blocks and Nf is the number of blocks per unit mass of substance having a given orientation. But $\Sigma\mu\cos\theta Nf(\theta)=\sigma$, the observed intensity of magnetization, so that the energy becomes

$$-\sigma H-\tfrac{1}{2}n\sigma_W{}^2.$$

In changing the field to $H+dH$ the intensity changes to $\sigma+d\sigma$ and $\sigma_W+d\sigma_W$, and substituting in the above expression we have for the change in magnetic energy

$$-\sigma dH-Hd\sigma-N\sigma_W d\sigma_W.$$

This estimate has neglected the possibility of a loss of energy, due, for instance, to the presence of a conductor in which currents are induced by the change in σ. We will assume that such conductors are not present. If they are, corrections must be applied.

The work done by outside forces in changing the field is

$$-\sigma dH.$$

Equating the work done to the change in magnetic energy and in heat content, we have

$$-\sigma dH=cdT-\sigma dH-Hd\sigma-n\sigma_W d\sigma_W$$

* n is the molecular field constant N_W expressed per unit mass instead of per unit volume.

c being the specific heat, or

$$dT = \frac{Hd\sigma + n\sigma_W d\sigma_W}{c}. \tag{14}$$

This is the formula given by Weiss and Forrer[17] except that in Eq. (14) a distinction is made between $d\sigma$, the change in the apparent magnetization, and $d\sigma_W$, the change in the "Weiss" magnetization, and that here the special conditions are pointed out under which the formula may be expected to hold.

The Experiments of Weiss and Forrer

In this section the experiments of Weiss and Forrer[17] on nickel are discussed in such a way as to bring out in how far the molecular field theory of Weiss can describe the magneto-caloric effect in high fields quantitatively, and what the nature of the discrepancies between theory and experiment is. In their paper the authors describe an exhaustive series of experiments on the magnetization of nickel. The range of fields used was up to about 20,000 gauss. The particular aspect of their work to be discussed here concerns the change in temperature accompanying a change in the applied field from some value H to zero. In fields of this order of magnitude the chief contribution to the magnetization is still the alignment of the blocks, and only for much higher fields would the increase in σ_W, the magnetization of each block, come in. This does not imply, however, that the change in energy or heat content may not be due primarily to the small increase in intrinsic magnetization. Indeed, it is easily seen that a very small change in σ_W will have much more effect on the energy because of the presence of the molecular field constant n in $n\sigma_W^2/2$, than a much larger change in the apparent magnetization due to the alignment of the blocks.

Writing $d\sigma = d\sigma_{bl} + d\sigma_W$, (the total observed change is due to the change in orientation of the blocks plus the change in magnetization of each block) and considering here only the part due to $d\sigma_W$, we have from Eq. (14). Let us calculate the temperature change due to a given change in σ_W.

$$dT = \left(\frac{H + n\sigma_W}{c}\right) d\sigma_W. \tag{15}$$

This equation is not well suited to a comparison with experiment because σ_W is not a directly observable quantity. We may, however, write

$$d\sigma_W = \frac{\partial \sigma_W}{\partial H} dH + \frac{\partial \sigma_W}{\partial T} dT \tag{16}$$

and substituting in Eq. (15) obtain

$$dT = \frac{\partial \sigma_W / \partial H}{(c/H + n\sigma_W) - (\partial \sigma_W / \partial T)} dH \tag{17}$$

[17] P. Weiss and R. Forrer, Ann. d. Physique **5**, 199 (1926).

where

$$\sigma_W = \sigma_0 \tanh \frac{\mu_B}{KT}(H + n\sigma_W). \tag{18}$$

In using this relationship it is tacitly assumed that H is parallel to σ_W. According to a previous section, this will hold approximately for temperatures not too near the Curie point, because even before $H=1000$ gauss the Barkhausen units are all sensibly parallel to H, and the magnetization has reached the final lining up of the blocks where $\sigma=\sigma_W(1-a/H)$. But near the Curie point where the Barkhausen units are broken up and the blocks are not lined up even in fields of the order of 20,000 gauss, only a part of the blocks will be magnetized parallel to H—some even in the opposite direction. In other words, near the Curie point H will not be as effective in increasing σ_W as at lower temperatures. This prediction we will proceed to verify. Limiting ourselves to temperatures below 570°K we may regard the coefficients of Eq. (17) as constant. This may be seen as follows. For nickel $\theta=630$°C, the saturation magnetization at $T=0$ is $\sigma_0=58$, and from the relation $\theta=\mu_B n\sigma_0/K$ we find $n=150{,}000$. From the magnetization diagram it is found that for $T<570°$, $\sigma_W>30$, and hence $n\sigma_W>4.5\times10^6$. Hence in Eq. (18) a change of H from 0 to 20,000 will change the argument $(H+n\sigma_W)$ of tanh by less than 2 parts in 450 or $\frac{1}{2}$ percent. From the nature of the function it follows that σ_W and its derivative will change by even less. This means that

$$\Delta T = \text{const}\,\Delta H \tag{19}$$

as Weiss and Forrer showed both theoretically and experimentally. They did not, however, evaluate the constant in Eq. (19), and this we proceed to do. From Eq. (18) it follows that

$$\frac{\sigma_W}{\sigma_0} = \tanh \frac{\theta}{T}\frac{\sigma_W}{\sigma_0}$$

$$n\frac{\partial\sigma_W}{\partial H} = \left[\operatorname{sech}^2 \frac{\theta}{T}\frac{\sigma_W}{\sigma_0}\right] \Big/ \left[\frac{T}{\theta} - \operatorname{sech}^2 \frac{\theta}{T}\frac{\sigma_W}{\sigma_0}\right]$$

$$\frac{T^2}{\theta\sigma_w}\frac{\partial\sigma_w}{\partial T} = -\operatorname{sech}^2 \frac{\theta}{T}\frac{\sigma_W}{\sigma_0}.$$

These equations are easily solved numerically, and the results, substituted in Eq. (17) for three values of the temperature, are shwon in Table II.

TABLE II. *The magneto-caloric effect in nickel.*

$t=100$°C	$t=200$°C	$t=300$°C
	From Eq. (17)	
$dT=0.38\times10^{-5}\,dH$;	$.90\times10^{-5}\,dH$;	$2.4\times10^{-5}dH$
	For $\Delta H=17{,}775$	
$\Delta T=0.068°$;	$0.16°$;	$0.42°$
	Experimentally* observed values are	
$\Delta T=0.065°$;	$0.13°$;	$0.32°$

* The experimental values are taken from the figure on page 194 of Weiss and Forrer's paper.[17]

The agreement for $t=100°C$ is remarkably good, but as we approach the Curie point ($t=357°C$) the observed value falls below the theoretical one, and it is suggested that this is due to the fact that for higher temperatures H is not parallel to σ_W in every block, and hence only a gradually decreasing component is effective.

Calculations for $T=\theta$ will not be attempted at this point because of the complexity of the phenomena involved.

The Experiments of Ellwood[6]

Perhaps the most interesting experiments on the magneto-caloric effect are those in Ellwood, because they concern themselves with fields of a few hundred gauss—just the region in which the readjustment between the various regions of spontaneous magnetization is taking place. It is in such fields that the detail of the potential energy curves (see Fig. 1) may be expected to make itself felt. There exists at all fields a magneto-caloric effect dependent on the change in spontaneous magnetization, called σ_W in the previous section, and this may be calculated with a considerable accuracy. Such a process however, cannot account for the results observed by Ellwood, and it would be desirable to attempt an analysis in the light of the foregoing. The fact that Ellwood's experiments were carried out on polycrystalline material makes such an analysis difficult, but the fact that this material consisted of two phases (ferrite+cementite) renders the situation quite hopeless. The experiments were of such a nature that there does not seem to be any reason why they might not be carried out on single crystals. Because of the fundamental importance of such experiments, certain results to be expected on single crystals will be pointed out in the following section.

One inference may be drawn, however, from the existence of a magneto-caloric effect at low fields, namely that in this region temperature agitation must be considered in calculating the magnetization of those substances which show an effect.

The Theory of Akulov

Based on the work of Mahajani,[18] Kornfeld[19] and Powell,[21] first Webster,[21] and then more in detail Akulov[22] developed a static theory of the magnetization curve. That is, given the potential energy E_p of a region as a function of the direction of magnetization, Akulov calculates the positions of the energy minima, and a sumes that the minima are the only points of the curve actually occupied. That this is a good approximation is shown by the correctness of the theoretical magnetization curve for iron crystals which he was able to construct. It can be shown quite generally that in such a static theory there can be no magneto-caloric effect. It follows that Akulov's theory can be accepted only so long as $dW-dE_p=dQ=0$ within the experimental error. The

[18] G. S. Mahajani, Roy. Soc. Phil. Trans. **228,** 63 (1929).
[19] H. Kornfeld, Zeits. f. Physik **22,** 27 (1924).
[20] F. C. Powell, Roy. Soc. Proc. **A130,** 167 (1930).
[21] W. L. Webster, Proc. Phys. Soc. **42,** 431 (1930).
[22] N. S. Akulov, Zeits. f. Physik **67,** 794 (1931).

relation is satisfied for iron as Akulov has shown. Let us apply it to nickel and cobalt. For nickel we may write

$$E_p = 2K(s_1^2 s_2^2 + s_2^2 s_3^2 + s_3^2 s_1^2) + \text{const.}$$

as in Eq. (5), from which it follows that

$$E_p(111) - E_p(110) = \frac{K}{6} \equiv \Delta E_p.$$

ΔE_p is the difference in energy of magnetization in the (111) and (110) direction. From a study of the component of I perpendicular to H, or deviation effect, Powell[8] has calculated $2K$ so as to fit the observations of Kaya[23] $2K = -94.8$ $I = -94.8 \times 500$ ($2K$ is γNI in Powell's notation). From this we find $\Delta E_p = -0.39 \times 10^4$ ergs/cc. ΔW, the difference in the amount of work required to magnetize nickel in the (111) and (110) directions is the area en-

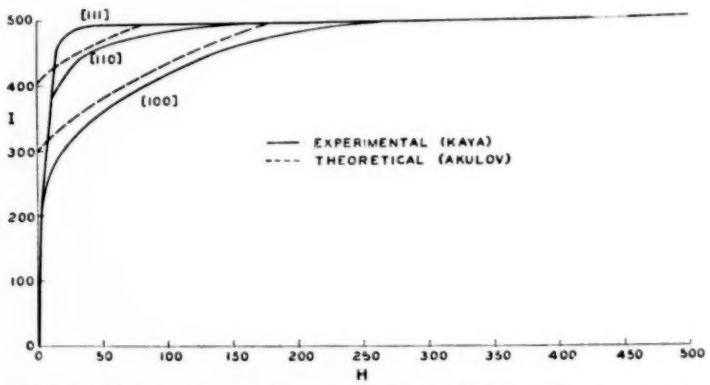

Fig. 4. The experimental magnetization curves of nickel in the principal directions as observed by Kaya, together with the corresponding theoretical curves as deduced by means of the static theory of Akulov.

closed between the corresponding magnetization curves. Using the curves published by Kaya, we find $\Delta W = -0.34 \times 10^4$ ergs/cc, which may be considered in satisfactory agreement with ΔE_p above. An actual plot of the theoretical magnetization curves in the (110) and (100) directions is shown in Fig. 4. The discrepancy between experiment and theory for the (100) direction is probably due chiefly to a correction that must be applied to account for the slope of the initial part of the curve. In the (110) direction the agreement is only qualitative. The theoretical curve was obtained according to Akulov's prescription for iron. The numerical value of $2K$ was taken as -94.8×500.

For cobalt, Powell[8] has shown that E_p may be written in the form

$$E_p = -K_1 I_z^2 - K_2(I_y^2 + I_z^2) \tag{20}$$

Powell found from the deviation effect that the difference in energy for a crystal magnetized in the direction of easy and difficult magnetization is

[23] S. Kaya, Sci. Rep. Tohoku Univ. **17**, 639 (1928).

$$\Delta E_p = -I^2(K_2 - K_1)$$
$$2I(K_2 - K_1) = 6.8 \times 10^3$$
$$I = 1.4 \times 10^3$$
$$\Delta E_p = -4.85 \times 10^6 \text{ ergs/cc.}$$

From the magnetization diagram given by Kaya[24] ΔW may be obtained by graphical integration and is found to be about -5.3×10^6. Whether or not this difference is an experimental error, it is hard to say. If it is not, we must assume that in cobalt there are changes in heat content for magnetization in the directions of difficult magnetization of the order of 10^6 ergs/cc which would correspond to temperature changes of the order of 0.03° C. Cobalt should be a very interesting substance for further experimentation. If the dis-

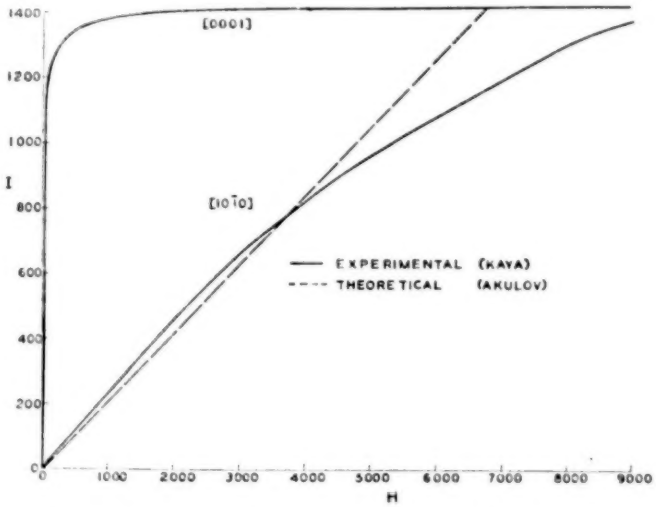

Fig. 5. The experimental magnetization curves of cobalt in its principal directions as observed by Kaya together with the corresponding theoretical curve as deduced by means of the static theory of Akulov.

crepancy between ΔE_p and ΔW is real, we must assume that a magneto-caloric effect is involved, and this in turn leads to the conclusion that a static theory such as Akulov's will not do. Instead of dealing with an equilibrium orientation, we must consider thermal agitation and the ensuing distribution of orientations as suggested in a previous section. Finally, it may be of some interest to see just what the above static theory predicts for the magnetization curve of cobalt in the direction of difficult magnetization. Using Eq. (20) above, it may readily be shown that up to saturation

$$I = \frac{H}{2(K_2 - K_1)} \tag{21}$$

In Fig. 5 the results of Kaya[23] are plotted together with Eq. (21), using $K_2 - K_1$ as found from the deviation effect, $2I(K_2 - K_1) = 6.8\times10^3$. The agreement is good except at high fields.

[24] S. Kaya, Sci. Rep. Tohoku Univ. **17,** 1157 (1928).

As to the nature of the necessary corrections, little can be said at present. One possibility is the introduction of temperature, as has been suggested. Another is the introduction of the random internal fields. As long as the regions of spontaneous magnetization are elongated in the direction of resultant magnetization, this will be negligible. But if they are not, we must write for the energy of a block $\mathfrak{y}(\boldsymbol{H}_e+\boldsymbol{H}_i)$, that is, take into account the internal as well as the external field. And finally there is the possibility that the crystals used in the experiments were not perfect, but locally distorted. This would necessitate the addition of an extra term in the potential energy function similar to that discussed by Becker,[14] and would involve a shifting of the positions at which E_p has a minimum. In how far each of these factors is actually important can be revealed only by further careful experimentation.

Summary

A summary regarding the process of magnetization is to be found at the end of a previous section. About the magneto-caloric effect we might say that,

(1) At high external fields changes in spontaneous magnetization I_W are probably alone responsible for the observed results, but that block structure does play a minor role near the Curie point.

(2) On the basis of Akulov's theory one would expect no magneto-caloric effect after the first steep rise in the magnetization of single crystals, except, of course, insofar as I_W, the Weiss spontaneous magnetization, is altered.

(3) During the steep ascent of the magnetization curve near the origin an effect is to be expected.

(4) Discrepancies between the experimental and theoretical magnetization curves (calculated on the basis of Akulov's static theory) of nickel and cobalt may possibly be due to the presence of a magneto-caloric effect. This point could be tested by experiments on single crystals.

(5) Ellwood's experiments on carbon steel in fields of the order of 200 gauss indicate that temperature agitation must be considered, in this steel at any rate, in calculating its magnetization curve.

THE MOBILITY OF NA^+ IONS IN N_2 AND H_2 AS A FUNCTION OF TIME

By Leonard B. Loeb
Department of Physics, University of California

(Received June 15, 1931)

Abstract

The mobilities of Na^+ ions from a Kunsman source have been measured in H_2 and N_2 using gases of considerable purity and time intervals ranging from 10^{-5} to 10^{-1} seconds. The method used was the Rutherford A.C. method using both sinusoidal and square wave form oscillations. With corrections for temperature and pressure included the method gives reduced absolute mobility constants for the ions good to about 10 percent. The results indicated three distinct classes of ions in H_2 and probably three in N_2. In H_2 there is a fast ion of mobility 17.5 cm/sec per volt/cm which is presumably the atom ion Na^+ which exists up to time intervals of 10^{-4} seconds. It then undergoes an abrupt transition to an ion of mobility of about 13.5 cm/sec per volt/cm whence, after some 10^{-3} seconds, it gradually transforms to the normal ion in H_2 which has an absolute mobility of 8.4 cm/sec. per volt/cm. The intermediate ion is presumably a single molecular addition product, (possibly water vapor) to the initial Na^+ atom ion which retains its charge. The final so called normal ion may result from a gradual growth of the ion cluster by further addition of molecules, or by a gradual interchange of one or two primarily attached molecules to molecules of impurity that are strongly attracted but less prevalent, gradually making a stable ion. In N_2 the initial ion observed up to 5×10^{-3} seconds has a mobility of 3.75 cm/sec. per volt /cm. and probably changes abruptly to an ion of about 3.0 cm/sec. per volt/cm at the end of the interval. At the end of about 10^{-2} seconds it has transformed to the normal positive ion of 1.6 cm/sec. per volt /cm mobility. The interpretation is similar to that suggested for H_2. The mobilities of 17.5 and 3.75 for Na^+ ions in H_2 and N_2 give the first opportunity to check the theoretical mobility equations since in these cases the nature of the ion is known. They show that the Langevin theory assuming forces of dielectric polarization of an inverse fifth power type yields values of the mobility that are about 20 to 40 percent too low. This result was to be expected since it seems unlikely that ordinary forces of dielectric polarization observed in weak homogeneous fields should be capable of extrapolation to the huge inhomogeneous fields existing within a molecular diameter or two of an ion. The amount of deviation is however gratifyingly small and should prove of value in extending the theory.

Introduction

IN THE many researches concerning the nature of gaseous ions little progress has been made in arriving at a definite conclusion as to the ultimate nature of the ion (i.e. whether it is a large cluster or a small ion)[1] under ordinary conditions. The work of Erikson[2] on the relatively abrupt change of mobility with age for positive ions in air and the work of the writer on mobilities in gaseous mixtures[1,3] have definitely indicated the preferential addition of some molecules to the already somewhat indefinite ion. In the latter work

[1] L. B. Loeb, Phys. Rev. **32,** 81 (1928).
[2] H. A. Erikson, Phys. Rev. **20,** 117 (1922); **24,** 502 (1924); **33,** 403 (1929); **34,** 635 (1929.)
[3] L. B. Loeb, Proc. Nat. Acad. Sci. **15,** 146 (1929); Phys. Rev. **35,** 184 (1930).

this action was shown to be a specific function of the chemical nature of the gas and the sign of the charge on the ion. Beyond this no definite knowledge of the nature of the ion could be derived, for these measurements indicated only *changes* of an abrupt sort in the ion which affected its mobility. Both workers, however, inclined to the belief that as a whole the ion was a complex of relatively few molecules, 2 or 3 at best, and that much of the reduction of the mobility was due to the attractive forces between molecules and ions not resulting in cluster formation.

It is clear that little progress can be made by such investigations unless the nature of the molecule actually carrying the charge (i.e., the nucleus of the ion cluster) can be studied. Heretofore many studies[4] have been made to determine the effect of the mass of the ion on its mobility. These all depended on assumptions as to the nature of the *initially ionized* molecule or atom (which was assumed to have retained its charge throughout). However, among all the researches done on this subject only those using as initial ions the radioactive recoil atoms, *detected by radioactive methods* were of any significance, and even these were of doubtful value because of the unknown size of the radioactive cluster torn off by recoil. The reason for the doubtful value of these earlier experiments could not at that time have been forseen. In the meantime, the immense amount of data on the transfer of energy between activated, excited, metastable and ionized molecules and atoms with neutral molecules, which have accumulated in recent years makes it most improbable that an initially ionized molecule of any ordinary gas (ionized by x-rays, radioactive radiations or ultraviolet light) has retained the charge in the 10^7 or more impacts with neutral molecules which occur in the ordinary periods of mobility measurement. Thus it is clear that in studying mobilities even under the most favorable conditions we have been completely in the dark as to the nature of the charged carrier, which for example, in H_2 may be a large organic molecule of low ionizing potential that may have in its many impacts annexed several other propitious companions. That such must in reality be the case in probably all previous mobility work follows at once from the fact that the collision frequency of ions in a gas is of the order of 10^9 collisions per second, and that even in the purest gases a purity of one part in 10^6 is exceptional at atmospheric pressure, (usually it is more nearly one part in 10^4 or 10^5). Thus the ion in one-tenth of a second can encounter from 100 to 10^4 molecules of an active nature with which change of charge or attachment may take place.

It is clear that what is needed in an analysis of the ultimate nature of the ions and their behavior as well as a test of our mobility theories is an investigation of ionic mobilities with *ions of a known nature*. Thus the measurements needed must be of such a sort that these ions can retain their charge, and at the same time the mobilities of such ions must be studied over intervals of time such that in a reasonably pure gas their chance of attachment is small. Now the positive ions of the alkali metals have ionization potentials far below those of any common gaseous molecules or organic impurities. They

[4] L. B. Loeb, Jour. Franklin Inst. **201,** 279 (1926). Gives summary of literature.

should thus be able to maintain their identity as the positively charged nucleus of positively charged aggregates indefinitely. Such ions are easily obtained in quantity from the Kunsman catalysts at a reasonably low temperature. To insure the fact that the ions have not picked up a molecule of impurity or formed a cluster such ions must have their mobilities measured in time intervals of the order of 10^{-4} or 10^{-5} seconds for gases which have a purity of better than one part in ten thousand. It was therefore planned to study mobilities of Na^+ ions from a Kunsman source using a high frequency alternating potential of square wave form and an alternating current method. The square wave form was desired so as to make the results as definite as possible. The gas initially chosen was H_2 since this gas is one of the easiest to purify of more reactive impurities and since the gas is least injurious for the Kunsman source.

The adaptability of the Kunsman sources to ion mobility work in N_2 and H_2 even up to atmospheric pressure was clearly shown at the outset of this work and the sodium catalyst kindly sent by Dr. Kunsman proved admirable for these experiments. The square wave form oscillator of a type originally designed by J. L. Bowman[5] and initially set up by J. E. McVay in this laboratory did not prove so satisfactory. Preliminary results obtained with such an oscillator were published in a letter to the Editor,[6] and are in fact substantially confirmed by later work (from $T=10^{-4}$ to 3×10^{-5}, $k=17$, $T=5\times10^{-4}$ to 10^{-4}, $k=12.6$, and above 5×10^{-4}, 10 or less). However, it is much to be doubted if any reliance can be placed on results obtained by this method as a more critical investigation has shown. Recourse was therefore had to a sinusoidal wave form which was adapted to this problem in several modifications. All results were in general agreement, the later techniques, however, being the only ones in which much faith could be placed. It fortunately turned out that the measurements in N_2 could largely be obtained by a high frequency commutator with far more satisfactory results.

Experimental Equipment and Procedure

Source

It was essential to have an equipotential Kunsman source which could be raised to such a temperature as to give a good ion emission (450° to 750°C) which at the same time did not give off too many vapors. A great deal of difficulty was encountered until a steatite stone insulating material called "Lavite" was found. This material when raw can be turned on a lathe threaded and drilled. It can then be baked to 1000°C for twenty-four hours and becomes an exceedingly hard material with relatively little shrinkage. With this as a base the heating element, a platinum spiral of 0.1 mm wire, was mounted between thin quartz plates, 0.1 mm thick and a thin sheet of platinum foil with catalyst already burnt on and reduced, was screwed over the open end of the mounting by the small brass nut. The assemblage is shown in Fig. 1 in cross section and is self explanatory. The diameter of the

[5] J. L. Bowman, Phys. Rev. **24,** 31 (1924).
[6] L. B. Loeb, Phys. Rev. **36,** 152 (1930).

open face of the catalyst was about 8 mm. The leads of heavy nickel from the platinum and from the coil were secured to the top of the lavite plug by brass clamps not shown. The whole was mounted in the heavy brass upper plate of the chamber and insulated from it by a quartz centering ring. The coil was heated by a storage battery and controlled by a rheostat, these elements being housed in grounded conducting cases to avoid electrostatic effects. This arrangement had a capacity, with the battery in the circuit, of some 660 cm as shown by direct measurement. Such a capacity when thrown into a tuned circuit above 5000 cycles during measurement could throw the circuit out of resonance by a serious amount. This limited the scope of the measurements considerably. The currents required for heating the source to a proper temperature varied with the gas and slightly with the pressure of the gas. Currents from 5.8 to 6.2 amperes were required in H_2 for pressures from 1 cm H_2 to 76 cm. In N_2 currents of the order of 4.2 to 4.5 amperes were required for the

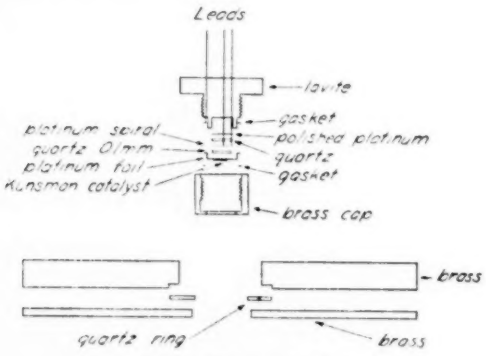

Fig. 1. Heater design.

same pressure range. The source was mounted as the upper plate of a parallel plate system (plate distance used being of the order of 1.6 cm with upper and lower plates 8 cm in diameter), the lower plate being connected with amber insulated leads to the electrometer circuit. The assemblage could be mounted, the plates rendered parallel and plate distance measured by cathetometer before placing in the chamber. The chamber was cleaned by the writer's standard technique[7] except that a concentrated $H_2SO_4 - K_2Cr_2O_7$ cleaning solution replaced the acids previously used. The gases used were tank H_2 or N_2 which were passed over the wrtier's standard purifying train of red hot Cu powder, powdered NaOH, $CaCl_2$, P_2O_5 and liquid air. In essence the gases were therefore of the best purity obtainable with the metal chambers used and the results at lower frequencies were comparable with previous results of the writer[9] in H_2.

The oscillators

A distrust of the wave form obtained from the Bowman oscillator as developed by McVay led the writer, on resuming the work in the autumn of

[7] L. B. Loeb and A. M. Cravath, Jour. Opt. Soc. Am. and Rev. Sci. Inst. **16,** 192 (1928).
[9] L. B. Loeb, Proc. Nat. Acad. Sci., **12,** 617, 677 (1926).

1930, to a critical study of the method. In the earlier work on the oscillator the wave form had been determined by the Lissajou figure obtained in a cathode-ray tube oscillograph, the potential to be studied being placed on the one pair of plates, while oscillations of the same frequency and proper amplitude picked up from the oscillating system itself and so changed in phase by capacity as to be 90° out of phase with the oscillation to be studied were placed on the other pair of plates. The behavior of the Lissajou figures as capacity was varied on the latter system convinced the writer that a rectangular figure obtained in this fashion was not as significant as desired relative to the true wave form of the oscillations. Recourse was then had to the Beddell-Reich oscilloscope for a further study. This instrument proved to be fairly useful for indicating the wave form in the region from 1000 to 5000 cycles. A great deal of trouble was encountered with the stabilization above

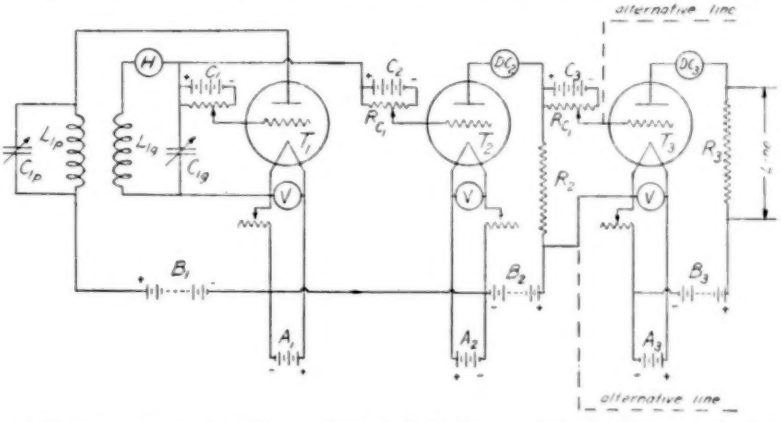

Fig. 2. Square wave form oscillator: T_1 and T_2 Radiotron UX 210 tubes. T_3 Radiotron UX 250 tubes. L_{1p} and L_{1g} Pacent honeycomb coils of appropriate inductance from 1500 turns to 500 turns. C_{1p} and C_{1g} either small radio condensers or glass condensers from 0.01 to 0.001 microfarad with 2 variable air condensers in parallel. $B_1 = 300$ volts. $B_2 = 300$ volts. $B_3 = 200$–400 volts. $C_1 = 27$ volts. $C_2 = 15$ to 40 volts as conditions altered. R_2 and $R_3 = 10{,}000$ ohms. $C_3 = 10$–30 volts, usually small.

such frequencies since the stabilizing oscillations leaked through into the timing circuit and the time axis ceased to be linear. Another difficulty lay in the fact that except for the lower frequencies while the instrument served for a good visual study any tracing or record of the wave form for measurement was impossible due to lack of adequate stabilization without distortion with the power available.* However, with its use the circuit depicted in Fig. 2 was developed. In some cases the circuit was applied directly to the measuring chamber as shown by the connections in Fig. 3, or the same connections were made across R_2 on the first stage amplifier. The detailed description of this system will not be given, the figures and the data in the legend being sufficient. In working out this system several months were spent and a large variety of

* Recently the writer has seen a very successful type of cathode ray oscillograph with a beautiful linear time axis up to 10^5 or more cycles built on the basis of improved argon rectifiers developed by Drs. Lauriston Marshall and Van Voorhis at Princeton. With these tubes it is possible that much progress can be made.

circuits tried. It will be noted that the potential of the oscillations as appled to the circuit varied from 0 to $-V_S$, while by means of a va.iable contact on a battery the 0 value was raised to a potential V_R above ground. V_S was always greater than $2V_R$ to keep ions from "working" across the plates. In the earlier work the ground was on the negative side and V_R was a retarding potential, the driving potential on the ions being $V_S - V_R$ and V_R being greater than $V_S - V_R$. Both methods worked equally well, the former being more convenient. A large number of measurements were made with this method in H_2. These measurements served to show that in general the ionic velocity was proportional to the field strength. The results were, however, inexplicably capricious until an oscillographic study revealed that the irregular behavior was caused by the fact that for each frequency used the value of the bias

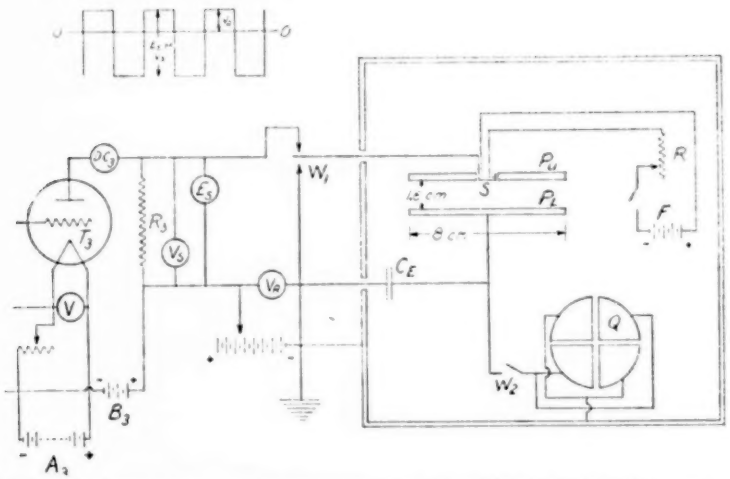

Fig. 3. Electrical arrangements for measurement: V_S = Kelvin multicellular voltmeter with capacity in series range 40–170 volts. E_S electrometer heterostatically connected for square waves. V_R = Hartmann-Brown d.c. voltmeter. W_1 = Switch for grounding or connecting ion sources to oscillations. S = source. P_U and P_L upper and lower plates. R = filament resistance, F filament battery electrostatically screened. C_E = grounding condenser to plate system, capacity 300 cm. W_2 = electrometer switch.

potential $C_2R_{C_1}$ was quite critical in that over-biassing made the upper half of the wave narrower than the lower half or vice versa. Since the mobility is computed for a uniform square wave by the equation $k = Nd^2/V_R$, where N is the number of half-cycles per second, (assumed equal), an inequality in the duration of the half-cycle results in a serious error. By working at the lower frequencies the oscilloscope showed when approximate equality of the upper and lower halves of the cycle was reached. Under these conditions the oscillations led to consistent values of the mobility. At higher frequencies this oscilloscopic study ceased to be possible and the square waves were abandoned. As this method of measuring mobilities indicated proportionality between ion velocity and field strength the square wave form was not considered essential and recourse was had to the more certain and accurate sinusoidal oscillations.

Sinusoidal oscillations of sufficient accuracy could be taken directly from the oscillator as in Fig. 4. In this case the amplitude of the oscillations cannot be varied without altering the frequency. While such oscillations may not be pure sinusoidal waves they have the advantage of steadiness and charging up the capacity of the ion chamber without throwing the system out of resonance as the ion chamber is cut in or out. This method was therefore the only possible one to use for the highest frequencies with existing capacities. Instead of varying the amplitude of the oscillations,the ground bias was varied by the bias battery V_R (Fig. 4) in such a fashion that that the field acting on the ions in each positive half-cycle could be increased or decreased. Since the distance the ions move depends on the area under the curve of the positive loop of the cycle multiplied by the mobility and divided by the plate distance,

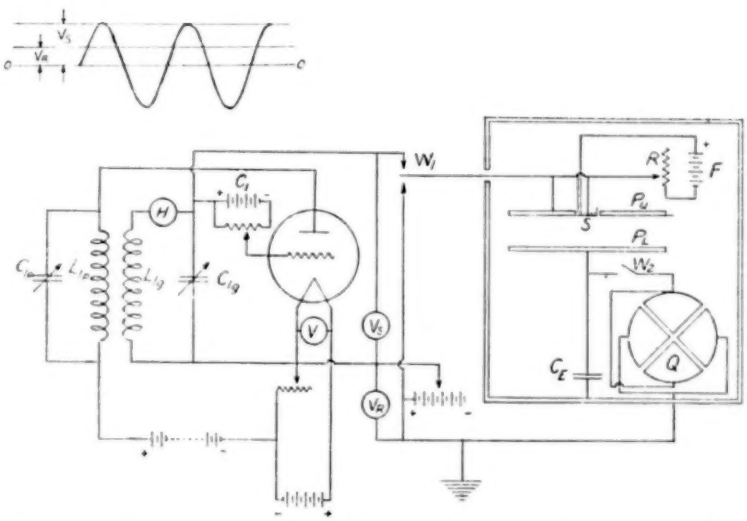

Fig. 4. Oscillator directly connected to measuring chamber, V_R variable. Symbols are similar to those in Fig. 2 and 3.

and as this area is varied by changing the bias V_R, this bias can be changed until the ions just cease to cross for the value of the product time times field strength contained under the positive loop as biassed.

Call V_S the root mean square value of the alternating sinusoidal potential call the mobility of the ion k, and let a and b be the intercepts of the sine curve with the line due to the bias potential V_R, then if T be the period of oscillation and d the plate distance, the ions will cross if

$$d = (2)^{1/2}\frac{V_S}{d}\,k\int_{a/\omega}^{b/\omega}\sin\omega t dt - \int_{a/\omega}^{b/\omega} k\frac{V_R}{d}\,dt$$

If $\theta = \omega t$, $dt = d\theta/\omega$ and $\omega = 2\pi/T$ we have

$$\frac{2\pi d^2}{(2)^{1/2}V_S T k} = \int_a^b \sin\theta d\theta - \frac{V_R}{(2)^{1/2}\,V_S}\int_a^b d\theta.$$

Calling $V_R/(2)^{1/2}V_S = A$ integration gives

$$\frac{2\pi d^2}{(2)^{1/2}kTV_S} = 2\cos(\sin^{-1}A) - A[\pi - 2\sin^{-1}]A$$

The right hand member of the equation, designated by ϵ, may be calculated as a function of A and plotted. Then

$$k = \frac{(2)^{1/2}\pi d^2}{V_S T\epsilon} = \frac{(2)^{1/2}\pi N d^2}{\epsilon V_S},$$

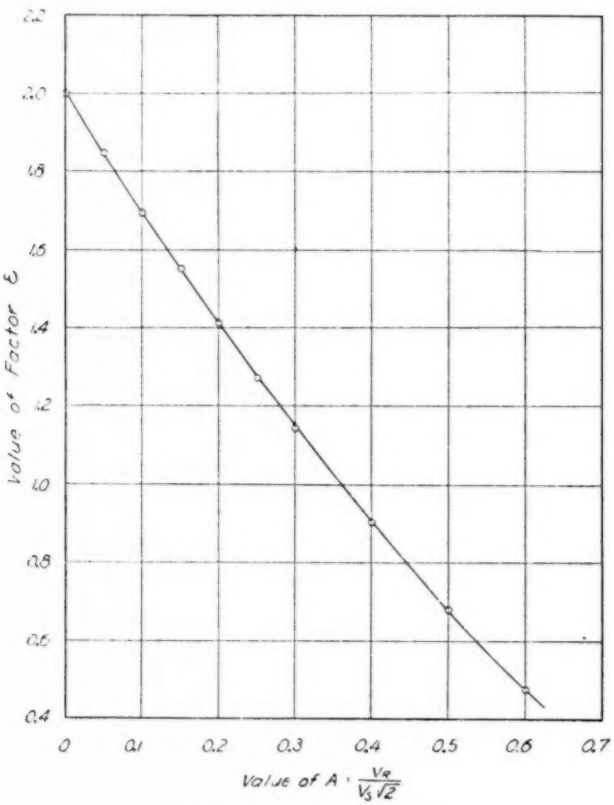

Fig. 5. Curve of ϵ against A.

where N is the frequency and ϵ is taken from the curve of Fig. 5 for the value of A corresponding to the ratio $V_{R_0}/(2)^{1/2}V_S = A$ obtained from the observed static voltmeter reading and the value of V_{R_0} for which the ions just cease to cross the distance d between the plates. A measurement using the oscillator directly is then achieved by keeping V_S constant and raising V_R until the ion current stops. If the oscillations are not accurately sinusoidal it is best not to have $V_{R_0}/(2)^{1/2}V_S$ too large as this accentuates the errors, which are most effective in changing the peak of the curve. Certain results obtained in the H_2 measurements shown in figure 12 are marked with question marks for just this reason.

To be more certain of the wave form other measurements were made with the oscillator and the first stage amplifier generating current in a coil L_2 coupled to a coil L_3 of the resonance circuit $L_3C_{R3}H$ in Fig. 6. The current in L_3 was varied by varying the potential B_2 in the amplifier. Hence the potential could be changed in $L_3C_{R3}H$ without changing the frequency. $L_3C_{R3}H$ was tuned with V_R and the plate system in the circuit (i.e. under the conditions of actual measurement).

With this arrangement either the potential across the static voltmeter system $C_V V_S$ could be kept constant and V_R changed to V_{R0} at which ions ceased to cross, or V_R could be set at 20–30 volts and the potential across $C_V V_S$ varied by varying the current in R_2 by means of the potential of the battery B_2. This latter method while by all odds the surest was most tedious

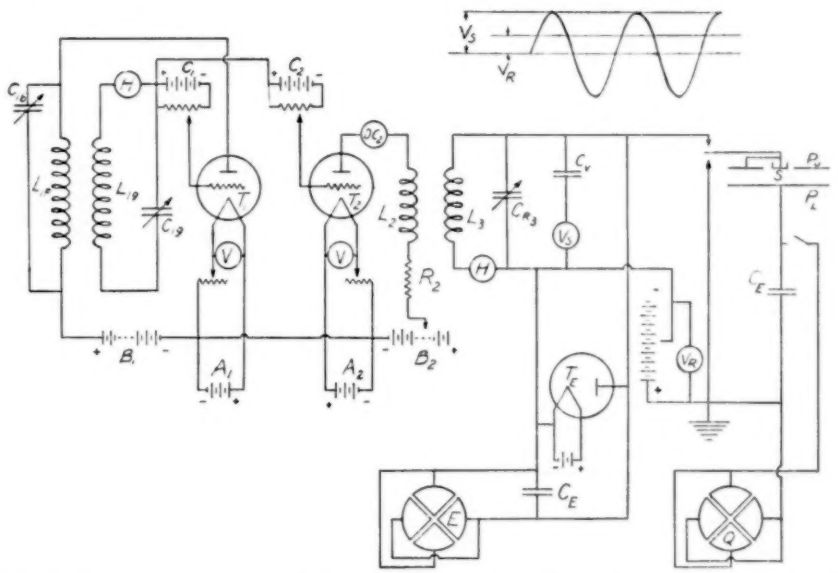

Fig. 6. Arrangement for tuned sinusoidal oscillations. L_2 = inductance in amplifier circuit coupled to L_3 in resonance circuit. C_{R3} = variable condenser in resonance circuit to tune it to the oscillating circuit. In general C_{R3} was kept as small as possible relative to L_3. E, T_E and C_E = electrometer rectifying circuit to measure the peak voltage of the oscillations. C_E = 0.002 microfarads. T_E = radiotron UX 299 tube.

and time consuming due to the slow period and low damping of the Kelvin multicellular static voltmeter used. An electrometer with rectifier used heterostatically served as a convenient voltmeter for rapid adjustment of the potential, but was not reliable within 1-2 volts in 100 for some unknown reason, generally reading a bit low. The slower method of measurement served to heat the gas unnecessarily and also to increase contamination.

Finally it was found that many of the measurements could be made by a square wave form commutator having 60 segments and capable of being rotated at 3600 r.p.m. With two auxiliary commutators and a series of gear ratios frequencies of alternation from about 5 per second to 3600 alternations per second of quite definitely square wave form could be obtained. The

measurements with commutator and oscillator where they overlapped agreed quite satisfactorily.

The frequencies of oscillation were measured for the oscillator from 500 to 10,000 cycles by means of a beat frequency oscillator made by the General Radio Company of Cambridge, Mass., and above 10,000 cycles by a precision wave meter of the same firm.

Measurements

The general procedure of measurement was to evacuate the ionization chamber to from 3 to 5 microns and then run in fresh H_2 or N_2 over hot cop-

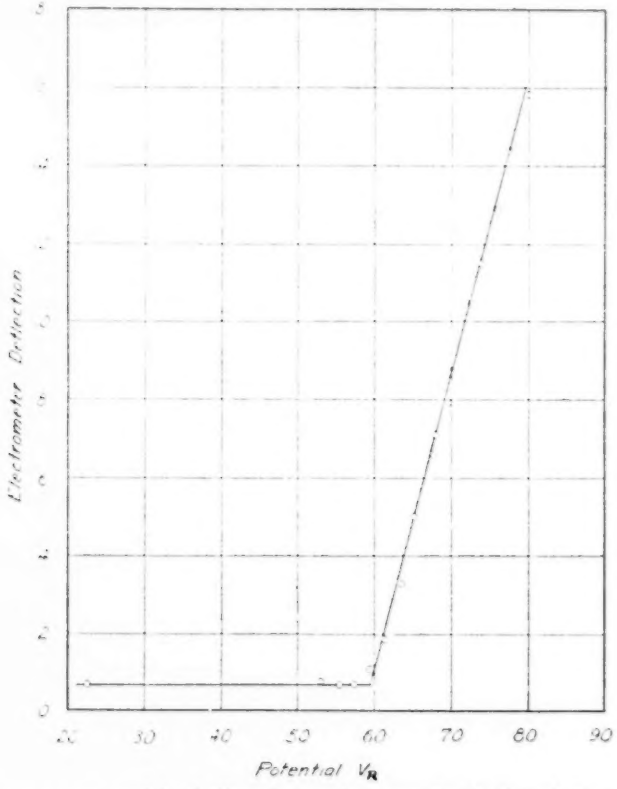

Fig. 7 Square waves, positive half-cycle less than negative half-cycle in ratio of about 1 to 1.3, using first stage and amplifier only. Pressure = 1.60 cm. Frequency = 6900 cycles. Mobility = 12.1. Hydrogen gas.

per, NaOH, $CaCl_2$, P_2O_5 and liquid air in the writer's standard purifying train.[9] The pressure was then measured on a standard barometer as well as on the McLeod gauge if low, and the filament current turned on at a specified time. The oscillator or commutator had been set at a given frequency and steadied down, the frequency being measured before and after the run. To make a reading the alternating potential was measured with the ion chamber in the circuit. The chamber was disconnected from the alternating source, electrometer disconnected and the alternations again applied to the chamber across the plates and through the condenser C_E. After 10 seconds the oscilla-

tions were cut off, the ground removed from the electrometer and electrometer connected to the collecting plate for 15 seconds (to control a small zero current due to space charge of positive ions) contact broken to the electrometer and the electrometer deflection noted. The sensitivity of the electrometer was 1500 mm per volt and the capacity of the electrometer system was some 350 cm. A series of values of currents were obtained for different values of V_S or V_R as the case might be, going up and down in potential around the region of the break point of the mobility curve. The temperature of the source usually increased with time, and this rendered the emission of Na^+ ions variable in time. As at rule, however, the current and temperature of the source steaded down after 20 minutes and reliable readings could be obtained over intervals of 20 minutes. It was undesirable to heat the gas any longer than necessary to

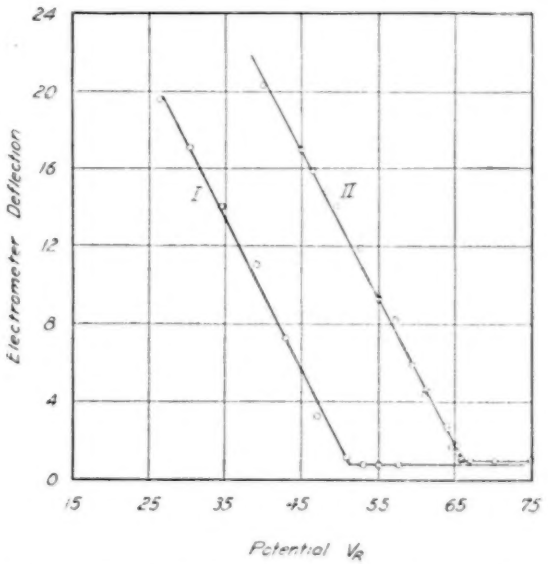

Fig. 8. Sinusoidal oscillations in hydrogen gas. Curve I from oscillator direct, varying retard bias potential V_R. Pressure = 0.51 cm. Frequency = 38,000 cycles. $V_S = 124$ volts, $V_{R_0} = 51.3$ volts. $\epsilon = 1.117$. $K = 19.7$ cm/sec per volt/cm. Curve II from tuned circuit activated by current from primary amplifier, varying retard bias potential V_R. Pressure = 1.61 cm. Frequency = 20,250 cycles. $V_S = 172.5$ volts. $V_{R_0} = 66$ volts. $\epsilon = 1.22$. $K = 22.9$ cm/sec per volt/cm.

obtain a curve on account of the temperature corrections, and also to avoid undue contamination of the gas. The measurements in general rarely lasted over 40 minutes. Occasionally two runs were made on the same sample of gas, but in most cases gas used for more than 1 hour was replaced by freshly purified gas. Pressures were read again at the end of a run and the change in pressure gave a good indication of the rise in temperature of the gas as a whole. In N_2 it was 8° in 30 minutes at 65 cm and in H_2 it was 10° in 40 minutes at the same pressure.

Typical current-potential curves obtained by the various methods outlined above are shown in Figs. 7, 8, 9 and 10 for which details are given in the legend. Fig. 7 was taken with the square wave form oscillator using only the

first stage amplifier. The frequency was 6900 cycles but the positive half-cycle was distinctly narrower than the negative half-cycle as viewed in the oscilloscope. Hence the calculated mobility was 12.1. If the mobility be increased by the estimated ratio of the width of the upper and lower half-cycles as seen in the fleeting glimpses in the oscilloscope the mobility should have been 1.3×12.1 or about 15.7 cm/sec, a value more or less in agreement with other values for the intermediate ion. The current potential curve it is seeh is nearly linear and the break point is sharply defined. Fig. 8 has two curves both obtained using sinusoidal oscillations of constant amplitude V_s

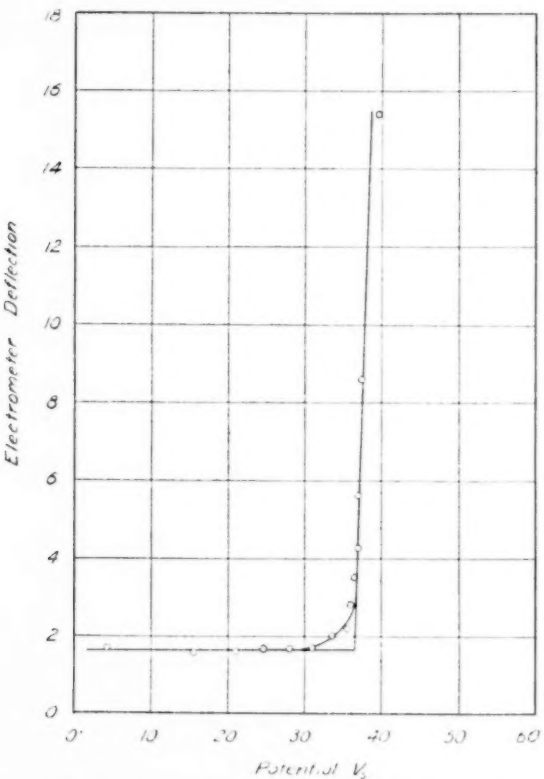

Fig. 9. Square waves from commutator in nitrogen with 10 percent hydrogen. Six segment commutator, gear ratio 1:1. Pressure = 2.03. cm. Frequency = 900 cycles/sec. Mobility = 3.58 cm/sec per volt/cm.

in which the bias potential V_R was varied. Curve I used the direct sinusoidal oscillations from the oscillator while curve II used the oscillations in the resonance circuit. The break points are again sharp and these ions are the very fastest ions in H_2 (i.e. those that have not had an opportunity to age). Figs. 9 and 10 show curves obtained with a square wave form commutator. Fig. 9 is for N_2+10 percent H_2 showing the intermediate ion, while Fig. 10 is for H_2 at 61 cm pressure. Both these indicate asymptotic feet due to transformation of ions while in the measuring field, those in H_2 being particularly pronounced. To estimate the intercepts in the curves of Figs. 7 and 8 is simple.

In the case of Figs. 9 and 10 the estimate of an extrapolated break point in the curves for the linear portions of the curves would seem to be the only proper procedure.

Interpretation of current-potential curves

The extrapolation raises the question of just what such curves signify, and what the break point means. With radioactive or other ion sources where saturation currents are easily obtained the shape of the mobility curve relative to the saturation curve enables a great deal to be determined about the ionic constituents present.[10] In the present case with a thermionic ion source

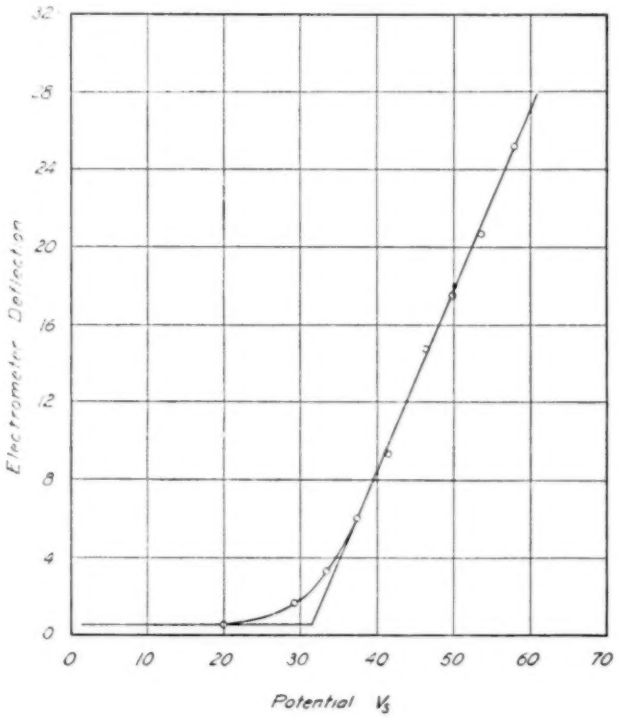

Fig. 10. Square waves from commutator in hydrogen. Pressure = 61.42 cm. Frequency = 78 cycles/sec. Mobility = 8.6 cm/sec per volt/cm, the value for normal ions.

such a study was impossible. The curves give the average velocities of those ion groups which *first* cross the electrode distance d. If ions of one mobility only are present then since the geometry of the system is quite regular the ions liberated first in the phase should get across at a very definite potential and a nearly linear increase of current should follow in the early portion of the curve. If two ions of widely different mobilities are present one might anticipate precisely the type of curves and transitions which appear for negative ions in air from 15 to 5 cm pressure using a photoelectric source.[11] The resolving power of the present method is, however, relatively low and differences

[10] L. B. Loeb, Jour. Franklin Inst. **196,** 537, 771 (1923).

[11] L. B. Loeb, Phys. Rev. **17,** 89 (1921); Jour. Franklin Inst. **197,** 45 (1923).

of 30 percent in mobility would with the positive ion sources used never be clearly resolved as two separate groups. Where ions of two mobilities are present, one of which changes to the other, in a time interval compariable with the time of crossing, the statistical nature of the transformation will result in a sort of hybrid current-potential curve representing the averge velocities of the ions with an asymptotic foot and an intercept for the lower nearly straight portion of the curve giving an intermediate value of the mobility. Such curves are readily deduced from theory for a statistical type of attachment.[11] The end of the asymptotic portion may or may not represent the fastest ion present, as it depends only on the sensitivity of the instruments and how nearly complete the transformation is in the time of measurement (i.e. on the number of ions crossing without transformation). Hence, assuming that in general only one type of ion is relatively stable after a given number of impacts in a gas due to impurities present; and thus that the time of transition is relatively short, one would expect the intercepts of the curves to be sharp where single stable groups are concerned giving constant mobilities, but asymptotic in time intervals covering the transformation process, and with the uncertainty of the saturation value giving, as extrapolated above, intermediate values of the mobility.

Where there may be several successive transformations with but a small difference in mobility of the ions formed the method of study used should yield a continuous series of mobilities as the time of observation, and hence the transformation, progresses. These should eventually approach some limiting stable value, namely that for the so-called normal ions in the gas. The method is thus capable of giving mobilities for the relatively stable ions, and indicating a succession of changes with time occurring where individual average mobilities are numerous in the regions where transformations occur, or where the ions are *not* clearly differentiated. It will be noted that in fact the results obtained are such as to be in complete accord with this discussion, a circumstances which will be discussed later in more detail.

Temperature correction

Before the final results obtained and their interpretation can be discussed, a final correction to be applied must be discussed. The mobility is measured in a chamber at constant pressure. As the mobility in the ordinary ranges of temperature is at constant density little affected by temperature, little account need be taken of the changes in temperature of the gas as a whole. However, the source of ions is at a temperature ranging from a very dull red heat to a rather bright cherry red (i.e. from about 500° to 750°C) while the lower plate is at the temperature of the heavy brass case of the ionization chamber. The upper plate which is electrically equipotential with the hot source may attain some 200°C towards the end of a measurement. Thus, a temperature gradient exists in the 1.6 cm of gas in the gap where the mobility is measured, which is a maximum in precisely the region where the ions are being studied. As the pressure is constant the gas density in the ion path varies inversely as the absolute temperature, and hence the mobility obtained

is higher in the ratio of the average absolute temperature than it would be computed from the initial conditions in the chamber. All mobilities must therefore be reduced in proportion to the ratio of initial temperature at which the pressure was measured to the average temperature in the gas path. This correction was exceedingly difficult to obtain inasmuch as experimental conditions preclude computations, though the energy input into the heating element for N_2 and H_2 enabled the relative conduction by the gas and by the metal to be determined. One estimate of the average temperature in the gap was achieved by measuring the mobility of the ions at atmospheric pressures with relatively impure gases and comparing the observed (assumed normal) mobility with those for normal ions in the gases. This method was used as an ultimate check on the temperature correction more directly determined. After mobilities had been measured the chamber was opened and six copper-constantan silver soldered thermocouples of No. 38 wire mounted on a thin mica leaf were placed along the axis of the upper and lower plates between them. The distances of the couples from the source were accurately measured by cathetometer and temperatures were measured in the gap as a function of time and at different gas pressures, with varying currents in the filament, corresponding to the currents actually used in measurement.

The temperature study showed that the temperatures given by the couples rose to a nearly steady condition within 5 minutes after the source was brought to temperature, it being customary gradually to raise the filament up to full current. Thereafter the temperatures changed relatively slowly at most 40°C an hour at the couple 1 mm from the source and 25° an hour at the lower plate. Changes in pressure made relatively little change in the couple temperatures, the temperatures being slightly lower for the same source temperature at higher pressures. The temperatures read on the couples for H_2 are shown plotted against distance from the source for the various couples in Fig. 11 in curve I. This curve is far from a linear gradient such as a convectionless gas should show under the conditions of 8 cm pressure with 1.6 cm plate distance, the upper plate being heated. The interpretation that the radiation from the source raised the gas-cooled couples above the gas temperature is obvious. Since the couples cool more rapidly than the gas by metallic conduction and radiation an estimate of the gas temperatures was made as follows. The filament was suddenly cut out and a series of timed readings of the temperatures in the gap were made. The measurements revealed that in less than 3 minutes in H_2 the couples had dropped to a linear gradient and thereupon the whole curve gradually fell at a somewhat more rapid rate than its rise after the first five minutes after turning on the current. The linear curve in H_2 is shown in Fig. 11, curve II, and gives an average gap temperature of 80°C, the room temperature being 22°C. In N_2 the temperatures were not quite as high, and the time to reach a linear gradient for the couples was longer. The average temperature was slightly lower for N_2 in all cases. The gradients were lower at pressures above 20 cm while the heating current required to give the same temperatures of the source was higher. This indicated some convection in the gas at these pressures. In view of the rela-

tively small variation in the average temperatures observed it was decided to correct the H_2 mobilities for 80° (or reduce them by a factor of 295/375 to give the true values), while for N_2 the average temperature of 55° was used and the correction factor was 295/350. The values yielded by these correction factors at atmospheric pressure gave mobilities in accord with the normal absolute mobilities to be expected of gases from this method, to wit about 8.6 cm/sec per volt/cm for H_2 and 1.6 cm/sec per volt/cm for N_2 within the certainty on these measurements. In any case it was clear that the above temperature correction, while if in error might change the absolute values by

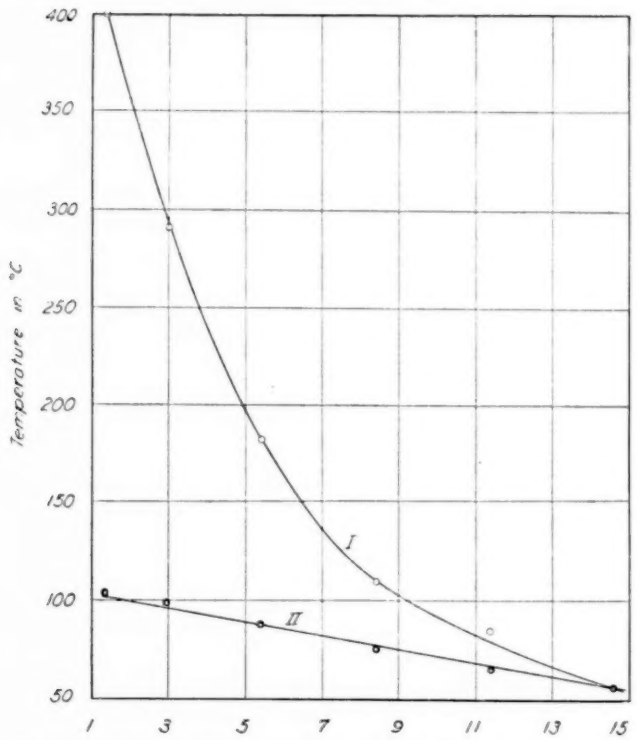

Fig. 11. Temperature gradient by thermocouples in H_2. Pressure 7 cm. I. Filament on. II. Filament off 40–60 seconds later.

possibly 10 percent, it would not seriously impair the value of the otherwise striking results.

Other than the density correction above, which also entailed a correction of the mobility for the initial gas pressure, no other correction was needed to deduce the mobility constant for the ions (i.e., the reduced mobility). The use of the inverse density law (law of Langevin) is justified in this case by wide experience and the recent results of Tyndall and Powell.[21] It was also verified in many of the present measurements. A very minute correction could have been made for the fall of potential across the auxiliary condenser C_E, it was however too small to include compared to the other uncertainties.

In conclusion therefore it may be stated that the results obtained measure

a sort of average mobility of Na^+ ions in H_2 and N_2 for the faster ions present at any time. Where only one stable class of ions is present at the time we obtain absolute values of the mobility by this method good to better than 10 percent.

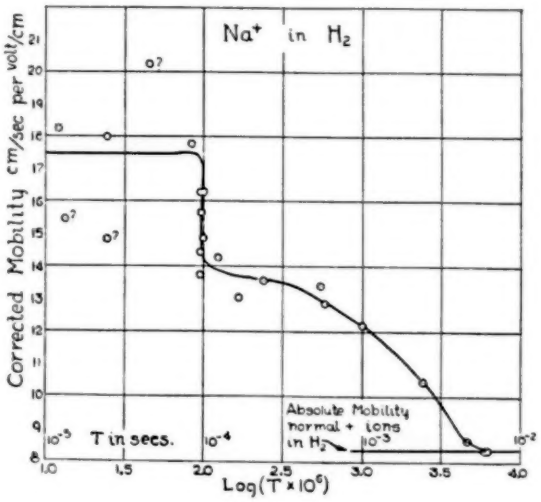

Fig. 12.

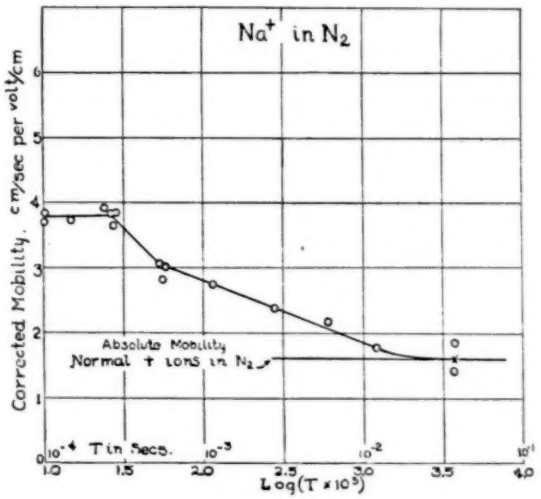

Fig. 13.

RESULTS

The results for the two gases H_2 and N_2 may be summarized by the curves shown for H_2 and N_2 respectively in Figs. 12 and 13. In these figures the reduced mobility constants are plotted against the logarithm to the base 10 of the time necessary for the ions to cross, i.e., the time of a square wave form oscillation or the half period of a sinusoidal oscillation. The two times are not exactly equivalent, but for the present purposes they suffice. The plots

on this scale have the effect of telescoping the results obtained over slightly different times together and accentuate the abruptness of the transitions. It is seen that both of the sets of curves agree in general outline. Within 10^{-4} seconds for H_2 and 5×10^{-4} seconds for N_2 or less, the ions have very high mobilities, around 17.5 cm/sec per volt/cm in H_2 and 3.7 cm/sec per volt/cm in N_2. At the end of these time intervals there is a more or less abrupt change in mobility to a stable ion of mobility 13.5 cm/sec in H_2 and about 3 cm/sec in N_2. The stability of the N_2 ion is not as clearly indicated as in the case of the H_2 ion owing to the impossibility of observing the mobility at intermediate time intervals with the commutator. After these time intervals both gases show a more gradual change in mobility with time, reaching eventually the so called normal value of the mobility usually encountered in these gases. This normal value is *not that usually given but is the real absolute standard of mobility for normal positive ions in these gases*, which have been indicated by Loeb,[10] Tyndall[12] and Grindley, and lately confirmed by Bradbury.[13] The abrupt change in mobility in H_2 is perhaps exaggerated by the action of impurity and possible variations in the ion path temperature. Different degrees of purity of the gas (time of sojourn or heating in the chamber, etc.) at this point had a marked effect on the mobility. On either side of this point, however, the purity made relatively little difference. The points with question marks attached to them were those taken with conditions that made absolute values doubtful, hence the value chosen for the mobility of the fastest ion in H_2 may be in error by as much as 5 or possibly 10 percent.

The facts are, however, quite definite that there are at least 3 different mobilities for a charged atom ion Na^+ in H_2 and probably as many in N_2. The first and fastest ions exist for lengths of time of 10^{-4} seconds in H_2 and 2×10^{-4} seconds in N_2. The second class of ions exist from 10^{-4} to 10^{-3} seconds in H_2, and possibly from 2×10^{-4} to 10^{-3} seconds in N_2, and the last class are the so-called normal ions in H_2 and N_2 measured above 10^{-2} seconds in relatively pure H_2 and above 10^{-2} to 10^{-1} seconds in relatively pure N_2.

Discussion of Results

From the fact that the Na^+ ion will retain its charge the following conclusion can be drawn concerning the first and fastest ion. The ions make on the order of 10^9 collisions with molecules per second. Granted a possible gaseous purity of one part in 10^4 molecules of these gases (a not unreasonable assumption) one can estimate that in H_2 in 10^{-4} seconds the ions can on the average meet but 10 or possibly less molecules of impurity. If on the average one in two collisions with such impurity molecules causes attachment of such molecules to the ion, then at the end of 10^{-4} seconds a goodly share of the Na^+ ions will have added one molecule. That the molecules attaching to the Na^+ ion to decrease its mobility must be impurity and not N_2 or H_2 molecules follows at once from the 10^5 impacts needed to attach and from the mixture work.[1] The sharpness of the drop also indicates that the process is probably

[12] Tyndall and Grindley, Proc. Roy. Soc. **A110,** 346 (1926); Phil. Mag. **48**,711 (1924).
[13] N. E. Bradbury, Phys. Rev. **37,** 1311 (1931).

the addition of a single molecule. Since we are measuring the fastest ions that cross in appreciably numbers, the downward parts of the curves of Figs. 12 and 13 represent an interval in which most of the ions have attached impurities. In N_2 the conditions are analogous, there being possibly less impurity than in H_2. What the impurity is one cannot say, but the probable contamination in these cases would most likely be water vapor, probably driven out from the heating element by the heating. Since the values assumed above seem reasonable, one may conclude that the chance of the faster ions in H_2 themselves being complex is unlikely. One may thus assume with considerable assurance that the ion of mobility of 17.5 cm/sec in H_2 represents the mobility of the Na^+ atom in ion in H_2. In N_2 the frequency was not pushed beyond 10^4 cycles and it may be that the Na^+ ion in pure N_2 has a still higher mobility than the value of 3.8 cm/sec noted. Further work is in progress to determine this. The significance of the actual values will later be discussed in connection with ion theories.

The second class of ion in both gases, then, as time goes on appears to alter its mobility in such a fashion that the separate steps are not clearly resolved. The behavior could be taken to indicate the formation of several intermediate stages of the clustering process, in which separate ions do not differ greatly in mobility (i.e., the addition of 1, 2 and 3 more molecules of some impurity to the first stage addition product), finally reaching some rather stable limiting size. Such an explanation would infer a rather complicated cluster ion of 4 or more molecules. On the other hand the subsequent steps might as simply be explained by assuming that the ions later pick up all sorts of molecules of heterogeneous character (some hydrocarbons of assorted character, etc.) which are present as still rarer impurities. Thus in this region of change the ions are quite heterogeneous in average mobility and the mobilities observed as time passes take on all sorts of progressively lower intermediate values. Eventually in some 10^{-2} seconds all ions have had an opportunity of rearranging themselves in harmony with their environment so that they are more or less uniform in structure, most ions having eventually only added one or two molecules of a relatively rare impurity, but one having a selectively high electrochemical affinity for a positive charge and giving the most stable ion. Such behavior would yield what we term normal ions, which have a more or less uniform mobility. The two processes outlined would then lead to a normal ion of nearly unique mobility, either by adding so many molecules that in more than 10^{-2} seconds the average constitution is the same (a molecule more or less little changing the ionic mobility) or else by interchanging its constitution so frequently that eventually the ions achieve a uniform composition as the addition product of some rarer but more strongly attracted molecules. As to which process is the true one, mobility measurements cannot at present say, though the writer is inclined to favor the latter process.

There is unfortunately not a single method whose resolving power is sufficient to answer the important question which is raised by these experiments as to the uniformity of the mobilities over a relatively large range. Some writ-

ers[14,15] purport to fine separate *classes* of ions of various velocities among normal ions. In no carefully controlled observations by the majority of the observers using the most diverse methods has this conclusion ever been verified. There have, however, been a large number of observations where the width of the velocity spectrum peaks observed in mobility measurements makes the question of a continuous distribution of mobilities within narrow limits among normal ions possible. In this group belong Erkison's,[16] La Porte's,[17] Zeleny's,[18] Van de Graaf's,[19] Tyndall[20] and Grindley's, and Bradbury's[13] observations, which owing to the nature of the methods leave much to be desired as regards resolving power. The recent admirable work of Tyndall and Powell[21] also raises the same question. The writer is inclined to believe that the width of the peaks of the latter are due to the dispersion of the ions through the use of the gauzes whose interpenetrating fields cause just such effects, as the writer[10] has shown. The writer is inclined to believe on the basis of measurements made in air using the simple Rutherford A. C. method on negative ions[10] that the close agreement in shape of the mobility-saturation ratio plotted against field strength, with the theoretical mobility curve based on the assumption of a single ion of definite mobility can only be reconciled with that assumption. Here again the question of resolving power is raised and it may well be that mobilities may be spread over a considerable range. Until this question is settled it is futile to go much further in speculating as to the nature of the second stage in the formation of the normal ion.

If an analogy to the second step in the formation of the ions is to be looked for in previous results it is probable that it might correspond to the change in mobility of positive ions with age observed by Erikson,[2,16] which is most interestingly influenced by water vapor and purity. However, the faster form of the positive ion in this case has a higher mobility than Erikson's and the change in mobility observed in these gases is more gradual. This later difference could be ascribed to the probable greater purity of the gases used (less impurities and hence a longer average transition period) and also to the fact that in this method the faster ions are always measured and hence the faster ions are measured in part in the longer time intervals, while Erikson measures the time for the average ion to transform. In addition the contaminations from ionization in Erikson's measurements were different from those encountered here which could in part account for the difference.

[14] J. J. Nolan, Proc. Roy. Irish Acad. **33,** 9 (1916); **36A,** 74 (1923); Phys. Rev. **24,** 16 (1924); also **25,** 101 (1925); Phil. Mag. **1,** 417 (1926).

[15] Haines, Phil. Mag. **30,** (1915).

[16] Erikson, Phys. Rev. **20,** 117 (1922).

[17] La Porte, Ann. de Physique **8,** 466 (1927).

[18] John Zeleny, Phys. Rev. **31,** 1114 (1928); **34,** 310 (1929); **36,** 35 (1930).

[19] Van de Graaf, Phil. Mag. **6,** 210 (1928).

[20] Tyndall and Grindley, Proc. Roy. Soc. **A110,** 346 (1926).

[21] Tyndall and Powell, Proc. Roy. Soc. **A129,** 162 (1930).

Theorectical Considerations

The fastest Na^+ ions in H_2 and N_2 if correctly interpreted as representing the mobility of the atom ion of sodium in these gases make possible the first real test of the existing mobility equations. Of the various equations developed two perhaps should be drawn on to compare with observations. One of these is the elastic solid ion theory of Langevin[22] which represents a good equation of this type. While questioned by Lenard and Mayer[23] it still furnishes an adequate basis for rough comparison though it may be deficient in details. This theory assumes an ion and molecule, the half of the sum of whose diameters is σ and whose charge does not affect its means free path. Since σ can be determined approximately from the radii of Na^+ ion and H_2

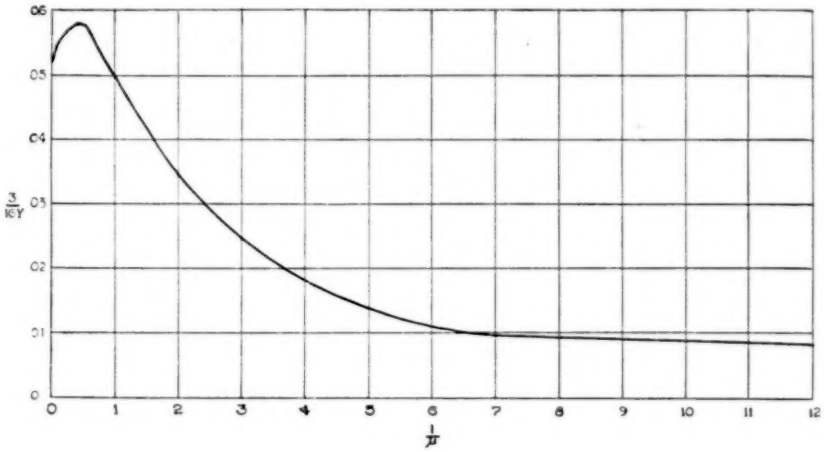

Fig. 14.

and N_2 molecules, as estimated from kinetic theory, the mobility can be easily computed from the Langevin equation that

$$k = 0.815(e/M)(\lambda/C)((M + m)/m)^{1/2}$$

where e is the charge, M the mass of the gas molecules, $\lambda = 1/\pi\sigma^2 N$, C the velocity of thermal agitation of the gas molecules, N = the Loschmidt number, and m is the mass of the ion. The most plausible of all ion mobility equations is, however, the full Langevin[24] equation assuming elastic-solid ions and molecules but including an attractive force between ion and molecule of the form $f = (D-1)e^2/2\pi N\sigma^5$; that is an inverse fifth power law of attraction based on the di-electric polarization of the molecule by the charge on the ion, where D is the dielectric constant of the gas. This has been verified mathematically in recent years by Hasse[25] and again carefully verified on the basis of its assumptions by H. A. Kramers at the writer's request in connection with another problem. The equation reads

[22] P. Langevin, Ann. Chim. Phys. **28,** 317, 495 (1903).
[23] H. F. Mayer, Ann. d. Physik **62,** 358 (1920).
[24] P. Langevin, Ann. Chim. Phys. **8,** 238 (1905).
[25] R. Hasse, Phil. Mag. **1,** 139 (1926).

$$k = \frac{3}{16Y} \frac{0.465}{\frac{\rho}{\rho_0}(D-1)_0 M_0)^{1/2}} \left(\frac{M+m}{m}\right)^{1/2}$$

where $3/16Y$ can be evaluated by the curve of Fig. 14 as a function of $1/\mu$, where μ is

$$\left(\frac{3(D-1)_0 e^2}{4\pi N \sigma^4 M C^2}\right)^{1/2}.$$

ρ and ρ_0 are the densities of the gas at any pressure and temperature and that at N.T.P., $(D-1)_0$ is the value of $D-1$ at N.T.P. and M_0 is the molecular weight of the gas. The relation between $3/16Y$ and $1/\mu$ is given by the curve shown in Fig. 14 and follows from the elastic solid impacts and the ratio of potential and kinetic energies of the ions and molecules. It assumes that the *dielectric polarization follows the inverse fifth power law to distances between centers of ion and molecule comparable with the quantity* σ. It happens that the factor $3/16Y$ for the Na^+ ions in H_2 and N_2 has a value nearly 0.505. In Table I are given the values of the mobilities computed on the two theories and the observed values for the mobilities of Na^+ in H_2, and Na^+ in N_2.

TABLE I.

	Langevin solid elastic	Observed	Langevin inverse fifth power law
Na^+ in H_2	48.7	17.5	10.25
Na^+ in N_2	14.9	3.75	2.72

The observed results it is seen fall in between the theoretical values, being far lower than the neglect of the electrical forces would lead one to expect, and yet larger than results to be expected from a consideration of the usual dielectric forces as well as solid elastic impacts. The conclusions to be drawn are very simple and should have been predicted. It is obvious that the dielectric forces must play some role so that the elastic solid theory falls very wide of its aim. On the other hand, the writer[4,26] has oftentimes pointed out that we have no right to assume that the value of the forces due to dielectric polarization at the point where the forces in this work are most important (i.e. at distances of the order of σ) are the same that one would get for forces of dielectric polarization produced in a weak uniform force field. In other words, when one gets to fields of the order of magnitude of that at 3×10^{-8} cm from a charge of 4.77×10^{-10} e.s.u. which are non-uniform fields of the order of 1.6×10^{8} volts/cm and less over the neutral molecules, the molecules and atoms are so distorted that the ordinary dielectric polarization can no longer be assumed to apply. Hence the law of force assumed, $(D-1)e^2/2\pi Nr^5$, is not strictly applicable in this region. One might venture to guess that under these conditions the forces must increase less rapidly as the distance r between ion

[26] L. B. Loeb, Kinetic Theory of Gases, McGraw-Hill, New York, 1927, p. 477; Phys. Rev. **32**, 81 (1928).

and molecule decreases. The result will be that the computed mobility would be higher than that computed above on the ordinary law of force. These results thus give us for the first time a definite indication of the order of magnitude of the deviations caused by the acknowledged deficiency in our best ion theory. Kramers also pointed out to the writer that the repulsive forces should be treated not as elastic solid forces but as repulsive forces of the type recently handled by the wave mechanics in the case of molecular interaction. It is likely that such a correction would have the effect of reducing the sharp maximum of the curve of Fig. 14. Whether the advances in the study of the molecular forces of distortion and repulsion by the wave mechanics will at this time make it possible to carry the analysis of Langevin further in line with these indications is doubtful. However, it is to be hoped that in the future the problem may be successfully solved, and the results above appear most suggestive in this connection.

In conclusion the writer wishes to express his gratitude to his friend and associate, Commander Telesio Lucci, of the Italian Navy, retired, Assistant in Physics at the University of California, for his invaluable assistance throughout the tedious course of these investigations.

LETTERS TO THE EDITOR

Prompt publication of brief reports of important discoveries in physics may be secured by addressing them to this department. Closing dates for this department are, for the first issue of the month, the twenty-eighth of the preceding month; for the second issue, the thirteenth of the month. The Board of Editors does not hold itself responsible for the opinions expressed by the correspondents.

An Interpretation of the Effect of Piezoelectric Oscillations on the Intensity of X-ray Reflections from Quartz

G. W. Fox and P. H. Carr[1] have reported an increase in intensity and number of spots on a Laue pattern through quartz, due to oscillation of the crystal slip as part of a piezoelectric oscillator. Radiation was used from a tungsten target running at 95 kv. As this voltage is considerably above the excitation voltage of the K series of tungsten (69.3 kv), the radiation which they used contained the K lines of tungsten in addition to the continuous spectrum. Any single wave-length in an x-ray beam will not in general fulfill the reflection conditions for any of the planes in a crystal if the crystal specimen is stationary. However, by a slight rocking motion of the crystal, various planes will be brought into the proper orientation for reflection of a given wave-length. The wave-length of the $K\alpha$ line of tungsten is so short (0.211A) that a very slight rocking of the crystal would allow a large number of high order reflections to take place. In the above experiment by G. W. Fox and P. H. Carr the slight rocking of the crystal by piezoelectric oscillation was sufficient to allow reflection of the strong $K\alpha$ or $K\beta$ line of tungsten by a number of the crystal planes. That only a very faint Laue pattern is produced by the non-oscillating crystal is due to the fact that the crystal thickness and primary beam intensity make the usual Laue pattern too weak to be seen. Monochromatic patterns of this sort somewhat similar in appearance to the usual Laue picture have been made by W. L. Bragg.[2]

There are three simple ways to check the correctness of this interpretation. (1) Lower the tube voltage to less than 69 kv so that the K lines will not be excited. The effect should disappear. (2) With the tube at 95 kv rock the crystal slip slightly mechanically. The same effect should be produced as by piezoelectric oscillation. (3) Make a Laue gnomonic projection of the pattern and calculate the $n\lambda$ values in the usual way. Most of these values should be multiples of the wave-lengths of $K\alpha$ or $K\beta$ for tungsten.

B. E. WARREN
Massachusetts Institute of Technology,
July 6, 1931.

[1] G. W. Fox and P. H. Carr, Phys. Rev. **37,** 1622 (1931).

[2] W. L. Bragg, Nature **124,** 125 (1929).

Corrected Relative Intensities of the X-ray Lines in the Tantalum L Series

In a paper which appears elsewhere in this number of the Physical Review, Allison and Andrew report, for the three stronger lines of the L series of tungsten (74), preliminary measurements of relative intensities which are widely different from those reported for the same lines of the L series of tantalum (73).[1] The error mentioned by Allison and Andrew in their footnote 11 is due to the use of an ionization chamber of faulty design in the tantalum measurements. This chamber was made of a piece of glass tubing 33 cm long. A cylinder of nickel gauze, 28 cm long, was placed just inside the inner wall of this tube and was kept at a potential of 170 volts. The end of the chamber nearest the crystal was closed with a brass cap with a slit in it, a flange on this cap extending a little distance into the tube. This cap was erroniously grounded. Thus, the ions formed by the x-ray

[1] Hicks, Phys. Rev. **36,** 1273 (1930).

beam immediately upon entering the chamber were repelled to the metal cap, instead of to the collecting rod which was placed inside the nickel gauze. The x-ray beam, then, travelled through an absorbing layer of methyl iodide about 5 cm long before ions were produced that reached the collecting rod. The length of this absorbing layer can be estimated only very roughly. On the assumption that the path of absorption was actually 5 cm long, the corrections in Table I have been computed, using the absorption coefficients for methyl iodide given by Allison and Andrew and data to be found in the paper on the tantalum *L* series intensities.

TABLE I. *Corrected relative intensities of lines in the tantalum L spectrum.*

Line	Correction Factor	Rel. Int. 30.6 kv	Rel. Int. at High voltage
l	2.4	3.6	3.6
α_2	1.1	11.	11.
α_1	1.0	100.	100.
η	.85	1.1	1.2
β_4	.58	5.4	6.4
β_1	.55	51.	57.
β_3	.52	6.8	7.4
β_2	.49	20.	20.
β_7	.47	.4	.4
$\beta_5+\beta_{10}$	.46	.5	(.5)
β_9	.46	.4	(.4)
γ_5	.38	.5	.6
γ_1	.35	10.	11.
γ_6	.34	.2	.2
γ_2	.33	1.7	2.0
γ_3	.32	2.3	2.7
γ_4	.30	.7	.8

The writer feels that these corrections are not any more than approximately ten percent accurate for the lines of wide wave-length separation, since the thickness of the absorbing layer of methyl iodide can be estimated only roughly. Nevertheless, application of these corrections bring the measurements on tantalum into much closer agreement with the results of Jönsson[2] than previously reported. They are also in fair agreement with the results of Allison and Andrew when the intensities are compared at corresponding voltages, as the relative intensities of the tantalum α_1, β_1, γ_1, lines are, as corrected and at 20 kv, 100:45:8.7 in comparison with 100:43.7:9.1 as reported for the corresponding lines of tungsten.

VICTOR HICKS

Research Laboratories,
Westinghouse Electric & Manufacturing Co.,
East Pittsburgh, Pa.,
July 2, 1931.

[2] Jönsson, Zeits. f. Physik **36,** 426 (1926).

X-ray Reflections from Oscillating Crystals

A few days ago B. Warren addressed to these columns a letter offering an explanation of the striking results of Fox and Carr,[1] who found that the Laue pattern of a quartz oscillator strengthened when the crystal was set into oscillation. Warren's explanation was so straightforward and plausible that the present writer decided to drop an alternative suggestion in the process of development even before the crucial tests proposed by Warren had been attempted.

Further discussion, however, threw some doubts upon the applicability of Warren's idea and so after indicating these I shall mention the alternative explanation which is easily capable of accounting for the facts, and which lends great interest to the experiments of Fox and Carr. The basis for Warren's interpretation is that there are probably a few strong lines of short wave-length in the incident radiation and that there is some jiggling of the crystal in the act of oscillating. An angle displacement introduced by the jiggle of less than one degree would bring many planes into the reflecting angle for such short wave-lengths and one might expect many spots not on the picture of a quiet crystal. Calculation shows however that since the reflection maxima have a width of several seconds, there should have been occasional strong spots from the quiet crystal. The experimenters make no mention of such spots. Moreover, the incident radiation filled an angle of almost two degrees. Under such conditions, rocking the crystal through less than one degree would have practically no effect on the total intensity of the Laue spots. True, a fraction of the spots might be enhanced but an equal number would be weakened. The tests proposed by Warren are surely still worth trying, but on the other hand a new suggestion is now in order.

My notion is to connect the phenomenon

[1] G. W. Fox and P. H. Carr, Phys. Rev. **37,** 1622 (1930).

under consideration with the known mosiac structure of crystals.[2] Quartz, it is true, occurs in fairly perfect ideal crystals and only selected pieces are suitable for piezoelectric oscillators. But the elastic motions during oscillation are of remarkable vigour. Their amplitudes are apt to be of the order of a wave-length of visible light. Now the shearing strength between adjacent "Zwicky" blocks is very low compared with that for two normal planes so that one might expect the oscillation to distribute the blocks through positions making appreciable angles with their equilibrium positions in the crystals at rest. In a block with 10^3 molecules on a side, a displacement of the outermost layer by one lattice spacing from its normal position would correspond to a rotation of about 8′. It will be shown that with the crystals used by Fox and Carr such a rotation would broaden the band of wave-lengths reflected in a spot to such an extent that the intensity of the spot could be increased 30 fold. This disturbance of the blocks becomes very plausible when one considers the fact that there is apparently a heat loss in the oscillator aside from the acoustic energy radiated into the air. Furthermore it is known that even the macroscopic motion of an oscillating plate is not uniform over its surface. First the crystal usually oscillates in more than one mode and the lowest—with the whole crystal in the same phase—need not be the strongest. Again different experiments have shown that there are often irregular quiet spots or unusually active localities on the face of an oscillator. Evidently the experiments of Fox and Carr may lead to important methods for studying the fine structure of crystals and the nature of piezoelectric oscillations as well.

An estimate of the effect can be made by the following argument. All sorts of simplifications are made in the interest of brevity but they do not affect the order of magnitude of the result in the case at hand. In particular the neglect of true absorption is justified by the fact that it will tend to influence the oscillating and the nonoscillating case in the same way, so that the relative intensity will be little changed by it except under special conditions. The reflected intensity $R(\lambda)$ from a crystal set to give a maximum reflection for the plane incident beam of intensity $I(\lambda_0)$ per unit wave-length range at wave-length λ_0 can be written

$$R(\lambda) = I(\lambda)(1 - e^{-\epsilon TG(\theta)B})$$

where ϵ is the coefficient of secondary extinction for the most favorable angle, T is the thickness of crystal traversed by the beam (assumed constant for all rays reaching the particular spot at angles close to $2\theta_0$). $G(\theta)$ is the distribution function giving the chance that a layer of the crystal will be oriented at the angle θ close to θ_0—the consideration of one angle instead of three suffices for our present purposes. The angle over which a perfect crystal would have maximum reflection is called β so that the product $TG(\theta)\beta$ represents the effective thickness of the crystal at the angle θ. The Gauss function would be appropriate for $G(\theta)$ but we might as well choose a simpler one so long as $\int_{-\infty}^{\infty} G(\theta)d\theta = 1$. The simplest is $G(\theta) = 1/\delta$ when $|\theta - \theta_0| > \delta$ and is otherwise zero. In this case assuming the range 2δ so small that $I(\lambda)$ is constant the integrated reflected intensity, $\int R(\lambda)d\lambda$ is approximately $I(\lambda_0) \cdot (1 - e^{-\epsilon T\beta/\delta}) \cdot \lambda_0 \cot\theta_0 \cdot 2\delta$.

We see that for values of δ/β small compared with ϵT the reflected intensity is proportional to δ. Now β is about 5″ so that even for $\delta \approx 8'$, ϵT should be greater than 70 which means for millimeter thick plates $\epsilon > 700$. This is a very moderate figure.

If we say that for the nonoscillating crystal the angular range δ of the blocks is about 15″ while under oscillation it goes to $\delta = 8'$ we see that the reflected intensities are in the ratio 1 to 30. This is more than enough to account for the photographs published by Fox and Carr.

R. M. LANGER

Mass. Inst. of Technology,
July 13, 1931.

[2] e.g. F. Zwicky, Proc. Nat. Acad. **15**, 816 (1929).

The Enhancement of Predissociation by Collisions

In continuing experiments upon the optical dissociation of iodine vapor it has been found that dissociation is produced in mixtures of iodine and argon (0.3 mm I_2, 3 cm A) by illumination with light of wave-length longer than 5100 A. Such light falls in the region of discontinuous band absorption rather than in the continuum and should produce as a pri-

mary product only ordinary excited molecules. Apparently these excited molecules which contain considerably more energy than the heat of dissociation undergo some change leading to dissociation upon collision with argon atoms as, indeed, Franck has already pointed out in discussing the quenching of the iodine fluorescence observed by him and Wood.

It seemed difficult, however, to understand how an argon atom, all of the excited levels of which lie over ten volts above the normal one could produce such an effect. It is possible that the effect of the argon might be to increase the probability of an already occurring predissociation. It has been pointed out elsewhere (Zeits. f. Physik **65,** 464, 1930) that such a predissociation is theoretically possible. (The perturbing states can be, however, the two 1_u states of the $^2P_{3/2}+{}^2P_{3/2}$ combination; *not* the 1_g state, as there stated, as was kindly called to my attention by R. S. Mulliken). Such an explanation may be made to seem more plausible by the following considerations. One of the selection rules for ordinary predissociation transitions is that J does not change, i.e., there must be a conservation of angular momentum. The angular momentum to be conserved can be thought of as being composed of two parts; the angular momentum of the iodine molecule itself and the angular momentum of the mutual motion of the centers of gravity of the molecule and argon atom. If only the total angular momentum is to be conserved the angular momentum of the iodine molecule or separating atoms after predissociation can have a variety of values. In other words the angular momentum can be distributed between the iodine atoms and the argon atom in a variety of ways. One might expect such a weakening of one of the restrictions upon the transitions in the iodine molecule to increase its probability.

In order to test this hypothesis spectra of discharges in pure iodine and in iodine-argon mixtures were compared. When an exposure made with the mixture is compared with one of suitable exposure-time made with pure iodine all bands of wave-lengths longer than about 5440 A seem to have the same intensities but the bands of shorter wave-length are considerably weakened in the spectrum of the mixture. Closer examination reveals that all bands of $v'>29$ are weakened, the quenching setting in fairly rapidly with increasing v'. Confirmatory results have been obtained in fluorescence experiments. The fluorescence was excited by illumination with light from an intense tungsten lamp. The fluorescence bands of wave-lengths longer than 5430A were cut to about 1/4 of their original intensity by 16 mm of argon, those of shorter wave-length being quenched much more severely, the additional quenching setting in only moderately rapidly with decreasing wave-length.

A detailed description and discussion of these experiments will soon be submitted for publication to the Physical Review. A quantitative study of the quenching of iodine fluorescence by argon is being undertaken.

LOUIS A. TURNER

Palmer Physical Laboratory,
Princeton, New Jersey,
July 14, 1931.

The Relative Abundance of N^{14} and N^{15}

In a recent letter to the Physical Review Birge and Menzel[1] have considered what relative abundances of the isotopes of carbon and nitrogen it is necessary to assume in order that the chemical atomic weights shall be consistent with Aston's values and Mecke and Child's[2] value for the relative abundance of O^{16} and O^{18}. The value which is required for the relative abundances of the nitrogen isotopes is $N^{14}:N^{15}=320:1$. This value agrees very closely with a preliminary value for this quantity which we have secured and this letter is for the purpose of reporting this result.

The method we are using depends on the relative intensities of the $NO\gamma$ absorption bands used by Naudé.[3] The determination by Naudé of the relative abundances of $N^{14}O^{18}$ and $N^{15}O^{16}$ molecules can be criticized on the following points: (1) he states that the $N^{15}O^{16}$ $^OP_{12}$ branch has the same intensity as the $N^{14}O^{18}$ $^PQ_{12}+P_2$ branch, while our microphotometer curves for the (1, 0) vibrational band show that the latter is the stronger; (2) even if these heads were of the same in-

[1] Birge and Menzel, Phys. Rev. **37,** 1669 (1931).

[2] Mecke and Childs, Zeits. Physik **68,** 362 (1931).

[3] Naudé, Phys. Rev. **36,** 333 (1930).

tensity, the fact could not be used to determine the relative abundances as done by Naudé, for the $N^{14}O^{18}({}^{P}Q_{12}+P_2)$ branch head is superimposed on the $N^{15}O^{16}\ {}^{O}P_{12}$ branch, so that it is difficult or impossible to determine what part of the absorption is due to each molecule. In view of these difficulties we thought it advisable to redetermine this ratio.

We have compared the relative intensities of the ${}^{O}P_{12}$ branches of $N^{14}O^{18}$ and of $N^{15}O^{16}$ directly by putting density marks on our plates using neutral wire screens[4] and as a source of light a hydrogen discharge tube whose intensity remains constant within about 1 percent. The $N^{15}O^{16}\ {}^{O}P_{12}$ branch is superimposed on the $N^{14}O^{18}\ {}^{O}P_{12}$ branch but they are well separated by the Hilger E 1 quartz spectrograph so that it is possible to estimate the contribution of each molecule to the absorption. Our preliminary result from 26 microphotometer curves for the ratio of $N^{15}O^{16}$ to $N^{14}O^{18}$ molecules is 0.551 ± 0.062. The probable error given represents only the error, if no systematic error is present. Using Mecke and Child's value for the ratio of O^{16} to O^{18} of 630:1, we get for the ratio of N^{14} to N^{15} the value 347:1 in satisfactory agreement with the ratio required by Birge and Menzel of 320:1. This result is preliminary for there are two possible sources of error: (1) the lines at the head of these bands may not give a true continuous absorption so that Beer's law may not hold (a possible error in Naudé's result also); (2) it is not certain that there are no superimposed bands of $N^{14}O^{16}$. Work is in progress to eliminate these possible sources of error. Our results have been obtained from the (1, 0) vibrational band and further checks will be secured from the (2, 0) band as well.

The study has been made on air nitrogen fixed by the Beckeland-Eyde and Haber processes and on nitrogen from Pennsylvania coal. We find no difference in relative abundances of the nitrogen isotopes in air nitrogen (17 microphotometer curves) and in coal nitrogen (9 microphotometer curves) within 3.4 percent, which is less than our probable error. Work is also being done on a sample of oxygen from Precambrian magnetite to see if the relative abundance of O^{16} and O^{18} is the same in this sample and in air oxygen.

Due to an improved hydrogen discharge tube which will be described elsewhere, exposures of the (1, 0) absorption band can be made in one minute and of the (2, 0) band in five minutes using the Hilger E 1 quartz spectrograph. The method requires only about 0.06 grams of oxygen element as NO in the absorption cell. The speed and small samples required makes this a good method for investigating the relative abundances of the oxygen isotopes in meteorites. Work on this problem is in progress in our laboratories.

HAROLD C. UREY
GEORGE M. MURPHY

Department of Chemistry,
Columbia University,
New York, New York,
July 13, 1931.

[4] See G. R. Harrison, J. O. S. A. and R. S. I. **18,** 492 (1929).

The Second Virial Coefficient

If the equation of state of a gas is written:

$$\frac{pV}{RT} = 1 + \frac{B}{V} + \cdots$$

the second virial coefficient, B, may be computed on the basis of classical statistics to be

$$B = 2\pi N \int_0^{\infty} (1 - e^{-E_q/kT}) r^2 dr$$

where E_q is the mutual potential energy of two molecules and r is their separation. In the deduction of this expression it is assumed that the energy is a continuous function of position in the momentum-configuration space of the system. Thus it fails to take into account quantized states which may arise in molecular collisions.

If we take as zero energy, that of two molecules at rest at infinite separation, we find upon examining the potential energy curve, let us say of helium, that the energy of the system of two molecules may be represented by a continuous spectrum when the total energy is positive and by a discrete spectrum when it is negative. Thus there will be certain regions of phase space corresponding to quantized energy states. By subtracting from the classical integral over all of the momentum-position space of the system, that part which comes from regions corresponding to quantized states, and in its place adding the sum over the discrete states in these regions, we should obtain the correct value of the virial

coefficient. When this process is carried through we find

$$B = 2\pi N\Big\{\int_0^\infty (1 - e^{-E_q/kT})r^2 dr - \int_{r_0}^\infty G[(-E_q/kT)^{1/2}](1 - e^{-E_q/kT})r^2 dr + \frac{1}{4\pi}\frac{h^3}{(2\pi mkT)^{3/2}}\sum_i p_i(1 - e^{-E_i/kT})\Big\}$$

where $G[(-E_q/kT)^{1/2}]$ is the error function. The second integral is to be taken over all values of r corresponding to negative E_q, that is from a separation r_0 where the potential energy curve of two molecules crosses the r axis, to infinity. The applicability of this expression is limited to temperatures for which the Boltzmann distribution function may be regarded as valid, and also where kT is at least as great as the lowest level in the discrete spectrum.

In general the discrete spectrum in the case of gas molecules where the potential energy falls off as $1/r^6$ will contain a finite number of levels. For two helium atoms there is only one level lying at approximately -2.4×10^{-16} ergs. Thus at 10°K, kT is still large relative to the dissociation energy of such a polarization molecule.

At a later time, a more detailed discussion of the deduction of the above formula will be given, as well as its application to the calculation of the virial coefficient of He at low temperatures.

J. G. KIRKWOOD
F. G. KEYES

Mass. Institute of Technology,
July 13, 1931.

BOOK REVIEWS

Handbuch der Astrophysik, Band III, Erste Halfte, Grundlagen der Astrophysik, Dritter Teil, x+473 pp., 44 figs., Springer, Berlin, 1930.

This treatise consists of four chapters, "Wärme Strahlung" by Professor Westphal, "Thermodynamics of Stars" by Professor Milne, "Die Ionisation in den Astrophären der Himmelskörper" by Professor Pannekoek, and "The Principles of Quantum Theory" by Professor Rosseland.

The first chapter treats the theory of black-body radiation, presented along well known lines without much reference to the most modern developments of quantum mechanics. It also includes a section on measuring instruments and methods, and on the determination of the constants of radiation.

The second chapter, which is the longest of the four, presents a relatively complete account of the application of thermodynamic considerations to the internal constitution of the stars, carrying the theory not much farther than to the state at which it existed at the time of the publication of Eddington's "The Internal Constitution of the Stars." Unfortunately it does not contain Professor Milne's own newer contributions in the field.

The third chapter gives a detailed account of ionization in the atmospheres of the stars from the point of view of the Saha formula with considerable reference to actual observational data.

The last chapter gives a good account of quantum theory from the point of view of the quantum mechanics as developed up to January, 1928.

The treatise exhibits the characteristic thoroughness of German undertakings, and is well printed and arranged.

RICHARD C. TOLMAN
California Inistitute of Technology

The Physics of Solids and Fluids. P. P. EWALD, TH. POSCHL, AND L. PRANDTL. Blackie and Son, 1930. xii+372 pp., figs. 93. Price. 17s. 6d.

The first part of this composite work (Pöschl) deals with the properties of solid bodies. It considers the ordinary elastic properties of solid bodies, such as the twisting of a rod, the extension of a spiral spring, the bending of a beam. There is included a discussion of the hardness test and a consideration of the conditions of rupture, with illustrations. The second part, Chapter III (Ewald), treats of the mechanical structure of solids from the atomic standpoint, with a good number of references. The successes and failures of the theory are indicated. The last three chapters (Prandtl) deal with the mechanics of fluids. The last chapter of nearly a hundred pages contains an interesting and reasonably elementary discussion of the flow of viscous fluids with applications to lubrication, pipe flow, paddle wheels and propellers, airplane wings and propellers, windmills, turbines, etc. The author is the director of the Aerodynamical Institute at Göttingen.

The whole work is a translation of parts of the recently published eleventh edition of Müller-Pouillet's *Lehrbuch der Physik.*

T. TOWNSEND SMITH
University of Nebraska

PROCEEDINGS
OF THE
AMERICAN PHYSICAL SOCIETY

MINUTES OF THE PASADENA MEETING, JUNE 15 TO 20, 1931

The 171st regular meeting of the American Physical Society was held at the California Institute of Technology, Pasadena, California, in the lecture hall, Room 201 of the Norman Bridge Laboratory of Physics, in affiliation with Section B of the American Association for the Advancement of Science, during the period June 15–June 20, 1931.

The sessions began on Monday morning, June 15, at 9 A.M., with President W. F. G. Swann, presiding, in the chair and Local Secretary for the Pacific Coast, L. B. Loeb, in attendance.

The mornings of June 15th, 16th and 18th were occupied by symposia, the papers being by invitation and covering the following topics:

SYMPOSIUM ON "THE PHYSICS OF CRYSTALS"

1. *On the Secondary Structure of Crystals*, by Fritz Zwicky, California Institute of Technology.

2. *Problems Connected with the Elastic and Electric Properties of Metal Crystals*, by P. W. Bridgman, Harvard University.

3. *Crystal Properties and Electron Diffraction*, by C. J. Davisson, Bell Telephone Laboratories.

4. *Experiments on Structure Sensitive Phenomena in Metal Crystals*, by Alexander Goetz, California Institute of Technology.

SYMPOSIUM OF "THE PRESENT STATUS OF THE PROBLEM OF NUCLEAR STRUCTURE"

1. *The Role of Mutual Mass in Nuclear Structure*, by W. F. G. Swann, Bartol Research Foundation.

2. *Recent Studies of Nuclear Stationary States*, by R. H. Fowler, Cambridge University, England.

3. *Problems of Hyperfine Structure*, by W. Pauli, Jr., Institute of Technology, Zurich, Switzerland.

4. *Hyperfine Structure and Nuclear Magnetism*, by S. A. Goudsmit, University of Michigan.

5. *A Theory of the Arrangement of Protons and Electrons in the Atomic Nucleus*, by W. M. Latimer, University of California.

SYMPOSIUM ON "THE PRODUCTION OF HIGH ENERGY ELECTRICAL PARTICLES

With a discussion of the recent experimental advances in the achievement of high energy radiations.

1. *High Voltage Cathode-Ray and X-Ray Tubes and their Operation*, by W. D. Coolidge, General Electric Company.

2. *Vacuum-Tube Experiment using Tesla Voltages*, by M. A. Tuve, Carnegie Institution of Washington.

3. *Methods for the Production of High Velocity Canal Rays which do not Require the Use of High Voltages*, by E. O. Lawrence, University of California.

4. *High Voltage X-Ray Tubes with Short Electron Path*, by C. C. Lauritsen, California Institute of Technology.

5. *Problems in the Development of High Voltage Technique*, by Drs. A. Brasch and F. Lange, Research Laboratory of the A. E. G., Germany.

On Wednesday morning, June 17th, the sessions of the Physical Society were suspended in order to permit the physicists to attend symposia by the astronomers and by the chemists, the latter being on the Molecular Force Fields.

The afternoons were devoted to excursions and more extensively to scientific discussions and visits to the laboratories of the California Institute of Technology.

On Tuesday evening a popular lecture was given by Dr. H. C. Arnold of the Bell Telephone Laboratories, in the open air amphitheater in Griffith Park, Los Angeles, entitled "Science Listens," with demonstrations.

On Friday morning, June 19, and again on Friday afternoon and on Saturday morning, June 20, the regular program of the Physical Society for presentation of ten-minute papers was carried out. There were twenty-nine papers presented on the regular program, as indicated in the Bulletin, with the following alterations.

Paper No. 10, "Differential Biological Effects Produced by X-rays and Gamma-rays," G. Failla and P. S. Henshaw, Biophysical Laboratory, Memorial Hospital, New York City, was transferred to the sessions of one of the biological societies at the request of the author, and a paper entitled "Diffraction Experiments with Monochromatic Molecular Beams," by I. Estermann, R. Frisch and O. Stern of Hamburg, was substituted in its place. The latter paper had through a misunderstanding been transmitted to the Chemical Society instead of being sent to the Physical Society for its sessions.

In addition, paper No. 19 was followed by a paper entitled, "The de Broglie Wave Spectrum from the Secondary Structure of Li F," by Thomas H. Johnson of the Bartol Research Foundation of the Franklin Institute. This paper had been submitted to the Secretary in time for inclusion but had never reached its destination. With the consent of the members present it was included at this point.

In addition to the three papers on the Supplementary Program three more papers were added to the program on Saturday morning. They were:

No. 33. "Modern Statistics from the Gibbsian Point of View," by Paul S. Epstein, California Institute of Technology, Pasadena, California.

No. 34. "The Effect of Inductance on the Electromagnetically Damped Galvanometer," by Thomas M. Dahn, California Institute of Technology, Pasadena, California.

No. 35. "A Search for an Electrostatic Analogy to the Gravitational

Red Shift," by Roy J. Kennedy and Edward M. Thorndike, California Institute of Technology, Pasadena, California.

On Friday evening, June 19th, a joint dinner was held at the Huntington Hotel for physicists, astronomers and mathematicians. Some hundred guests attended and adjourned thereafter to attend the lecture by Astronomer Hubbell of the Mt. Wilson Observatory.

The only item of business which came before the meeting was the question of the date and place of the December meeting of the American Physical Society on the Pacific Coast. *It was moved, seconded and voted* to hold the 174th meeting of the American Physical Society in Le Conte Hall, University of California, at Berkeley, December 18th and 19th, 1931.

The Pasadena meeting of the American Physical Society was unquestionably the most successful meeting ever held on the Pacific Coast. Attendance during the symposia was well above two hundred and the attendance at the regular meetings was above a hundred.

The American Physical Society desires to go on record as expressing its appreciation of the splendid program and the many provisions for the comfort of its members which were arranged by the local committee of the California Institute of Technology.

L. B. LOEB,
Local Secretary for the Pacific Coast

1. A revision of values of e/m from the Zeeman effect. J. S. CAMPBELL and W. V. HOUSTON, *California Institute of Technology.*—The preliminary values of e/m obtained from the Zeeman separations of Cd λ6439 and Zn λ6362, and reported last year, are revised on the basis of a redetermination of the current-field ratio of the solenoid used. The method of calibration permitted this ratio to be determined at the solenoid currents and temperatures which prevailed during exposures. The g-factors have been corrected to take account of the influence of neighboring triplet terms. Some of the plates have been remeasured. The values of e/m so obtained, 1.7578 with a probable error of 0.06 percent from Cd λ6439, and 1.7576 with an error of 0.05 percent from zinc 6362, are 0.16 percent lower than the accepted spectroscopic value. Possible disturbance of the g-factors, from the approach of terms other than those of which account has been taken, cannot at present be estimated.

2. The absorption spectrum of ClO_2. HAROLD C. UREY AND HELEN JOHNSTON, *Columbia University.*—The absorption bands of ClO_2 have been investigated using Hilger E1 and Hilger E185 quartz spectrographs. In all 125 bands have been measured from λλ5040–3300. These follow the formula

$$\tilde{\nu} = 19795.4 + 719.34(v_1' + \tfrac{1}{2}) - 2.817(v_1' + \tfrac{1}{2})^2 + 304.82(v_2' + \tfrac{1}{2}) - 2.487(v_2' + \tfrac{1}{2})^2 - 4.892(v_1' + \tfrac{1}{2})(v_2' + \tfrac{1}{2}), - \tilde{\nu}''$$

where $v_1' = 0, 1, 2, \cdots$, $v_2' = 0, 1, 2, \cdots$, and $\tilde{\nu}'' = 0$, 528.8, 727.0, 857.7 and 1471.3 cm^{-1}; the latter appears to be a harmonic of the 727.0 frequency. We have not been able to find evidence for the $v_1' = v_2' = 0$ level unless there is a considerable perturbation of this level. The isotope effects which we have observed follow the formula

$$\tilde{\nu}_{35} - \tilde{\nu}_{37} = 5.37(v_1' + \tfrac{1}{2}) + 0.80(v_2' + \tfrac{1}{2}) - 14.4, \text{ if } \tilde{\nu}'' = 526.2$$

and

$$\tilde{\nu}_{36} - \tilde{\nu}_{37} = 5.37(v_1' + \tfrac{1}{2}) + 0.80(v_2' + \tfrac{1}{2}) - 11.2, \text{ if } \tilde{\nu}'' = 0.$$

Calculation of the isotope effect for a molecule of this kind shows that the isotope effect for the normal level is larger than can be expected if the least possible vibrational energy is $\frac{1}{2}h(\nu_1+\nu_2+\nu_3)$

The formula given above does not apply to bands of shorter wavelength than about λ3300. Beyond this point another formula must be used as pointed out by Goodeve and Stein (Trans. Far. Soc. **25,** 738 (1929)) though we have measured only a few bands as yet in this region.

3. New infrared absorption bands in water. JOSEPH W. ELLIS. *University of California at Los Angeles.*—New absorption bands have been found for water at 1.74μ (5750 cm^{-1}) and 1.79μ (5590). Absorption in this region diminishes considerably with rising temperature but no noticeable shift of band centers occurs as with other water bands. The maxima may be interpreted respectively as combinations of 2.79μ (3580), 6.1 (1640) and 19.5 (510); and 2.90 (3450), 6.1 and 19.5. 6.1μ is a well-known water maximum, 2.79 and 2.90 are components of the 3μ region resolved by Kinsey and others through Raman scattering, whereas 19.5 is somewhat hypothetical. It has been cited by Rawlins and Taylor (Infrared Analysis of Molecular Structure, p. 61) as characteristic of water but I have failed to find it in the literature. Whether it is to be identified with the gradual approach toward a maximum near 20μ in the absorption and reflection spectra of Rubens and Ladenburg is uncertain. Since the present model of the H_2O molecule scarcely permits so low a characteristic frequency the 19.5μ band is here assigned to a water polymer. The well-known 4.7μ (2130 cm^{-1}) band of water and ice, which disappears in water vapor, can be interpreted as a combination of 6.1 and 19.5μ. Bands analogous to all of the water bands characterize the water of crystallization in selenite.

4. Infrared absorption bands of hydrogen cyanide in gas and liquid. FREDRICK S. BRACKETT AND URNER LIDDEL. *Smithsonian Institution and Fixed Nitrogen Research Laboratory.*—The absorption spectra of both gaseous and liquid hydrogen cyanide have been investigated by means of an automatic spectrograph in the region from 7,000 *A* to 20,000 *A*. This region yields 15 absorption bands in the liquid, three of which have been observed also in the gas, with a displacement from liquid to gas to higher frequencies of from 104 cm^{-1} to 145 cm^{-1}. These, with the exception of one weak band, have been identified as harmonics and combination frequences of fundamentals at 14μ, 4.7μ, and 3.04μ, designated δ, ν_2, ν_1, respectively. The second and third harmonics of the 3.04μ fundamental are observed as doublets in the gas with separations of 47 cm^{-1} and 50 cm^{-1} yielding moments of inertia 21×10^{-40} g.cm^2 and 18×10^{-40} g.cm^2, respectively. The combination frequency of $2\nu_1+\nu_2$ yields a doublet separation of 50. cm^{-1} giving a moment of inertia 18×10^{-40} g.cm^2. This work is in entire agreement with that of Badger and Binder (Phys. Rev. **37,** 800 (1931)) both as to wave-lengths, approximate values of moments of inertia, and interpretation in terms of fundamental modes of vibration. The band $4\nu_1$ observed by them at 12,636 cm^{-1} in the gas was observed in the liquid displaced to lower frequencies by 136 cm^{-1}.

5. The auroral spectrum. JOSEPH KAPLAN. *University of California, Los Angeles.*—The recognition of unusual band spectrum phenomena in the weak auroral radiations, have led to an almost complete reproduction of the auroral spectrum. The Franck-Condon rule for band intensities is strikingly violated. First positive bands of nitrogen which are normally four-headed, possess only strong single heads. The comparison of the upper atmosphere to a discharge tube without walls gave the clue to the present experiments. It was thought that a continuous discharge through a tube would so modify the surface as to reproduce the aurora spectrum. This has been done in a striking manner in electric discharges in air at 10^{-3} mm. The discharge was marked by rapid chemical cleanup of the air and a subsequent disappearance of the discharge. It was during the flickering stage that the best reproductions of the aurora were obtained, an interesting fact in view of the pulsating types of luminosity which have been observed in auroral displays. Both of the above band spectrum phenomena are explained on the hypothesis that the nitrogen molecule predissociates. This is particularly interesting since the afterglow of active nitrogen was obtained in the same tube for the first time in uncondensed discharges. The writer has elsewhere given an explanation of the long life of the afterglow in terms of predissociation. The present experiments therefore are evidence that the auroral displays are electrical discharges at low pressures under conditions which are ideal for the production of the nitrogen afterglow.

6. New emission bands in mercury vapor. J. GIBSON WINANS. *University of Wisconsin.*—The spectrum of an electrodeless discharge through mercury vapor showed a group of eight bands with short wave limits at 2494, 2488, 2482, 2476, 2470, 2464, 2458, and 2450. It showed also a continuous spectrum with different intensity maxima between 5000 and 2050. The band limits 2482 and 2464 are uncertain since they are concealed by mercury lines. The bands 2476 and 2470 were first observed by Stark and Wendt and 2458 and 2450 by Miss Brzozowska. Rayleigh resolved the 2476 band into closely spaced components and Condon suggested that they might be "diffraction bands." Miss Brzozowska has shown that these components converge like the rotational lines in a single band. The emitter of these bands is uncertain. The closely spaced components are not close enough to be rotational lines of Hg_2. The bands were observed in three different tubes prepared with different samples of mercury. They appeared when the HgH bands did not; and they are not observed in absorption or in fluorescence. Heating, which destroys the 4850 band and greatly enhances the 3300 band produces no effect on this group. Considering them as single bands, their frequencies and intensities can be correlated with potential energy curves. A probable emitter is Hg_2^+.

7. Features of the spectra of thulium, ytterbium, and lutecium under different excitations. ARTHUR S. KING. *Mount Wilson Observatory.*—The work is a continuation of the investigation of rare-earth spectra in the electric furnace, arc and spark for temperature classification and the segregation of neutral and ionized lines in the range λ2950 to λ6800. Distinctive characteristics have appeared for each element. The lutecium spectrum is of special interest on account of its large variety of line-groups, each brought out by certain physical conditions, and also the hyperfine structure of a large proportion of its lines. The prevailing hyperfine pattern when resolved has three components equally spaced, usually degraded in intensity toward the red; while unresolved lines appear to have the same pattern in varying degrees of closeness. The ytterbium lines require in general the excitation of the arc or high-temperature furnace, only five out of about 400 listed being classed as low-temperature lines. Distinct hyperfine structure is absent. Enhanced lines are prominent, and by a comparison of arc and spark spectra, were grouped according to their response to spark excitation. Preliminary examination of the thulium spectrum showed the furnace excitation expecially favorable for high intensity and easy reversal of Tu I lines. The absence of hyperfine structure in thulium furnishes the only exception thus far observed among rare-earths of odd atomic number.

8. Investigations in the spectral region between 20 and 40μ. JOHN STRONG. *National Research Fellow. California Institute of Technology.*—A reststrahlen apparatus was employed for the experiments. This apparatus has advantages over former arrangements in that it does not require large crystal mirrors, the crystals may be quickly interchanged to give various wave-lengths, and the major part of the air in the optical path may be kept dry with P_2O_5. The transmission of several gases in the spectral region 20–33μ has been investigated. SO_2 showed strong absorption at 20.75μ. This band is believed to be one of its fundamentals. The reflectivity of SO_2 at 20.75μ and 8.7μ was found to be zero. Raman data for SO_2, CCl_4, $CHCl_3$ and $(C_2H_5)_2O$ are compared with the absorption of these gases. The transmission of lacquer, glass and amorphous quartz films was determined in the region 20–33μ. β-MgO was found to have a reststrahlen near 23μ. This material reflects 80 percent of the 23μ CaF_2 reststrahlen. Potassium iodide was found to be transparent to wave-lengths greater than 33μ.

9. Graphical determination of all crystal lattices from x-ray powder method data. WALTER SOLLER. *University of Arizona.*—The crystal analysis of solid substances available only in powdered form has in general been limited to the more symmetrical crystal structures. Analytical methods are too complex to have any practical value. The present graphical methods, because of their limitations to the more symmetrical systems and the x-ray interference due to interpenetrated lattices, give reliable results only for a limited number of substances. An x-ray diffraction pattern analyzer for all crystal lattices is discussed in this paper which should make crystal analysis for all solid substances possible. From an analytical discussion of the series of angles of x-ray reflections from lattice planes it is shown that an apparatus could be constructed which at once would indicate this series for any lattice of all crystal systems with the exception of the tri-clinic lattice. With this apparatus the lattice of any solid substance can be identified

by matching the diffraction pattern of the substance with some pattern indicated on the apparatus. A definite procedure is possible in using the apparatus, so that the higher symmetry lattices are eliminated in order of higher symmetry until the correct match is obtained. This procedure identifies the tri-clinic lattice by the elimination of all the lattices higher in symmetry. From the setting of the apparatus for the match of the diffraction pattern all the parameters of the unit lattice cell, as well as the identification of the planes from which each reflection is coming, are obtained directly. The parameters of any unit lattice cell including the tri-clinic are also obtained by three definite settings of the apparatus distinct from the identification setting. This second determination of parameters serves as an entirely independent check of the first.

10. Diffraction experiments with monochromatic molecular beams. I. ESTERMANN, R FRISCH AND O. STERN *Physical Chemical Institute, University of Hamburg, Germany.*—A beam of helium atoms with de Broglie wave-lengths distributed according to Maxwell's law was diffracted from a LiF crystal surface which served as a crossed grating. By means of a slit, (practically) monochromatic portions of the resulting spectrum were selected; these portions were then diffracted from the surface of a second LiF crystal. At the diffraction angle corresponding to the wave-length thus selected, a diffraction maximum was observed. The intensities of the maxima for the different de Broglie wave-lengths were found to correspond to the Maxwell distribution of velocities in the original beam. First and second order diffraction maxima were observed.

11. Transition from a glow discharge to an arc. S. S. MACKEOWN. *California Institute of Technology.*—Results of an experimental study of the abnormal cathode drop and of the transition of a glow discharge to an arc lead to the following theory. As the current density to the cathode in the abnormal cathode drop increases, a larger number of electrons are freed from the cathode by positive ion bombardment. These electrons come primarily from active spots due to impurities on the cathode, and produce ionization which is localized near the active spots. Due to the high mobility of the electrons a high positive space charge results which increases the electric field near the active spots and consequently the electrons emitted therefrom. This process is cumulative and proceeds rapidly until the field at the active spot increases sufficiently to produce "field electrons" from the cathode due to the high electric field, and an arc results.

12. The electro-optical shutter. HAROLD W. WASHBURN, *University of California, Berkeley. Introduced by Ernest O. Lawrence.*—A solution of the electric circuit of the electro-optical shutter, taking into account distributed constants, was obtained to see what error is made in assuming lumped constants. The results showed that, for the leads from spark gap to Kerr cell up to about one meter in length, the more exact solution differs from the approximate solution mainly by a 10 percent third harmonic and other smaller higher harmonics. Experiments on the effect of the Kerr cell capacity on the time of cut-off were made and the differences of time thus measured were found to agree approximately with those calculated. A short calculation showed that these differences of time were very nearly independent of the time taken (up to 10^{-8} secs.) for the voltage across the spark gap drop. An experiment employing short leads (10 cm), with a resistance too small for effective damping, from the spark gap to Kerr cell showed that oscillations sufficient to reopen the shutter did not occur. Calculation predicts this when the period of oscillation is about equal to the time of voltage drop across the gap. Experiments have been started on the breakdown of liquids which indicate that the rate of progression of the breakdown is much more rapid than in air since the voltage gradients are greater.

13. The production of ultra-short undamped electromagnetic waves. G. V. POTAPENKO. *California Institute of Technology.*—Ultrashort electromagnetic waves have been obtained by the extension of the method of Barkhausen and Kurz. This method utilizes electronic oscillations which can be obtained in a vacuum tube when grid has a high positive potential relative to the plate and filament. When to such a tube a circuit is connected the energy of oscillations is a maximum when the time necessary for the electrons to go from the filament to the plate and back is equal to natural period of this circuit. By increasing the grid potential and filament current it is possible to obtain an electronic oscillation until a frequency of 10^9 per second is

reached. Further increase of frequency is prevented by overheating of the filament. From the author's theoretical investigation it follows that in a circuit connected to the tube, oscillations can be produced if the natural period of a circuit is two, three, etc., times shorter than the period of electronic oscillations. By a method based on this theory the author obtained oscillations the frequency of which exceeds many times the frequency of electronic oscillations. Undamped waves of a few centimeters were obtained. Report will be followed by demonstrations.

14. Electron lenses. C. J. DAVISSON AND C. J. CALBICK. *Bell Telephone Laboratories, New York.*—Electrons or other charged particles on passing through an aperture in a charged conductor receive rather sharp deflection in the distorted electrostatic field there encountered. A mathematical investigation of these deflections reveals that for apertures of simple geometry, such as slits in cylinders and circular holes in plates, the interaction between the distorted field and incident electrons is similar to the interaction between an optical lens and incident light rays. The field about a slit has the properties of a cylinderical lens. It has a focal length which is independent of the width of the slit, and electron images real and virtual are formed in accordance with the simple laws of geometrical optics. The field about a circular hole in a plate is the analogue of a spherical lens. Its focal length is given by the formula $f=2V/(G_2-G_1)$, where V represents the energy of the incident particles in equivalent volts, and (G_2-G_1) represents the difference, which existed before the hole was formed, between the potential gradients on the two sides of the plate. The diameter of the hole is not involved. The focal length of the field about a slit is given by the same formula. The results of these calculations are verified by experiment.

15. Nuclear scattering of high velocity electrons by thin foils. H. V. NEHER, *California Institute of Technology.*—Work on nuclear scattering of electrons by thin foils has led to the following conclusions: (a) A more critical criterion for single scattering is obtained which depends on the shape of the curve connecting ρ, the amount of scattering, with angle. (b) Secondary electrons may be eliminated by applying stopping potentials equal to one-half the energy of the primary beam. (c) Dependence of scattering on energy of primary beam is found to agree well with either Mott's equation or with the relation k/V^2, but is at variance with the classical relativistic theory. (d) Comparison of values of scattering for Al, Ag and Au shows that ρ increases faster than Z^2. (e) Either Mott's or Rutherford's equation gives the correct angular dependence for Al. The latter also gives the correct dependence on angle for Ag and Au. Mott's equation is not applicable for these heavy elements. (f) Experimental absolute values for scattering for Al compared with theory give $\rho=1.32$ of the value given by Mott's equation. This relation is valid within the ranges $\theta=95°-173°$, $V=56-145$ KV. (g) Secondary electrons coming from the foil are distributed according to the simple cosine law. (h) No evidence of loss of energy due to radiation is found up to one-half the energy of the primary beam.

16. The absorption of hydrogen positive rays in helium and argon. ROBERT E. HOLZER. *University of California, Berkeley.*—The absorption of H^+, H_2^+ and H_3^+ ions with velocities corresponding to accelerating potentials between 200 and 1800 volts was observed in helium and argon by means of an apparatus similar to that previously described (Phys. Rev. **36,** 1204 (1930)). The absorption of all of the ions, in helium is lower than in hydrogen. Measurements of the absorption of H^+ and H_2^+ ions in helium at 900 volts agree with the previous measurements of Dempster (Phil. Mag. **3,** 115, (1927)) within the limits of experimental error. The absorption coefficients for hydrogen ions in helium decrease in size in the following order H_3^+, H_2^+, H^+. The absorption coefficients for hydrogen ions in argon are larger than in helium or hydrogen. H_2^+ is absorbed more strongly than H_3^+ in argon as in hydrogen but not as in helium. Since the ionization potential of H_2 is nearly equal to the ionization potential of A and widely different from the ionization potential of He, it appears that the neutralization of a positive ion is very probable when it is moving among gas molecules, the ionization potential of which is the same as the ionization potential of the molecules from which the ion was produced. The absorption coefficient of H^+ in argon rises with increasing velocity between 300 and 1800 volts. It is smaller than H_3^+ at 300 volts but larger at 1800 volts. A rise in the absorption curve with increasing velocity has been observed for electrons in various gases in certain velocity ranges. The rise

in the absorption curve for protons in argon does not occur in the same velocity range as the rise in the absorption curve for electrons in argon. Whether or not the phenomenon is similar to the Ramsauer effect for electrons must be decided by further investigation.

17. Effects due to the bombardment of platinum by mercury ions. JOSEPH E. HENDERSON AND EDITH GIDEON. *University of Washington.*—Positive ions of mercury, formed by ionization of mercury vapor at 50°C, were accelerated and made to pass as a beam against a platinum surface. This platinum surface was so arranged that the positive ion current incident upon it could be measured with and without secondary electron emission from the surface. This arrangement permitted both the rate of cathodic disintegration and the secondary electron emission to be studied under identical conditions. The rate of disintegration was found to increase linearly with the accelerating voltage applied to the positive ions up to about 1200 volts after which the rate remains constant as far as carried. The secondary emission likewise increases linearly up to 1200 volts after which it decreases markedly. This implies that there is an intimate relation between the rate of disintegration and secondary electron emission due to the positive ions. Wax vapor was present in the apparatus.

18. High velocity mercury ions. E. O. LAWRENCE AND D. H. SLOAN. *University of California, Berkeley.*—At the Los Angeles meeting of the American Physical Society last December the authors described a method of successive accelerations of a beam of mercury ions as they pass through a column of hollow cylinders connected alternately to opposite terminals of a radio frequency oscillator. Using a tube with 30 such cylinders, with 35,000 volts applied at a frequency of 8535 kilocycles, a beam of singly charged mercury ions with 1,050,000 electron volts equivalent energy, was obtained. The magnitude of the ion velocity was checked by electrostatic deflection of the beam. The effects of secondary electrons due to positive ion bombardment of the collector, and of photoelectrons due to x-rays originating in the ion source and in the accelerators can be eliminated, leaving the actual high velocity ion current of 5×10^{-9} amperes.

19. Mobilities of Na^+ ions in N_2 as a function of time. LEONARD B. LOEB. *University of California.*—The measurements of mobilities of Na^+ ions from a Kunsman source in relatively pure H_2 over different time intervals using a sine wave form oscillator and the Rutherford alternating current method recently reported on (minutes of the 170th meeting of the American Physical Society, May 2, 1931) were extended to Na^+ ions in N_2 gas. The measurements yielded a mobility of 3.8 cm/sec per volt/cm from 10^{-4} to 5×10^{-4} seconds. At this point the mobilities dropped fairly rapidly to a value of about 3 cm/sec per volt/cm thereafter falling gradually to about 1.6 cm/sec per volt/cm the value normally found in N_2 in intervals of 10^{-2} or more seconds. The fastest mobility is presumably that of the Na^+ ion in N_2. The others are probably addition products of Na^+ with molecules of impurity present. The first rather sharp drop is presumably due to the addition of a single molecule of fairly common impurity (H_2O vapor). The gradual change may be due either to the gradual growth of a cluster, or the gradual picking up by all ions of some common impurity molecule of large size with high ion affinity but present in small amounts. The value 3.8 cm/sec of the Na^+ ion mobility in N_2 gives the first real test of our theoretical mobility equations. It is higher than the value of 2.7 cm/sec for the complete Langevin equation for inverse fifth power law attractions, but far less than the value 14.9 cm/sec from a law assuming solid elastic impacts.

19A. The de Broglie wave spectrum from the secondary structure of LiF. THOMAS H. JOHNSON, *Bartol Research Foundation of the Franklin Institute.*—The de Broglie wave diffraction patterns produced by the reflection of a beam of hydrogen atoms from a cleaved LiF crystal surface, formerly reported, consisted of both a primary set of spectra from the array of ions on the surface and of a set of secondary spectra, the directions and amount of the dispersion of which were characteristic of a periodicity on the surface of the order of 50A parallel to the 100 cleavage planes. The secondary spectrum has recently been photographed at grazing incidence in the 100 azimuth using a ribbon shaped beam with an angular aperture of 24′ of arc. The secondary spectrum at 2.5° incidence extended to ten times the width of the incident beam, but there was still no evidence of a minimum between the specular beam and the secondary

spectrum though this should have appeared if the cracks were regularly spaced at distances as great as 250A. The most plausible interpretation seems to be that the secondary structure under the conditions of the experiment was not characterized by a regular spacing. At angles still closer to grazing the reflected beam was cut off by the step-formed structure of the surface.

20. The relation of atmospheric space-charge to turbulence and convection. JOSEPH G. BROWN, *Stanford University.*—Von Schweidler, in 1908, showed theoretically that in a still atmosphere under the influence of a potential gradient of 90 V/m a positive space-charge would accumulate in a layer next to the earth's surface due to the migration of the ions in the air-earth current. The maximum density of this space-charge would be 0.25 esu/m^3 at the surface and it would fall to zero at 15 meters above the surface. The mean value of the space-charge at 7.5 meters above the surface, measured at Stanford University, amounts to 0.05 esu/m^3 at 7 A.M. This is the time of day when the air has been quiet for the longest period and the fact that the space-charge approaches closely to the theoretical value of 0.07 esu/m^3 for this elevation shows that the condition assumed by von Schweidler is actually approached. Continuous simultaneous records of space-charge and wind velocity have been obtained for one year. The mean diurnal variation of each has been computed for each month and for the entire year. A comparison of these variations shows a very clear inverse relation. It is believed that this relation is the result of the formation of the positive layer when the air becomes quiet and its dispersion by the turbulence and convection which accompany wind.

21. The temperature variation of the specific heat (C_p) of CO_2 at 65.3 kg/cm² pressure; the specific heat (C_p) of helium as a function of pressure. E. J. WORKMAN, *National Research Fellow, Bartol Research Foundation of the Franklin Institute, Swarthmore, Pennsylvania.*—The ratio of C_p at a pressure of 65.3 kg/cm² to C_p at a pressure of one atmosphere has been measured for CO_2 over the temperature range 45 to 100°C. Measured values for this ratio are as follows: 1.87 at 45°C; 1.58 at 50°C; 1.38 at 80°C and 1.27 at 100°C. Considering the relatively small temperature variation of the specific heat (C_p) of CO_2 at a pressure of one atmosphere, the enormous increase in the above ratios at a pressure of 65.3 kg/cm² arises from the large temperature variation of the specific heat at the higher pressure. Incomplete measurements at a pressure of 180 kg/cm² give an indication that this ratio may increase to 10 or 12 in the temperature region 40 to 50°C. The specific heat (C_p) of helium at 50°C shows no measureable variation with pressure in the pressure range 10 to 120 kg/cm². In the case of helium the probable error does not exceed 0.2 percent.

22. An electromagnetic theory of sight and color vision. S. R. COOK. *Stockton, California.*—The paper sets forth a new theory of sight and color vision. In this theory the electromagnetic (light) energy is transformed by the visual purple and the rods and cones into alternating electric and magnetic potentials. These alternating electric and magnetic potentials are transmitted through the fibers, nuclear cells and synapses to the ganglion cells, whence the electric energy is transferred to the brain as neuro-energy along the optical nerve. The rods interpret intensity only while the cones interpret color. There are five areas of cone receptors, corresponding in general to red, yellow, green, blue, and violet. Each of these five areas interpret their respective wave-lengths (colors) primarily, but they are also capable of relatively wide tuning. The yellow receptors, for instance, are capable of interpreting, not only the yellow portion of the spectrum, but also wave-lengths well into the red and into the green. The theory might aptly be termed a radio theory as it assumes that the electromagnetic energy of the light waves is transformed in a manner similar to the transformation of electromagnetic radio wave energy. The theory explains color blindness by assuming either that the receptors for the special color are wanting, or that they are defective in their tuning. Residual images are hypothetically explained on the assumption that energy is stored up in the nuclear cells. This energy being later delivered to the ganglion cell, and thence to the optic nerve. By assuming that conduction through the nuclear cells are electrolytic rather than electronic, the theory explains the difference between the velocity of neuro-energy and electronic conduction. The alternating potentials are conducted through the synapses by condenser action. The theory is suggestive only and awaits confirmation.

23. Note on the relation of wave-length to color sensation. C. A. RINDE. *College of the Pacific.*—At the Cleveland meeting of the American Physical Society last December the author presented evidence, based upon measurements of the retinal areas sensitive to monochromatic light at varying wave-lengths, suggesting the possibility of five primary chromatic sensations, red, yellow, green, blue, and violet. Curves were plotted showing the range of wave-length capable of stimulating each of five separate chromatic receptor mechanisms; and it was asserted that the stimulation of a particular receptor mechanism by any light within its range would produce a specific sensation, regardless of the location of the wave-length within the given range. Further work using a didymium glass filter, in accordance with a suggestion by Dr. M. Luckiesh at Nela Park, tends to corroborate these results, both as to the existence of primary yellow and as to the production of the yellow sensation by light from which the so-called "yellow" wave-lengths of the spectrum are absent.

24. On the magneto-caloric effect. FRANCIS BITTER. *Westinghouse Research Laboratories, East Pittsburgh, Pennsylvania.*—The magneto-caloric effect is the reversible evolution of heat accompanying a change in the magnetization of a substance. Its physical significance is that the change in energy accompanying a change in magnetization is partly due to work done at the expense of thermal agitation. The effect in ferromagnetic substances in strong fields depends on the change in energy of spontaneous magnetization and is essentially governed by the energy term $n\sigma^2/2$, where n is the molecular field constant and σ is the intensity of magnetization per unit mass, as was shown by Weiss and Forrer. For low fields, however, other processes take place, for instance the rotation of magnetization of small regions which may be related to Zwicky's blocks. The temperature agitation determines the distribution of directions of magnetization of the various regions. The existence of a magneto-caloric effect in fields up to a few hundred gauss, as found by Ellwood, shows that temperature agitation plays a significant rôle in small as well as in large fields. A magneto-caloric effect depending on crystal orientation and on mechanical distortions is predicted and discussed, and it is pointed out that a quantitative interpretation of experiments on single crystals might be possible.

25. Asymetric Zeeman patterns at intermediate strengths of field in Ca I. WM. BENDER. *Yale University. (To be read by title.)*—The theoretical Zeeman pattern, based on Darwin's Wave Mechanical treatment (Proc. Roy. Soc. **115**, p. 1, 1927) was worked out for the $^3D-{}^3P$ transitions in Ca I, for $\omega=1.55$ cm^{-1} corresponding to a field of 32,500 gauss. Marked asymmetries in the pattern are expected since $\omega:\beta$ for the ^3D levels is 1.60. Measured lines in general with theoretical predictions well within the probable error throughout the entire pattern. Radiation in the field opposite the "forbidden line" $j=2\rightarrow j=0$ ($2^3P_0-4^3D_2$) came out in excellent intensity though somewhat broad, the position of the corresponding field lines $m=1, 0, -1\rightarrow m=0, 0, 0$ being observed at 104.91, 103.22, 101.30, as against the theoretical values, 104.80, 103.10, 101.47, all measured in cm^{-1}, from the mean multiplet center. The relative intensities for these "forbidden lines" was measured as 2.1: 4.1: 1 as against the theoretical values of 2.04: 4.01: 1. Evidence for "forbidden field radiation" associated with $2^3P_1-4^3D_3$ in the form of three distinct blocks at approximately the position given by the theory, was found although the density of deposit on the plate is quite small, in this case. Polarization plates confirmed the theoretical predictions in a striking manner, particularly in the densely overlapping field patterns associated with $2^3P_2-4^3D_2$, and $2^3P_2-4^3D_1$.

26. Probabilities of inelastic collisions. CLARENCE ZENER. *National Research Fellow California Institute of Technology.*—The probability of an inelastic collision has been found quite generally to be approximated by $(IS)^2$. Here $I=2\pi/h\int_{-\infty}^{\infty}X(t)dt$, where X is the matrix element with respect to the initial and final states of the mutual interaction of the two systems. X is obtained as a function of time by allowing the centers of gravity of the two colliding systems to obey classical mechanics in the potential resulting from averaging over all the internal coordinates. S is approximately $exp(-\tau_c/\tau_0)$. τ_0 is the pseudo period of oscillation h/σ, σ being the magnitude of the difference in the internal energy before and after collision. τ_c is the time of collision, for which a definite expression may be found in any specific collision. Thus if the closest distance of approach, p, is so large that the motions of the centers of gravity are

nearly linear, then $\tau_c = 2\pi p/v$, where v is the mean of the initial and final mutual velocities. If the collision is head-on, and if the average mutual energy is positive and varies as $exp(-\lambda R)$, then $\tau_c = \pi/\lambda v$.

27. Photoelectric absorption of ultra-gamma radiation. HARVEY HALL AND J. R. OPPENHEIMER. *University of California, Berkeley.*—A relativistic theory of the photoelectric effect, based on the relativistic quantum electrodynamics and the relativistic Dirac equation for a single electron, is developed and applied. The cross-section for photoelectric absorption of very hard radiation by electrons bound to a nucleus is computed. For this hard radiation, with $\lambda << h/mc$, we obtain

$$\sigma \backsimeq 1.9 \times 10^{-22} Z^5 \lambda.$$

The results of the theory are compared with the experimental results of Chao and Tarrant on the total absorption of the gamma rays of ThC'' by various elements. For elements of intermediate atomic number (Cu) the agreement between theory and experiment is satisfactory; the deviations from the Compton absorption found experimentally may be explained by the photoelectric absorption of extranuclear electrons. For the heaviest elements the theory gives an absorption fifty times that observed. The discrepancy is much too large to be explained by experimental error, or by errors introduced by approximations used in deriving and applying the theory. The present theory leads to incorrect results when applied to the interaction of electrons with light of such extremely short wave-length.

28. Comparison of the classical electron orbital models with the probability density $\Psi\Psi^*$ of the Schrödinger and the Dirac solutions of hydrogen-like atoms. H. E. WHITE. *University of California, Berkeley.*—It is well known that the solutions of Schrödinger's non-relativistic wave-equation for hydrogen-like atoms may be represented graphically by interpreting $\Psi\Psi^*$ as a probability density. All three of the probability density factors $\Phi_m\Phi_m^* \cdot (\Theta_{m,l})^2 \cdot (R_{n,l})^2 = \Psi\Psi^*$ may be represented graphically and compared in some detail with the electron orbits of several classical models. An attempt to combine the probability density factors and form some graphical representation of $\Psi\Psi^*$ has resulted in the construction of a mechanical device or model which when set in motion and photographed gives a good representation of the *electron-cloud*. Photographs representing the magnetic states $m = 0, \pm 1, \pm 2, \pm 3, \cdots$ for $1s$, $2p$, $3d$, $4f$, $2s$, $3p$, $4d$, $5f$, $3s$, $4p$, and $5d$ electrons have been made.

In a similar manner the Dirac electron, which includes the electron spin, may graphically be compared with the classical electron orbits. In this more complete case with S, L and J, the angular distributions $(\Theta_{m,l,j})^2$ differ considerably from the Schrödinger distributions. It is of interest to point out in this connection that not only are the ${}^2S_{1/2}$ states spherically symmetrical but also the ${}^2P_{1/2}$ states. The correspondence with the classical models, including electron spin, is quite remarkable. On the other hand, the radial distributions $(R_{n,l,j})^2 \cdot 4\pi r^2$ on both the Schrödinger and Dirac theory, are so nearly identical that the difference between the two, being of the order of the fine-structure constant α, cannot be shown graphically. This is just as would be expected from the classical analogy. The probability density $\Psi\Psi^*$ for the Dirac electron becomes zero at $\Theta = 0$ and π only and at $r = 0$ and ∞ only.

29. The motion of a Dirac electron in a magnetic field. L. D. HUFF. *California Institute of technology.*—Solutions of the Dirac wave equation representing a free electron moving in a uniform magnetic field are obtained. The functions are similar to those obtained by Landau and by Uhlenbeck and Young as solutions of the Schrödinger equation. A wave packet is constructed representing a beam of electrons passing through a slit. The results agree with the classical predictions to terms of the order of the de Broglie wave-length of the electron divided by the radius of curvature of its classical path. For experimental cases this ratio is of the order 10^{-8} to 10^{-10}. Hence it is concluded that the difference between magnetic deflection measurements of e/m and other determinations cannot be explained as a quantum effect.

30. On the relative abundances of isotopes. HAROLD C. UREY AND CHARLES A. BRADLEY, JR. *Columbia University.*—If the relative abundances of atomic nuclei represent an equilibrium distribution at any temperature, that temperature must be the temperature of the

sun at the time the planets were formed. An alternative hypothesis is that equilibrium existed at some previous higher temperature and has been *"frozen"* since then. But the relative abundances can hardly be those established at such a higher temperature, for this would require that the atoms turn into radiation in just such a way that this equilibrium mixture would remain. To test the question by thermodynamic considerations it is necessary to know (1) the activity coefficients of atomic nuclei in the body of a star, (2) the energy changes, and (3) the entropy changes of the reactions involved. For reactions of the type

$$C^{12} + O^{17} \rightarrow C^{13} + O^{16},$$

the activity coefficients need not be known and the entropy change is zero or small unless the temperatures are so high that nuclear energy levels are excited and the densities so high that the activity coefficients cannot be regarded as determined by the net nuclear charge only. The energy changes are known from the atomic masses and using the known relative abundances of the nuclei, it is possible to calculate the supposed temperature of equilibrium. The temperatures calculated in this way form a number of such reactions are fantastic. We conclude that either (1) these simple thermodynamic considerations cannot be applied under the extreme conditions of the sun for unknown reasons, or (2) the mixture of the isotopes on earth is not an equilibrium mixture at any temperature.

31. The spectra of high current vacuum arcs. ARTHUR S. KING. *Mount Wilson Observatory.*—The experiments were designed to supplement previous work in which arcs carrying very large currents had been studied. Small metallic rods, or copper tubes containing pulverized metal, were used as electrodes in a vacuum chamber at a pressure of about 5mm. The voltage of a large generator was applied directly to these electrodes, forming an arc of very brief duration and intense brightness. The current often reached 2000 amperes at 110 volts, the electrodes burning apart to a gap of about 5 cm. The spectra examined were of iron, titanium, copper, magnesium and silicon. The lines appearing were largely those of the ionized atom, the relative strength of neutral and enhanced lines indicating a degree of ionization of the same order as that obtained in a high-capacity spark in air. Doubly-ionized lines of silicon appeared. The features of reversal and strong widening, often unsymmetrical, which in the high-current arc in air were useful in the grouping of neutral lines, are found in the vacuum high-current arc for lines of the ionized atom. It is possible thus to group the enhanced lines having similar behavior and to judge their relative energy levels. The neutral lines, though much weaker, also show the differences in structure characteristic of the different temperature classes.

32. The work required to remove a field electron. JOSEPH E. HENDERSON AND RALPH E. BADGLEY. *University of Washington.*—Electrons were drawn from a two micron platinum filament by means of an intense electric field. This field was secured by using the filament as the inner conductor of a cylindrical condenser. The outer conductor was of copper and was perforated, permitting some of the electrons to pass through it. Surrounding this conductor was another copper cylinder which was at the same potential as the filament, less a small variable potential tending to accelerate the electrons. Observation of the magnitude of this small variable potential, when the electrons just reached the outer cylinder, provided a means of measuring the work done by the field in removing an electron from the filament. The value of this was found to vary from more than 10 volts to 4.3 volts as the field was increased. The value of 4.3 volts is apparently approached asymptotically. The pressure in the apparatus as measured by an ionization guage was 2.9×10^{-8} mm of mercury.

33. Modern statistics from the Gibbsian point of view. PAUL S. EPSTEIN. *California Institute of Technology.*—Demonstration of models illustrating the differences of the Planck, Einstein-Bose, and Fermi types of statistics.

34. The effect of inductance on the electromagnetically damped galvanometer. THOS. M. DAHM, *California Institute of Technology.*—When an inductance term is included in the pair of differential equations governing the galvanometer, it is found that the results are especially applicable to the design of a galvanometer of short period and critical damping intended for the study of irregular currents, such as those produced by muscular action. Determination of the

nature of the roots of the cubic auxiliary equation is facilitated by the introduction of one parameter the value of which is determined by the inductance and resistance of the circuit and by the undamped period of the instrument, and a second determined by damping coefficient and period. Four types of transient motion are found possible—damped oscillatory, critical, doubly critical, and overdamped. A galvanometer that would be overdamped or critically damped if without inductance can be made overdamped, critical, or oscillatory by proper choice of inductance. Similar changes in behavior of an underdamped galvanometer can be produced if the damping is greater than $4\sqrt{3}/9$ times critical damping. At this value the cubic has a triple root, giving double critical damping with terms e^{mt}, te^{mt}, and t^2e^{mt} for a particular value of inductance, all other values giving oscillatory motion.

35. A search for an electrostatic analogy to the gravitational red shift. ROY J. KENNEDY AND EDWARD M. THORNDIKE, *California Institute of Technology*.—An attempt is made to determine whether the frequency of light is effected by a difference in electrostatic potential between the source of light and the measuring apparatus. The source is an electrodeless discharge in mercury vapor. It can be raised about 53,000 volts above ground by an x-ray transformer. The apparatus for measuring the change in frequency of the light is a quartz interferometer of the Michelson type with a difference in the lengths of its paths of about 560,000 light waves. It is in an evacuated case which in turn is in a thermostated water bath. Twelve exposures have been measured, six with the lamp about 53,000 volts above ground and six with the lamp grounded. The change in frequency produced by this potential was: $\Delta\nu/\nu$: about 1 part in 5.6×10^8. The probable error was about one third as large as this. It is hoped to investigate this small positive effect to see if it is real or whether it is caused by some systematic error.

AUTHOR INDEX TO ABSTRACTS OF PASADENA MEETING

Badgley, Ralph E.—see Henderson
Bender, William—No. 25
Bitter, Francis—No. 24
Brackett, Fredrick S. and Urner Liddel—No. 4
Bradley, Charles A., Jr.—see Urey
Brown, Joseph G.—No. 20

Calbick, C. J.—see Davisson
Campbell, J. S. and W. V. Houston—No. 1
Cook, S. R.—No. 22

Dahm, Thomas M.—No. 34
Davisson, C. J. and C. J. Calbick—No. 14

Ellis, Joseph W.—No. 3
Epstein, Paul S.—No. 33
Estermann, I., R. Frisch and O. Stern—No. 10

Frisch, R.—see Estermann

Gideon, Edith—see Henderson

Hall, Harvey and J. R. Oppenheimer—No. 27
Henderson, Joseph E. and Ralph E. Badgley—No. 32
——— **and Edith Gideon**—No. 17
Holzer, Robert E.—No. 16
Houston, W. V.—see Campbell
Huff, L. D.—No. 29

Johnson, Thomas H.—No. 19A
Johnston, Helen—see Urey

Kaplan, Joseph—No. 5
Kennedy, Roy J. and Edward M. Thorndike—No. 35
King, Arthur S.—No. 7
————No. 31

Lawrence, E. O. and D. H. Sloan—No. 18
Liddel, Urner—see Brackett
Loeb, Leonard B.—No. 19

Mackeown, S. S.—No. 11

Neher, H. V.—No. 15

Oppenheimer, J. R.—see Hall

Potapenko, G. V.

Rinde, C. A.—No. 23

Sloan, D. H.—see Lawrence
Soller, Walter—No. 9
Stern, O.—see Estermann
Strong, John—No. 8

Thorndike, Edward M.—see Kennedy

Urey, Harold C. and Helen Johnston—No. 2
———**and Charles A. Bradley, Jr.**—No. 30

Washburn, Harold W.—No. 12
White, H. E.—No. 28
Winans, J. Gibson—No. 6
Workman, E. J.—No. 21

Zener, Clarence—No. 26